Cranfield University

Ravinka Seresinhe

Impact of aircraft systems within aircraft operation: A MEA trajectory optimisation study

School of Aerospace, Transport and Manufacturing

Centre for Aeronautics

Aerospace Engineering Division

PhD Thesis

2011 – 2014

Supervisor: Dr. C.P. Lawson

September 2014

This thesis is submitted in partial fulfilment of the requirements for the degree of Doctor of Philosophy.

Abstract

Air transport has been a key component of the socio-economic globalisation. The ever increasing demand for air travel and air transport is a testament to the success of the aircraft. But this growing demand presents many challenges. One of which is the environmental impact due to aviation. The scope of the environmental impact of aircraft can be discussed from many viewpoints. This research focuses on the environmental impact due to aircraft operation.

Aircraft operation causes many environmental penalties. The most obvious is the fossil fuel based fuel burn and the consequent greenhouse gas emissions. Aircraft operations directly contribute to the CO_2 and NO_X emissions among others. The dependency on a limited natural resource such as fossil fuel presents the case for fuel optimised operation. The by-products of burning fossil fuel some of which are considered pollutants and greenhouse gases, presents the case for emissions optimised operations. Moreover, when considering the local impact of aircraft operation, aircraft noise is recognised as a pollutant. Hence noise optimised aircraft operation needs to be considered with regards to local impacts. It is clear whichever the objective is, optimised operation is key to improving the efficiency of the aircraft.

The operational penalties have many different contributors. The most obvious of which is the way an aircraft is flown. This covers the scope of aircraft trajectory and trajectory optimisation. However, the design of the aircraft contributes to the operational penalties as well. For example the more-electric aircraft is an improvement over the conventional aircraft in terms of overall efficiency. It has been proven by many studies that the more-electric concept is more fuel efficient than a comparable conventional aircraft.

The classical approach to aircraft trajectory optimisation does not account for the fuel penalties caused due to airframe systems operation. Hence the classical approach cannot define a conventional aircraft from a more-electric aircraft. With the more-electric aircraft expected to be more fuel efficient it was clear that optimal operation for the two concepts would be different. This research presents a methodology that can be used to study optimised trajectories for more-electric aircraft.

The study present preliminary evidence of the environmental impact due to airframe systems operation and establishes the basis for an enhanced approach to aircraft trajectory optimisation which include airframe system penalties within the optimisation loop. It then presents a suite

of models, the individual modelling approaches and the validation to conduct the study. Finally the research presents analysis and comparisons between the classical approach where the aircraft has no penalty due to systems, the conventional aircraft and the more-electric aircraft.

When the case studies were optimised for the minimum fuel burn operation, the conventional airframe systems accounted for a 16.6% increase in fuel burn for a short haul flight and 6.24% increase in fuel burn for a long haul flight. Compared to the conventional aircraft, the more electric aircraft had a 9.9% lower fuel burn in the short haul flight and 5.35% lower fuel burn in the long haul flight. However, the key result was that the optimised operation for the more-electric aircraft was significantly different than the conventional aircraft. Hence this research contributes by presenting a methodology to bridge the gap between theoretical and real aircraft-applicable trajectory optimisation.

Acknowledgements

I thank GOD for the faith, patience, strength and all other blessings given during my life.

This research would have not been possible if not for the support and guidance by Dr. Craig Lawson. I thank him for giving me the opportunity to be involved in the Clean Sky research and for all the time he dedicated to my research and supervision. I would like to thank Professor Marin Guenov and Professor Howard Smith for always giving their support especially in acquiring grants for funding conference publications. I also thank Diane and Elizabeth for helping out with all administrative matters.

This research has been a remarkable journey for me and I was fortunate enough to have great colleagues and supervisors. Dr. Lawson and Dr. Madani were extremely helpful when there were technical challenges that needed to be resolved and I thank them for their insight. Even though the PhD research was an individual task, I had the privilege of working with two outstanding gentlemen within the Clean Sky team. Together with Mr. Daniele Quaglia and Mr. Ahmed Shinkafi, we worked as a team. We had philosophical arguments, technical debates and brainstorming sessions which were invaluable to my research. I thank them for the great support and team atmosphere which was created. I hope I contributed to your work as much as you did to mine.

I thank my parents for the support and guidance they have given throughout my entire life and this achievement is a testament to their unwavering help and advice. I would not have been able to do this research without the financial support of my father or the academic values instilled by my mother. I would also like to thank my parents-in-law Mr. Terrance Perera and Mrs. Nalinka Perera for their invaluable support and their willingness to help me in my time of need.

Finally I would like to thank my lovely wife and son for the patience and support they have shown. They have been an endless source of inspiration for me to better myself and a constant voice of encouragement driving me to be the best I could be. Most importantly they have been the reason to smile in times when I had doubts about myself throughout this journey.

Table of Contents

List of figures

List of tables

Nomenclature

Units and Abbreviations

°C	Celsius
2-D	Two Dimensional
3-D	Three Dimensional
AC	Alternate Current
ACARE	Advisory Council for Aeronautics Research and Innovation in Europe
ADM	Aircraft Dynamics Model
ADP	Air Driven Pump
AEA	All Electric Aircraft
AGL	Above Ground Level
AMC	Acceptable Means of Compliance
APU	Auxiliary Power Unit
ASHRAE	American Society of Heating, Refrigerating and Air conditioning Engineers
ASM	Airframe Systems Model
ASTM	American Society for Testing and Materials
ATA	Air Transport Association
ATM	Air Traffic Management
atm	Standard atmosphere
BADA	Base of Aircraft DAta
CAA	Civil Aviation Authority (UK)
CFG	Constant Frequency Generator
CO_2	Carbon Dioxide
CS	Certification Standards
CTRLS	Controls
DAE	Differential Algebraic Equations
dBA	A-weighted Decibel
DC	Direct Current
DOF	Degrees-Of-Freedom
EASA	European Aviation Safety Agency
EC	European Commission
ECS	Environmental Control System
EGT	Exhaust Gas Temperature
EHA	Electro hydro-static Actuator
ELA	Electrical Load Analysis
EMA	Electro Mechanical Actuator
ELMC	Electric Load Management Centre
ENADOT	Electric Network Architecture Design Optimisation Tool
EPNL	Effective Perceived Noise Level
FAA	Federal Aviation Authority
FBW	Fly By Wire
FL	Flight Level
ft	feet

GATAC	Green Aircraft Trajectories under Air Traffic management Constraints
Gen.	Generator
g/m^3	Grams per cubic meter
HP	High Pressure
HPC	High Pressure Compressor
Hyd	Hydraulic
ICAO	International Civil Aviation Organization
ID	Integrated Technology Demonstrator
IDEA	Integrated Digital/Electric Aircraft
IDG	Integrated Drive generator
IFE	In-Flight Entertainment
IM	Induction Machine
INM	Integrated Noise Model
INMTM	Integrated Noise Model / Management of Trajectory and Missions
IP	Intermediate Pressure
IPC	Intermediate Pressure Compressor
IPS	Ice Protection System
ISA	International Standard Atmosphere
ITD	Integrated Technology Demonstrator
K	Kelvin
KCAS	Knots Calibrated Air Speed
kg	Kilograms
kg/s	Kilograms per second
kN	kilo Newton
kt	Knots
kVA	kilo Volt-Ampere
kW	kilo Watt
L/s	Litres per second
LAMAX	A-Weighted Maximum Sound Level
lb/sec	pounds per second
LP	Low Pressure
LWC	Liquid Water Content
M	Mach number
m	Metres
m^2	Square metres
MEA	More Electric Aircraft
mg/N.s	Milligrams per Newton per second
MTM	Management of Trajectory and Mission
MTOW	Maximum Take-Off Weight
N	Newton
NASA	National Aeronautics and Space Administration (USA)
NO_X	Nitrous Oxides
NSGA	Non-dominated Sorting Genetic Algorithm
PAX	Number of Passengers
PMS	Power Management System

PMSM	Permanent Magnet Synchronous Machine
PNLTM	Tone-Corrected Maximum Perceived Noise Level
RNAV	Area Navigation (formerly random navigation)
RWY	Runway
s	Seconds
SAE	Society of Automotive Engineers
SEL	A-Weighted Sound Exposure Level
SFC	Specific Fuel Consumption
SGO	Systems for Green Operations
SID	Standard Instrumental Departure
SL	Sea Level
SPS	Secondary Power System
SRM	Switched Reluctance Machine
SSPC	Solid State Power Controller
STAR	Standard Terminal Arrival Route
T	Temperature
T-O	Take-Off
TAI	Thermal Anti-Ice
TE	Technology Evaluator
TRU	Transformer Rectifier Unit
V	Volt
VHF	Very High Frequency
VOR	VHF Omnidirectional Range
VSCF	Variable Speed Constant Frequency
W	Watts
WP	Way Point

Symbols

γ	ratio of specific heat of air
ε	efficiency of the heat exchanger
φ	ratio between the ambient and the aft compressor temperatures
γ	Flight path angle (radian)
χ	Heading angle (radian)
c	Specific fuel consumption (milligrams per Newton per second)
C_p	Specific heat capacity of air (Joule per kilogram per Kelvin)
Φ	Geodetic latitude (decimal degrees)
λ	Geodetic longitude (decimal degrees)
μ	Bank or roll angle (radian)
A	Wall area of cabin (square meter)

D	Drag magnitude (Newton)
g	Gravitational acceleration (meter per second per second)
h	Altitude (meters)
H_e	Heat load from electrical equipment (Watt)
H_P	Sensible heat for passengers and crew (Watt)
H_s	Heat load due to solar radiation (Watt)
L	Lift magnitude (Newton)
m	Mass (kilogram)
$\dot{m}_a$	Air mass flow (kilograms per second)
P_e^b	Ratio between the ambient and cabin pressures
P_{net_EECS}	Net power for the electric ECS (Watt)
$\dot{Q}$	Bleed air power (Watt)
$\dot{q}_{aero}$	Aerodynamic heating (Watt)
$\dot{q}_{anti}$	Anti-icing energy requirement (Watt)
$\dot{q}_{sensib}$	Sensible heating (Watt)
$\dot{q}_{convec}$	Convective cooling (Watt)
$\dot{q}_{evap}$	Evaporative cooling (Watt)
$\dot{q}_{ke}$	Kinetic heating (Watt)
R_E	Earth radius (meters)
T	Thrust (Newton)
T_c	Average cabin temperature (Kelvin)
T_e'	Ratio between the ambient and cabin temperatures
T_e	Exit temperature (Kelvin)
T_i	Inlet temperature (Kelvin)
T_s	Outside skin temperature (Kelvin)
U	Thermal conductivity of the cabin skin (Watt per meter per Kelvin)
V	Aerodynamic speed (meters per second)

1 Introduction

Aviation has become an important instrument for economic growth which has resulted in a global rise in demand for air transport services. This growth is accompanied by operational hazards, negative effects on the environment and unsustainable operational expenses.

It is estimated that air transport moves over 2.2 billion passengers annually and that by the year 2050 the current commercial aircraft fleet will be doubled. Moreover, it is expected that within the next 20 years, demand for air travel will increase between 4-5% per year. [1]

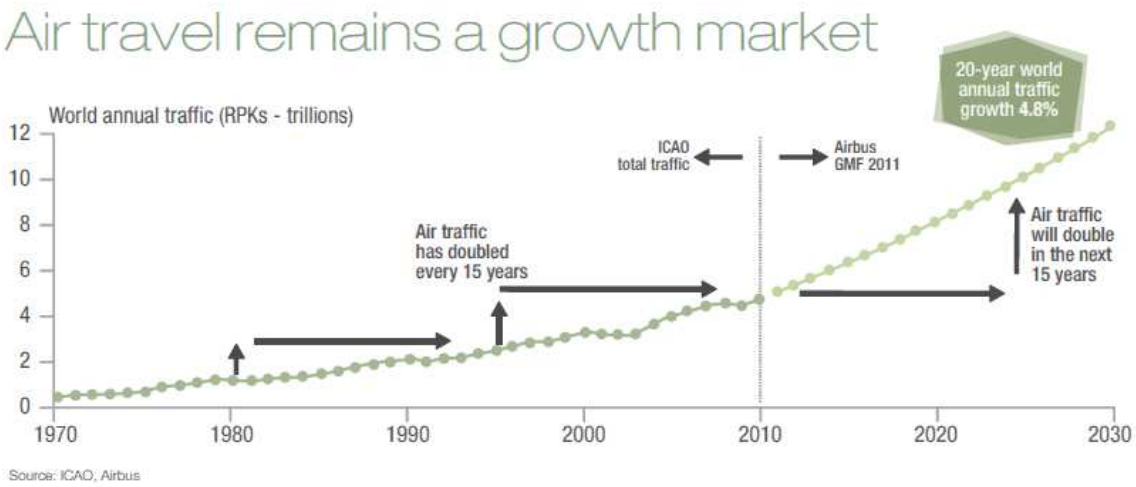

Figure 1-1: Air travel growth [2]

This expected growth in aviation has significant effects on the global environment. Waitz et al. [3] highlights noise, local air quality and climate change as some of the key areas that need to be addressed within the topic of aviation and its impact on the environment.

1.1 Aviation's impact on the environment

The expected annual growth rate of 4.7-4.8% over the next 20 years in air travel (in terms of revenue passenger kilometres) [4] means that in the future, aviation may have a greater negative environmental impact. The challenge will be to have more aircraft operating more of the time yet have a lesser adverse environmental impact overall compared to the present. Consequently, it has become the priority project of the Advisory Council for Aeronautics Research in Europe (ACARE), to achieve ; a 50% reduction of the perceived noise compared to average noise levels in year 2000, a 50% cut in CO_2 emissions per passenger kilometre and an 80% cut in NO_x emissions compared to year 2000 [5]. All these goals directly affect not only how an aircraft is operated but also how an aircraft is designed and built.

Moreover, ACARE has identified that more efficient aircraft, more efficient engines and improved air traffic management will be the key contributors to achieving the objectives [1].

1.2 The airframe systems impact

The aircraft is a system of sub-systems which is operated to achieve the necessary functions. The components in the sub systems require energy to operate and produce their desired outputs, whether it is an essential component (required to maintain safe flight) such as an air data computer or a non-essential component (not required to maintain safe flight) such as a beverage maker in the galley.

Aircraft systems are of vital importance for any aircraft. The systems may differ between different types of aircraft. It may also differ between aircraft of the same type. Typically the aircraft systems are powered either, pneumatically, hydraulically, electrically or in most cases by a combination of the three. Moreover, the aircraft engines provide the power for the aircraft systems. This power which is separate from the propulsive power is often referred to as secondary power. This secondary power extraction from the aircraft engines causes a penalty which can be quantified by studying the fuel consumption or the specific fuel consumption of the engine.

The conventional large commercial aircraft which includes almost all aircraft with the exception of the Boeing 787 series has three main types of power sources to run the systems on-board. Systems on-board the aircraft such as the environmental control system (ECS), ice protection system (IPS) as well as some other minor systems are run by pneumatic power. Systems such as the primary and secondary flight control surface actuation and, landing gear actuation are powered by the aircraft hydraulic system. Systems such as the communication and navigation system, the lighting, the galley, and the in-flight entertainment are operated by the electrical network.

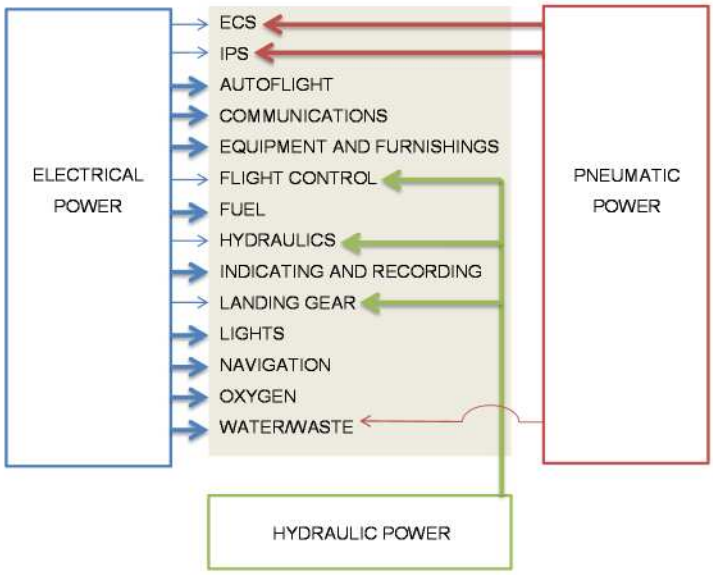

Figure 1-2: Airframe systems – typical power type

The demands on bleed-air and power off-takes are dependent on the aircraft size and the engine type. Moreover, there is a loss of potential thrust and a rise in the specific fuel consumption due to off-takes, as shown in Figure 1-3. In addition, engines with smaller cores are expected to have a greater deterioration of performance due to off-takes in comparison to engines with larger cores. [6]

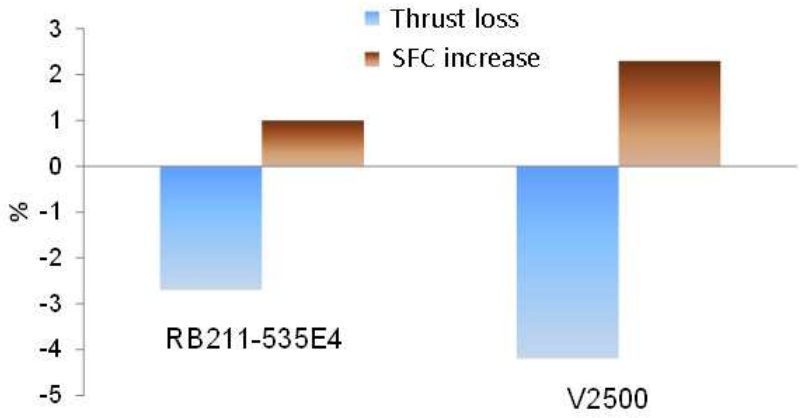

Figure 1-3: Effect of typical aircraft off-take requirements [6]

Giannakakis et.al, [7] states that keen focus on the effects of secondary power extraction began following the 1970s oil crisis.

1.3 The MEA and its evolution

In recent times, with the rising fuel costs and the emphasis on more environmentally friendly aircraft technologies, major focus has been placed on designing and producing more electric aircraft.

An aircraft with all secondary power systems operating electrically can be thought of as an AEA (All Electric Aircraft). The definition of a MEA can be derived as; an aircraft where the majority of the systems or a higher percentage of systems compared to conventional aircraft, are powered electrically.

For the purpose of this research the “more electric aircraft” has been defined as an aircraft which uses proportionally more electrical secondary power than a legacy or conventional aircraft. An “all-electric aircraft” can be defined as an aircraft that uses only electrical secondary power, by dispensing with hydraulic and pneumatic power [8]. Feiner [9] suggests that aircraft with all electric secondary power systems are expected to “cost less, be more reliable and be less expensive to operate”. He also goes on to say that benefits include reduced design complexity, reduced parts count, easier aircraft modification and less environmental impact. It is further endorsed by Arguelles et al in [5], where the MEA is highlighted as a pathway to achieving a lower environmental impact due to aviation. Moreover, it means that future aircraft will possibly have most equipment operating through electrical power.

ACARE lists the MEA as an enabler to reach the 2020 goals. [10] However, with the projected advances in aircraft architecture and aviation in general will most likely be inadequate to meet the stringent ACARE 2020 targets. But the targets set out provide the motivation for aviation and aircraft technologies to advance rapidly. The significance of the MEA as an enabler is the basis for this research to study optimised operations of MEA.

It is interesting to note that legacy aircraft such as the Bristol Brabazon and the Vickers Valiant V-Bomber which were aircraft of the mid 1950s, used electricity to power many of the systems and components on-board [11]. However the architectures of these aircraft were not the basis for further development of MEA due to the level of available technology at the time and the lack of maturity of efficient electrical distribution technology. Thus, pneumatic and hydraulic alternatives were introduced and developed. The challenges and the benefits of the MEA concept are discussed in detail in [12], [13] and [14].

1.4 Trajectory optimisation

The scope for improvement of aircraft efficiency has also been extended to the aircraft operations domain. With global aviation growing at a fast rate, the traditional navigation and guidance measures need to be improved to achieve more robust and efficient aircraft operation, to reduce the environmental impact. Trajectory and trajectory optimisation plays a key role in aircraft operation.

The classical approach to trajectory optimisation has neglected the impact of the airframe systems power off-takes. A typical approach consists of aircraft dynamic representation, engine performance and environmental impact models such as emissions and noise assessment.

The airframe systems operation is vital in representing real aircraft behaviour as it consumes a sizeable proportion of the aircraft engine's power which has a knock-on effect on the fuel burn and consequently the optimisation of aircraft trajectory.

Moreover, it is very important to establish from the outset that the concept of "*more-electric aircraft trajectory optimisation*" cannot be discussed by ignoring the airframe systems, since an aircraft can only become more electric by substituting the conventional pneumatic and hydraulic powered systems with electrically powered systems. Hence in the topic of trajectory optimisation for future MEA, needs to represent the airframe systems within the problem definition.

1.5 Clean Sky

In order to address the challenges of aviation in Europe, the European Commission (EC) initiated the Clean Sky program.

The Clean Sky program is organized into six Integrated Technology Demonstrators (ITDs) and the Technology Evaluator (TE) to evaluate the outputs of the ITDs. Systems for Green Operations (SGO) ITD address the novel and more efficient ways of managing aircraft energy, as well as aircraft trajectory and mission. This work is carried out as part of System for Green Operations (SGO) ITD and involves the development of a multi-objective optimisation framework for planning environmentally efficient trajectories to provide quantitative estimates of the energy used by them with a view to improving their efficiencies.

The Clean Sky program is the successor to a long line of projects in Europe which addressed environmentally friendly aircraft. These include; Totally Integrated More Electric Systems (TIMES) [15], Power Optimised Aircraft (POA) [16], and the More Open Electrical Technologies (MOET) [17] studies.

1.6 Objectives

The research question was based on; *"trajectory optimisation of more electric aircraft"*. Specifically, ***"How can design and operation aspects of aircraft be combined to achieve more efficient and environmentally friendly future aircraft?"***

In order to answer the research question, the following objectives were established;

- A critical review on secondary power systems on past and present aircraft
- A new robust methodology for the sizing of the electrical loads on an aircraft
- Formulation of robust and accurate relationships between power extraction and SFC change by using engine performance models validated for a variety of off-design conditions including power extractions
- Creating integrated models which included satisfactory complexity but which were also computationally efficient.
- Studying the combined effects of systems operation and trajectory optimisation

1.7 Intended contribution to knowledge

The research aims to provide a methodology to enhance the classical approach to aircraft trajectory optimisation by including the airframe systems power off-take penalties within the optimisation loop; thereby assessing optimum operations for novel more-electric aircraft.

In summary it is to design, simulate, analyse and assess the environmental impact of the electrical loads and electrical distribution system for a given aircraft and consider the effect of the trajectory on the systems as well as the effect of systems on trajectory.

1.8 Organisation of the thesis

The thesis is organised in the following structure.

- Literature review to identify the scope of the problem, the required model and case study developments and the overall methodology.
- Overall methodology of the study

- Discussion on the environmental impact of airframe systems off-take penalties to establish the need to study airframe systems performance within the aircraft trajectory optimisation scope.
- Discussion on the electrical load analysis tool which helps quantify the conventional aircraft electrical loads. This is the basis to the MEA systems where the conventional loads are accompanied by more electric systems which replace the conventional pneumatic and hydraulic systems.
- Discussion on the off-takes interface model development which enables to correct the baseline engine fuel flow (which does not include penalties due to power off-takes) to account for power off-take penalties.
- Discussion on the final modelling set-up which was used in a trajectory optimisation framework to generate the results.
- Discussion on the results for a short haul and long haul case study.
- The conclusions and further improvements that can be made.
- A list of references.
- Appendices which include supplementary data which were used to facilitate the research.

2 Literature review

2.1 The MEA evolution in commercial aircraft and the consequences for initial aircraft design

The secondary power system should be designed to achieve the lightest weight, highest efficiency, least complexity and highest cost effectiveness. [18] However, compromises need to be made in all design aspects. The MEA concept does offer a number of advantages over the conventional systems configuration. It is predicted to have greater overall efficiency, less complexity and higher cost effectiveness. The MEA is expected to present a weight penalty, but the advances of high power density electronics has been significant and the overall benefits of the MEA are expected to outnumber the disadvantages. Within this research, aspects such as the mass, maintainability and cost differences between the conventional and more-electric aircraft are not considered. The focus is on the power consumption of the two technology types and all other aspects are considered to be comparable.

The enhanced performance due to electrically driven subsystems, versatile power management due to a single power source, microprocessor based monitoring, control and protection, improved reliability and maintainability compared to bleed and hydraulic systems and reduced aircraft weight due to the combination of the above mentioned, makes the more/all electric aircraft concepts much more appealing. [19]

However, in order to understand the future aircraft secondary power systems which are expected to be more-electric, the secondary power systems of past and present aircraft needs to be analysed in detail.

One of the most effective methods to do a study on the design of the secondary power system is to review past and present aircraft so that an understanding of the design can be established by looking at proven systems and configurations. Since it is impractical to review each variant of each model from every manufacturer, a subset of aircraft has been chosen with varying characteristics such as manufacturer, number of passengers, service entry year, maximum take-off mass and number of engines. The discussion is structured as a timeline to represent the evolution of the secondary power system.

Table 2-1: Subset of commercial aircraft of interest

Aircraft	Manufacturer	Service entry year	Max Take-Off mass (kg)	No. of passengers (Maximum density)	No. of engines
B727-200	Boeing	1964	83,900	189	3
L-1101*	Lockheed	1968	195,045	400	3
DC-10*	McDonnell Douglas	1971	196,406	399	3
A300*	Airbus	1974	170,500	266	2
MD-80	McDonnell Douglas	1980	63,503	172	2
BAe146	British Aerospace	1983	38,102	94	4
B757-200	Boeing	1983	115,680	228	2
A320*	Airbus	1988	73,500	180	2
B767-300ER	Boeing	1988	186,880	350	2
B747-400	Boeing	1989	396,890	524	4
MD-11	McDonnell Douglas	1990	273,300	323	3
A340-300*	Airbus	1993	275,000	440	4
A330-200	Airbus	1994	230,000	380	2
Avro RJ115	BAE Systems	1995	43,091	94	2
MD-90	McDonnell Douglas	1995	70,760	172	2
B737-600	Boeing	1998	66,000	132	2
B717-200	Boeing	1999	49,895	106	2
B777-300*	Boeing	2004	299,370	550	2
A380-800*	Airbus	2005	560,000	853	4
B787-8*	Boeing	2012	227,930	250	2

*Discussed in more detail

Data for the Airbus A300, A320-100, A340-300, A330-300, and A380-800 were gathered from [39] and [40]. Data for the McDonnell Douglas DC-10, Boeing 737-600, B747-400, B767-

300ER, B777-300ER and the B717-200 were derived from [39] and technical specifications in [41]. Details for the Boeing MD-11 and MD-80 were gathered from [42], details for the Boeing MD-90 were gathered from [43].

2.1.1 Lockheed L-1011 Tristar

L-1-1011 Hydraulic system - The L-1011 hydraulic system consists of four independent hydraulic systems. Each system is pressurised by engine-driven variable displacement pumps. The system operates the flight control, landing gear, and the door and locking mechanisms. Systems 1 and 2 have the capability of being pressurised by engine 1 or engine 2 engine-driven pumps using a power transfer unit. System 3 and system 4 can be pressurised by engine 2 or engine 3 engine-driven pumps. [20]

L-1-1011 Pneumatics **-** There are three independent air cycle refrigeration packs, providing the necessary ventilation to the passenger and crew compartments, on the L-1011. The system is capable of maintaining a reasonable level of comfort with only one system operating. Moreover it is capable of providing 150 cubic metres of air per minute when all three conditioning packs are operating. Galley units, lavatories, forward and mid electrical centres, and the cargo holds are ventilated, temperature regulated and pressurized where necessary. [20]

L-1-1011 Electrical system - The L-1011 has three 90 kVA generators which were paralleled automatically to a tie bus, in normal operation. A fourth generator is installed on the APU. The system also comprises of four transformer rectifier units, a battery, and a static inverter. The battery was capable of providing power to the instruments, lights, and radio for about 40 minutes. [20]

According to [21], “the continuous average demands throughout discrete phases of the aircraft flight envelope was the basis for determining the electric system capacity”. Loads required for flight, passenger comfort, and utility loads, such as galleys and lights, were included in the continuous load consideration. Loads related to the fuel, hydraulic, environmental control, avionics, and other flight support systems were classed as essential loads and amounted to about 70kVA. The maximum continuous loads occurred during a “cold-night cruise” and amounted to 168kVA.

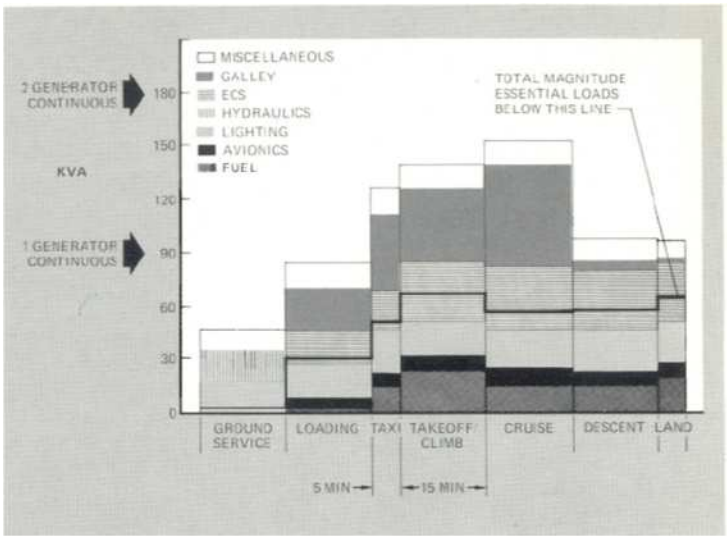

Figure 2-1: Electrical Load profile – L-1011 [21]

2.1.2 McDonnell Douglas DC-10

DC-10 Hydraulic system - The DC-10 includes three separate hydraulic systems with completely separated fluids. The system uses reversible hydraulic power transfer units to transfer the power between the three systems.

The power for each system is generally provided by the hydraulic pumps driven by two engines. However, in the case of an in-flight emergency or ground power, electric driven pumps on engine system 3, supply the power. An air-driven dropout generator is used in an all engine-out scenario. Redundancies for flight controls are provided using dual power actuators on the ailerons and elevators, by using split upper and lower rudders with separate actuators, by using dual actuators for each flap and slat and by using dual powered systems for the stabilizer trim, brakes and steering. [22]

DC-10 Pneumatics - The DC-10 has three pneumatic systems each associated with an engine. These systems are identical. The engines are the primary source of air for the systems. The APU provides an alternate source when required. The system functionality includes air conditioning, anti-icing, heating, ventilation and engine starting. The tasks are divided between the systems. Air conditioning pack 1, the left wing anti-icing, forward lavatory ventilation, lower galley ventilation and forward cargo compartment heating is supplied by pneumatic system 1. Pneumatic system 2 supplies air conditioning pack 2, heating for the centre and aft cargo compartments and the ventilation for the aft lavatories. Air conditioning pack 3, right wing anti-icing, upper VHF antenna anti-icing and pressurization of the portable water system are run by pneumatic system 3. [22]

DC-10 Electrical system - According to [22] the DC-10 aircraft uses a three-channel parallel engine CSD (Constant Speed Drive) driven electrical system. It also uses an isolated single-channel APU driven electrical system. Each of the channels consists of air-cooled brushless generators with oil-lubricated bearings, generator control units, generator relays, bus tie relays, generators and control assemblies. The APU channel is similar to the main channels but the bus tie relays are replaced with auxiliary power relays.

The generators used in the system are Westinghouse 90kVA generators. According to [22] the DC-10 had the most complex electrical system in an aircraft operated by American Airlines at the time (1970's). It incorporates features such as automatic paralleling of the generator buses at the touch of a button and complex preferential logic for auto-land.

The following illustration from [23] is the electrical load profile of the DC-10.

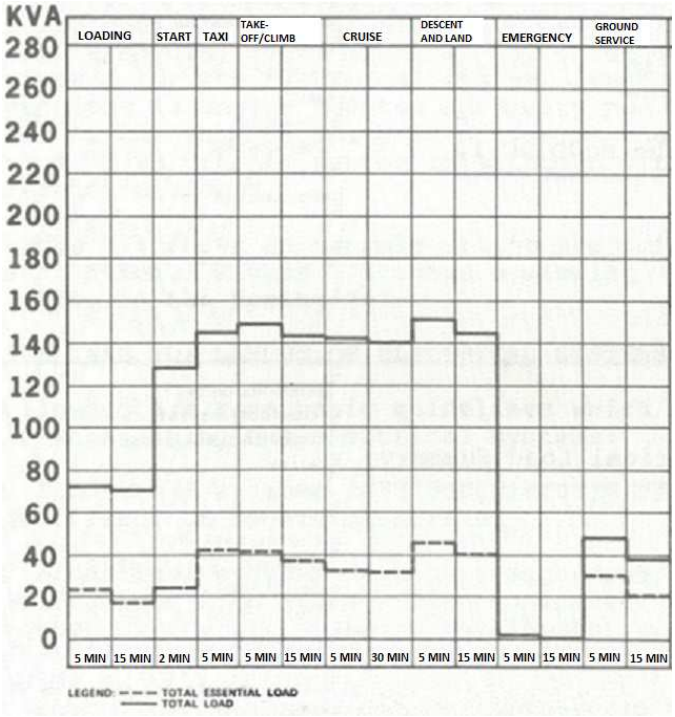

Figure 2-2: DC-10, electrical load profile [23]

2.1.3 Airbus A300

A300 Hydraulic system - The Airbus A300 has three completely independent hydraulic systems each of which has its own reservoir of fluid. The system is pressurised to 3,000 psi and is operated by engine-driven pumps. Capability of transferring power from one system to another is realised by using two non-reversible power transfer units. The system supplies power to the

primary and secondary flight control surfaces as well as to the landing gear actuation, steering, and braking systems. [24]

A300 Pneumatics - The pneumatic system on the A300 supplies bleed air for engine starting, air conditioning and pressurisation, hydraulic reservoir pressurisation, wing anti-icing and portable water tank pressurisation. The bleed air is obtained either from the engines, APU or the ground air supply units. Moreover, the thrust reverser and the engine air intake ice protection are achieved by using two independent pneumatic systems on each aircraft engine. [25]

A300 Electrical system - The electrical system on the A300 consists of four AC buses (AC1, AC2, AC ESS, and AC EMER), two DC buses (DC NORM and DC ESS), three transformer rectifier units, three 25A/h batteries, a static inverter, an APU generator, and a generator connected to each of the two aircraft engines. [26]

Each generator is rated at 90kVA and is of the brushless air-cooled type. Moreover the inverter is rated at 750VA and each transformer rectifier unit at 4200VA. [27]

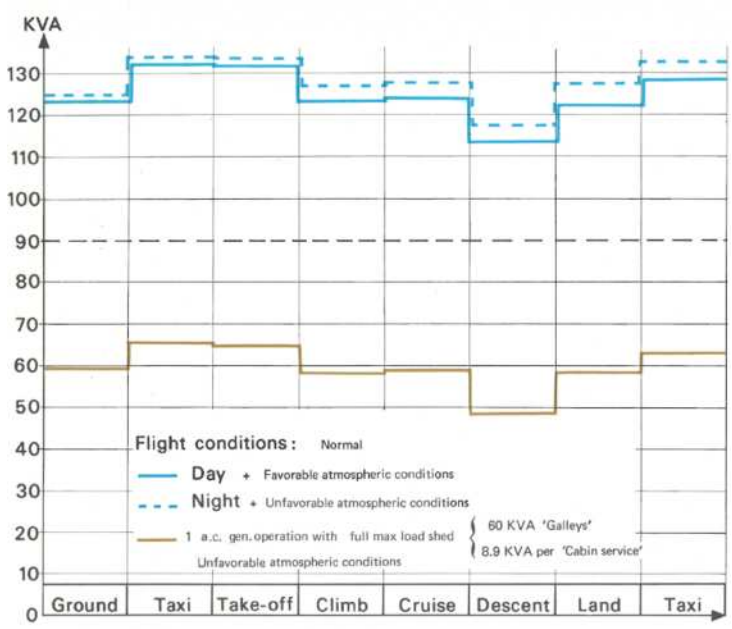

Figure 2-3: Electrical load profile – A300 [27]

2.1.4 Airbus A320

A320 Hydraulic system - The A320 hydraulic system consists of three continuously operating hydraulic systems, each with its own reservoir and normally operating at 3000 psi. The system does not permit the hydraulic fluid to be transferred from one to another channel. It should be

noted that when the system is powered (in an emergency situation) by the ram air turbine the operating pressure drops to 2500psi. [28]

The hydraulic system operates the primary and secondary flight control surfaces, the landing gear actuation and the landing gear park and alternate braking. [29]

A320 Pneumatics - The A320 pneumatic system supplies high pressure air for air conditioning, engine starting, wing anti-icing, water pressurization and hydraulic reservoir pressurization systems. The sources for high pressure air consists of the engine bleed system, the high pressure ground connection and the APU load compressor. The three sources are interconnected by a cross-bleed duct which allows the changes between the sources as required. A leak detection system is in place to check if there is any overheating in areas with hot air ducts. [30]

A320 Electrical system - The A320 electrical system consists of two three-phase generators, each driven by an engine and producing 90kVA of 115/200V 400Hz AC power. The system also contains a third identical generator which is run by the APU. The system uses a generator control unit to control the outputs of each generator. The system is capable of being connected to a ground cart when necessary and a ground power control unit protects the network by controlling the external power contactor. Moreover, the system also contains an emergency generator which would be driven by the blue hydraulic channel and is capable of supplying 5kVA of three phase 115/200V 400Hz AC power. [31]

In the case where all generators fail and only the batteries are supplying electrical power to the aircraft, an inverter is used to convert the DC power to 1kVA of 115V 400Hz AC power which is then supplied to the essential bus. The automation of this process depends on whether the aircraft is travelling at less or more than 50 knots. [31]

The system uses two transformer rectifiers to convert the AC power to 28V DC power. Each rectifier is capable of supplying up to 200 amperes of DC current. The electrical system uses two batteries which are permanently connected to the two hot buses. These have a normal capacity of 23 ampere-hours and each consists of a battery charge limiter which monitors the battery charging and the contactor. [31]

The A320 was the first airliner to use the digital FBW (Fly-By-Wire) concept [11] building on the analogue FBW system designed for Concorde.

2.1.5 Airbus A340

The Airbus A340 has a similar top level architecture in terms of the secondary power system to the Airbus A320. The air conditioning, engine starting, wing anti-icing, water pressurisation, and hydraulic reservoir pressurisation is carried out by the pneumatic system using high pressure bleed air from one of the following systems; the engine bleed system, APU load compressor or the high pressure ground connections. [32]

The hydraulic system is also very similar to the Airbus A320 in terms of the loads that it powers. The hydraulic systems powers the actuation of the primary and secondary flight control surfaces, the normal, alternate and park braking, the nose wheel steering, and the landing gear actuation. [33]

As with the pneumatics and hydraulics, the top level characteristics of the electrical system are similar to that of the A320. The primary supply is an 115V, 400Hz three-phase current supplied by engine driven generators rated at 75kVA each or an APU generator rated at 115kVA or two ground supply carts each rated at 90kVA. The DC system is a 28V system which uses two transformer rectifier units rated at 200A as converters. It also has two main batteries rated at 37Ah and a static inverter rated at 2.5kVA. The system also has two additional transformer rectifier units rated at 2.8kVA, one connected to the essential buses and the other dedicated to the APU. [34]

2.1.6 Boeing 777

The Boeing 777 can be described as a conventional aircraft in terms of the actual electrical loading but an innovative and advanced aircraft in terms of the electrical distribution system.

It has two 120kVA integrated drive generators, an APU generator, four transformer rectifier units, a main battery connected to the hot battery bus and a APU battery connected to the APU battery bus. The system also comprises of an inverter and a ram air turbine generator. [35]

According to [36] the Boeing 777 has an advance and sophisticated load management system compared to the conventional architectures. The ELMS (Electrical Load Management System) consists of three primary power panels. These primary panels contain ELCUs (Electronic Load Control Units) which control and protect high power loads such as high power fan, pump and motor loads in the ECS, electrical, fuel, landing gear, and hydraulic systems. These control

loads higher than 7kVA. The system also has four secondary power panels. These are supplied by the primary power supplies and supply power to secondary loads.

2.1.7 Airbus A380

The Airbus A380 is the world's first large civil aircraft to use a more electrical architecture with a variable frequency power generation. The aircraft has four 150kVA variable frequency generators producing three-phase power of between 370Hz and 770Hz. It also uses two 120kVA constant frequency APU generators which produce three-phase power at 400Hz. [37]

According to [37] the A380 uses 15kVA for cabin lighting, 120-240kVA of intermittent power for the galleys depending on the meal service, 90kVA of permanent power for galley cooling and about 50-60kVA permanent load for the IFE (In-Flight Entertainment) (which is about 100W/seat). These make up the majority of the main electrical loads.

The A380 architecture has a 28V DC system which converts power from the AC bus via transformer rectifier units. The DC system provides power to the critical loads in case of an interruption, through the main DC bus. The DC system supplies power to the control computers and charges the batteries as well. [37]

2.1.8 Boeing 787

According to [37] the Boeing 787 has the greatest number of features of a MEA. The aircraft uses 'bleedless' engines and the ECS is powered through an electrically driven compressor. [38] states that the hydraulic architecture is similar to the conventional system but with the exception of the centre hydraulic system being powered by two electric driven hydraulic pumps instead of the traditional Boeing air turbine driven pumps.

The main power generation on-board the aircraft is achieved by two 250kVA variable frequency starter/generators per engine which produce three-phase AC power of 230V with a frequency range of 360-800Hz. It should be noted that by using the 230V AC architecture rather than the 115V AC architecture the current that is carried for equipment with similar loads is less. This results in the decrease in conductor loss of electricity which manifests itself by allowing the wire sizes to be reduced. The aircraft also has two 225kVA APU starter/generators. Moreover, the system has the capability to convert the 230V AC power into the more conventional 115V AC and 28V DC forms to support the necessary equipment. The electrical system on the Boeing 787 also converts the 230V AC power to ± 270V DC power via

autotransformer rectifier units and the power is used to supply the environmental control system and for engine starting. [37]

2.1.9 Trends and Analysis

Figure 2-4 shows a plot of engine driven generator capacity against the maximum take-off mass. This is a typical relationship used for systems sizing at the aircraft conceptual design stage.

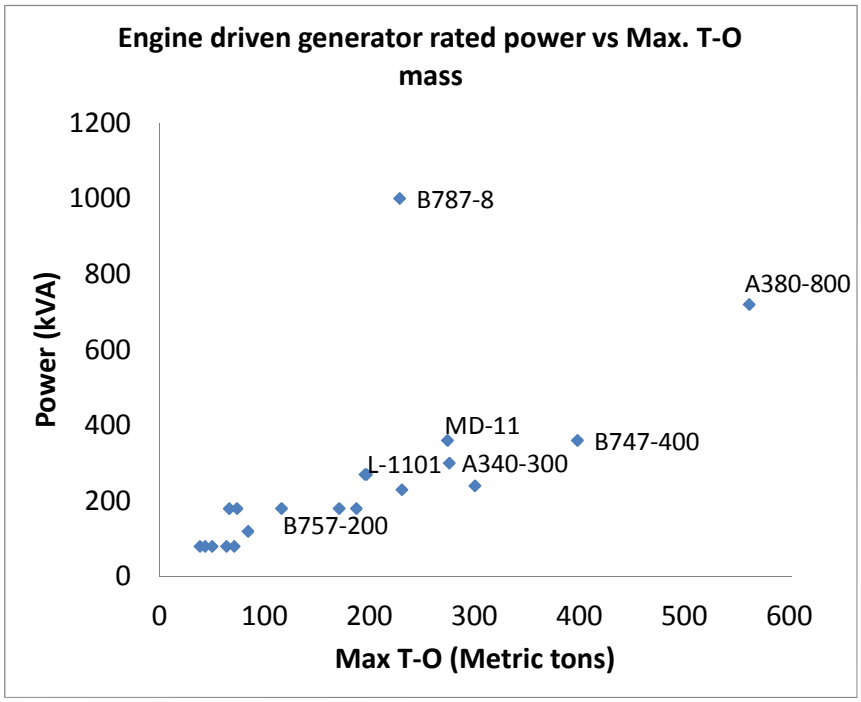

Figure 2-4: Total engine driven generator capacity vs maximum take-off mass

The data shows that for aircraft (considered in the study) having a maximum take-off mass below 70,000kg, the generator capacity remains the same most of the time. This amounts to 80kVA. The exceptions here are the Boeing 737-600 which has an installed electrical generator capacity of 180kVA at just 66,000kg (maximum take-off mass). Most aircraft within the range of 70,000kg to 190,000kg had a total generating capacity of 180kVA. Here again the Boeing 727-200 stood out as the exception, with a total capacity of 120kVA. Interestingly the Airbus A380-800 falls within the expected threshold even though the electrical architecture is very different to that of preceding Airbus aircraft. As expected the Boeing 787-8 stands out from the rest of the aircraft. It is interesting to note that the total generator capacity of the Airbus A330-200 which has a similar weight as the Boeing 787-8 is 23% of the Boeing 787-8 generator capacity.

The electrical load on the aircraft is also affected by the number of passengers on-board the aircraft. In general when the number of passengers increases, more galley equipment is required to maintain acceptable levels of comfort. Moreover the cabin lighting requirements as well as the in-flight entertainment requirements increase as well.

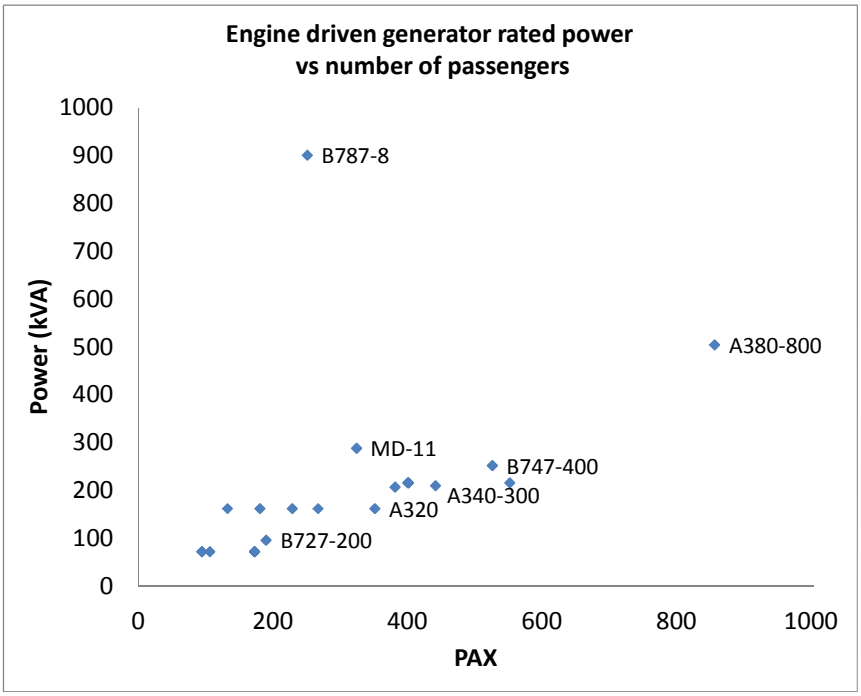

Figure 2-5: Total engine driven generator capacity vs number of passengers in the maximum density configuration

When the electric generating capability per passenger is observed (see Figure 2-5), it shows that in most cases 0.5 – 1kW is required per passenger. Certain significant characteristics are also observed. Firstly the Airbus A320 had a higher power per passenger value than any other Airbus aircraft. It is about 18.5% higher than the Airbus A380. The data suggests that the A320 may be fitted with generators which had a higher rating than required. The continuous development of systems and increasing passenger comfort by introducing innovative electrical systems in the future may have been the motivation behind this. A similar sort of deviation can also be seen on the Boeing 737-600. The number of variations for the Boeing 737, up to the 737-900ER, suggests that the generator rating may have been driven by the potential expansion of the aircraft in terms of both size and technology.

It is clear that certain characteristic technologies are also highlighted in the analysis shown below. For example as expected the Boeing 787-8 has the highest power to passenger ratio

of any aircraft. With more electrical systems on-board compared to any other aircraft the total electrical load is much higher and thus the power to passenger ratio is also higher.

At the other end of the scale, the Boeing 777-300 has a much lower generating capacity than expected. In fact it has a higher maximum take-off mass and passenger count than the Airbus A340-300, but has a lower electrical generation capacity. It should be noted that the Boeing 777-300 had an innovative electrical distribution system with the ELMS (Electric Load Management System). Hence even though the electrical loading is potentially the same as equivalent aircraft, the efficiency gained manifests itself in the overall sizing of the aircraft. Also the four-engine layout of the A340 lends itself to greater redundancy which, may in part explain the higher generating capacity compared to the two-engine Boeing 777.

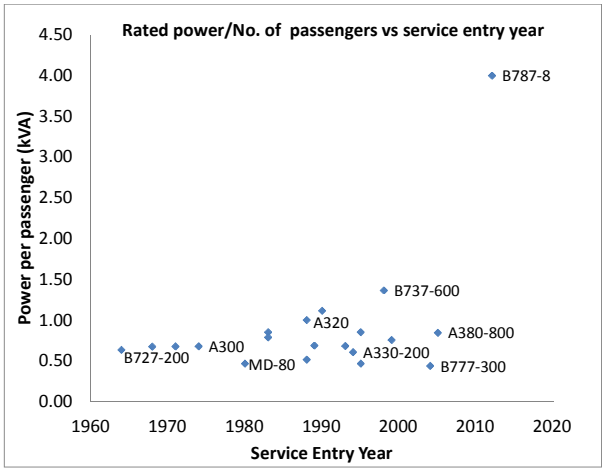

Figure 2-6: Total electrical generating power to passenger ratio against aircraft service entry year

Figure 2-6 shows the trend for electrical power per passenger against the service entry year. It shows a very interesting trend for the conventional aircraft (excluding the Boeing 787-8). A majority of the aircraft have a power per passenger ratio of between 0.5 and 1.0. It has remained in this threshold throughout. As expected the Airbus A320 is an exception as well as the Boeing 737-600. It is interesting to note that more electrical equipment (connected to passenger comfort and various other systems) has been added to the aircraft, yet this ratio has been in the same threshold. In part this may be explained by the technology advances made in the generation and distribution systems. The increase of specific system efficiencies may also contribute to balancing the ratio between the thresholds. In any case it is a good indication for conceptual aircraft design. As expected the Boeing 787-8 is in a league of its own, with a ratio of more than 4.0. This can be used as an initial estimate in the conceptual design of MEA.

The study takes conceptual design of the electrical loading one step further by studying available data on electrical load profiles of aircraft. By analysing the trends for the Lockheed Tri-star, Airbus A-300 and the DC-10, empirical correlations were constructed to observe the accuracy of relating the electrical load and generator sizing to conceptual design parameters such as the maximum take-off mass and maximum number passengers.

For the purpose of this study a standard flight profile with seven flight segments was used. The flight was assumed to be at night with unfavourable atmospheric conditions. The following are the results;

$$P_{Ground} = 0.55 * P_{Taxi} \quad (1)$$

$$\mathrm{P_{Taxi}} = ((-2 \times 10^{-4} * \ln \mathrm{PAX}) + 0.0018) * \mathrm{MTOM} \quad (2)$$

$$\mathrm{P_{Take-Off}} = ((-8 \times 10^{-5} * \ln \mathrm{PAX}) + 0.0012) * \mathrm{MTOM} \quad (3)$$

$$\mathrm{P_{Climb}} = ((5 \times 10^{-5} * \ln \mathrm{PAX}) + 0.0005) * \mathrm{MTOM} \quad (4)$$

$$\mathrm{P_{Cruise}} = \mathrm{P_{Climb}} \quad (5)$$

$$\mathrm{P_{Descent}} = ((-1 \times 10^{-4} * \ln \mathrm{PAX}) + 0.0014) * \mathrm{MTOM} \quad (6)$$

$$\mathrm{P_{Land}} = \mathrm{P_{Taxi}} \quad (7)$$

P, is the electrical load in terms of kilo-Watts at the corresponding flight segment denoted by the subscript, PAX is the number of passengers for the maximum seating density layout and MTOM represents the maximum take-off mass in kilograms.

The data suggests that the typical electrical load during the taxi phase and the landing phase are the same. The taxi phase represents the taxi out phase. It should be noted that the taxi phase duration represents loads which are occurring for 5 minutes or more whereas the landing phase represents loads occurring for 15 minutes or more. Thus even although the relationship between the parameters is the same; the landing phase represents continuous loads (defined as loads occurring for at least 15 minutes continuously) and the taxi phase represents intermittent loads defined as loads occurring for at least 5 minutes but less than 15 minutes). The duration of the segment is not considered since the analysis is focused on the maximum possible load permissible at any given time during each segment of flight.

Figure 2-7 and Figure 2-8 show the results of the review.

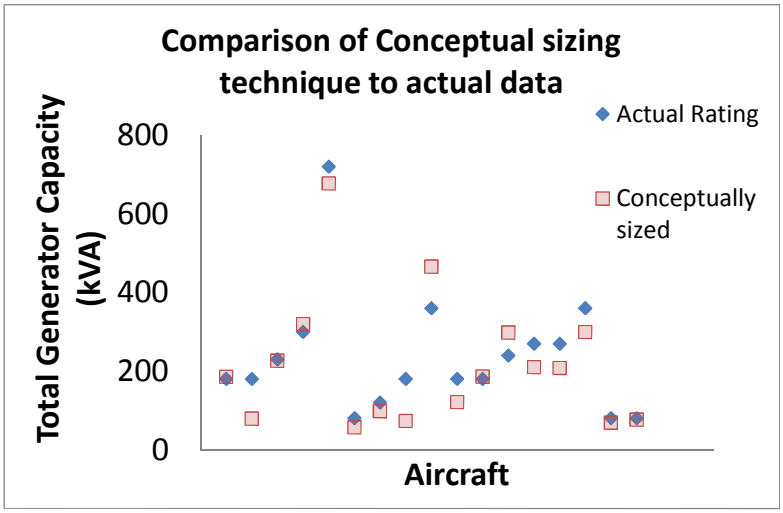

Figure 2-7: Deviation between actual data and conceptually sized results for aircraft total electric generator capacity

As can be seen most results have a degree of deviation. Although in the case of the Airbus A300, Airbus A330-200, Boeing 767-300ER, and MD-90 the deviation was less than ±5%. Moreover the Airbus A340-300 and Airbus A380-800 were within a ±10% deviation range. But 11 out of the 17 aircraft models studied showed a deviation of greater than ±14%.

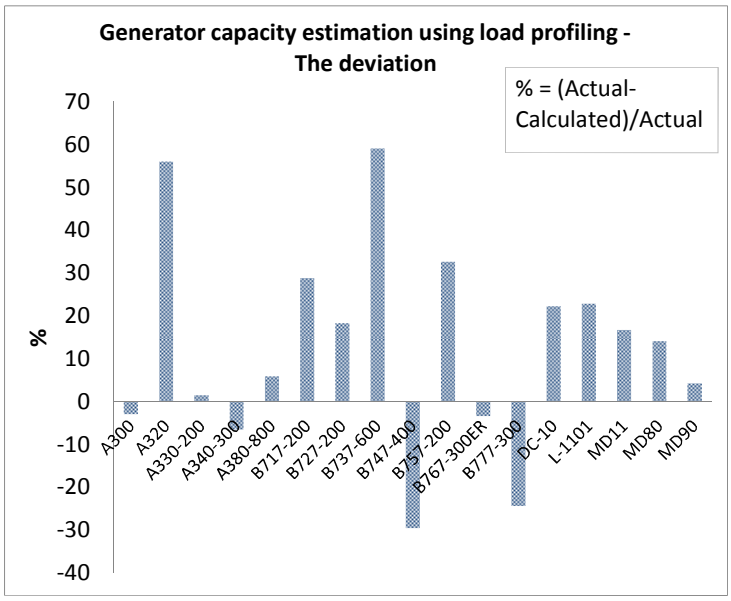

Figure 2-8: Deviation between actual data and conceptually sized results as a %

Furthermore, the analysis with conceptual sizing parameters did not show any logical reason for a particular deviation. Moreover from Figure 2-8, it can be seen that the electrical load per passenger does not present a uniform trend and this is also true for Figure 2-7. It is not possible to predict the scatter in both these graphs which makes it difficult to apply a correction factor.

The analysis suggests that the conceptual sizing method is highly accurate in certain aircraft while in others it is in-accurate. This leads to the conclusion that a more robust method is needed to size the electrical load requirement and that it should be applicable to any aircraft.

2.1.10 Summary

This section presents a review of the evolution of the electrical loading in commercial aircraft by discussing the electrical load and distribution system qualitatively and detailing the electrical load profiles where data were available. The pneumatics and hydraulics systems are also briefly discussed to show the evolution of non-electrical loads in previous aircraft being transformed to electrical loads in the MEA concept.

It is concluded that the electrical load on-board the aircraft is the key driver for the generator size and rating. Moreover, it is also concluded that with current design going in favour of the MEA concept, it is no longer acceptable not to consider in detail, the design of the electrical loads and distribution system at the conceptual and preliminary design stage. This is endorsed by the step change shown by the Boeing 787-8 as discussed in the study and also with the lower than expected generator rating of the Boeing 777-300. Both aircraft had significant changes in technology; the Boeing 787 is terms of the electrical loading and the Boeing 777-300 in terms of the distribution architecture.

The study also critically reviews the available data on in-operation aircraft generators with respect to their ratings, the maximum take-off mass of the respective aircraft, the number of passengers, and the service entry year of the aircraft to form trends and correlations. It is concluded that the generator sizing does not present a clear relationship with any of the general conceptual sizing parameters making such correlations inadequate for use in the detail design stage. This is as expected since the current practice is to do a complete electrical load analysis at the detail design stage when all components are fully defined. This is endorsed by the fact that established literature such as [44], [45], [11], [46], [23], [47] and [48] mainly discuss the type of configurations but not a detailed process on how to size it. Yet again it can be stated that perhaps the importance of the impact of the electrical system in a conventional aircraft is less significant than that of a MEA. The study presented in section 3, clearly shows that the Boeing 787-8, which can be considered to be a MEA, has nearly a 1000 kVA engine driven generator capacity. The Airbus A300 which has a slightly lower mass (comparatively to other aircraft studied) and a slightly higher number of passengers (comparatively to other aircraft

studied) only has a total of 180 kW of generator capacity. This not only shows the evolution of the electrical system, but also indicates to the impact that the MEA concept has on aircraft design.

Hence having a clear concise methodology to estimate and size the electrical loading, distribution and generation system for the MEA concept at a conceptual and preliminary aircraft design stage is of great importance.

2.2 Electrical load sizing – conventional and more-electric

The aircraft conceptual design and preliminary design procedures are well documented in a number of publications including [23], [46], [44], and [45]. There is a large volume of literature describing the development of electrical components for conventional and future aircraft as well. Roskam [23] as well as airframe manufacturers [27], [21] provide aircraft level electrical load profiles, but a numerical sizing method based on historical data or otherwise, is not provided. CAA (UK) [49] provides the guidelines on how to perform an analysis and is aimed at the detailed design phase.

By using conceptual sizing methods which rely on statistical fitting, an approximation of the total engine mounted generator rating may be obtained. The “Tot Elec” curve in Figure 2-9 represents the published engine mounted generator capacity [11]. It was found that these results, which were predicted using conceptual sizing techniques, showed significant deviations from the published data. More importantly, the total generator rating alone is not adequate for further design and analysis at a preliminary design stage and a more robust systematic prediction of required power levels is needed.

The f(MTOW) represents the generator capacity calculated as a function of the MTOW. The f(PAX) represents the generator capacity calculated as a function of the number of passengers in the maximum density configuration. The f(MTOW,PAX) is when the MTOW and the PAX are both used as variables. To keep the data consistent during the statistical fitting, PAX and MTOW variables are for the maximum passenger density configuration for each aircraft type.

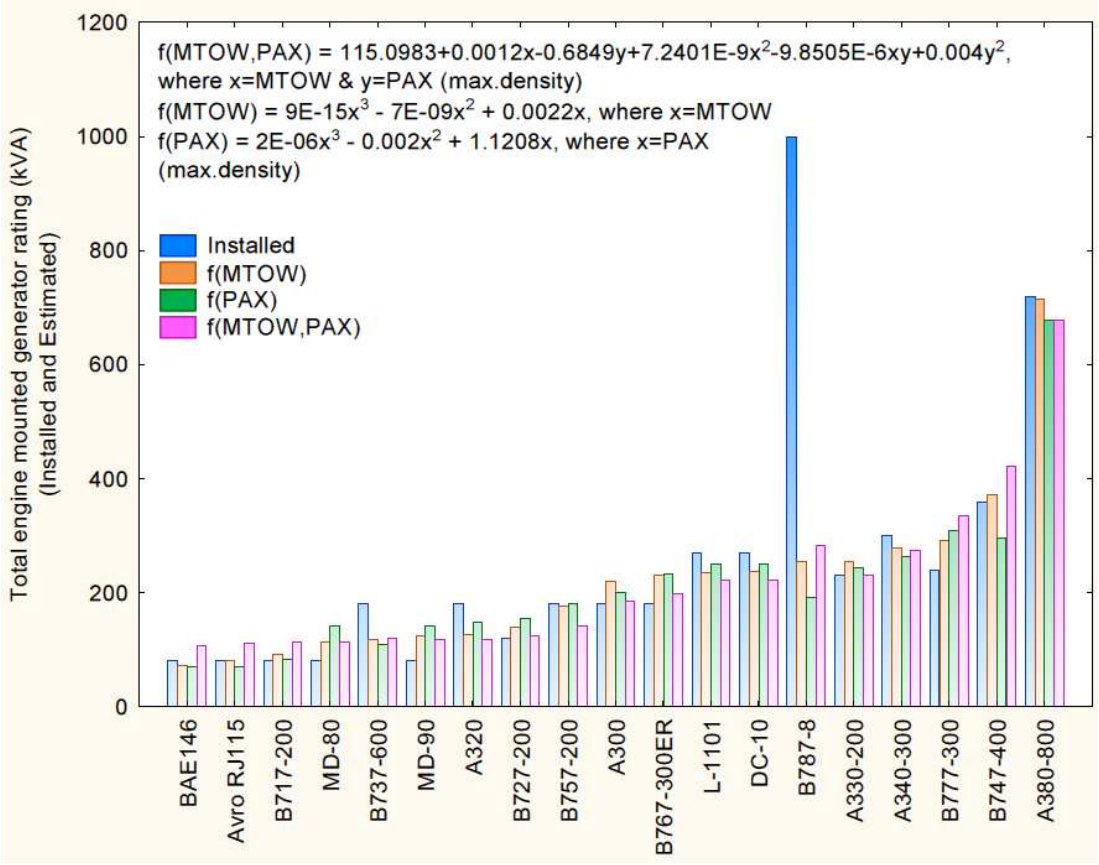

Figure 2-9: Estimated vs published total engine mounted generator ratings

$$f(MTOW, PAX) = 115.0983 + 0.0012X - 0.6849Y + 7.2401x10^{-9}X^2 - 9.8505x10^{-6}XY + 0.004Y^2 \quad (8)$$

$$f(MTOW) = 9x10^{-15}X^3 - 7x10^{-9}X^2 + 0.0022X \quad (9)$$

$$f(PAX) = 2x10^{-6}Y^3 - 0.002Y^2 + 1.1208Y \quad (10)$$

X is the mass of the aircraft and Y is the number of passengers in the maximum density configuration. The equations were constructed after a thorough trend analysis using regression techniques.

The aircraft electrical system requirements are heavily dependent on all other aircraft systems. The consumer components of the electrical system are solely dependent on other aircraft systems. The generation and distribution architecture is decided upon the technology level and power consumption of the components required for the systems. This process can only be done at a detail design stage since only at this stage will all components be fully defined. Hence the understanding of the capacity of the electrical system at the preliminary design stage is limited to a prediction achieved using empirical methods which rely on conceptual sizing

methodologies and previous experience. This limits the ability to provide more efficient tailor-made solutions for each type of aircraft. It was observed that throughout the range of aircraft studied in this research, the installed generator capacity was at times much higher than expected for the mass and passenger count of the aircraft. MEA will most likely have varying electrical loads among different aircraft types. To maintain the efficiency of MEA, , it is important to have prediction tools which will enable designers to provide tailor-made solutions which are not over-sized.

The ASTM F2490-05e1 (standard guide for aircraft electrical load and power source capacity analysis) sets the standard for the aircraft electrical system sizing. Yet this is only achievable through a full aircraft electric load analysis and can only be conducted once all the electrical components of the aircraft are decided upon. Hence it can only be completed after the detail design phase of an aircraft. An example is given by the Civil Aviation Authority (CAA) UK in [49] and it can be seen that each component needs to be listed and then a full analysis carried out. The procedure is quite straightforward, and the total power is summed up in each flight phase according to which electrical components would be needed to operate in a given flight phase. However, the procedure relies heavily on manufacturer data. Due to the sheer number of different manufacturers for various components, only the airframe manufacturer could calculate the electrical loads accurately due to the lack of availability of data. Moreover, this could only be done once all the electrical equipment was established.

2.2.1 Conventional electrical power demands

The conventional large aircraft has systems run purely on electricity as well as systems which require electrical power but use pneumatic or hydraulic power as the main type of power. Hence to get a better understanding of what components are run by which type of power, it is worthwhile to discuss certain systems briefly.

Environmental Control System (ECS) - The ECS carries out the essential functions of ventilation and pressurisation as well as thermal regulation. Typically in the conventional aircraft the ECS is powered mainly by the bleed air extracted from the engines hence it is pneumatically powered. However certain equipment necessary to maintain the functionality of the ECS are powered electrically. The re-circulation fans, many pressure regulating valves, the monitoring and controlling computers, and a variety of controllers are run electrically.

Ice Protection System (IPS) - The IPS is in charge of providing ice and rain protection. One of the primary concerns for the IPS is the build-up of ice on the wing and the majority of the energy required by the IPS is to carry out wing anti-icing. In the conventional large aircraft, the wing anti-icing is typically done using hot bleed air extracted from the engines. Hence the main power is in pneumatic form. However, for the anti-icing of probes, the wipers, the ice detectors, the anti-icing and de-misting of cockpit windows, and the operation of some valves and most controllers, electrical power is used.

Hydraulic System - The hydraulic system in conventional large aircraft is tasked with the actuation of flight control surfaces. Most components in the system are powered by engine driven pumps pressurising the hydraulic fluid for transmission. Controllers and measurement valves in the system are powered electrically. Typically, hydraulic reservoirs are pressurised using engine bleed, thus introducing a pneumatic power component as well.

Fuel system - It is typical to have electrically powered pumps for engine feed in fuel systems of large conventional aircraft. But it is also common to have jet pumps (which uses fuel as the working fluid) to carry out less critical tasks, such as transfers to the outer tanks. The monitoring and measuring systems are also typically powered by electrical power.

Other systems - Systems such as the lights, navigation, communication, auto pilot, flight control system, indicating and recording, and water and waste systems are typically powered by electricity.

A comprehensive description of airframe systems and airframe system architectures are given in [11].

A typical conventional secondary power breakdown is shown below in Figure 2-10.

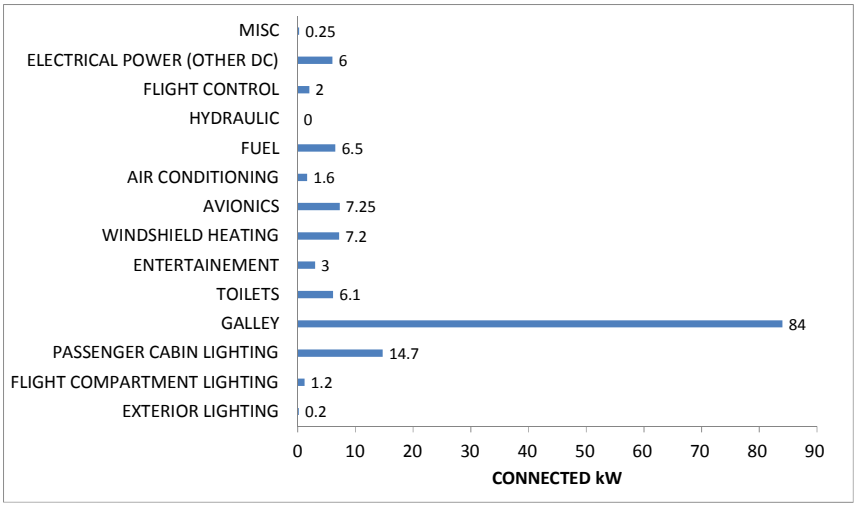

Figure 2-10: DC-10 power demands at a typical cruise [23]

2.2.2 More electric secondary power demand

Two separate studies done by airframe manufacturers and research centres such as the National Aeronautics and Space Administration (NASA) give an indication of what loads would be present in a typical all electric secondary power system for civil passenger aircraft.

The following illustration shows the estimated loads for 300 passenger tri-engine aircraft. [50] These are a result of studies conducted by the NASA Lewis Research Centre to assess the operational, weight and cost advantages for commercial transport aircraft with all-electric secondary power systems.

The following is an illustration on the load results found in the studies.

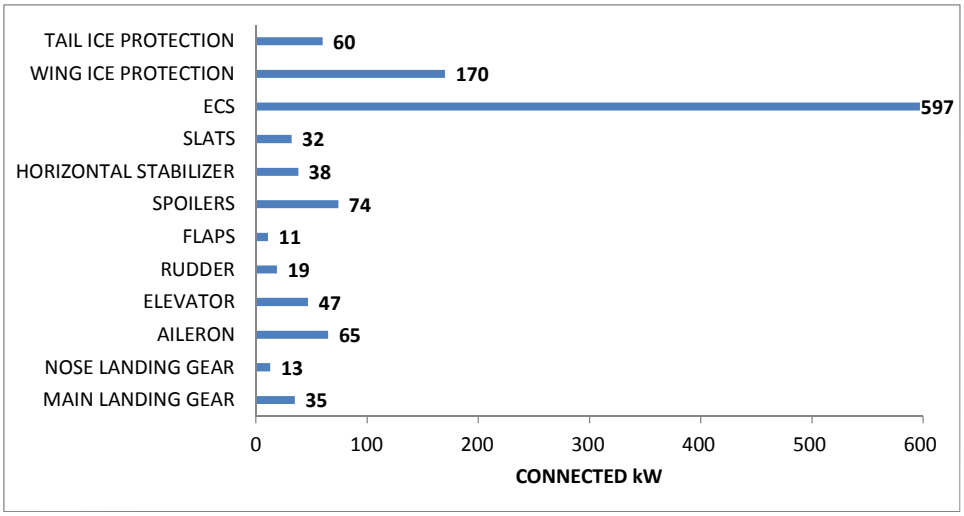

Figure 2-11: Electric load demands – 300 passenger, tri engine aircraft [50]

A further separate study by NASA on a 600 passenger, 4 engine aircraft produced the following preliminary estimates.

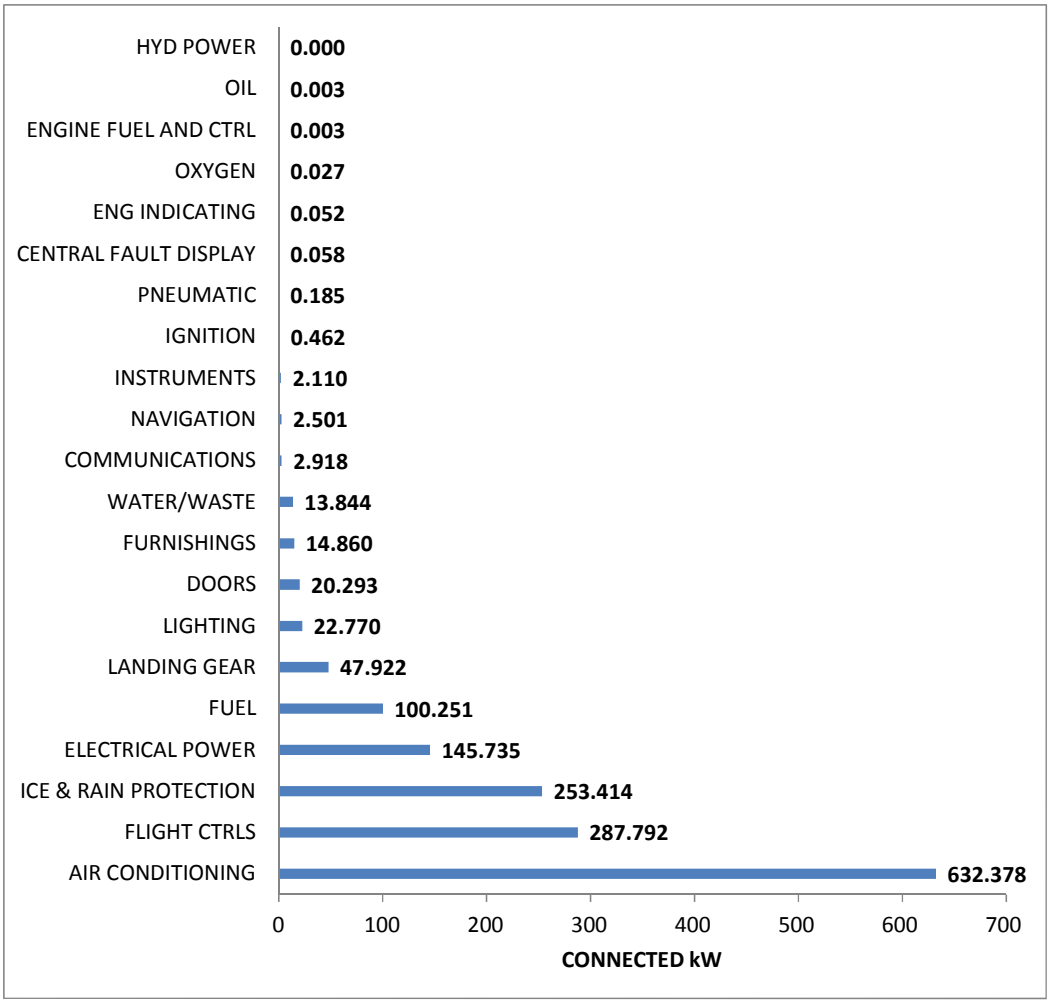

Figure 2-12: Electric load demands – 600 passenger, four engine aircraft [9]

The two studies, though focusing on MEA, were done for different aircraft sizes. The loading details of the studies cannot be directly compared due to the differences in the breakdown of loads. However, there are certain observations which are common in both cases. The ECS is established as the largest power user by a considerable margin. Other major power users are the, IPS and the flight control actuators; all three of these loads are not powered electrically in the conventional configurations. More data on MEA sizing is needed to form empirical relations for systems sizing. However, more importantly accurate prediction tools are required to prevent over-sizing of the electrical system.

2.3 Future aircraft electrical architectures

The scope of this study is based on the power requirements of the airframe systems. The losses and efficiencies of the electrical distribution and generation systems have not been addressed in detail within the modelling and simulation process. In most current aircraft the power factor of the entire electrical system in between 0.8 and 0.85. This is dependent on the overall technology level of AC components in the system. A higher power factor translates in a higher percentage of apparent power being converted to real power. As a conservative approach a typical power factor of 0.8 has been assumed for the conventional and more-electric AC components. Losses in converters have been neglected and constant generator efficiency has been assumed where necessary. The detailed modelling of the distribution and power generation system is not in the scope of this study and the losses are negligible at the aircraft level. Detailed descriptions of typical aircraft electrical conversion equipment such as TRUs, inverters, contactors and circuit breakers can be found at [51], [52], [53] and [11] respectively.

However, it is worthwhile discussing the potential future aircraft electrical architectures. According to [54] the most likely the source for the future electrical system would be a 270 V DC power source, from which 28 V DC and 115 V AC would have to be drawn. In order to do these conversions, current aircraft utilize AC-to-DC rectifiers, DC-to-AC inverters and DC-to-DC choppers. If the source is VSCF generator system then solid-state bi-directional converters can be used to condition the variable frequency into a fixed frequency. It is stipulated that the future electric architecture will require a significant amount of power electronics. The loads and the sub-systems of the future architecture will have a large number of inter-connections which would result in a variety of dynamic interactions; hence power electronics would be absolutely necessary for system functionality. The power electronics would have three major tasks. The first task would be the on/off switching of loads. In conventional systems this is done by mechanical switches and relays. The second task would be to control the electric machines and the final task will be the conversion of power and regulation of the voltage. Detailed information on solid state power controllers and the SSPC technology is documented in [55].

With regards to the power generation the PMSM, the SRM and the IM are predicted to be the most suitable options. [56]

Maldonado et.al [57] provides detailed information about DC-to-AC converters, DC-to-DC converters and electric load management centres (ELMC) which were used in the MADMEL (Management and Distribution system for a More-Electric Aircraft) program funded by the United States Air Force. The MADMEL program aimed to design, develop and demonstrate an advanced electrical power generation and distribution system for a MEA.

2.4 Power off-takes

Typically an aircraft engine is capable of providing bleed-air off-takes and shaft power off-takes. The bleed-air provides cabin pressurization and ventilation as well as airframe anti icing [58]. Moreover, it is also used to pressurize the hydraulic reservoir and the water tanks. Rolls-Royce [58] states that ideally the bleed-air should be extracted at an early stage of the engine cycle, preferably the early stages of the compressor. But it also confirms that in order to maintain appropriate temperatures and pressures, the bleed-air may need to be extracted at a later compressor stage.

Tagge et.al, [14] estimated the following bleed-air requirements, shown in Figure 2-13, for a 207 passenger, twin engine aircraft which was sized by the Boeing Commercial Airplane Company [59].

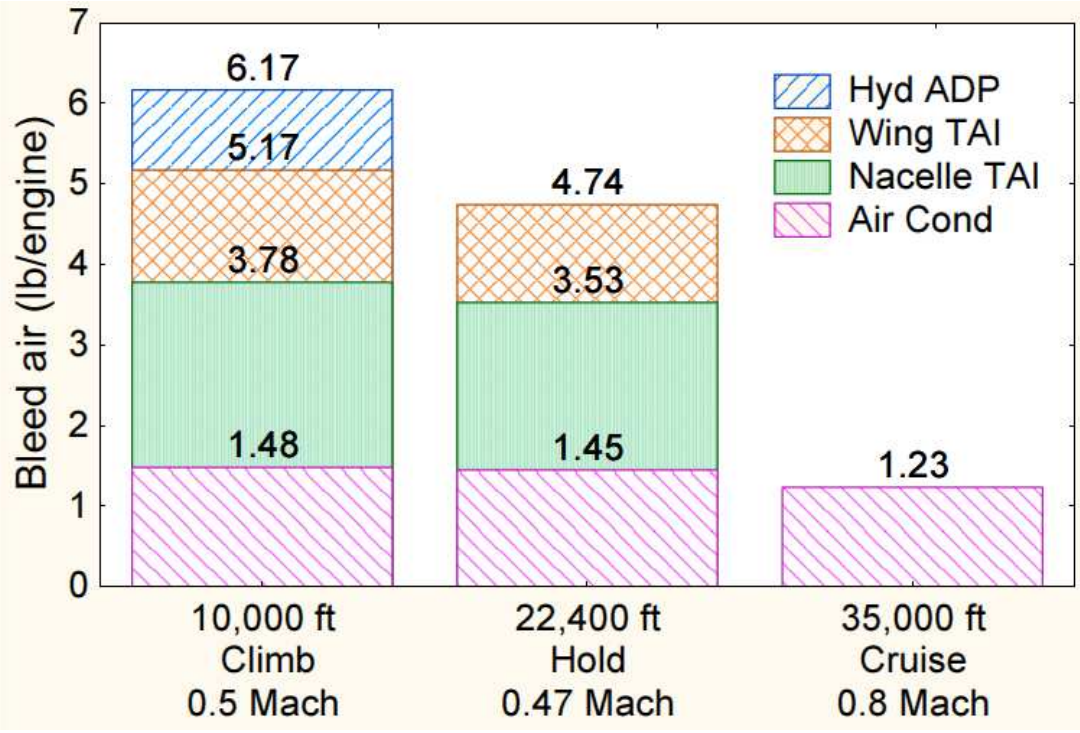

Figure 2-13: Bleed airflow requirements – IDEA study by NASA [14]

From an engine design perspective the permissible bleed-air and shaft power extraction allowances in engines vary significantly but in all cases the installed aircraft systems will have a significantly lower requirement than the respective engine's capability. Appendix 1 shows some of the bleed-air and shaft power allowances in past and present large commercial turbofan engines. The scheduling of off-takes, especially bleed-air, has many conditions, hence for this comparison; the aircraft services bleed-air provisions at the highest engine operating conditions have been summarized. The shaft off-take allowances are compared by studying the maximum continuous power available for the electrical generator drive pad. The summary is listed in "*Appendix B: Characteristics of past and present large commercial turbofan engines*".

Figure 2-14 illustrates bleed air provisions for various engines. Figure 2-15 shows engine shaft driven electrical generation capacity for several engines.

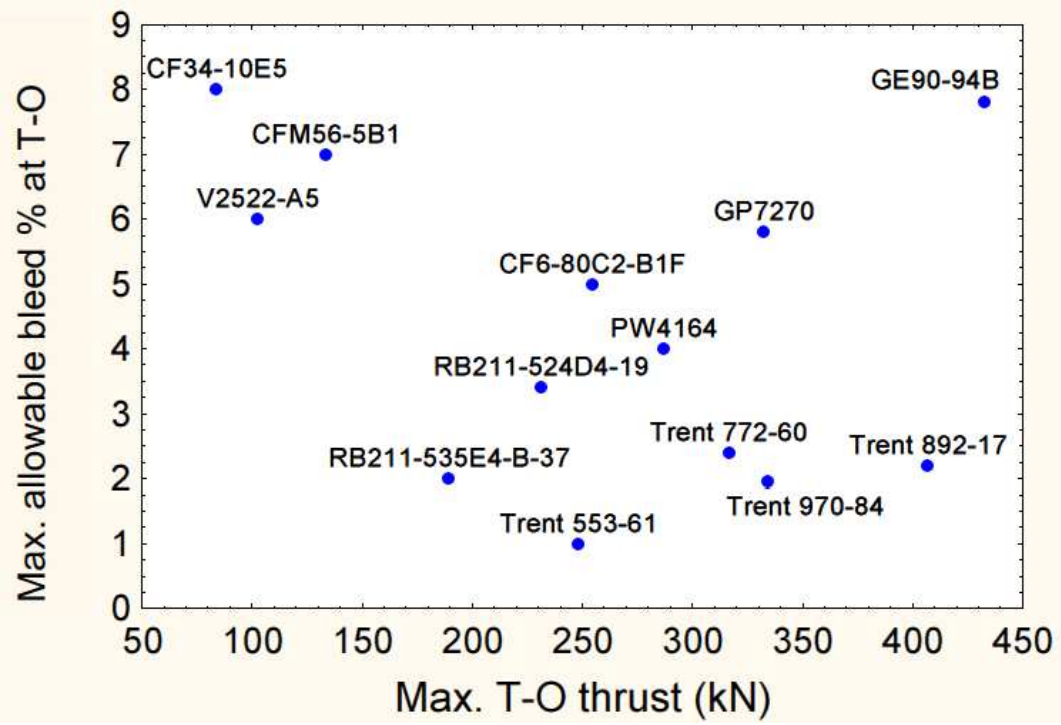

Figure 2-14: Typical aircraft services bleed-air allowances in large commercial turbofan engines

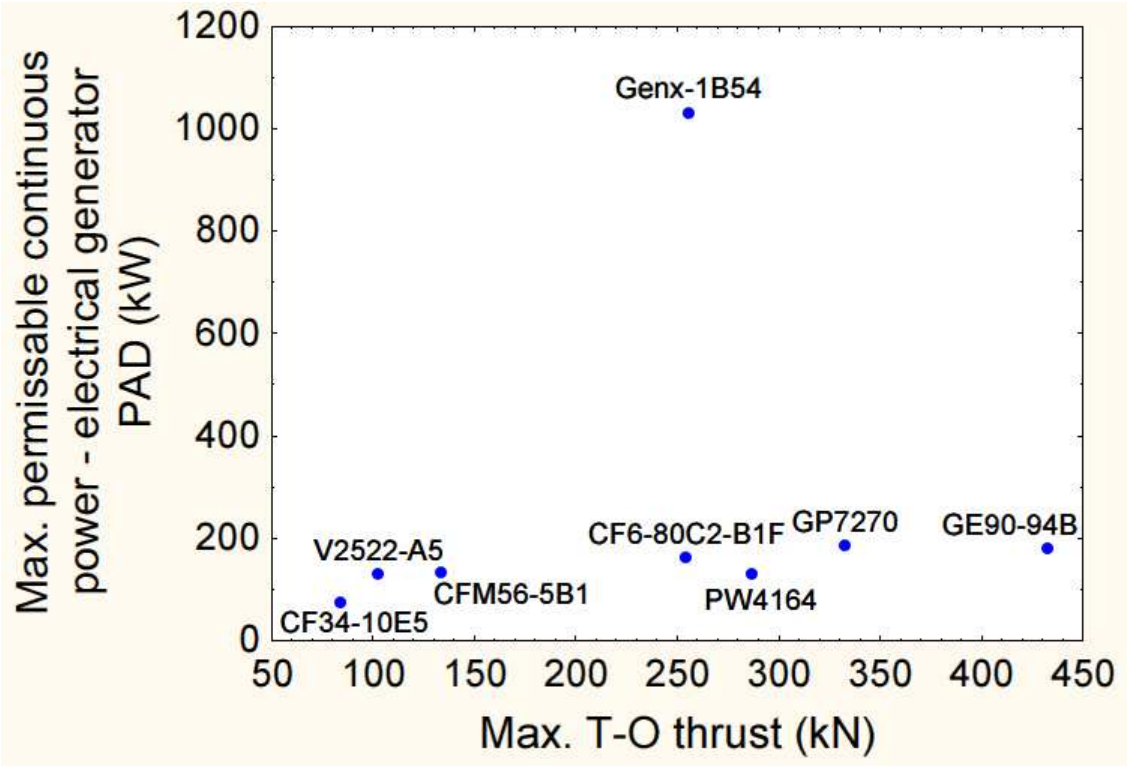

Figure 2-15: Typical electrical generator pad power availability in large commercial turbofan engines

With the MEA concept, studies have shown that the shaft power requirement will further increase due to the increase in the electrical loads. As shown in Figure 2-15, the Boeing 787 and the corresponding GE GEnX-1B54 engine confirms this rise in shaft power demand.

Figure 2-11 shows the estimated loads for a 300 passenger tri-engine aircraft [50]. These are a result of three studies conducted by the NASA Lewis Research Centre to assess the operational, weight and cost advantages for commercial transport aircraft with all-electric secondary power systems.

2.4.1 Approaches for off-take penalty calculations

A method of off-take penalty calculations is presented by the SAE [60];

It states that once bleed-air is extracted from the compressor, a penalty can be calculated in terms of an increase in the fuel flow which is required to maintain a constant thrust. Moreover, as a first approximation the increase can be quantified as;

$$\Delta W_f = 0.0335 \left[\frac{T_{tb}}{2000}\right] w_b \qquad (11)$$

ΔW_f is the increase in the fuel flow

T_{tb} is the turbine inlet temperature in Rankine

w_b is the bleed air flow rate in lb/sec

If a constant shaft power is extracted from the engine during a portion of the aircraft mission, the trip fuel penalty can be calculated by;

$$\frac{W_{f0}}{P(SFC)_p} = \frac{L/D}{(SFC)_{th}}\left[\left(e\ exp\frac{(SFC)_{th}\tau}{L/D}\right) - 1\right] \quad (12)$$

W_{f0} – Trip fuel weight required to carry fixed or variable weight

P – Power being consumed

$(SFC)_P$ – Specific fuel consumption for power

L – Lift

D – Drag

$(SFC)_{th}$ – Specific fuel consumption for thrust

e – Base of the Napierian (natural) logarithm

exp – Exponent

τ – Mission time duration under evaluation

Error! Reference source not found. uses the Breguet range equation to estimate the fuel penalty for the given flight with $(SFC)_P$ which, adds the effect of “fuel penalty due to off-takes” is estimated as a first approximation.

These methods are only useful for a first approximation. Moreover, they do not take into account the changes in the flight conditions such as the altitude and the flight Mach number. Therefore, this simplified approach cannot be used to estimate the penalties for a typical flight envelop, where various operating conditions are experienced by an aircraft.

Another method is found in [7]. This method presents formulations to calculate the efficiency drop in the engine core due to off-takes.

For shaft power off-takes, the drop in engine efficiency is;

$$\frac{\eta_{CO}^{*}}{\eta_{CO}} = 1 - \frac{P_{PO}.\eta_{tr}.\eta_{pr}}{T.V_0} = 1 - \frac{2.P_{PO}.(BPR+1)}{T.\left[BPR/\left(\eta_f\eta_{lpt}\right)+1\right].(2V_0+ST)} \quad (13)$$

η_{CO}, η_{CO}^{*} - Engine core efficiency before and after the extraction off-takes

P_{P0} – shaft power off-take extracted

η_{tr} – Engine transmission efficiency

η_{pr} – Engine propulsive efficiency

T – Engine net thrust

V_0 – Aircraft flight velocity

BPR – Engine by-pass ratio

η_f – Fan isentropic efficiency

η_{lpt} – Low pressure turbine isentropic efficiency

ST – Engine specific thrust

For bleed-air off-takes, the drop in engine efficiency is expressed as;

$$\frac{\eta_{CO}^{*}}{\eta_{CO}} = 1 - \frac{2.W_b\Delta h_b.(BPR+1)}{(1-\beta).T.\left[BPR/\left(\eta_f\eta_{lpt}\right)+1\right].(2V_0+ST)} \quad (14)$$

$$\beta = \frac{W_b.ST.(BPR+1)}{T} \quad (15)$$

W_b – Bleed-air mass flow

Δh_b – Bleed-air enthalpy increase through the core

β – Ratio of bleed-air mass flow upon core mass flow

The drop in the engine efficiency can then be used to calculate the SFC penalty [7]. The baseline SFC will still have to be estimated by using an engine performance code or published numerical methods.

This method looks at the off-takes from an engine design perspective. Moreover, since the method relies on having good estimates for the efficiency values of engine specific components, it is difficult to adapt it to an aircraft performance study where the engine will undergo various operating scenarios. Also, the above mentioned values could be subject to significant change. Hence a more straightforward method which could be adapted to performance studies, where variables can be easily estimated, is required.

2.5 Trajectory optimisation

Betts [61] provides a comprehensive insight into the methods that can be applied to aircraft trajectory optimisation. It discusses elements such as non-linear programming, optimal control and numerical analysis which are required to specify methods to solve trajectory optimisation problems. It also provides dynamics programming and genetic algorithms as alternatives to the more popular and computationally efficient optimal control approach. It mentions that the attractiveness in genetic algorithms lie in the fact that they are incredibly simple to apply without detailed understanding of the system being optimised. Nevertheless they are not computationally competitive compared to optimal control techniques.

The approach for this study has been to use genetic algorithms as optimisers. It is accepted that optimal control theory is the common approach in solving trajectory optimisation problems. But optimal control theory requires parameterisation for controls and states of the problem and typically uses gradient based techniques to find the solution. Gradient based optimisers are local minimum optimisation techniques.

The vision within the Clean Sky SGO mission trajectory management was that many aspects such as real/forecasted weather, airframe systems penalties, operational business models and engine degradation could be included within the trajectory optimisation loop to closely represent real aircraft behaviour. Certain aspects of these representations, especially the weather which is not limited to the wind but also influences icing and contrails, cannot be easily parameterised without losing significant accuracy. Moreover, model development was done by

a number of different institutions, which makes parameterising all aspects un-realistic due to resource constraints and proprietary rights.

To overcome these issues, genetic algorithms, which does not need heavy parameterisation techniques as with optimal control theory, were preferred within the research which finds globally optimal solutions.

However, this is a compromise, since the uses of GA's are expected to present challenges such;

- Computationally inefficient in comparison to gradient based optimisers
- In-efficiencies in handling a large number of input variables
- Producing results closer to the optimal solution rather than the local optima.

Within this research, the genetic algorithm was used as a black box. The parameters of interest were the number of generations and number of population that was required to find feasible solutions for the optimisation problem. Typically within the algorithm evolution usually starts from a population of randomly generated solutions, and is an iterative process, with the population in each iteration being referred to as a generation.

The necessity of systems consideration in trajectory optimisation, the model setup, frame work and test cases are explained in detail in the following chapters.

2.6 GATAC framework within Clean Sky

Greener Aircraft Trajectories under ATM Constraints (GATAC) is a multi-objective optimisation framework for planning, generating and optimising environmentally friendly trajectories. The software was co-developed by the University of Malta and Cranfield University for the SGO ITD under Clean Sky.

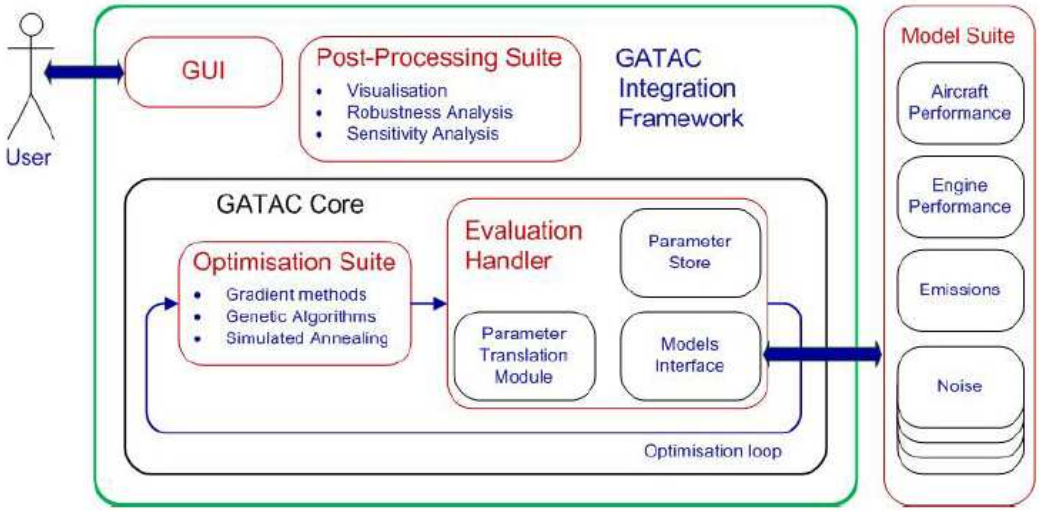

Figure 2-16: GATAC Integration Framework Architecture [62]

The overall optimisation block diagram of a generic problem using GATAC is shown in Figure 2-16. Further reading on GATAC can be found in [63].

The framework included three optimisers which were conceptualised as per the requirements of the overall SGO work.

- Non-dominated Sorting Genetic Algorithm Multi-Objective (NSGAMO)
- Multi-Objective Tabu Search (MOTS)
- Hybrid Optimiser (HYOP)

The NSGAMO, which has been used in this study, is capable of performing multi-objective optimisation under constraints and is based on Genetic Algorithm (GA) optimisation techniques. Further reading of the development and performance of the NSGAMO can be found at [64]. The MOTS optimiser is described in [65].

3 Methodology

The methodology for the study was initiated by performing a critical literature review. Afterwards the following topics were identified as enablers to achieve the objectives and the aim of the research.

- Establishing the significance of the penalties caused by the airframe systems on aircraft operation, thus establishing the basis on the need to represent airframe systems within the trajectory optimisation scope
- Developing an electrical load sizing tool to determine electrical loads and the consequent power off-takes for conventional and more electric secondary power systems
- Developing robust and computationally efficient equations to calculate the fuel penalties due to power off-takes, thereby interfacing airframe systems performance and engine performance
- Creating an integrated model for both conventional and more electric aircraft which include, engine performance, airframe systems performance, off-take penalty representation and emissions modelling.
- Result orientated analysis and comparison of conventional and more-electric aircraft trajectory optimisation.

4 Environmental Impact Assessment, on the Operation of Conventional and More Electric Large Commercial Aircraft

In order to conduct such a study, it was essential to establish key definitions and limitations. In particular, for the purpose of this study, only technology advances in the airframe systems are considered. Hence a conventional aircraft is defined as an aircraft which uses pneumatic, hydraulic and electrical systems comparable to most operational aircraft today.

The More Electric Aircraft (MEA) is defined as an aircraft with all major airframe systems powered electrically.

A key limitation of the study is that it does not take into account more electric or all electric aircraft engines and it is based on current high by-pass commercial turbofan engine performance.

The objective was to study the difference of conventional and more electric aircraft system power usage for a given flight trajectory.

4.1 Case studies

The baseline aircraft considered in the case studies was a twin engine short range aircraft with a maximum passenger capability of 180. The baseline engine was a twin spool turbofan engine capable of producing a maximum static take-off thrust of 121 kN at ISA+30 ^{0}C.

For the preliminary performance analysis, two test trajectories were studied [66]:

- Amsterdam Airport Schiphol – Franz Josef Strauss International Airport Munich
- London Heathrow International Airport – Amsterdam Airport Schiphol

All test cases included constraints to represent air traffic management, aircraft performance and engine performance limitations [66]. These were generated in a separate trajectory optimisation study. For this research, they were used as pre-defined flight trajectories. The merits of the trajectories, the feasibility and the accuracy is discussed in [66].

The trajectories are shown below in Figure 4-1 to Figure 4-4 for the Amsterdam to Munich and London to Amsterdam cases.

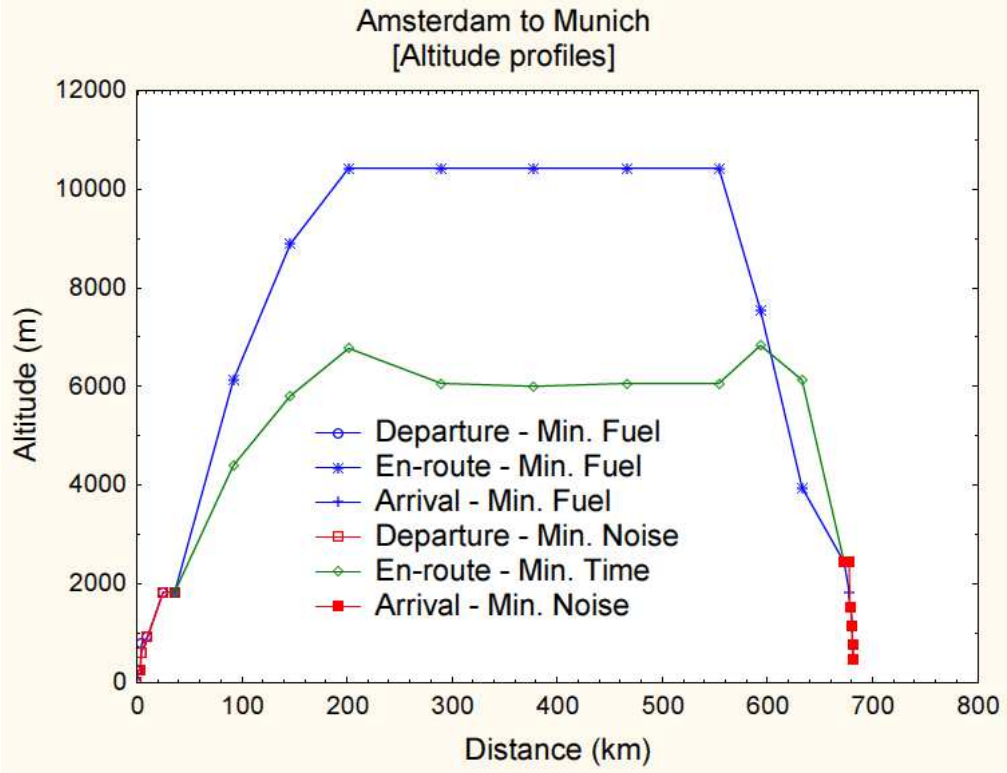

Figure 4-1: Amsterdam to Munich – altitude profile [66]

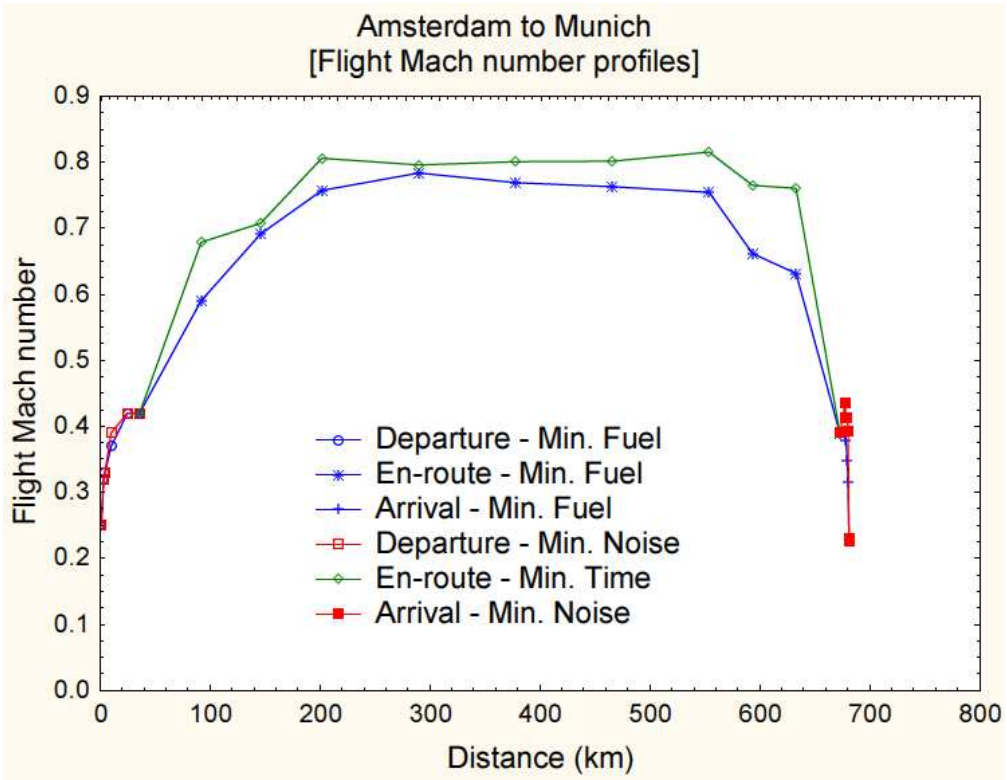

Figure 4-2: Amsterdam to Munich – flight Mach number profile [66]

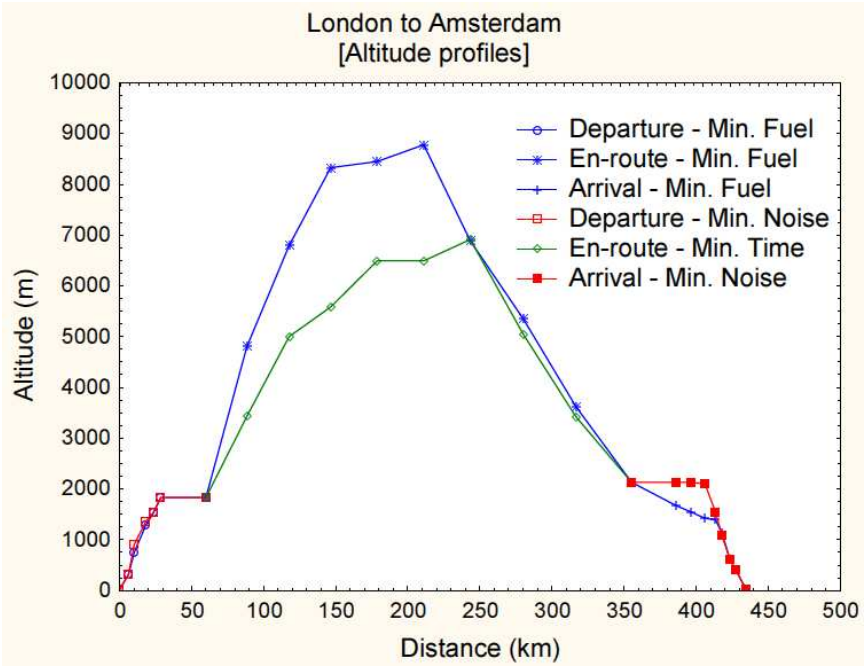

Figure 4-3: London to Amsterdam – altitude profiles [66]

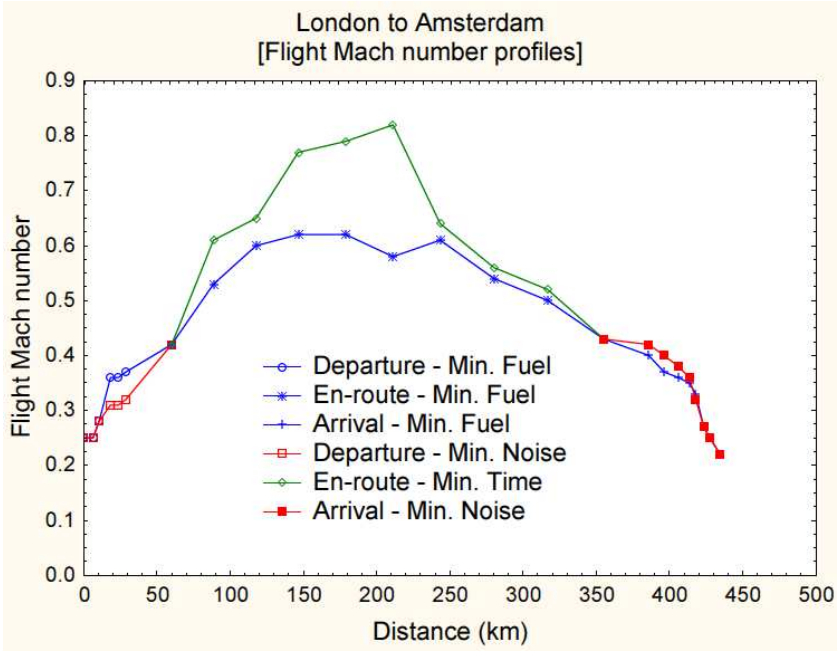

Figure 4-4: London to Amsterdam – flight Mach number profile [66]

4.2 Aircraft systems model

4.2.1 Conventional aircraft systems model

The conventional aircraft model consisted of a pneumatic ECS, pneumatic IPS, hydraulically actuated control surfaces and the conventional electrics.

The specification and the description for the aircraft systems model are documented in [67] and [68].

The pneumatic ECS model was validated as per data in [68], the IPS model was verified as per [69] and the electrical model was validated at a systems level by using [70] and at an aircraft level using [27] and [21]. The models used in this section were the basis for further developed models described in §6 and §7.

4.2.2 MEA systems model

The MEA systems model consisted of an electric ECS, electrical IPS, electrical actuators for flight controls and the conventional electrical loads.

The electrical ECS was modelled to have comparable performance as the pneumatic ECS. However, an electrical compressor was used to draw in ram air rather than extracting bleed air from the engine. The electrical ECS was validated by using data in [71] and the conventional electrical load was calculated by the electrical model mentioned above.

The electrical IPS was modelled to represent an electro-thermal system which used heating element on the anti-icing surfaces. The electrical actuators were based in known parametes of electro-mechanical actuators. The loads for the electrical IPS and the electrical actuators were estimated as per [9].

This study used the trajectory data shown previously, to assess the impact on the aircraft systems operation.

4.3 Results

4.3.1 Conventional aircraft

By using the results obtained from the trajectory optimisation study, the conventional aircraft systems model was simulated and the results were analyzed. The electrical generator was simplified by using a constant efficiency of 85%.

The results obtained for the London to Amsterdam case are shown in Figure 4-5 to Figure 4-8.

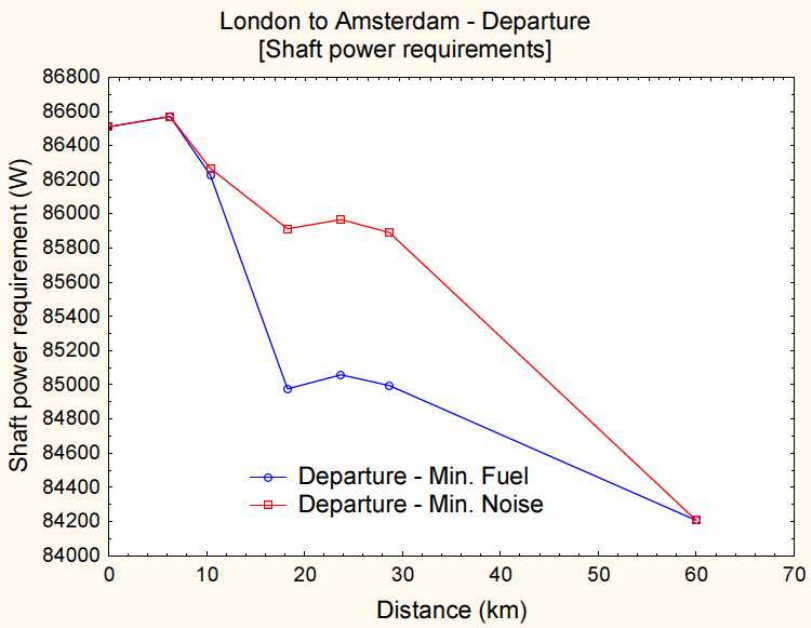

Figure 4-5: London to Amsterdam – departure – shaft power variation

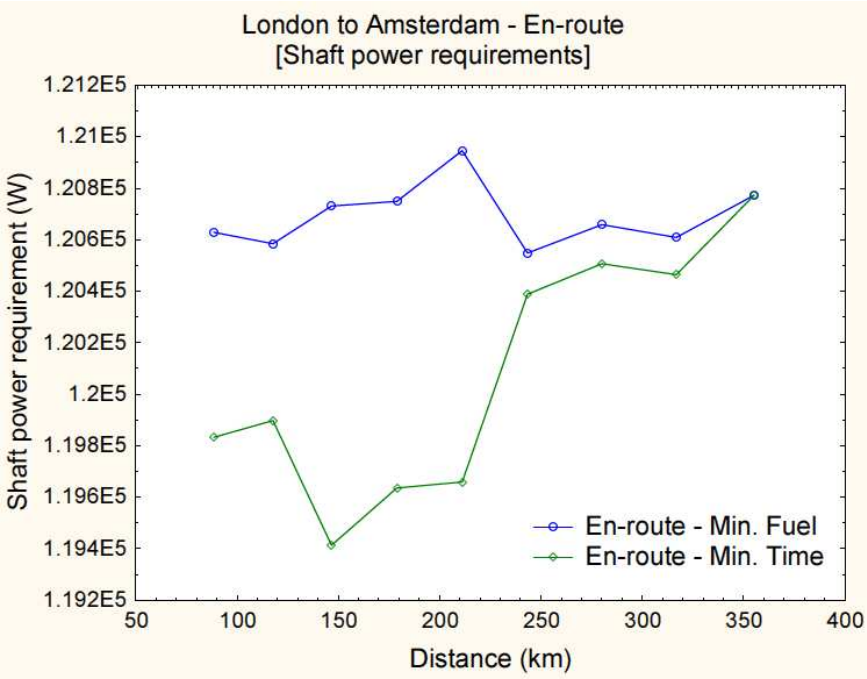

Figure 4-6: London to Amsterdam – en-route – shaft power variation

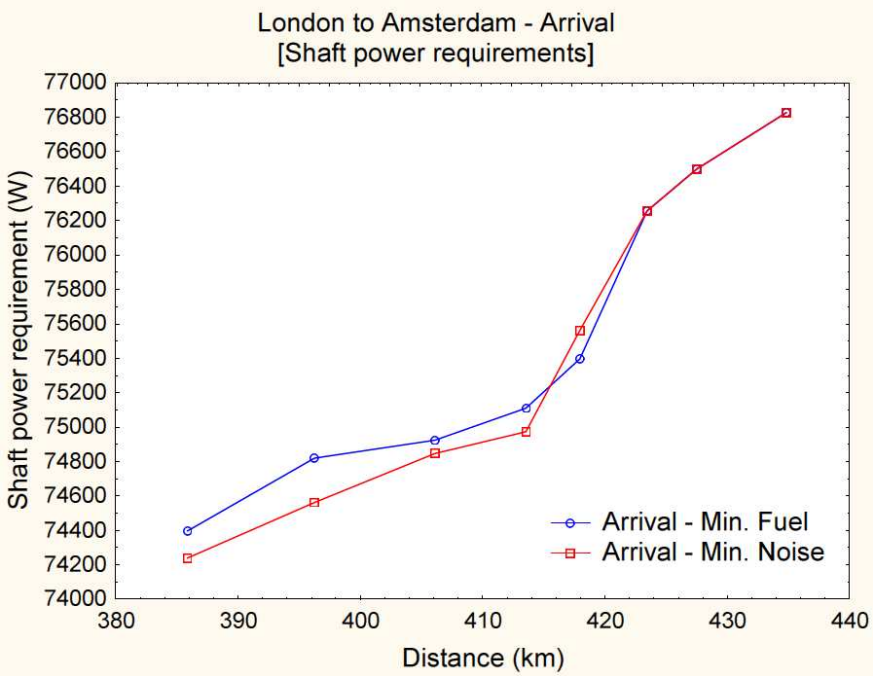

Figure 4-7: London to Amsterdam – arrival – shaft power variation

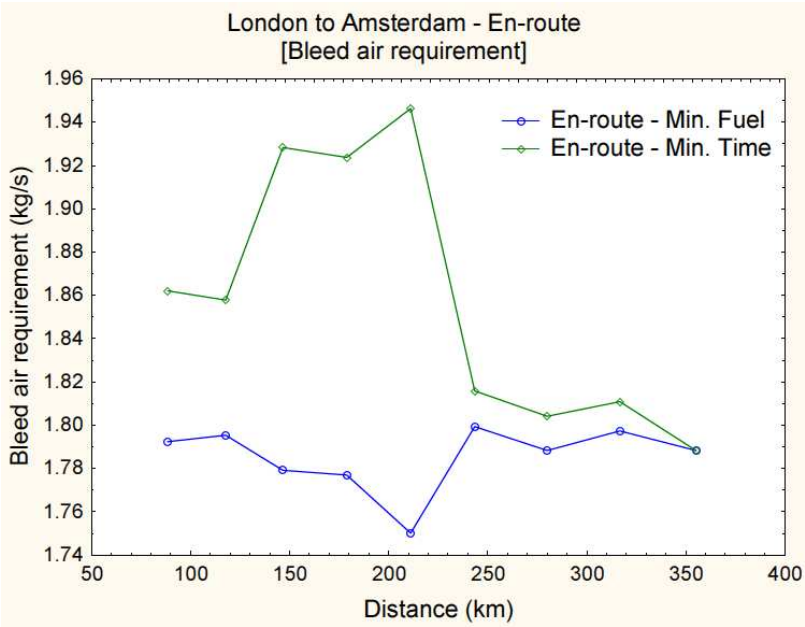

Figure 4-8: London to Amsterdam – en-route – bleed air requirement

It was observed, that the shaft power requirements and bleed air requirements vary depending on flight conditions. But the magnitude of the variation was small. Therefore, it was concluded that the change in fuel penalty due to off-takes would not significantly affect the gains between the various optimisation objectives. Moreover even though Figure 4-8 shows that the bleed air requirement is sensitive to the flight conditions, in real aircraft engine operation the bleed rates are usually fixed for different flight phases.

Similar effects can be observed for the Amsterdam to Munich case in Figure 4-9 and Figure 4-10.

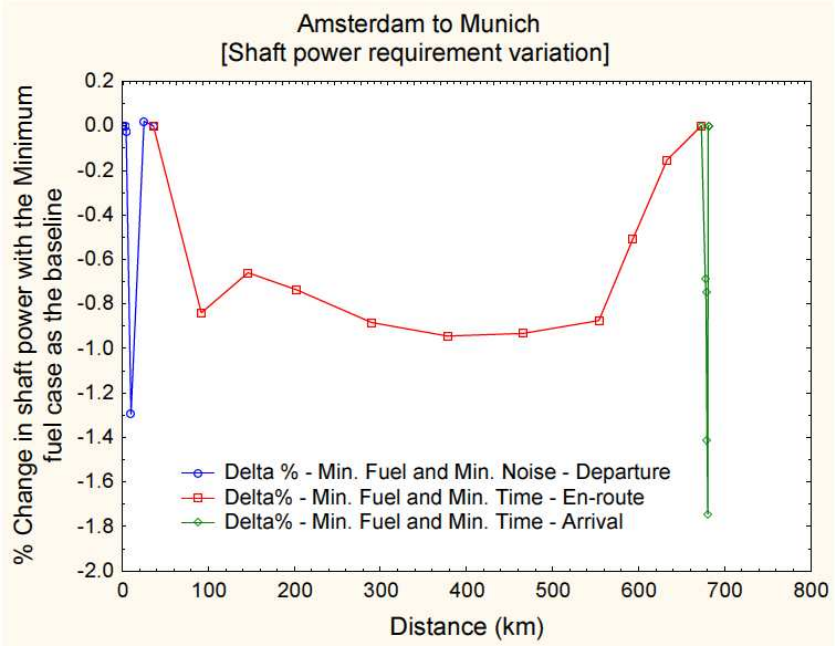

Figure 4-9: % Change in the shaft power requirement with the minimum fuel trajectory as a baseline

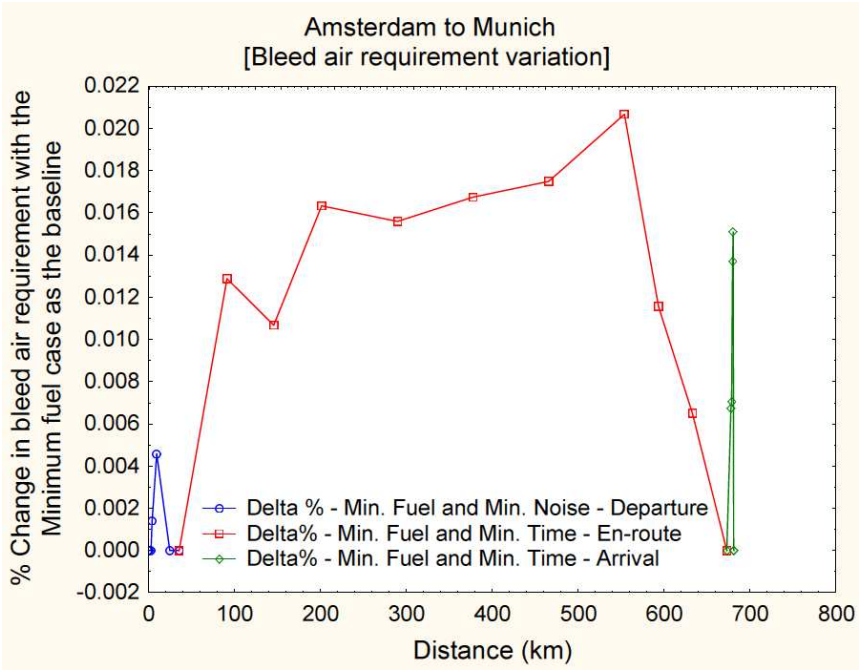

Figure 4-10: % Change in the bleed air requirement with the minimum fuel trajectory as a baseline

Both cases showed similar trends for both shaft power and bleed air requirements. It was interesting to note from Figure 4-5, that for the London to Amsterdam case the minimum noise case has the higher demand at departure. But from Figure 4-9 (Amsterdam to Munich case), the minimum fuel trajectory has a greater demand in shaft power. This disparity clearly shows that the influence of the trajectory on the systems is quite complex and a multi-disciplinary study such as this is needed to understand the complexities.

Yet on the other hand, all results for the conventional aircraft systems showed that the magnitude of the change in shaft power or bleed air requirements respective to each trajectory are small. Therefore, it can be concluded that the conventional aircraft systems off-takes would not affect the trajectory optimisation significantly.

4.3.2 MEA

A more interesting scenario was the MEA which, due to the peculiarities of the technical approach adopted, showed an entirely different perspective of aircraft systems impacts on optimal flight trajectories.

The following assumptions were adopted in order to simulate the MEA systems:

- Any flight point within the threshold of 4572 m and 6706 m is likely to have severe icing conditions and the IPS will be fully operational.
- By using the 80/20 rule it was estimated that the average power for flight control actuation would be 36% of the peak power [72].

The results of the MEA analysis for the London to Amsterdam case are shown in Figure 4-11 to Figure 4-14.

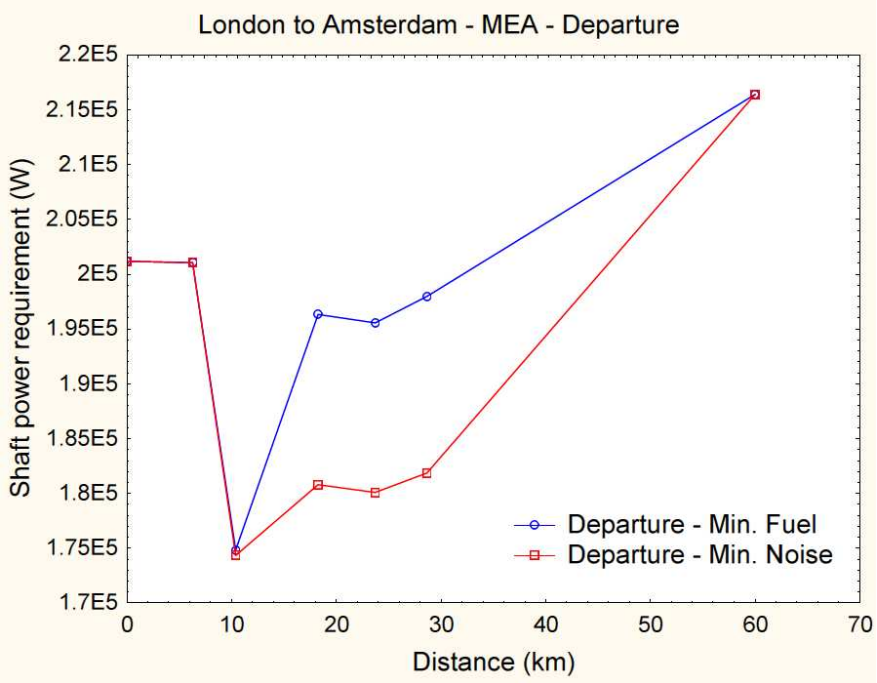

Figure 4-11: Shaft power requirement for London to Amsterdam – MEA – Departure

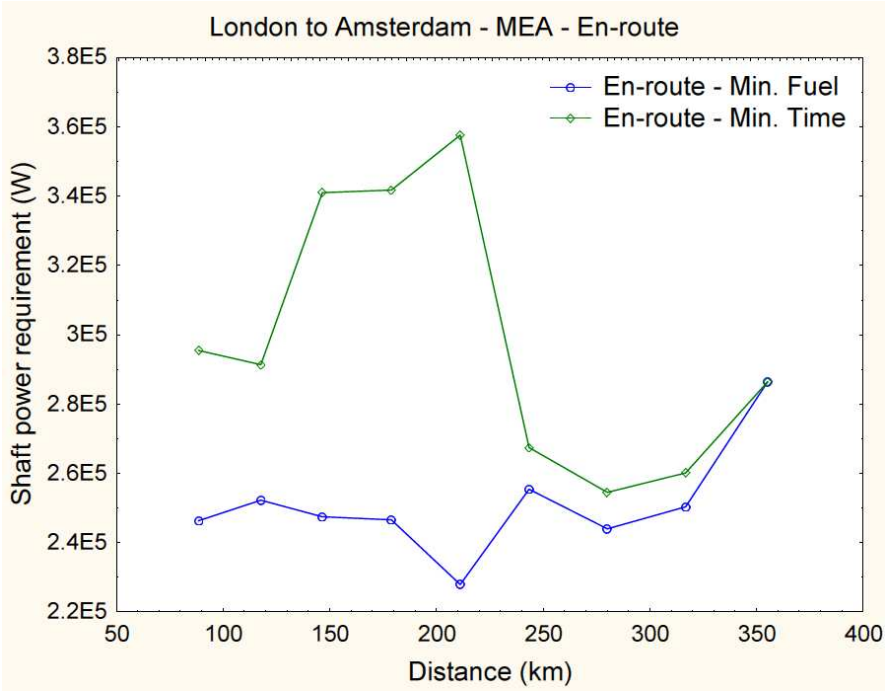

Figure 4-12: Shaft power requirement for London to Amsterdam – MEA – En-route

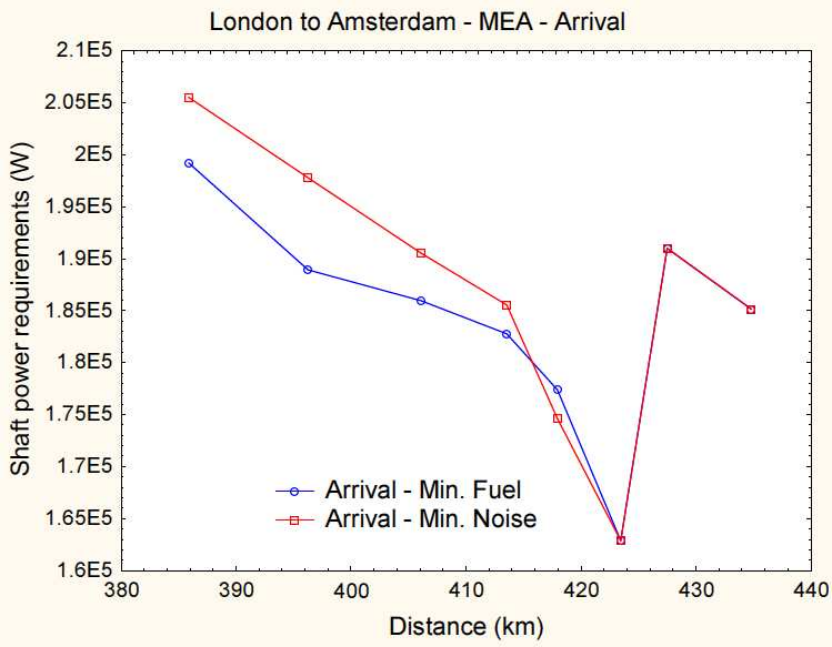

Figure 4-13: Shaft power requirement for London to Amsterdam – MEA – Arrival

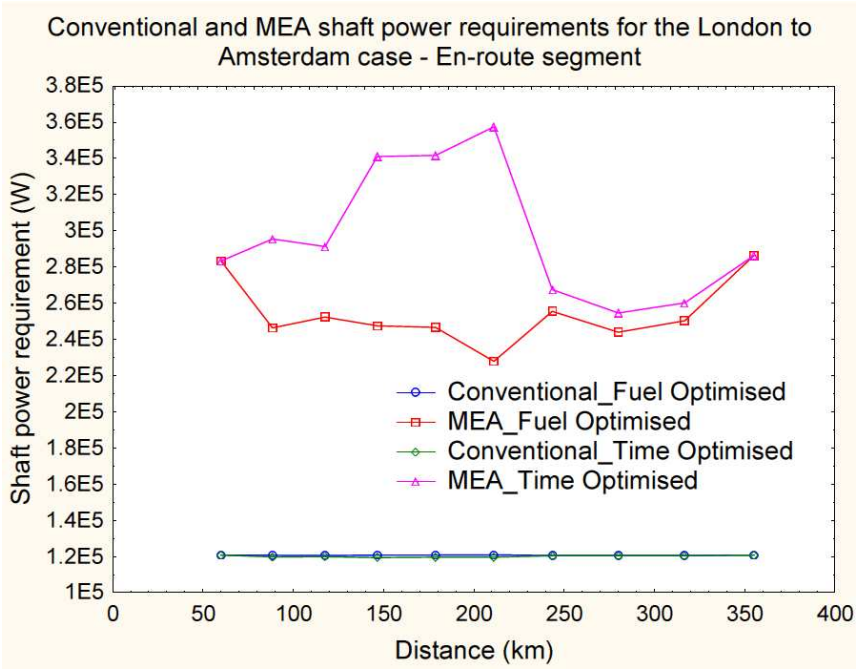

Figure 4-14: Increase in the shaft power requirement compared to the conventional aircraft for the London to Amsterdam case

As expected, there was a significant increase in the electrical load. The major contributors were the electrical ECS and the IPS. Moreover it was also observed that during the en-route segment, where the aircraft operates for a majority of the time, the differences in the effects of the applied optimisation criteria were significant.

From Figure 4-14 it is observed that the MEA showed an average increase of 110% over the conventional aircraft for the en-route segment when the trajectory was optimised for fuel burn (i.e., minimum fuel consumption). When the trajectory was optimised for time (i.e., minimum flight time), the increase was about 148%. Moreover, the difference in the shaft power requirement, between the fuel and time optimised trajectories was about 18%, whereas in the conventional aircraft, the shaft power requirements changed only by about 0.4% between the fuel and time optimised en-route segments. However, it should be noted that these figures only represent the shaft power requirements and that the total secondary power requirements for the conventional aircraft must include the primary pneumatic loads as well. For this particular aircraft, during the en-route segment, the pneumatic ECS power consumption was estimated in the order of 330 kW to 360 kW.

There are some key characteristics that were observed:

- The total secondary power requirement for the conventional aircraft was higher than the MEA.
- The MEA shaft power requirement was much greater than the conventional shaft power requirement.
- The total power requirements did not vary greatly with respect to the trajectory, in the conventional aircraft.
- The total power requirement, even though less than the conventional aircraft (yet still significant), varied significantly with respect to the trajectory, in the MEA.

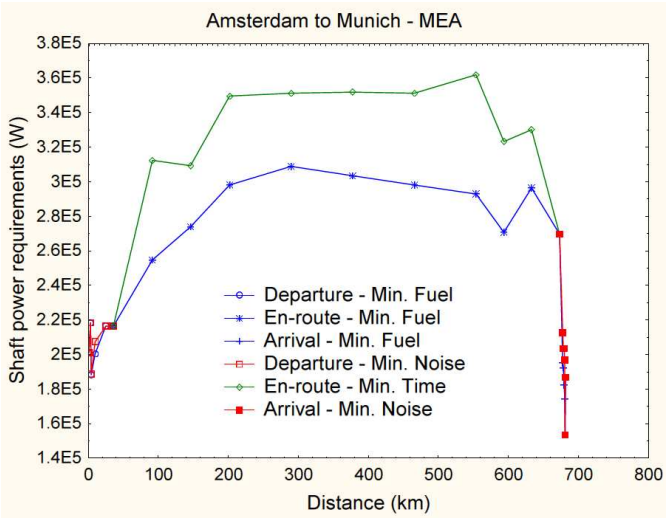

Figure 4-15: Shaft power requirement for Amsterdam to Munich - MEA

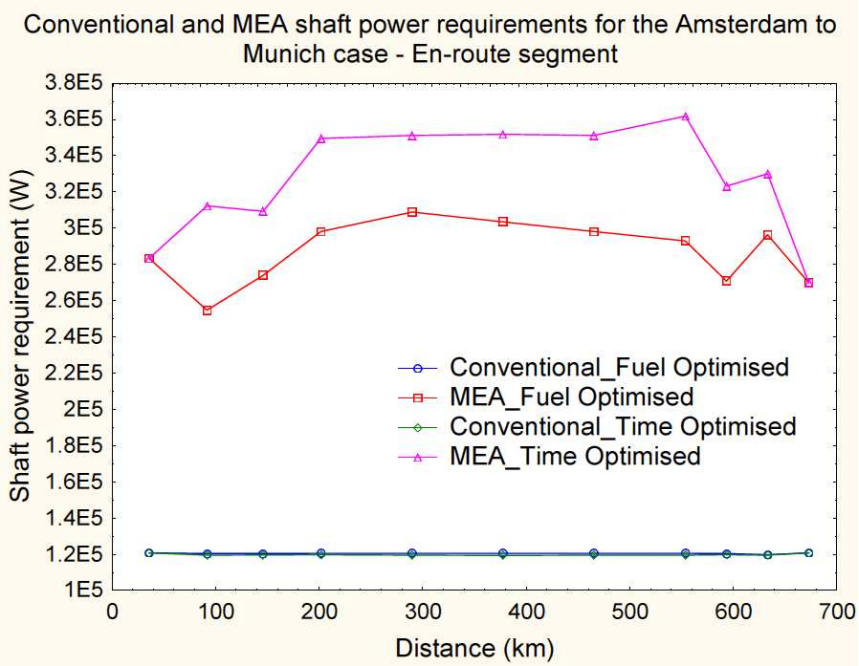

Figure 4-16: Increase in the shaft power requirement compared to the conventional aircraft for the Amsterdam to Munich case

For the Amsterdam to Munich case, it was observed that the average increase in the shaft power requirement during the en-route segment for the fuel optimised trajectory compared to the conventional aircraft was 138%, while in the time optimised trajectory there was an average increase of 173%. Moreover, in the MEA configuration the change in the shaft power requirement between the fuel optimised and time optimised trajectories was about 14% while in the conventional configuration it was only 0.6%.

As in the London to Amsterdam case, the primary pneumatic loads were estimated and were between 330 kW to 360kW. Similar characteristics were observed for this case as well.

An en-route flight trajectory currently flown by many aircraft, between Heathrow and Schiphol was also considered, in order to benchmark the increases in the shaft power requirement due to trajectory. The trajectory profiles are listed in [66].

The results of this additional case study are shown in Figure 4-17.

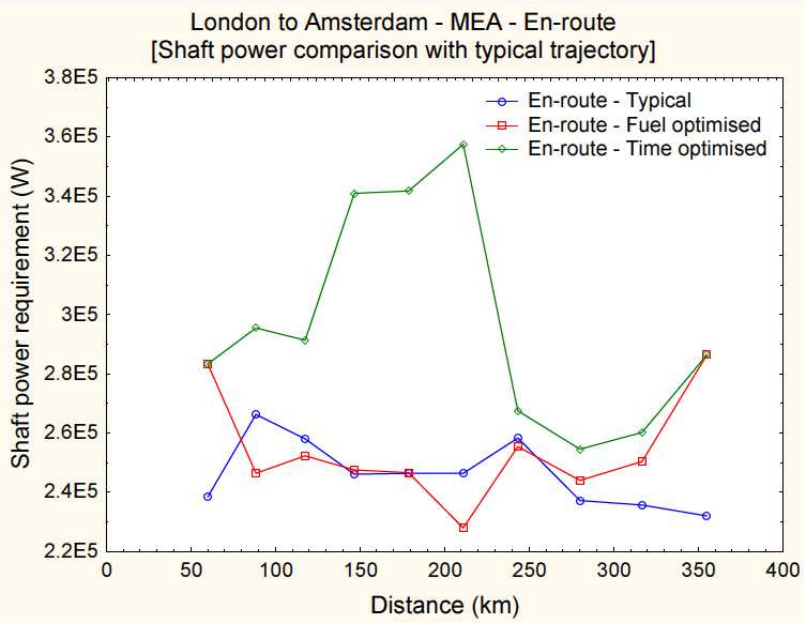

Figure 4-17: Comparison of MEA power requirement for typical, fuel optimised and time optimised trajectories for the London to Amsterdam en-route segment

It was observed that the fuel optimised and time optimised trajectories had different shaft power requirements in comparison to a typical trajectory. The magnitude of the change was significant, more so for the flight time is optimised. Moreover it is expected that by accounting for the power off-take penalty due to systems, a better comparison of the trajectories can be made and thus a better assessment of the environmental impact due to aircraft operation.

4.4 Summary

This section presented an initial study on the effects of aircraft systems on trajectory optimisation processes and vice-versa. In addition to conventional systems, it presented the MEA as a case where the systems have significantly higher power off-take demands of varying magnitudes during the different flight phases. The significant change in the fuel burn has an important effect on MEA trajectory optimisation studies. The main conclusion is that the optimality of the computed aircraft trajectories can be significantly improved by representing the aircraft systems requirements within the optimisation loop, particularly for MEA applications.

5 Electrical load sizing methodology to aid conceptual and preliminary design of large commercial aircraft

With the increasing electrical load in future aircraft, more demand is naturally placed on analysing and preparing for design challenges, in the preliminary design stages of the electrical network. This was one of the main observations of the critical review conducted (see §2.2).

Moreover, by analysing the results in Figure 2-9 it is clear that in choosing the generator ratings other factors such as development costs and availability of off-the-shelf products have played their parts.

The deviation seen in Figure 2-9 for the Boeing 787-8 and the evidence in Figure 2-10 and Figure 2-11 indicates that with the development of more electric technologies, the electrical load requirements of aircraft vary widely even within the same size range. One of the reasons for this variation is due to the choice of design for the sub-systems. The electric loads will be dependent on which sub-systems are migrated from pneumatic, hydraulic or mechanical power usage to electrical power usage. Moreover, the level of technology of the components of each electric sub-system will also affect the electrical loading requirements of the aircraft. Hence using off-the-shelf generators will be an extremely inefficient option which will significantly impact the aircraft and systems performance with the possible risk of oversizing of the generators and distribution network.

This presents the case for designing electrical generators according to the specificities of an aircraft. In order to achieve this efficiently the design process needs to be addressed as early as possible in the aircraft design stage.

This is further endorsed by Feiner [9] who says that the “power capacity must be estimated early in the aircraft’s design cycle in order to support engine development”. Hence to achieve this efficiency, a robust and adaptive electrical load sizing and analysis tool is needed, which can incorporate uncertainties such as future component loads and also adapt to changes in the design requirements through the aircraft development cycle.

Moreover, it also facilitates the initial steps in relating aircraft level objectives to system level choices, the importance of which is extensively discussed in [73]. Also with novel concepts in operation and optimisation of aircraft operation, the effects of systems need to be considered with great care [74]. To facilitate this, methodologies need to be in place at the early design

stage to calculate the power requirements of the airframe systems to a reasonable level of accuracy and detail.

In summary, the following methodology for electrical load sizing tries to overcome the limitations of empirical methodologies currently used at the preliminary design stage. This is achieved by using a generic baseline electrical load architecture which, can be adapted and modified to any aircraft, conventional or more electric. The method bridges the gap between a predicted generator load based on conceptual sizing methods, and the precise electrical load analysis which can be done at the detail design stage.

5.1 Methodology – electrical load sizing & analysis tool

Esdras and Liscouet-Hanke [75] presents a methodology developed at Bombardier which relies on predicting the electrical loads at a systems level by studying the trends in the power consumption of past and present aircraft. Since the more electric concept is relatively new, a more robust methodology where the component loads are considered needs to be adapted. This enables the methodology to then be adapted to a more electric design, simply by adding characteristics of electrical components, needed to design more electrical airframe systems architectures.

The following illustration shows the architecture on which the developed model is based on.

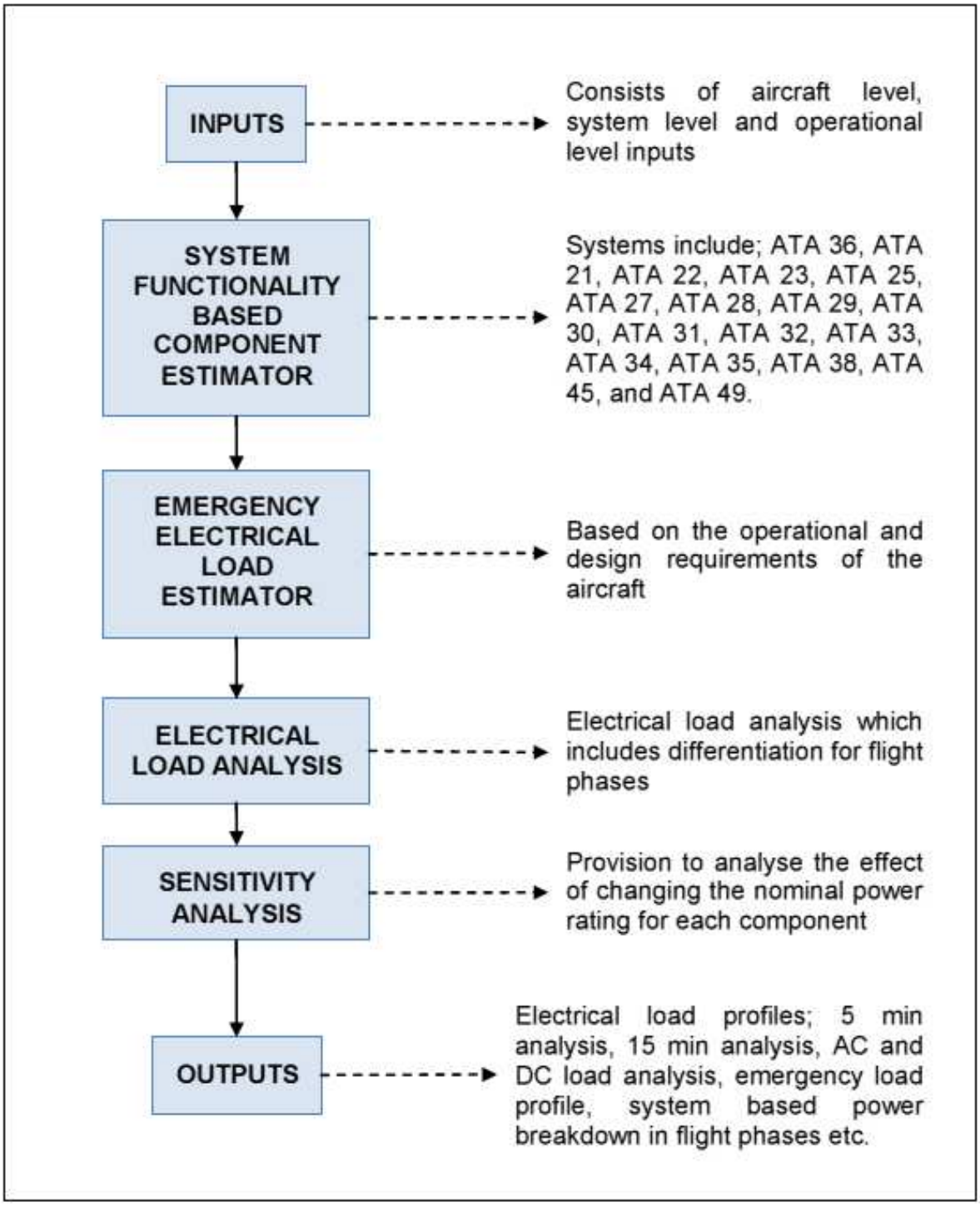

Figure 5-1: Architecture of electrical load analysis tool

The development of this tool was carried out with the intention of aiding the preliminary design process of an aircraft. The tool is designed such that it can be adapted to a conventional configuration or an all-electric configuration. The baseline configuration is the conventional system. To achieve the all-electric configuration, all systems components which are powered

non-electrically can be easily replaced by electrically powered equivalent equipment within the tool itself. The model has been implemented by using Microsoft Excel and the Visual Basic programming language.

The inputs for the model are classified under three categories. Firstly, there are the aircraft level inputs. These inputs are used to size the basic configuration of the each system. Furthermore, it has system level inputs which relate to various system functionalities and operational level inputs. These inputs are used to allocate the minimum equipment lists to each of the sub-systems. The operational level inputs are restricted to only include provision for simultaneous operation of the same equipment. The operational inputs cannot be used to simulate a potential flight where certain components may be switched on or off at random, since the purpose of this tool is to aid the design process in which the highest loading scenarios are analysed. The list of inputs is shown in Appendix 1.

The system based component estimator receives information from the inputs and estimates the minimum number of components needed to achieve the required level of system functionality. Characteristics of functionality related to each different system are used as constraints in the component estimator. This ensures that regardless of the aircraft level inputs, the minimum required system functionality is achieved each time in each system.

The main task of the emergency load estimator is to define which electrical equipment in each system is essential to the aircraft. “Essential” in this context is defined as the minimum equipment list needed to maintain safe flight. By having pre-defined functions that are essential to safe flight, the emergency load estimator assigns a tag to each component; assigning it as essential or non-essential defining that particular electrical component to be flight critical or not. The logic for the emergency load estimator was derived by studying the electrical bus equipment lists and the essential bus equipment for the Airbus A320 and the Airbus A430 series. It also calculates the loads on the essential buses of the aircraft and is herewith referred to as the emergency load. The logic is limited to the conventional architecture. Hence for more electric aircraft studies, each new component needs to be defined either essential or non-essential according to the design requirements of the aircraft.

The electrical load analysis is the core module of the tool. This extracts all the information from the component estimator and the emergency load estimator and lists all equipment and related

data. It then couples the data with the “operational matrix”, which enables it to calculate the electrical load profile.

The operational matrix contains vital information needed to perform the electrical load analysis.

Table 5-1: Format of component related information for electrical load analysis (ELA)

ID	T_{opr}	V_{opr}	N_{opr}	GR	T-O	CL	CR	DE	LO	LA	L_p
A1	c	115VAC	1	0	0	1	1	1	0	0	n

ID – Component ID (Includes component name, number of components, nominal power usage)

T_{opr} – Defines the operation time (Continuous or Intermittent)

Intermittent loads are defined as loads occurring for duration of 5 minutes or less whereas continuous loads will operate for duration of 15 minutes or more.

V_{opr} – Nominal operational voltage

N_{opr} – Number of components operating simultaneously

GR – “Ground” phase

T-O – “Take-Off” phase

CL – “Climb” phase

CR – “Cruise” phase

DE – “Descent” phase

LO – “Loiter” phase

LA – “Landing” phase

L_p – Defines the priority of the load (On an essential, shed or normal bus)

Since the intention of the sizing tool is to size the electrical system with design constraints (design for worst case scenario), the duration of the flight phase is not taken into consideration

here. It is simply a case of where a load qualifies or has the possibility as being classed operational in each flight phase. A separate model is to be developed to analyse the load in flight operation which incorporates constraints related to time such as instances or operation and duration of operation and well as constraints related to power usage (% of the nominal power usage for equipment with variable power consumption).

For example for an AC load to be registered as a continuous load in “cruise” phase on a 115 VAC normal bus;

$$P_{NCR} = ID[ID_N = \text{“name”}, (ID_{NO} \geq 1) \cap (ID_P > 0)] \cap (T_{opr} = \text{“c”}) \cap (V_{opr} = \text{“115 VAC”}) \cap (N_{opr} \geq 1) \cap (CR = 1) \cap (L_p = \text{“n”}) \quad (16)$$

Where;

P_{NCR} is the condition for active power for a named component under the “cruise” flight segment to be registered

ID_N is the unique name assigned to the component

ID_{NO} is the number of components of the same name

ID_P is the accumulated nominal power of components of the same name

$$ID_N = f\,(AL_{in},\ SL_{in}) \quad (17)$$

Where;

AL_{in} are the aircraft level inputs

SL_{in} are the system level inputs

A relation for each component needs to be constructed by looking at what affects the quantity of components at system and aircraft level.

For example, the quantity of Very High Frequency (VHF) radios needed for communication is directly related to the number of pilots so,

$$ID_{VHF} = f\,(AL_{in\_pilots}) \quad (18)$$

For the estimation of the number of cabin lamps required to maintain the required luminosity of the cabin the cabin volume and the type of lighting also affect the result. Thus a combination of aircraft level and system level inputs affects the result.

$$ID_{Cabin\_Lamps} = f\,(AL_{in\_cabin\ volume},\ SL_{in\_Lighting\ type}) \tag{19}$$

The load priority is based on the system architectures of typical regional, short range and long range aircraft. The loads are categorised as essential or non-essential. Essential loads shall operate without disruption in the case of an emergency, thus are given a much higher priority over the other loads. These would typically operate under “essential” buses. All other loads are classed as “non-essential” and are not critical to maintain safe flight. Allocations are also made for loads that can be shedded.

The ID_P is derived from a database within the tool. The database contains equipment data such as the nominal power usage and the mass, of electrical components used in aircraft.

The tool estimates the loads on a conventional electrical system. It is also imperative that the more electric aircraft, which was the motivation of the study, be analysed as well.

This tool can be combined with an electrical ECS, electro thermal IPS, Electro-Hydro static Actuators (EHA) or Electro-Mechanical Actuators (EMA) and any other more electric subsystems to analyse the electrical loading of an MEA.

The results of the tool are presented as a set of graphs and data values for ease of use. The tool gives overall loading values per flight segment, categorised by the voltage Bus type (AC, DC, AC SHED, DC SHED, AC ESS or DC ESS), by system designation (ATA chapter number), priority level (essential or non-essential) and operational time (continuous or intermittent).

5.2 Validation

Due to the lack of data, the generated electrical load profiles cannot be validated by direct comparison. Hence a separate validation strategy has been developed.

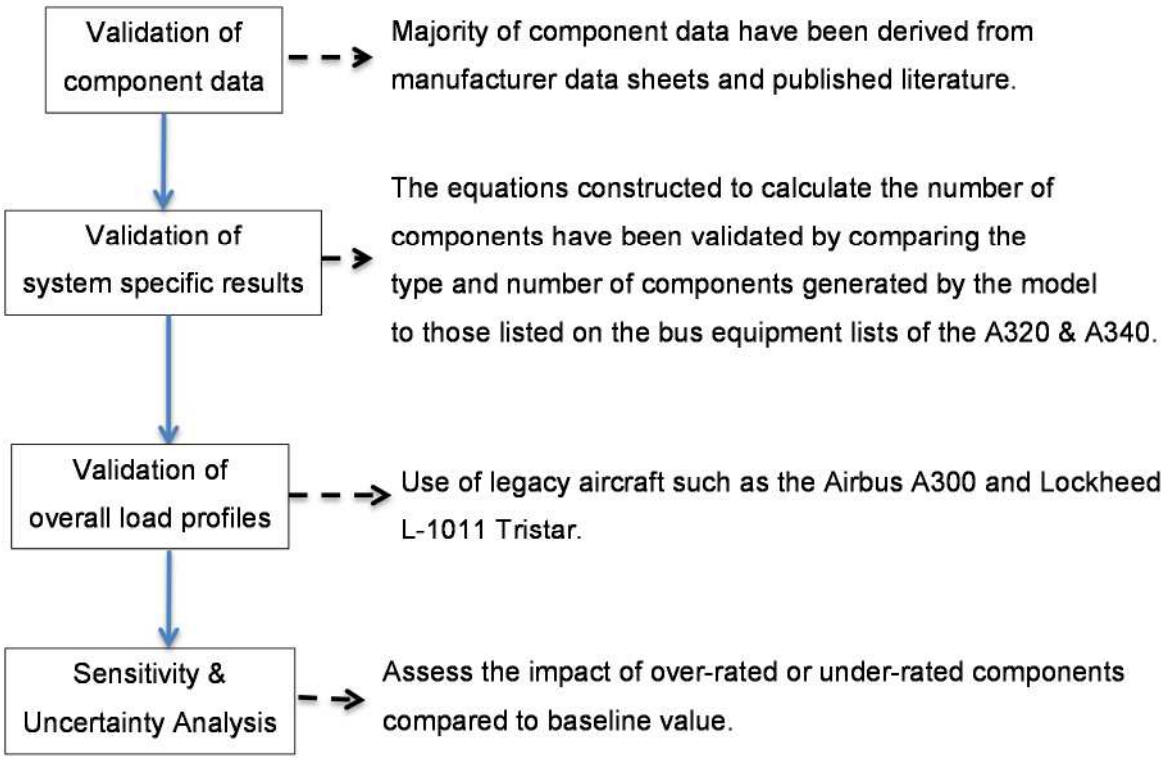

Figure 5-2: Validation strategy

Due to the complexity and demands of the aircraft secondary power system, each individual sub-system needed to be analysed and included in the design process of the tool, in order to achieve a satisfactory level of robustness. The system level power was the accumulated power of the components which were required to achieve the functionality of that particular system. This meant that at each of the calculation steps; component level, system level and aircraft level, there was the possibility of errors, and errors at the component level could be amplified at the aircraft level. To avoid such a scenario, a bottom-up validation strategy where component data, systems level results and aircraft level results were checked against published data, was needed. The validation strategy was based on the above requirement.

The choice of aircraft used in the validation procedure was based on the availability of data.

5.2.1 Validation of component data

Data sheets for components include(but not limited to) the following manufacturers; Eaton Aerospace, Ebm-papst, Aerospace Controls Corporation, GE Measurement & Control Solutions, Parker (Aerospace), South Bend Controls, Goodrich (Aerospace), Dynon Avionics,

Hartzell Aerospace, International Water-Guard Industries Inc, Adahan Carmeli Engineeing Co., Thales, Sarasota Avionics, Teledyne Controls, L-3 Communications, Columbia Research Laboratories Inc., Honeywell, Rockwell Collins, United Instruments Inc., Gables Engineering, Northrop Grumman Corporation, Avtech Tyee, Allied Signal (now Honeywell), Sermat Aero, B/E Aerospace, Aerolux, Astronics Corporations, Flight Display Systems, Pacific Precision Products and SensorsONE. Publications include [76], [77] and [47].

5.2.2 Validation at systems level

In order to perform electrical load analysis at an aircraft level accurately, the inputs from the systems need to be within satisfactory ranges. To test the performance of the tool at a systems level, the tool was simulated to represent the Boeing 777-300. [70] lists the electrical loads for an "engine out" scenario (with a single main generator operating) in the cruise segment.

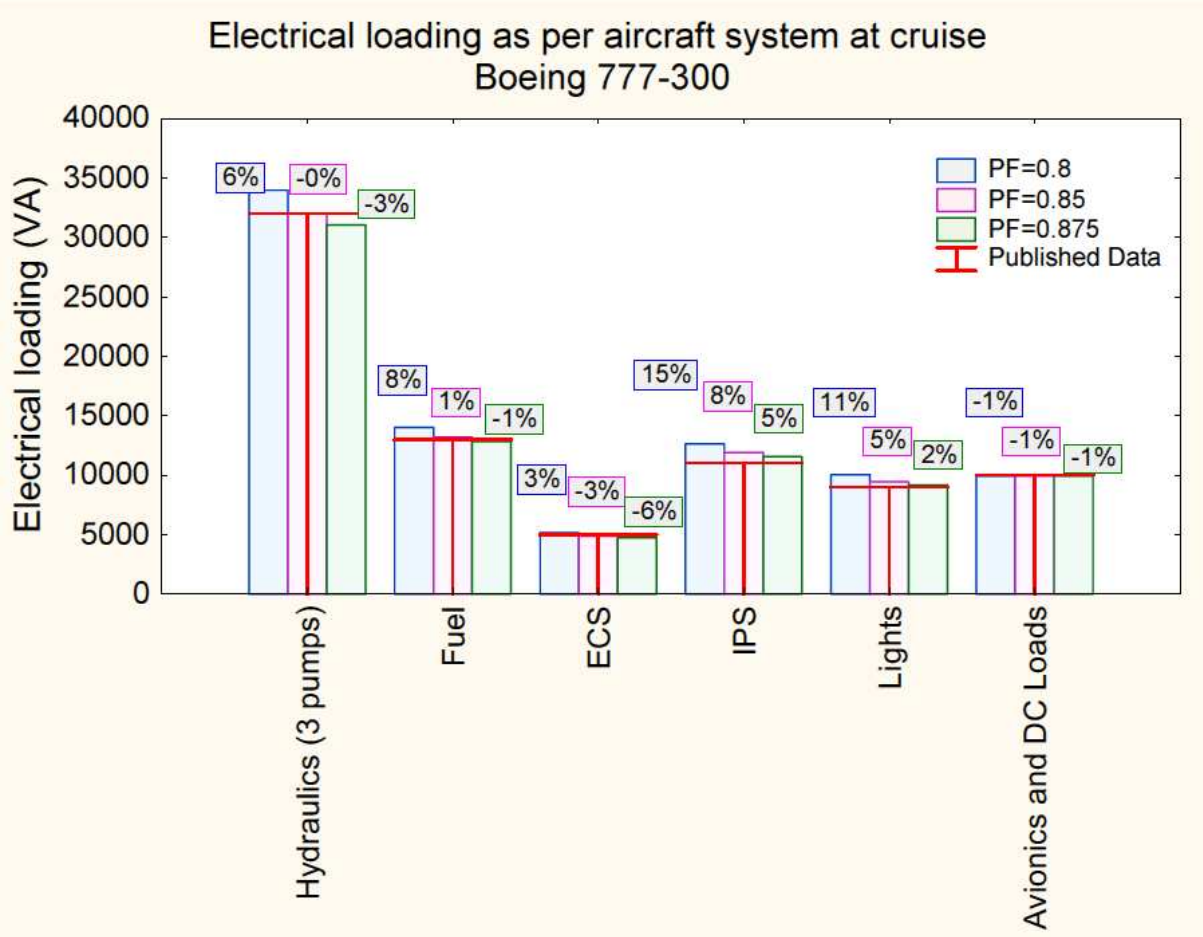

Figure 5-3: Electrical load at cruise (engine out scenario)

The tool computes the electrical load as a real power in kilo Watts. For comparison with the available data, a subset of typical power factors were used to convert the AC power component

to an apparent power in volt amperes. The results showed that with a typical power factor of 0.85 the deviation was less than 10%. Even with a conservative power factor of 0.8, for an advance distribution such as the Boeing 777 architecture, the deviation was less than 15%, clearly indicating that the model calculates the systems level power requirements satisfactorily. The validity is further increased since six aircraft systems, which are characteristically different, were compared.

It must be noted that the above sub-systems in Figure 5-3 were assumed to be fully operational and not compromised due to the engine out scenario. This is a valid assumption as all sub-systems listed are required to function to the respective minimum requirement to maintain safe flight. Engine out scenarios will result in power down sequences where non-essential systems such as in-flight entertainment and galley services are some of the first loads that would be shed.

5.2.3 Validation at an aircraft level through comparison of electrical load profiles

Airbus A300 (List of inputs specified in "*Appendix A: List of inputs for the A300 case study for the ELA"*); When the Airbus A300 electrical load was simulated the following results were obtained. Airbus [27] provides data for the A300 electrical load analysis. The flight scenario used in the simulations for validation, is the "cold night cruise" where the worst possible conditions are assumed such that all electrical equipment may be used at least once.

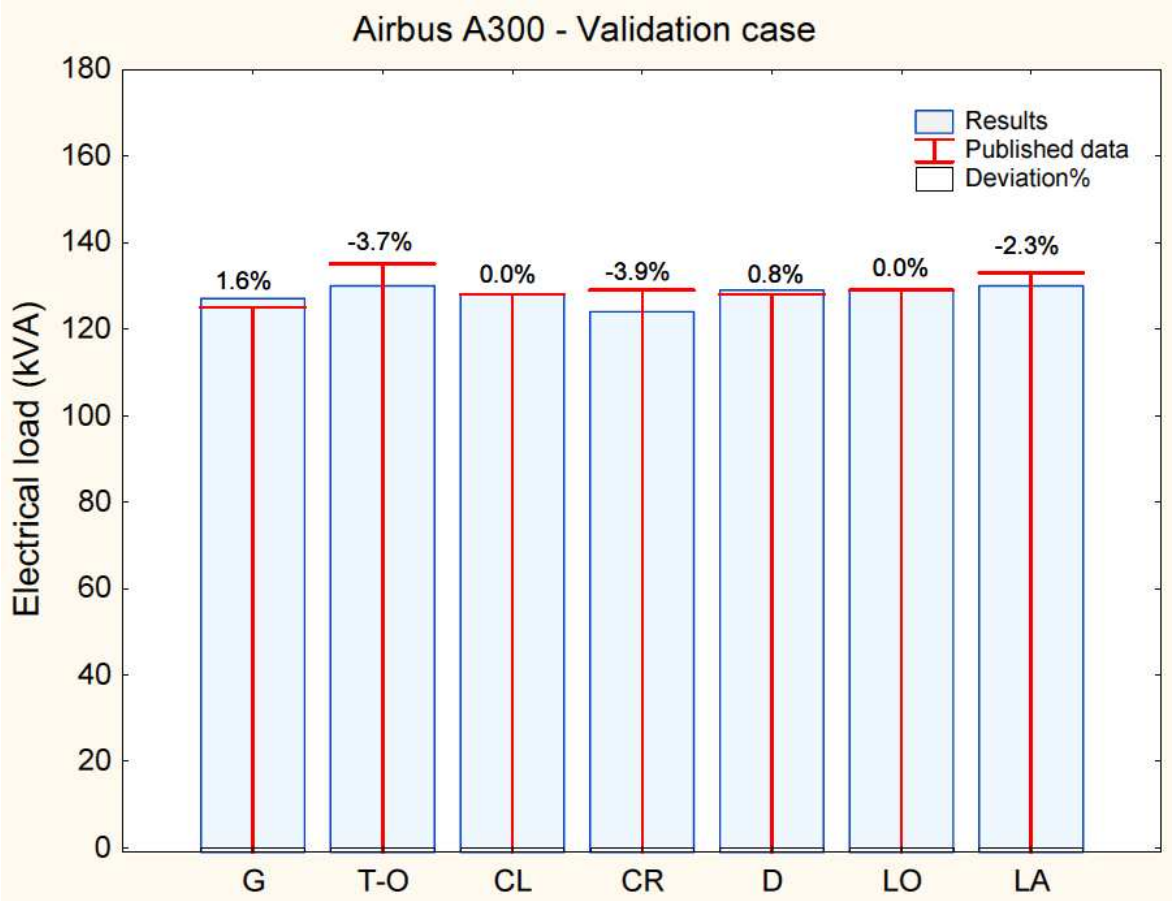

Figure 5-4: Airbus A300 study

As can be seen an accuracy of more than 95% was achieved in all flight segments. It should be noted that the scenario simulated was a “cold night cruise” in which all electrical equipment operated at least in one flight segment. The power factor used was 0.8.

Lockheed L-1011 Tristar; The same process as for the Airbus A300 was repeated for the Lockheed Tristar, to observe the robustness and accuracy of the methodology and development tool, for aircraft from different manufacturers incorporating different design philosophies. [21] provides the data for the electrical load analysis of the L-1011 Tristar. The flight scenario used was a “cold night cruise”.

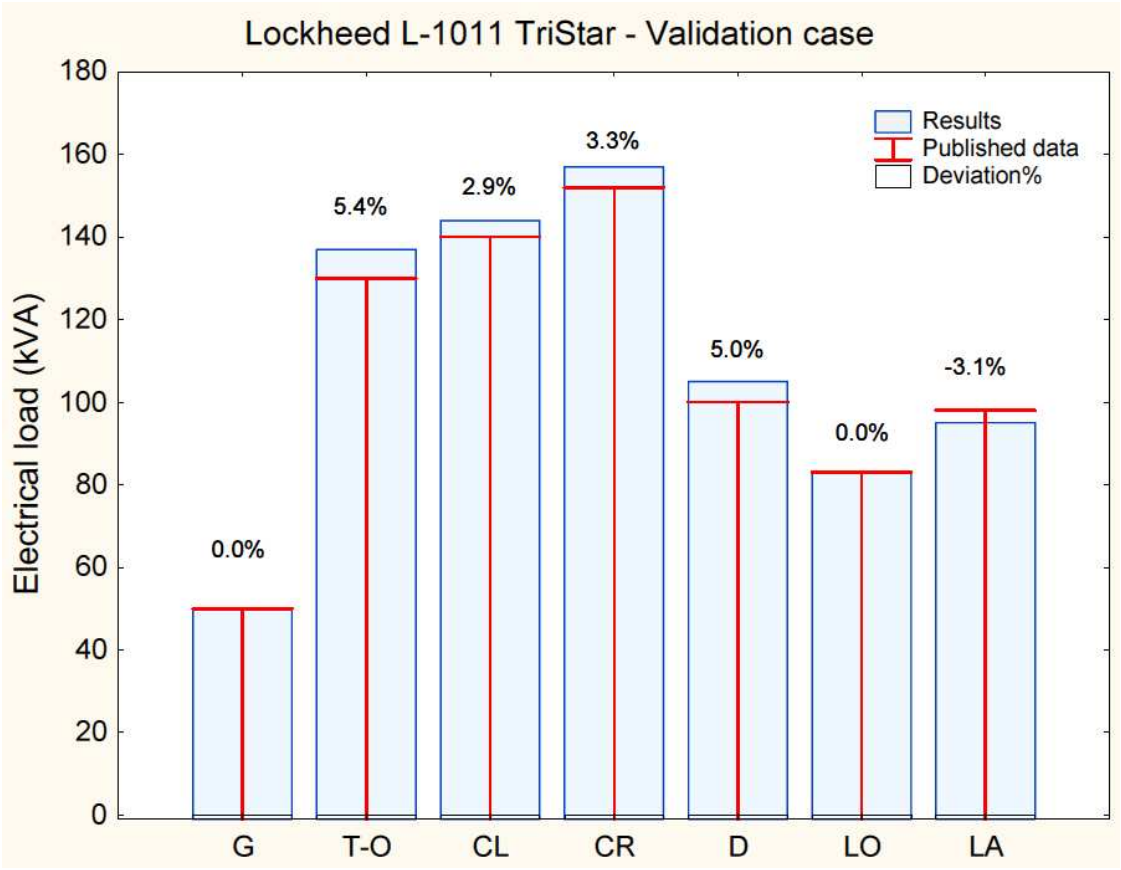

Figure 5-5: Lockheed L-1011 Tristar study [21]

As in the case of the Airbus A300, an accuracy of at least 90% was achieved within all flight segments. Each electrical component was operational for at least one of the flight segments. The power factor used was 0.8.

5.2.4 Sensitivity and un-certainty analysis

The work presented in this section relies on a key assumption; -

"The power-to-weight ratios of functionally similar electrical components are similar if not the same, in conventional commercial large aircraft."

Many aircraft use commercial off-the shelf products to fulfil many functionalities. By analysing available data on lighting components, fuel pumps, galley equipment, sensors, avionics equipment, in-flight entertainment equipment and many others, the above assumption can be justified.

To illustrate this, the electrically operated fuel booster pump characteristics were studied for the Airbus A330 [78], Airbus A430 [78] and Boeing 747 [79] series aircraft.

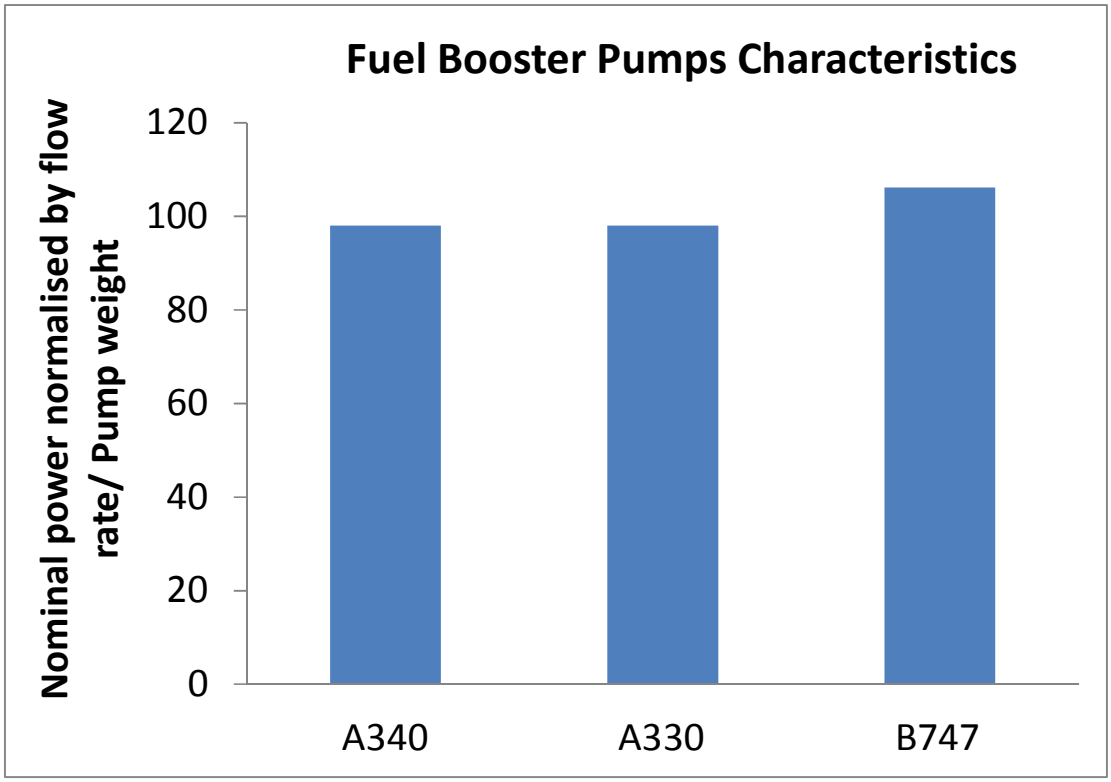

Figure 5-6: Fuel booster pump characteristics

The Airbus A330 and Airbus A340 uses the same pump while the Boeing 747 has a very similar power to weight ratio once the performance of the pump is normalised by the flow rate to get a similar functionality.

In order to justify that the methodology is appropriate and that the assumption is valid, an uncertainty analysis was conducted. Within the study it was established that each electrical component could vary between 85% and 115% of the generic nominal power listed in the database.

This type of analysis is needed since, during the development cycle of the aircraft many technologies especially those related to electrical equipment evolve rapidly. So the final electrical components in the aircraft, though functionally similar, may have different power consumption ratings than a previously established baseline. A sensitivity analysis helps determine the effect of variations at the component level to the aircraft level electrical loading. Moreover, the ± 15% can be applied to all components to find the extreme, but this would be a conservative approach that may lead to over-design. So in this study, the approach has been to apply a random change, with ±15% as the limits, to each component and to perform a thorough sensitivity and un-certainty analysis.

Due to the lack of data, individual distributions for the variation of the nominal power, for a specific component across the large commercial aircraft range, could not be established. So a conservative range for the nominal power was established using results obtained from Figure 5-3. Here, it was observed that for a power factor of 0.8, the IPS total load varied by 15%. This was the basis of the range. This range was based on two assumptions. Firstly it assumed that the Boeing 777-300 had an overall power factor of 0.8 and is the worst case scenario. It was also assumed that each component in the system contributed equally to the variation. This meant that each component in the system on-board the actual aircraft was operating at 85% of the nominal power to those in the generic database. Hence the range of ±15% was established.

Each component was assigned a random power based on the above limit at each iteration of the process. Figure 5-7 shows that the range of ±15% of the nominal value covered all published ratings. It is for the beverage maker on board the aircraft. Similarly every other component power was randomly changed as per a normal distribution.

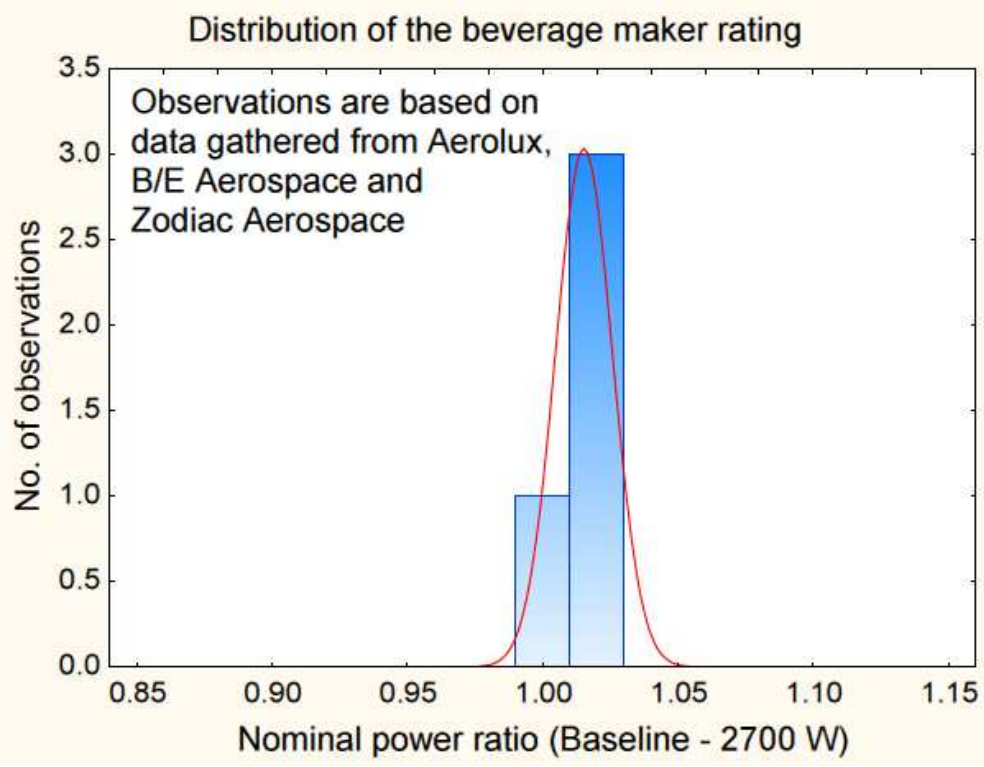

Figure 5-7: Distribution of the operating power for typical a beverage maker – estimated for this research study

Each flight segment was analysed to observe the effect of the uncertainty of the component power.

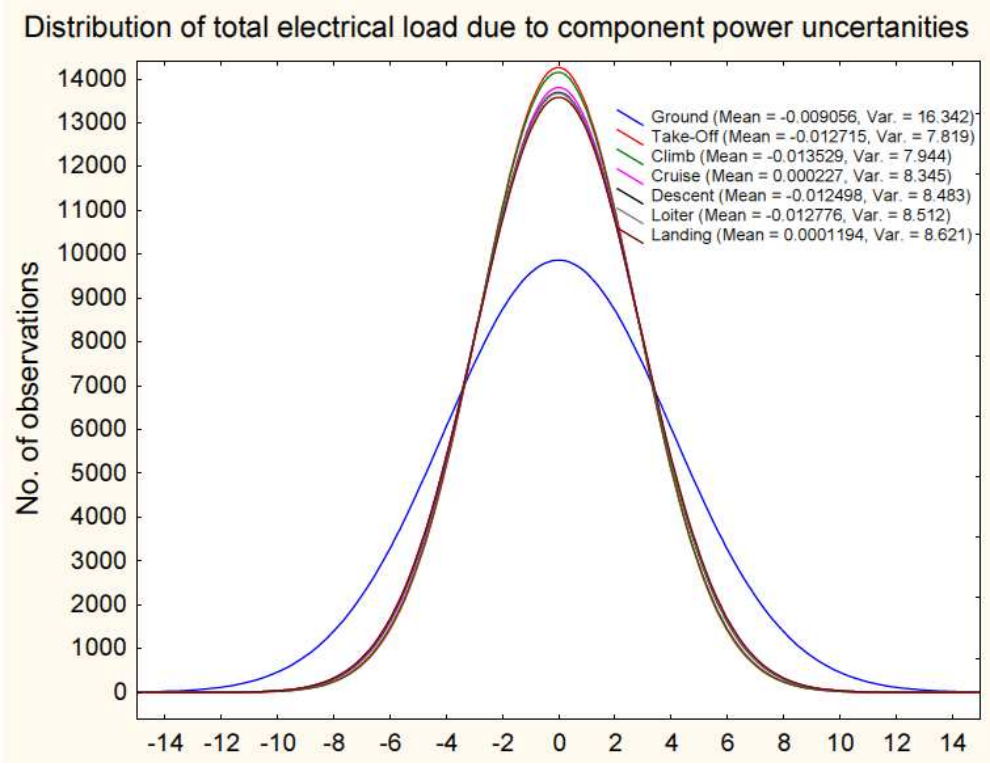

Figure 5-8: Uncertainty analysis for each flight segment

The following is a summary of the results;

Table 5-2: Results summary of uncertainty analysis

	Percentage of cases falling within the limit range						
Limit range	**Ground**	**Take-Off**	**Climb**	**Cruise**	**Descent**	**Loiter**	**Land**
Within 2.5% of baseline	40	62	61	60	58	58	59
Within 5% of baseline	76	93	92	92	92	92	91
Within 7.5% of baseline	95	99.6	99.6	99.4	99.6	99.6	99.5

Within 15% of baseline	100	100	100	100	100	100	100

The results indicate that nearly all cases fall within 85% of the baseline case. With the exception of the “Ground” segment, a majority of the cases fall within 99% of 7.5% of the baseline calculation. This indicates that the total electrical load change for the aircraft is not affected significantly due to the change in the power for a component. Moreover, the limits of 85% to 115% are conservative in the sense that it allowed for a greater deviation than that which would be expected in functionally similar components across the commercial aircraft range. This justifies the use of a generic database to design the electrical system of an aircraft at the preliminary stage. Moreover, it also confirms that relating the components on a functionality basis for each system provides results with far greater accuracy than using conceptual sizing parameters.

This result can be summarised by saying that more than 95% of the cases simulated with varying degrees of component operating power falls within a 7.5% deviation of the overall aircraft electrical load calculated using the generic component database and as expected 100% of the cases fall between a 15% deviation limit.

The results of the uncertainty analysis shows that this methodology is robust, such that the load for each flight segment is computed independently and that it relies on the operation of components, rather than conceptual design parameters.

Since the methodology relies on the component operation, it makes it robust in adapting to new technology. For example, in the avionics field there is great demand for integrated solutions which perform multiple functions. This results in some conventional avionics equipment being obsolete. Moreover, it also means that the power requirement for such an integrated solution would not be a fixed amount but would vary in different flight conditions. By using the operational constraints included in the methodology, the tool can be adapted to incorporate such technology for study, at the preliminary electrical system design stages.

5.2.5 Overall validation of work

As stated by Feiner in [9] the “initial power is estimated by scaling previous designs or by estimating power on a per-passenger basis during the advanced aircraft configuration studies.”

Moreover, this means that the much of the electrical distribution and generation design can only take place once the other system components are fully defined.

By using generic components as a baseline and by relating the system components to the aircraft level, systems level and operational level requirements, a full electrical load analysis can be achieved in the preliminary design stage. This has a distinct advantage over using conceptual metrics such as the maximum take-off weight and the number of passengers to size/re-size the systems. Moreover, the design of the electrical system can now be done in parallel to the other systems. At the detailed design stage, once the other system components are fully defined, by simply varying the characteristics of the components such as the nominal load the preliminary Electrical Load Analysis (ELA) can be adjusted to provide the final electrical load profile and analysis required for certification. This makes the methodology robust in design as well as post design analysis, giving it the capacity for it to be adapted and modified to different design and operational conditions.

5.3 Results

One of the primary objectives of this research was to provide a methodology to size the electrical load. The tool developed, will produce electrical load profiles which will enable designers to estimate the capacity of the electrical power sources namely the generators and the Auxiliary Power Unit (APU) by incorporating allowances for distribution and efficiency losses. The default setting of the simulation is a cold night cruise where worst possible conditions are assumed. This follows the certification requirements in which the aircraft should be able to supply the maximum possible electrical load at any given time.

Three case study aircraft were chosen. The case studies were chosen such that both short range and long range aircraft were represented.

1. A long range aircraft with 4 engines, 440 passengers, and a range of 13,700 km.
2. A short range aircraft with 2 engines, 180 passengers and a range of 6,150 km.
3. A long range aircraft with 4 engines, 524 passengers and a range of 13,450 km.

All aircraft are considered to have fly-by-wire technologies. The continuous loading is discussed since this is the primary factor which influences the sizing of the primary electrical generation.

The aircraft level results for each case study are presented and the similarities between the operational aircraft power consumption and the case study aircraft power consumptions are discussed. This is followed by a discussion of the tool's ability to calculate the emergency power requirements of a given electrical architecture, as well as the individual bus loading. It should be noted that only the split-bus architecture has been used since it is the typical configuration in most commercial passenger aircraft in operation at present.

The results then present the tools ability to breakdown the power usage in terms of sub-systems within the aircraft secondary power system. Finally, the results show the tool's adaptability to design and analyse a more electric secondary power system.

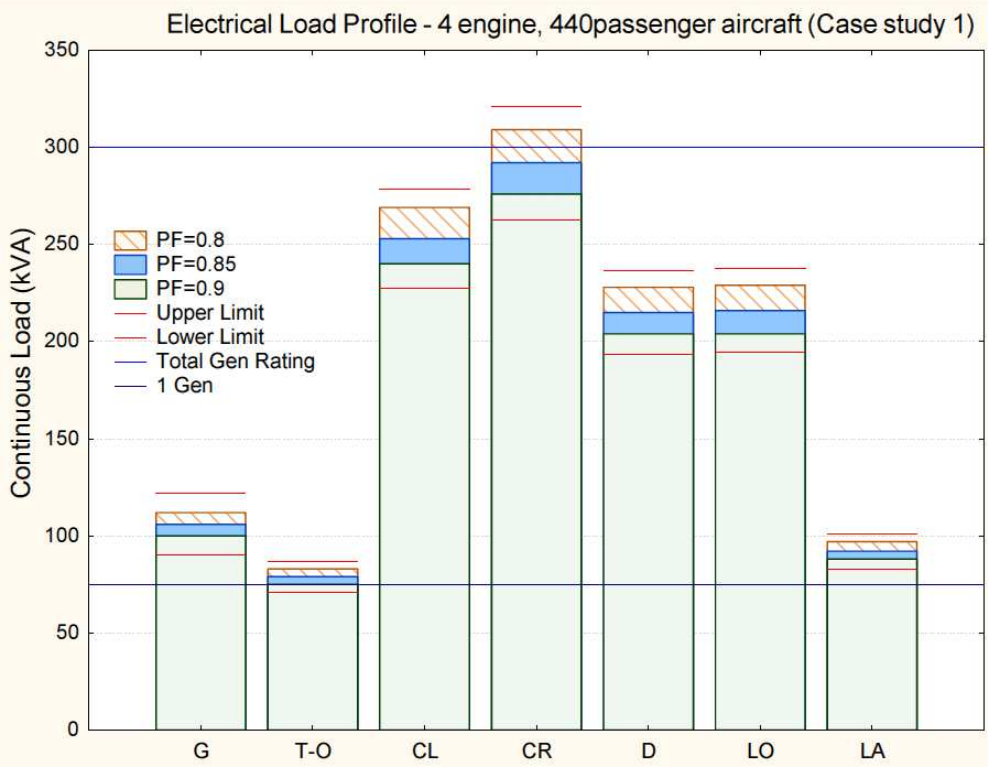

Figure 5-9: Case study aircraft 1 – ELA

The characteristics of *Case study 1* are similar to that of the Airbus A340-300. The A340 has a total rated capacity of 300 kVA and is shown on the graph for easy comparison(Blue Horizontal lines represent the total and single generator ratings). *Case study aircraft 1* requires

a maximum of 282 kW. If a power factor of 0.85 is assumed, the maximum load required will be 292 kVA. This compares well with the total engine mounted generator rating. But it should be noted that a safety factor needs to be considered to avoid over loading the system. This leads the result to be slightly oversized, but still within a very accurate range for preliminary design.

As can be seen on Figure 5-10, the power requirements for C*ase study aircraft 2* with 180 passengers, with a maximum range of 6150 km, with fly by wire technology, and 2 engines is presented.

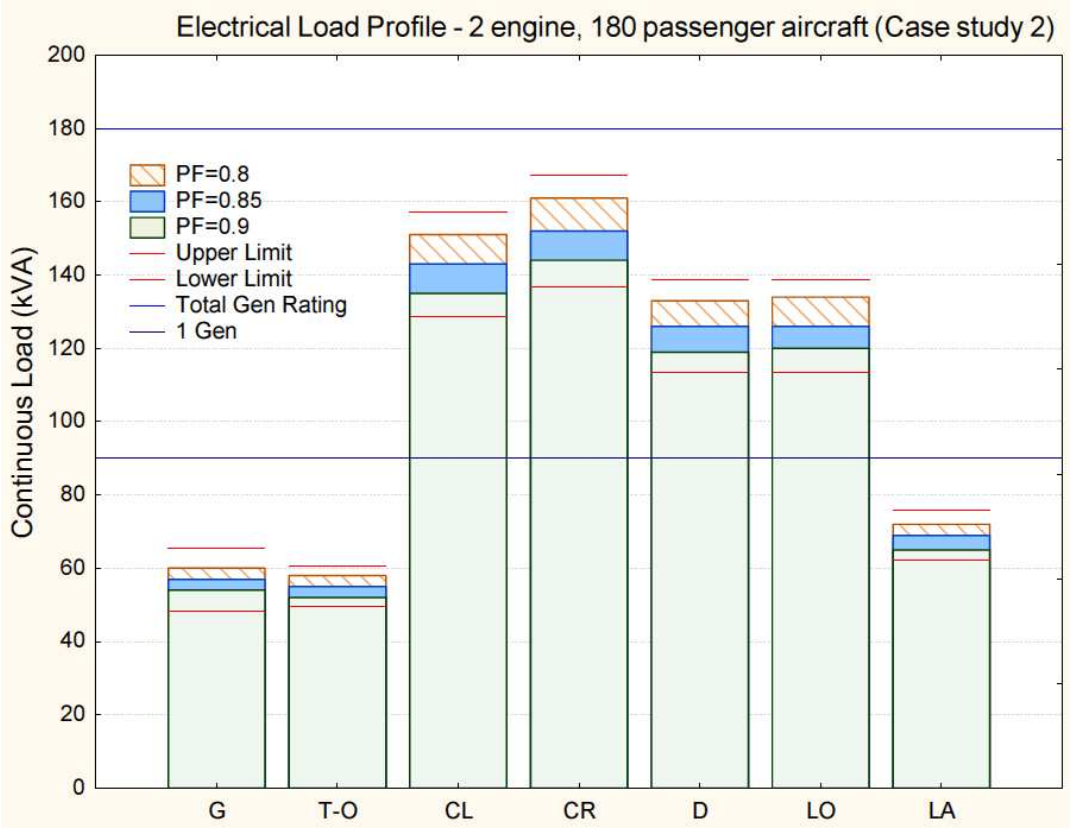

Figure 5-10: Case study aircraft 2 - ELA

The results show that maximum load required is about 150 kW. This translates into about 161 kVA for a power factor of 0.85. If the Airbus A320 is considered, the aircraft is a twin engine, 180 passenger aircraft with a maximum range of about 6150 km. It has a total rated capacity of 180 kW. The generator ratings for the A320 are shown on the graph for easy comparison. In this case the model seems to provide a result which is about 11% less than a comparative aircraft. This is still within an acceptable range at the preliminary design stage.

Case study 3 which is comparative to the Boeing 747-400 was included in the study, since both previous case study aircraft had Airbus aircraft as comparatives. Moreover, the methodology developed in this research was intended to be as generic as possible. Hence it was expected to perform well regardless of the airframe manufacturers and their bespoke design methodologies.

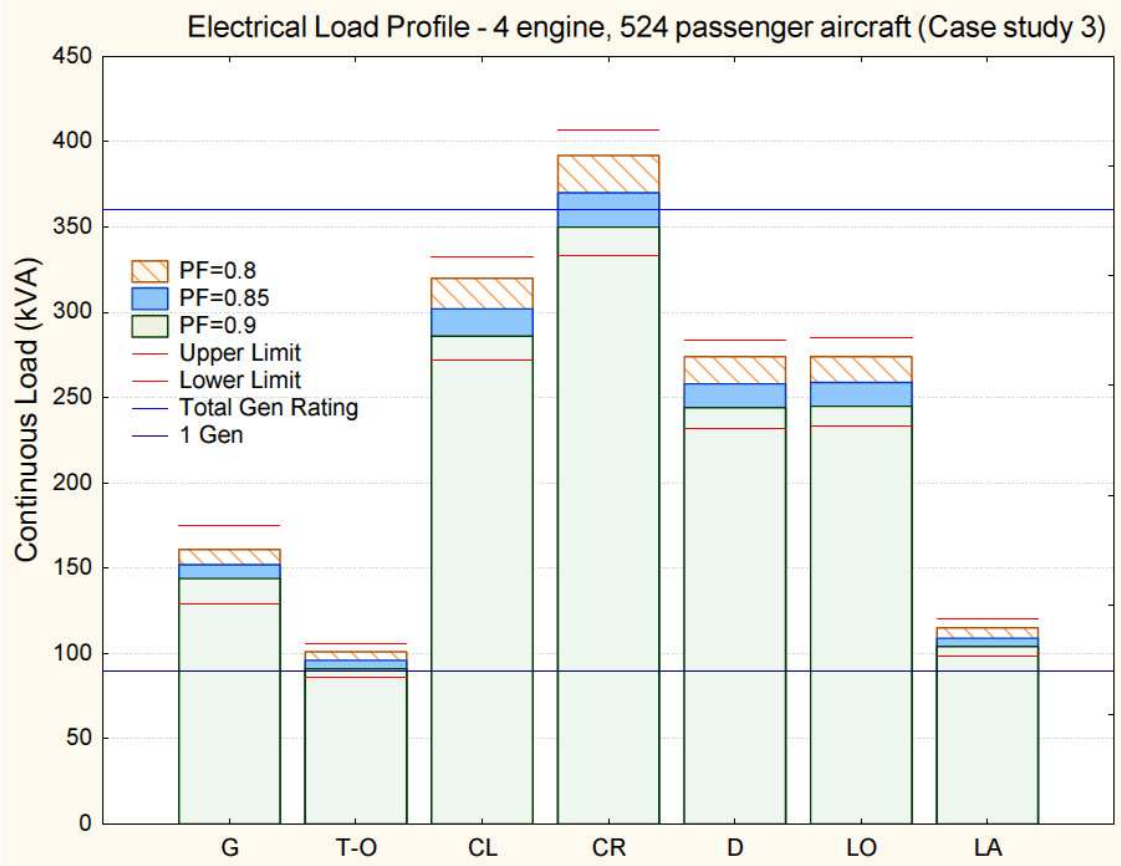

Figure 5-11: Case study aircraft 3 – ELA

Case study aircraft 3 requires a maximum electrical load of about 368 kVA at a power factor of 0.85. The Boeing 747-400 has a total engine mounted generator capacity of 360 kVA. The generator ratings for the B747-400 are shown on the graph for easy comparison. Hence the result is well within range of the comparative aircraft.

Each load analysis profile has an upper and lower limit. This is to account for any uncertainty that may be caused due to the uncertainty of the choice of components at the detailed design stage. The limits are a result of the uncertainty analysis discussed previously and make sure the sizing range accounts for more than 99% of the different configurations possible.

The assessment of the electrical power required during an emergency is critical to size the ram air turbine and establish the load shedding as well as size the emergency power supply buses. Figure 5-12 provides results showing the capacity of the essential and vital loads that need to operate during an emergency in *Case study aircraft 2*. For example these loads will be the loads operating on the essential bus and the shed bus on distribution systems with split bus architectures.

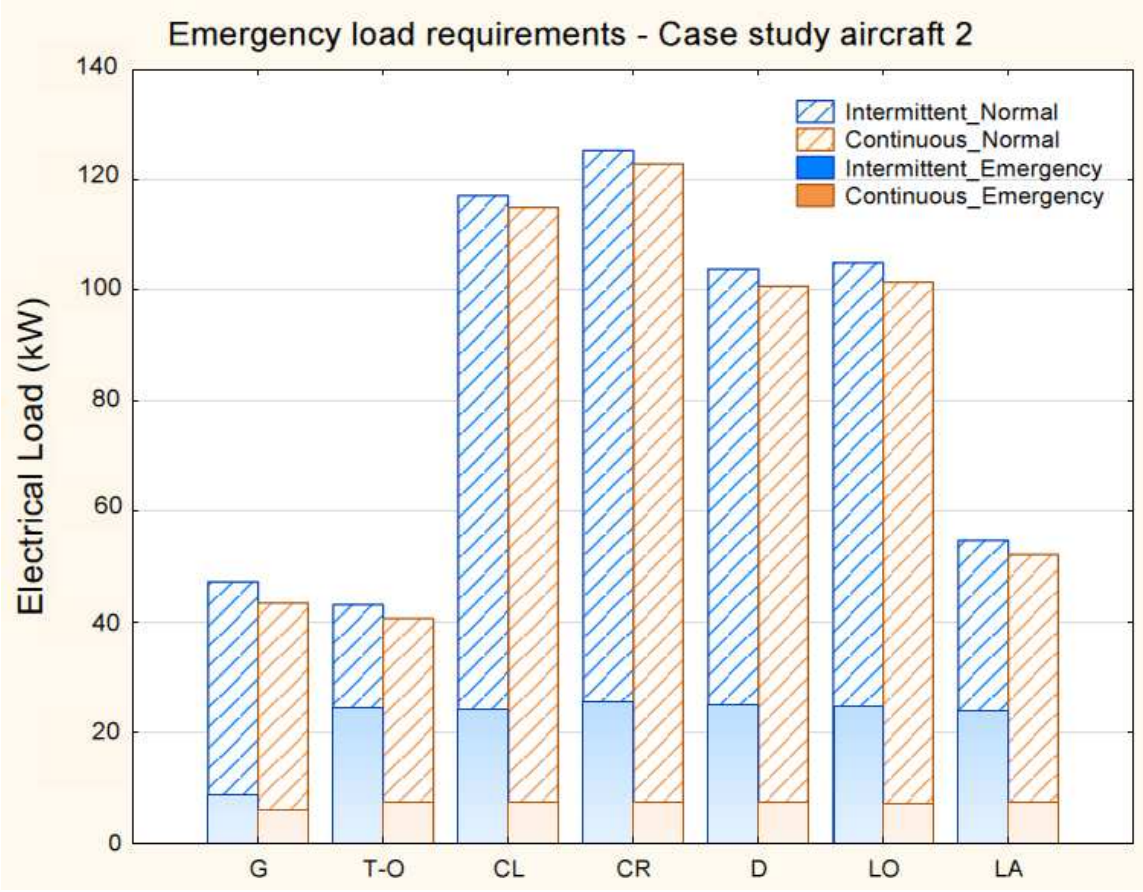

Figure 5-12: Emergency power analysis for 5 minute duration – Case study aircraft 2

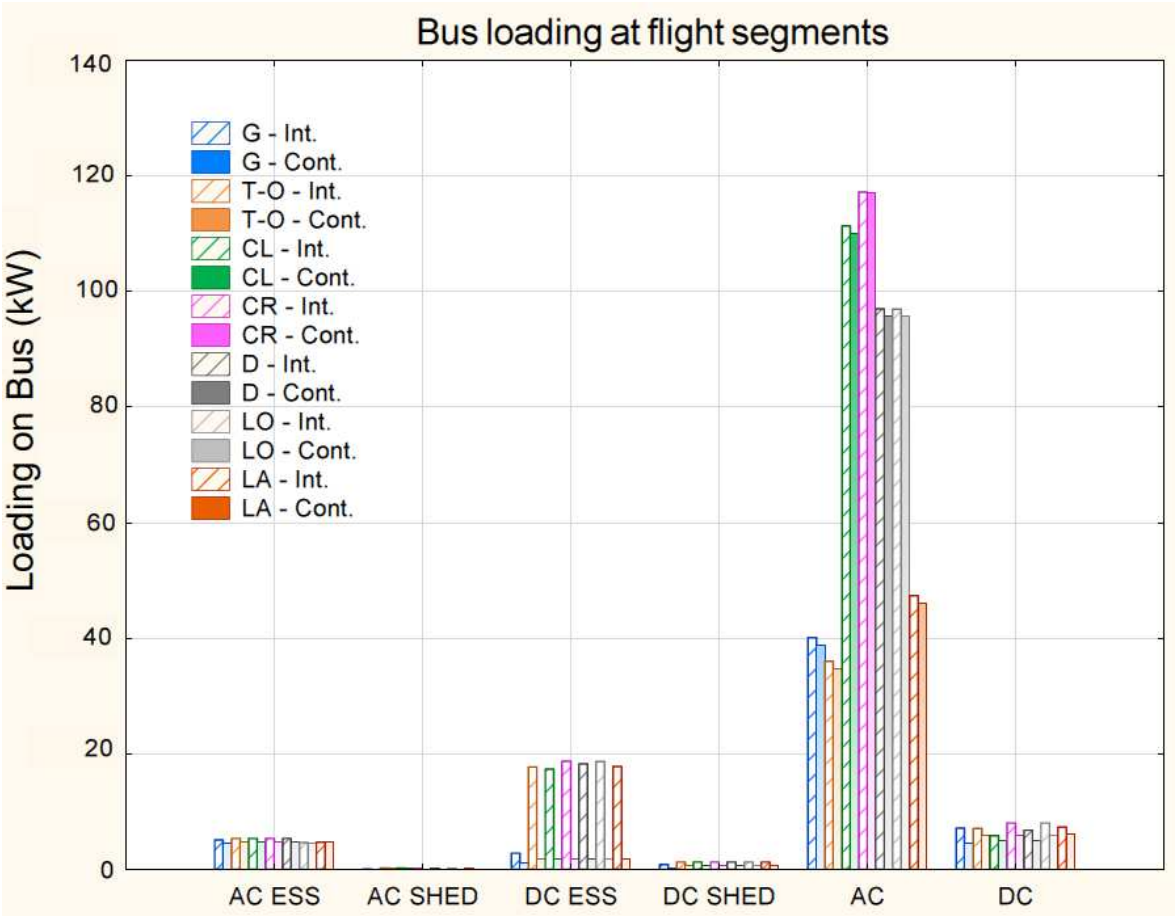

Figure 5-13: Electrical power requirements as per priority of load – Case study aircraft 2

In order to estimate the sizes of power conversion equipment, emergency power sources, and establish load shedding schedules, details of the operating conditions of each load and its priority needs to be assessed. As discussed previously the tool evaluates and lists loads under six categories as shown in Figure 5-13 and the analysis provides a method of sizing the buses or load management centres as required by the distribution architecture.

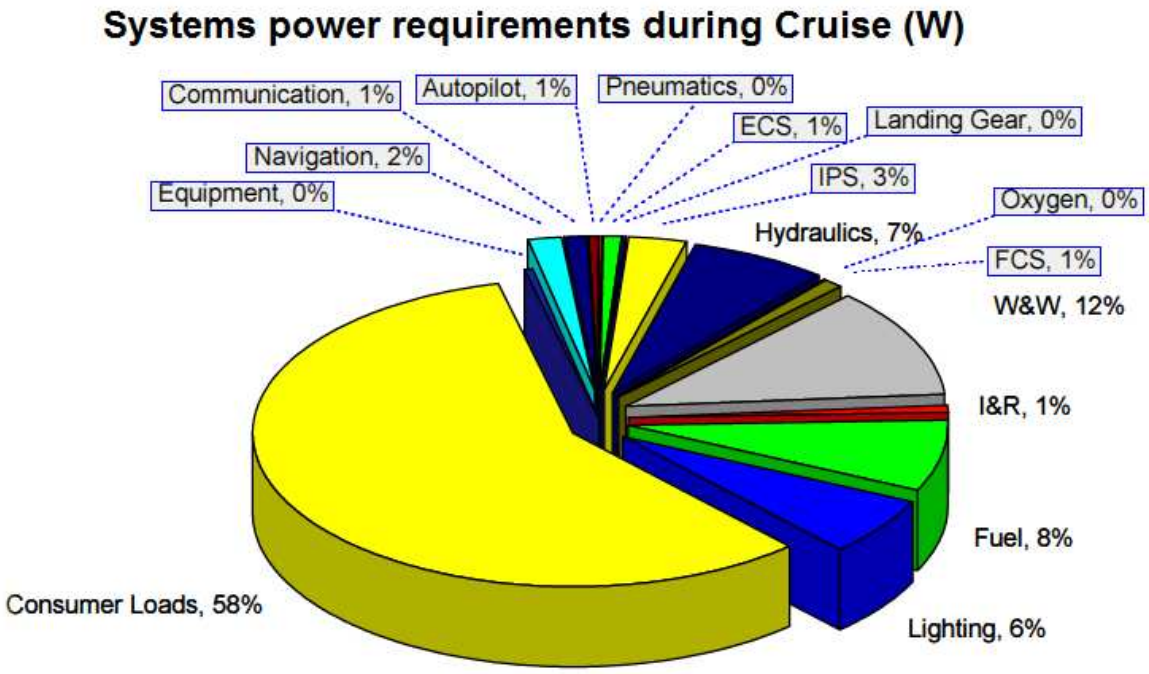

Figure 5-14: System loads (electrical) during the cruise phase – Case study aircraft 2

Figure 5-14, shows the breakdown of electrical power usage during the cruise, as per the ATA chapter. As expected ATA 25 which includes the galley and the in-flight entertainment, is the biggest user of electric power while ATA 38 which includes the water heaters and vacuum generators for the lavatories consume 12% of the electric consumption which makes it the second largest consumer of electric power.

The sensitivity analysis performed by the tool is also important to assess the impact of a component at the aircraft level power consumption. This provides the basis to judge the sizing or re-sizing of the electrical sources without repeating a further electrical load analysis which increases the efficiency and the robustness of the design procedure itself.

Once the baseline aircraft and the baseline architecture of the systems is established within the tool, mathematical functions can be formulated to represent the electrical power requirement of each airframe system so that further design analysis can be conducted on variants which have similar systems architectures.

The following is the correlation for the pneumatics and ECS electrical power consumption for *Case study 2*. The ECS in this test case provides pressurization, temperature regulation and ventilation. The pneumatics provides the bleed air required to run the ECS and IPS. The results

from the system level analysis can be summarised by factorising and grouping parameters related to sub-functions of the system. Since certain equipment have multiple functionalities, this grouping of terms can be done in many ways and the following is just one example. In this form, the power consumption for the system level components such as controllers of the system and the aircraft level parameters which affect the power consumption are grouped separately. It is only a method of expression for the system power consumption which can be derived by following the bottom-up electrical load sizing approach detailed above.

$$P_{ECS+Pneu} = 30(N_{PC}+N_{ZC}+8N_{BF}) + 17(N_{APU}+1) + 4(31N_{CP}+48N_{AC}-8) + [14(N_{RAM}+10N_{E}+6N_{RF})-N_{E}+8N_{RF}] +152N_{CC} \quad (20)$$

N_{PC} - number of pressure controllers

N_{ZC} - number of zone controllers

N_{BF} - number of blowers in the avionics compartments

N_{APU} - number of APU

N_{CP} - number of conditioning packs in the ECS

N_{AC} - number of avionics compartments

N_{RAM} - number of ram air inlets

N_{E} - number of engines

N_{RF} - number of re-circulation fans

N_{CC} - number of cabin compartments

A numerical relationship for each sub-system power requirement can be formed as above. This is achieved by relating aircraft level and system level parameters to the minimum equipment needed to achieve the functionality of a given sub-system, and a generic data set containing typical power consumption values for each electrical component in the sub-system.

To calculate the power usage at different flight stages, co-efficients can be used to multiply $P_{ECS+Pneu}$. At ground (which is defined as prior to engine start up and passenger boarding) the co-efficient for the 5 minute load is calculated as 0.0105 and 0 for the 15 minute load. For all

other flight phases the 5 minute load co-efficient will be 1 and the 15 minute load co-efficient will be 0.8623.

This process can be done for all systems to simplify the relationship between the functions, components, power usage and operations (as per flight phases). This information can then be used to re-size the systems themselves or design and adapt systems for aircraft families.

5.4 Adaptability and implementation in a MEA design

This model was adapted and implemented for a design of a more electric aircraft electrical system. Since all systems now run on electricity, the electrical load analysis included additional loads. These loads represented the pneumatic and hydraulic loads in the conventional aircraft which will be substituted by electrical components.

The significant loads were the electrical environmental control system compressor which draws in ram air, the electrical heating devices/mats for the electric wing and tail anti-icing / de-icing systems and the electrically powered actuators.

Moreover, the electrical components such as bleed computers in the pneumatics and leak measurement valves in the hydraulic system in the conventional configuration were made redundant.

To test the adaptability of the tool, *case study 2* was converted into a MEA. The summary of the loads are shown below;

From [71] a benchmark for an electrical ECS power demand was derived. It suggests that for a typical hot day cruise at 40,000 ft, a typical electrical ECS will consume about 1.17 kW/per passenger for ventilation, pressurisation and cooling of the cabin. An in-house developed electrical ECS simulation tool was tested at similar conditions for the "*case study 2*" aircraft. The ISA deviation to represent the hot day was calculated using [80]. The electrical power for the compressor was based on (21), (22) and (23)

$$P_{net\_EECS} = W'UAT_c \tag{21}$$

$$W' = mT_e' \left[P_e^b - 1 + \frac{\varepsilon}{\varphi}(\varphi - 1)(\varphi - P_e^b) \right] \tag{22}$$

$$b = \left(\frac{\gamma - 1}{\gamma} \right) \tag{23}$$

Where,

P_{net_EECS} - net power for the electric ECS

U - thermal conductivity of the cabin skin

A - wall area of the cabin

T_c - cabin temperature

m – mass flow rate of air

T'_e – ratio between the ambient and cabin temperatures

P_e^b – ratio between the ambient and cabin pressures

ε- efficiency of the heat exchanger

φ – ratio between the ambient and the aft compressor temperatures

γ – ratio of specific heat of air

This model calculated a ratio of 1.21 kW/per passenger for *case study 2* during a hot day cruise flight at 40,000 ft. It was a deviation of 3.8% thus the model was accurate to be used in further analysis. The avionics cooling load which is relatively low compared to the cooling of the cabin was not accounted for, since the equations presented above are for a simplified electrical ECS.

The maximum power for the wing ice protection was interpolated using Figure 2-11 and Figure 2-12 as 136.8 kW.

Due to the availability of data the maximum loads for the actuators were scaled as a first iteration using the maximum number of passengers as a sizing factor from Figure 2-11. It should be noted that detailed actuator models would provide more accurate power predictions, and that a first approximation is used to demonstrate that the tool developed in the research is capable of being adapted to MEA electrical load analysis.A summary of the actuator loads is shown below;

- Slats – 19 kW
- Horizontal stabilizer – 23 kW
- Spoilers – 44 kW

- Flaps – 7 kW
- Rudder – 11 kW
- Elevator – 28 kW
- Ailerons – 39 kW
- Landing gears – 29 kW

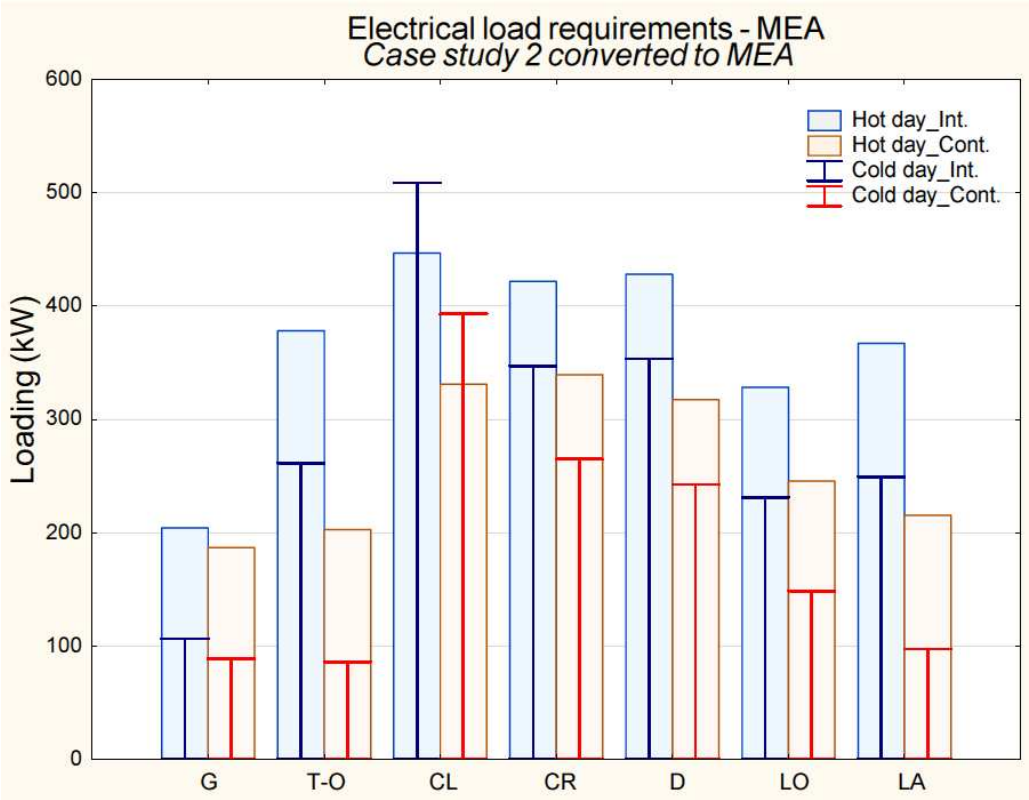

Figure 5-15: Electrical loading for *more electric case study 2 aircraft*

Figure 5-15 gives a top level indication as to what challenges MEA design will face. The obvious challenge is the significantly higher electrical load demands that must be satisfied by the electrical generation."Int." refers to intermittent loads and "Cont." refers to continuous loads.

Moreover, it also presented a challenge in choosing the design case. For example by simulating the electrical ECS it is clear that the design case is a hot day cruise. Yet if this condition is selected for the overall aircraft loading study, the loads from the IPS may not be represented. On the other hand, if a cold night cruise is selected, then the risk of icing is very high, hence the IPS loads will be at a maximum. But the maximum possible loads for the ECS will not be represented, thus if sized for this condition, it will not be adequate to run the electrical

ECS. Hence intelligent power management solutions will be required to satisfy both scenarios and avoid oversizing of the electrical system.

Figure 5-15 shows that the sizing case this instance is the climb segment during a cold night cruise. Yet in all other segments, the hot day cruise requirements are greater.

Moreover, the illustration below shows that the electric ECS accounts for about 52% of the total electrical load during a hot day cruise. The cruise altitude is 35,000 ft and the cruise Mach number is 0.8.

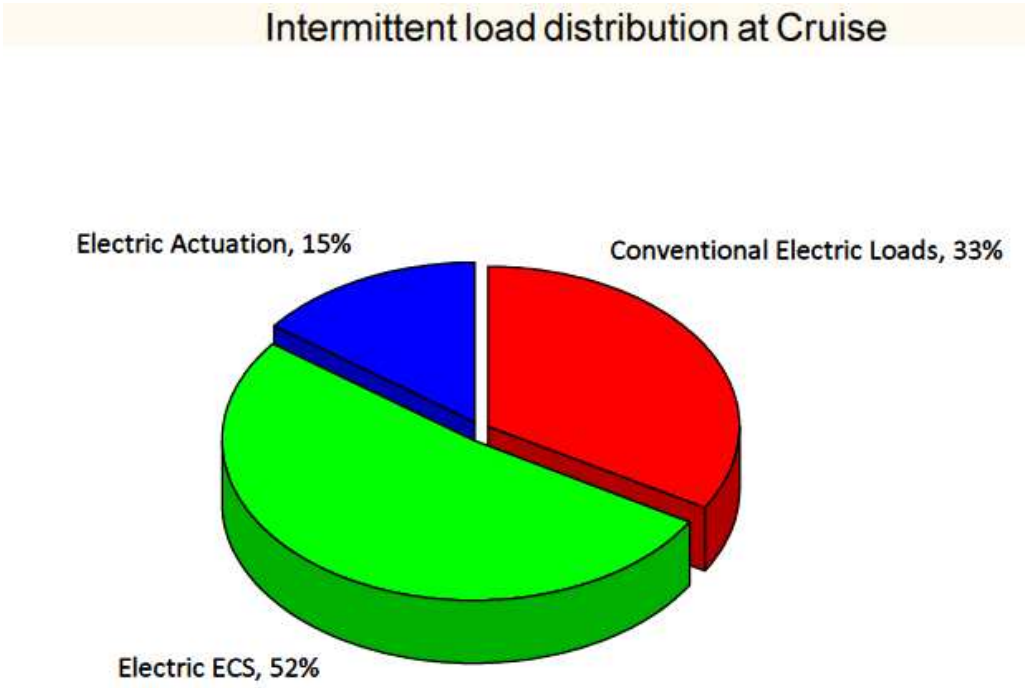

Figure 5-16: Distribution of loads at cruise in the *MEA case study 2*

5.5 Summary

The tool discussed within this section has been developed to size the electrical loads of an aircraft (at the preliminary design stage) with relation to aircraft level, system level and operational level inputs and constraints. As part of the validation procedure, a sensitivity analysis has been incorporated in to the tool itself, thereby showing the user the impact of an over-rating or under-rating of a component compared to the baseline calculation using the generic component database. The methodology was successfully validated at component, system and aircraft level.

The methodology can be applied to any aircraft thus providing a means of sizing the electrical load at the preliminary design phase. The tool can also be adapted to incorporate additional components to satisfy future aircraft systems. The robustness and efficiency of the design process can be increased by using the sensitivity analysis which is in-built in the tool.

In converting case study 2 into a more electric aircraft, it was observed that the conventional electric load is only 33% of the total load. This re-establishes the significance of the electrical sizing, design and analysis at the preliminary design stage of the aircraft. Moreover, this methodology and the consequently developed sizing tool provides a solution to improve the design of the aircraft electrical system at the early stages of the design process.

6 Methodology to predict the fuel penalties due to power off-takes in large commercial turbofan aircraft

After conducting a critical review of the methods available (see §2.4) the k_P method was chosen as the baseline for further development.

The k_P method, presented in [81] represents the off-take penalties by a factor which relates the off-take power to net thrust ratio and the increase in the SFC due to off-takes.

In order to fully understand the k_P method, the trends of the impact of off-takes need to be understood.

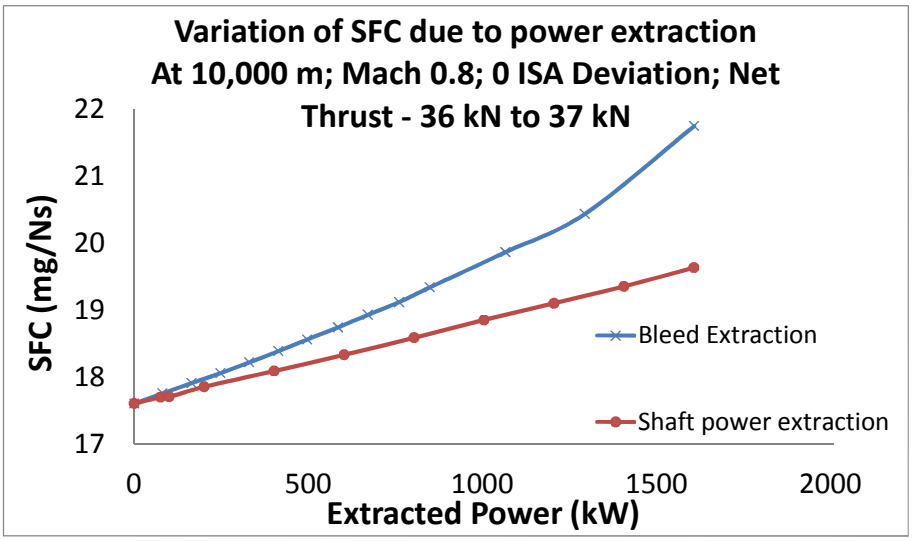

Figure 6-1: Bleed vs shaft power off-take

Figure 6-1 shows that the SFC increases linearly with the amount of extracted power for shaft power extraction. For bleed-air extraction, the variation is nonlinear. The k_P is defined as the slope of the curve between the change in SFC and the extracted power normalised by the thrust produced. This is shown in Figure 6-2. Hence by definition; in the case of shaft power extraction, at a given set of engine operating conditions, k_P is a constant, but when bleed is extracted k_P will take the shape of a straight line. This is shown in Figure 6-2. The parameter k_{P_B} will represent the k_P values at bleed extraction and K_{P_S} will represent k_P values at shaft power extraction.

$$k_P = \frac{\Delta SFC/SFC}{P/T} \tag{24}$$

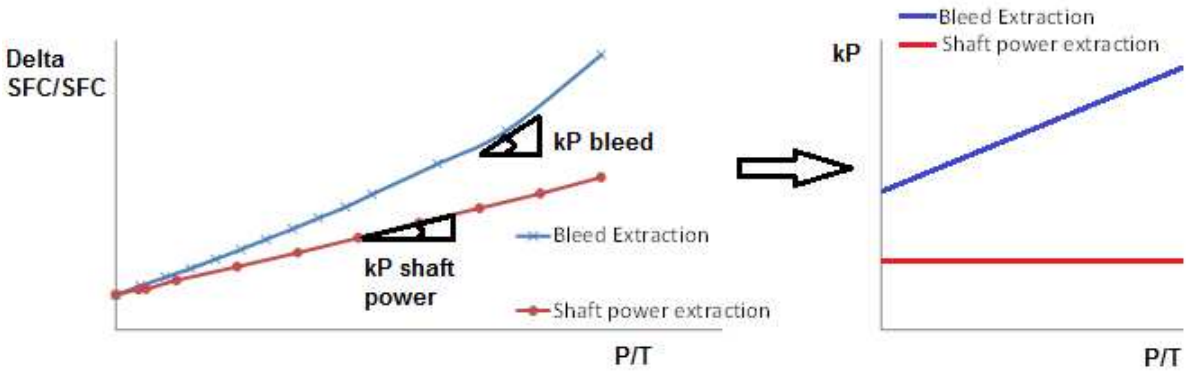

Figure 6-2: Definition of k_P

In order to provide a numerical method to calculate the bleed-air off-takes a further constant k_{P_B} has been defined.

$$k_{P\_B} = \frac{dk_P}{d(P/T)} \tag{25}$$

From the analysis and as shown in Figure 6-2, it was observed that in the case of bleed-air off-takes, k_P, takes the form of;

$$y = mx + c \tag{26}$$

The research showed that the influence of "c" (the intercept of the function) was negligible and that (26) can be approximated in the "y = mx" form.

So (25) can be simplified as;

$$k_{P\_B} = \frac{k_P}{(P/T)} \tag{27}$$

The study in [81] presents a methodology to calculate the fuel penalty due to shaft power off-takes as a function of k_P. The initial findings in [81] shows that there is a significant variation of k_P with respect to the flight Mach number and the altitude. Thus a single k_P value is not sufficient for the engine performance envelop. The study was limited to extracting shaft power from a single shaft of a turbofan engine. This study extends this research to complete the analysis by using a thoroughly validated engine model, shaft power off-takes from all shafts, bleed off-takes, and more operating conditions of the engine.

6.1 Baseline and validation

Off-takes are a result of the integration between the airframe and the engine. The airframe systems demand the off-takes and the aircraft engine supplies the power. It was observed that to create a suitable methodology, this fact was essential. The methodology developed should take into account the flight conditions such as the altitude, flight Mach number and also the engine performance such as the availability of thrust and the engine cyclic parameters.

It was further observed that, to reduce the complexities, a numerical method needs to be developed, which would avoid using engine cycle based thermodynamic calculations. To facilitate this, a vast study was conducted on engine performance with and without off-takes. The objective was to analyse the data, perform regression studies and formulate numerical relationships between the operating altitude, flight Mach number, operating thrust and the fuel penalty.

To perform such a study an accurate simulation tool of a baseline engine is required. The TURBOMATCH code developed at Cranfield University, analyses design point and off-design point calculations for gas turbines. As a baseline a Rolls Royce RB211-524-D4 engine was modelled.

In order to validate the engine performance, the simulation results were compared to data produced from an engine deck supplied by Rolls Royce for a RB211-524D4 engine. "*Appendix C: Design and off-design performance points used in validation of engine simulation*" lists 23 performance points where engine manufacturer deck data was available and the same conditions were simulated using the TURBOMATCH scheme for the modelled engine and compared.

To test and validate the performance of the entire thermodynamic cycle a number of key parameters were chosen for comparison. These included the gross thrust, net thrust, SFC, fuel flow, inlet mass air flow, HPC inlet temperature and the EGT. The validation results are shown in Figure 6-3 and Figure 6-4.

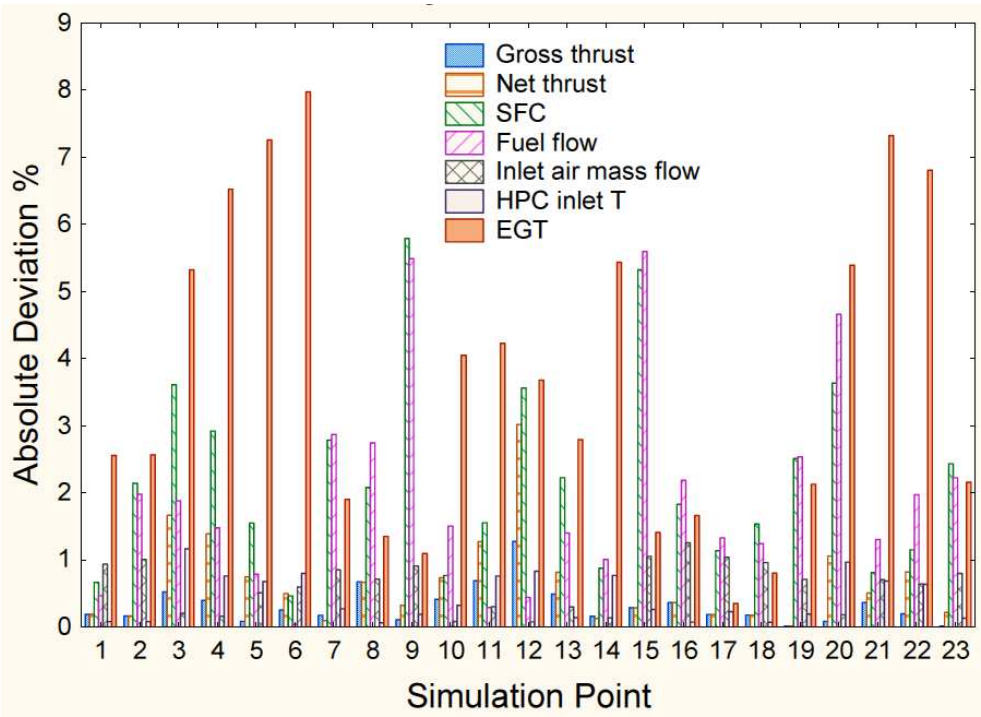

Figure 6-3: Validation results for each design and off-design condition

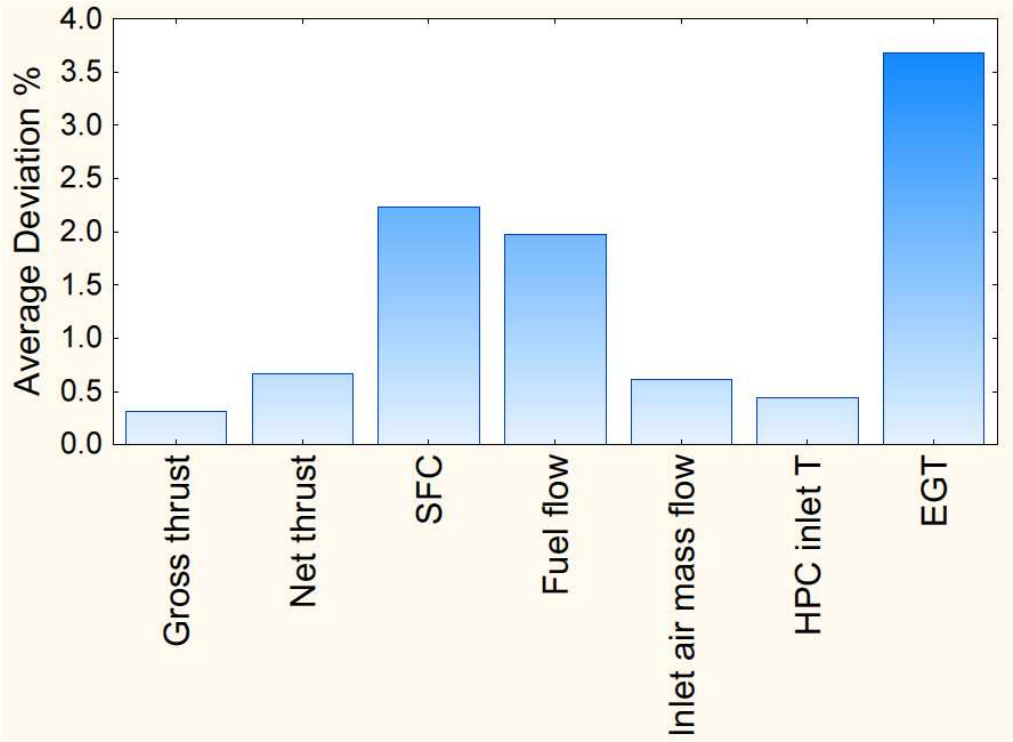

Figure 6-4: Summary of baseline engine validation

The average deviation for both design and off-design conditions was well within an acceptable range. Moreover, since many parameters related to different stages and outcomes of the

engine was considered in the validation, the model was acceptable for further detailed analysis of off-design conditions; namely off-takes.

6.2 Engine performance – uninstalled

The baseline engine was simulated at varying conditions to study the un-installed performance throughout a typical flight envelop. The key variables for this study were the altitude, flight Mach number, the net thrust and the specific fuel consumption. The un-installed performance study had no shaft power off-takes or customer bleed-air off-takes.

The uninstalled engine performance can be summarized by the following graphs shown in Figure 6-5, Figure 6-6 and Figure 6-7.

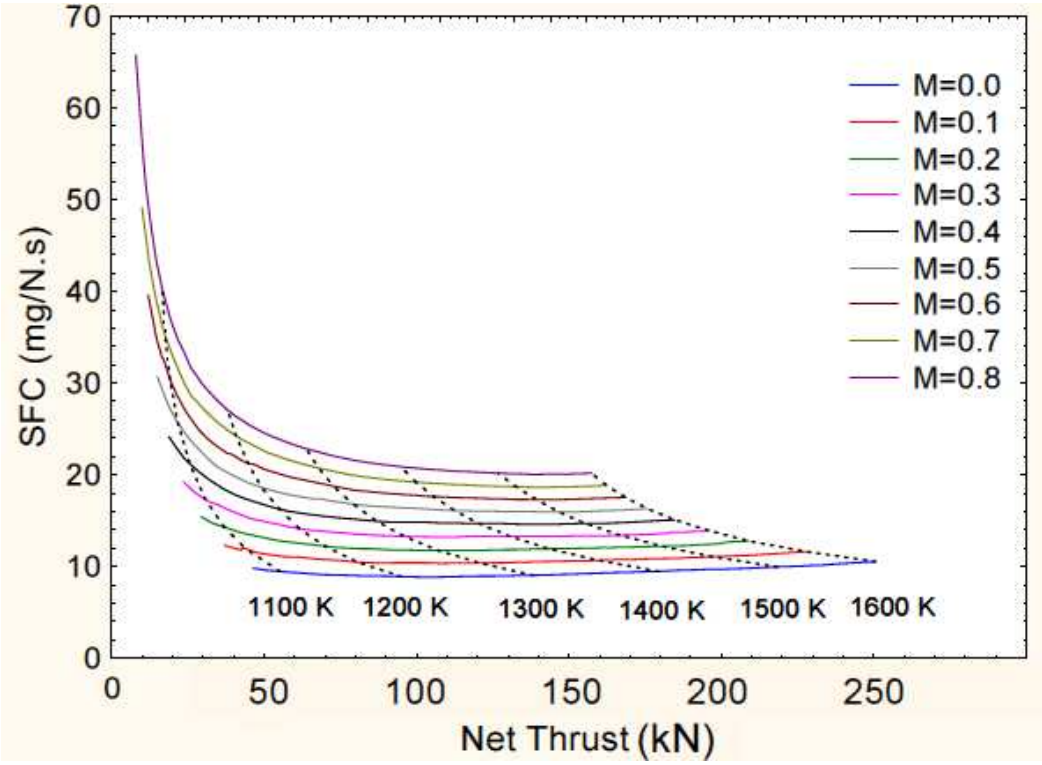

Figure 6-5: Un-installed engine performance at sea level, ISA conditions

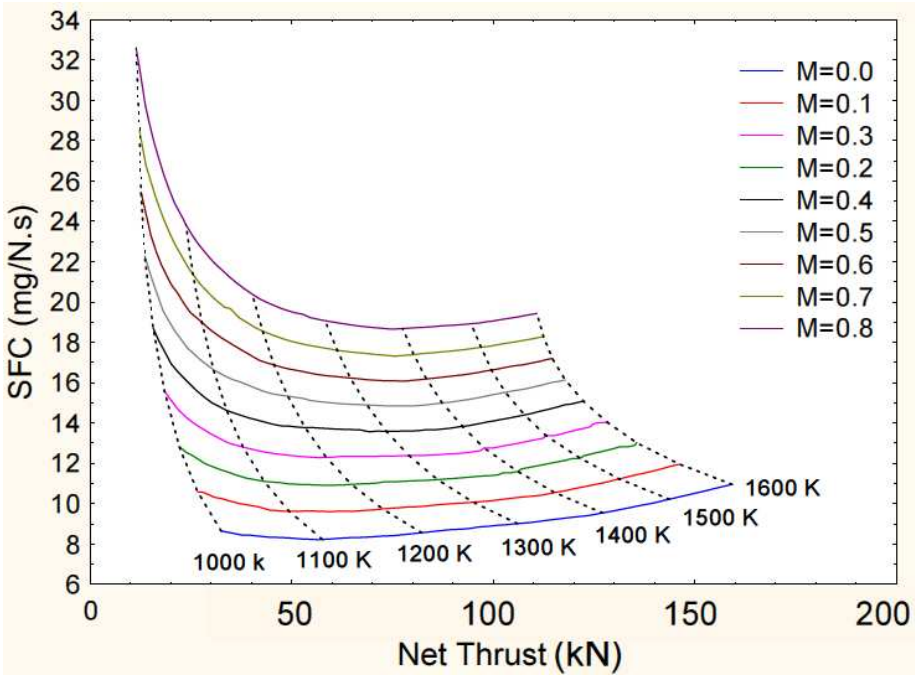

Figure 6-6: Un-installed engine performance at 5,000 m, ISA conditions

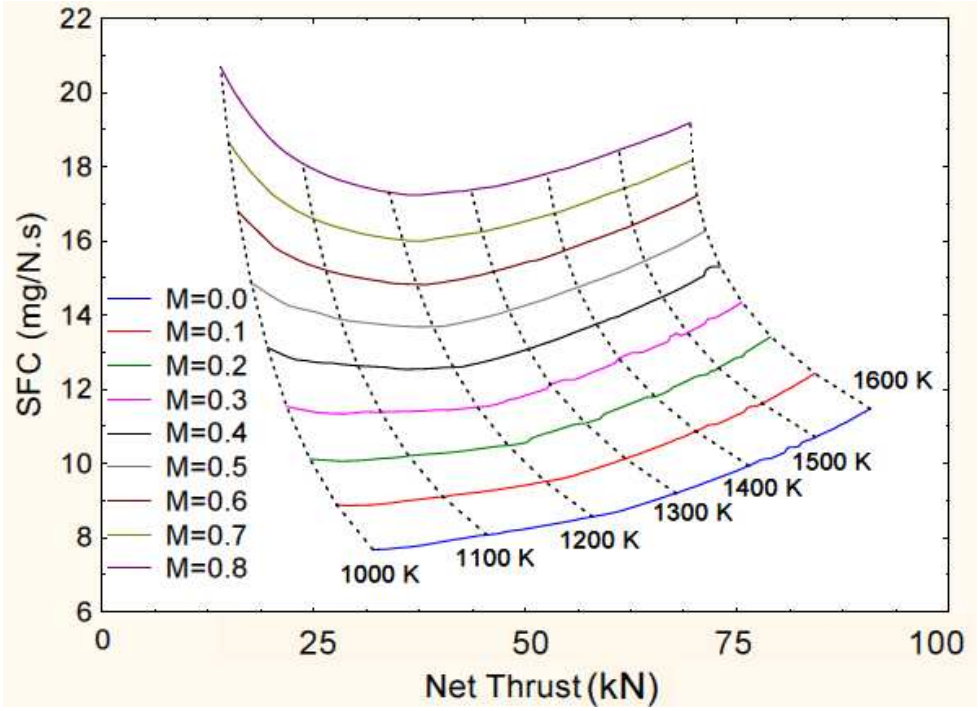

Figure 6-7: Un-installed engine performance at 10,000 m, ISA conditions

The trends observed here, served as verification since it complied with established turbofan engine performance trends.

6.3 Results & Findings

To analyse the effects of the off-takes, the baseline engine was simulated with and without off-takes for various different altitudes, flight Mach numbers and net thrust levels.

6.3.1 Bleed off-takes

The bleed-air extraction was simulated in both the HPC and the IPC in the engine. The summary of the findings are shown in Figure 6-8 to Figure 6-11.

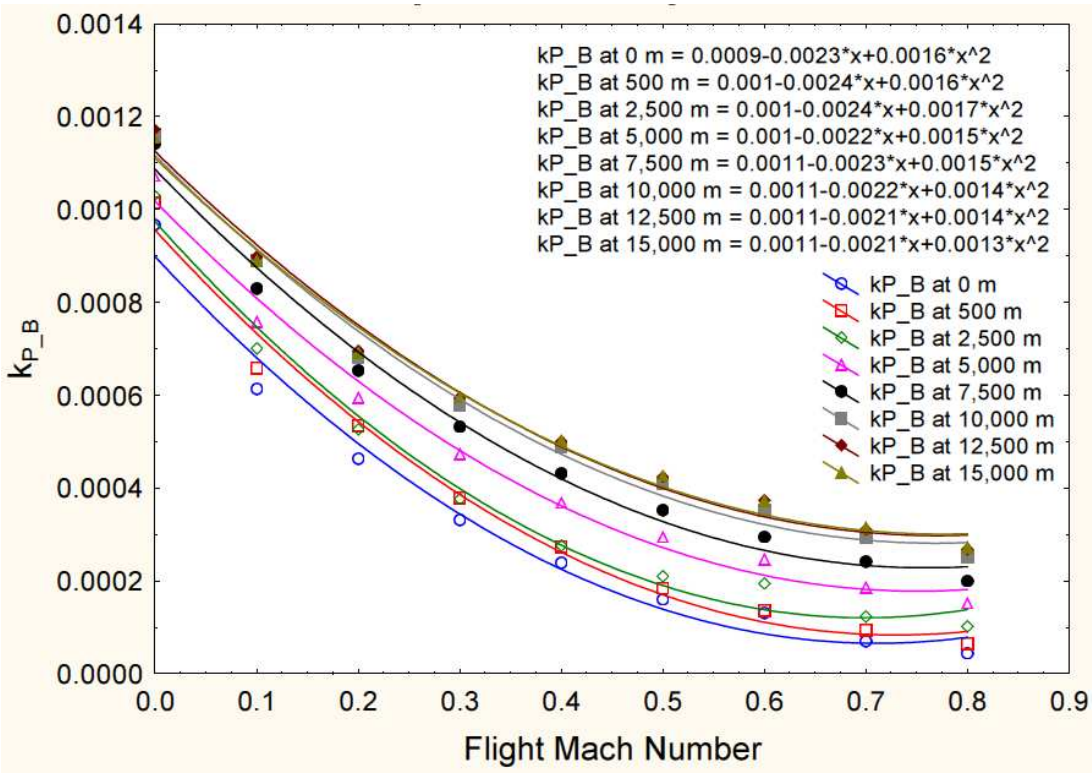

Figure 6-8: IP bleed-air extraction penalty (2-D) representation

The bleed power extraction can be calculated using the following relationship;

$$P_b = \dot{m}_b . C_p . \left(T_{bp} - T_{amb}\right) \tag{28}$$

P_b – Extracted bleed air power

$\dot{m}_b$ – Extracted bleed air flow

C_p – Specific heat capacity at the bleed extraction port

T_{bp} – Temperature at Bleed extraction port

T_{amb} – Ambient temperature

It is assumed that all the energy of the extracted air is exhausted and that it is not used in any energy recovery loop.

The results for the IP bleed air extraction penalties can be summarised as;

$$k_{P\_B} = 0.0009 - 0.0023M + (3.0845 \times 10^{-8})h + 0.0015M^2 + (1.8779 \times 10^{-9})Mh - (9.9046 \times 10^{-13})h^2 \quad (29)$$

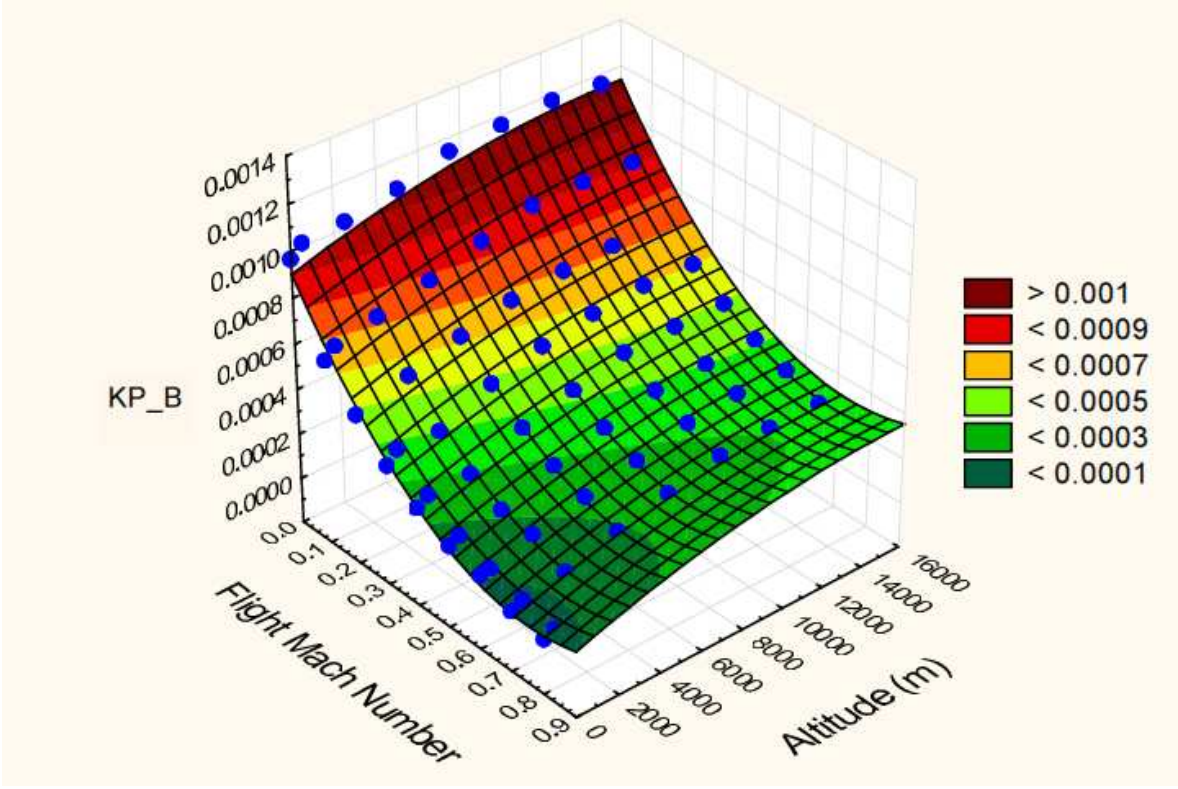

Figure 6-9: IP bleed-air extraction penalty (3-D) representation

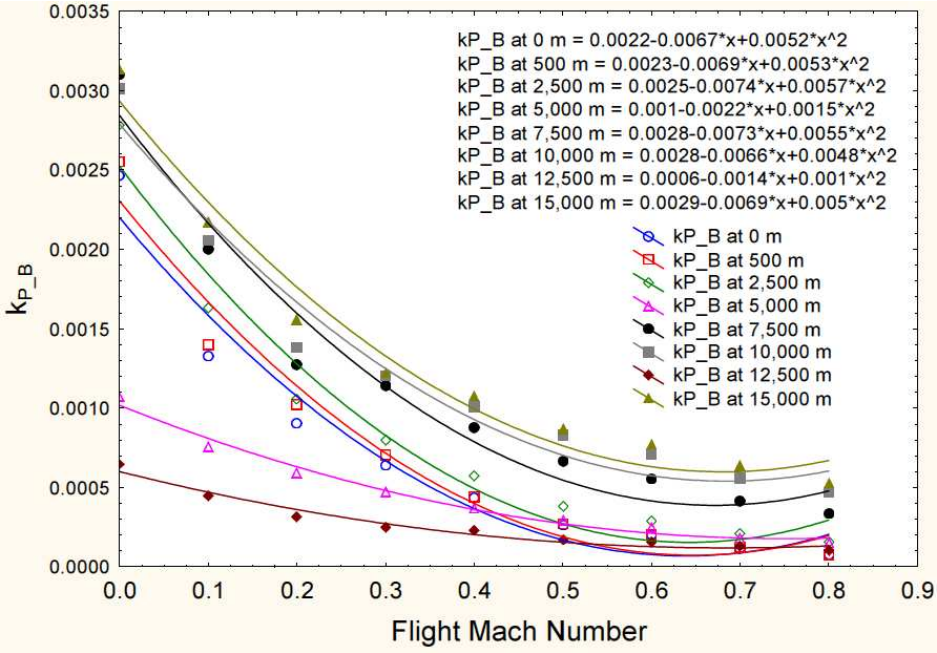

Figure 6-10: HP bleed-air extraction penalty (2-D) representation

The results for the HP bleed air extraction penalties can be summarised as;

$$k_{P\_B} = 0.0021 - 0.0059M - (7.4079 \times 10^{-9})h + 0.0043M^2 + (3.1755 \times 10^{-8})Mh + (9.9335 \times 10^{-13})h^2 \quad (30)$$

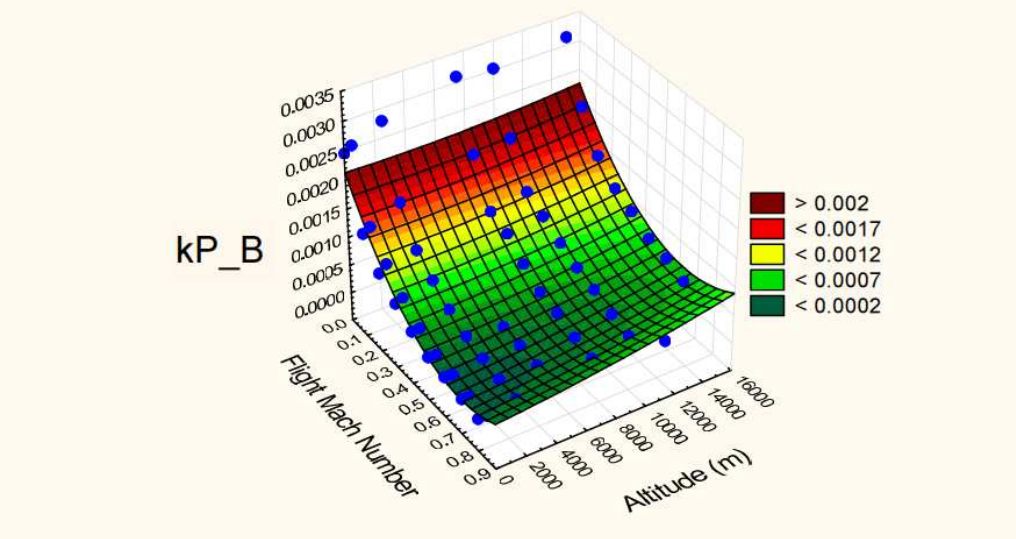

Figure 6-11: HP bleed-air extraction penalty (3-D) representation

The findings suggest that the variation of the "impact due to bleed-air extraction" can be expressed as a function of the altitude and flight Mach number. This is plotted in Figure 6-10

and Figure 6-11. A further analysis was conducted to compare the penalties between the different stages of bleed air extraction. This is shown in Figure 6-12.

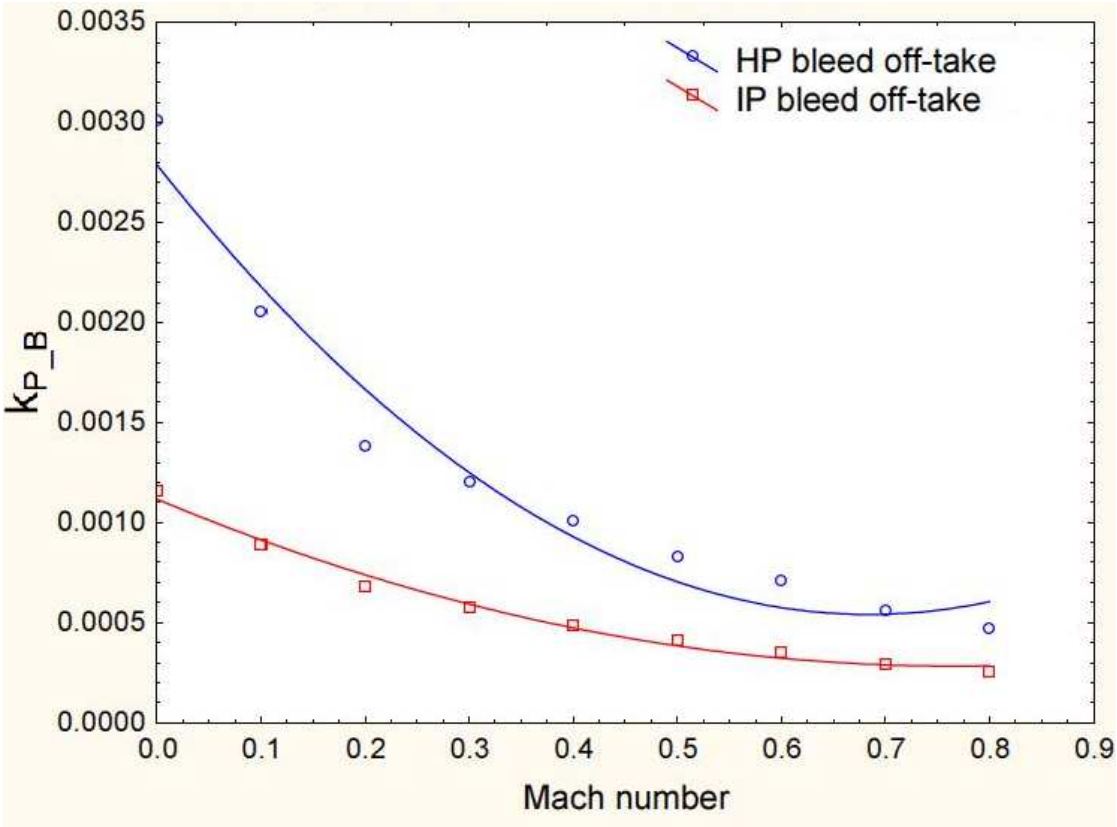

Figure 6-12: Comparison of the "*bleed-air* extraction *impact*" from different stages of the engine at 10,000 m

These findings suggest that for this particular engine, extracting bleed-air from the IPC is more efficient than extracting air from the HPC. However, as the Mach number increases (see Figure 6-12), the curves show trends of convergence, from which it could be inferred that the difference in the penalties decreases.

The results also give an indication to the sensitivity of the engine to off-takes. In the HPC, at low flight Mach numbers, the maximum bleed-air that can be extracted is limited. The penalties caused in these conditions are significantly higher than the numerical formula would predict. This suggests that at the operating limits of the engine, especially under very high or very low operating speeds, the engine is more sensitive to power extractions than at other conditions.

6.3.2 Shaft power off-takes

Shaft power was extracted from the LP, IP and HP shafts of the engine. The summary of the findings are shown in Figure 6-13 to Figure 6-16.

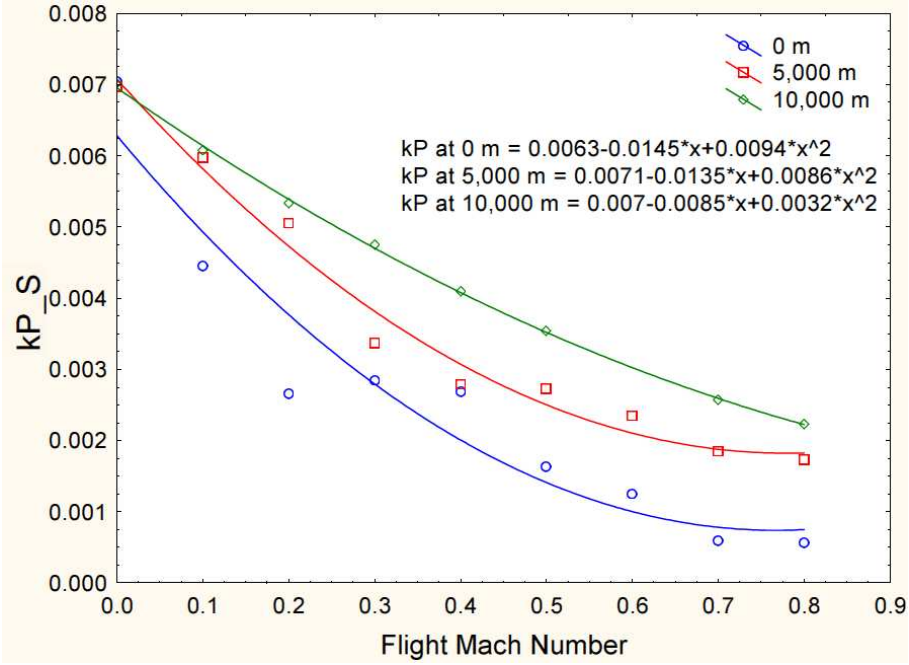

Figure 6-13: HP shaft off-take extraction penalty (2-D) representation

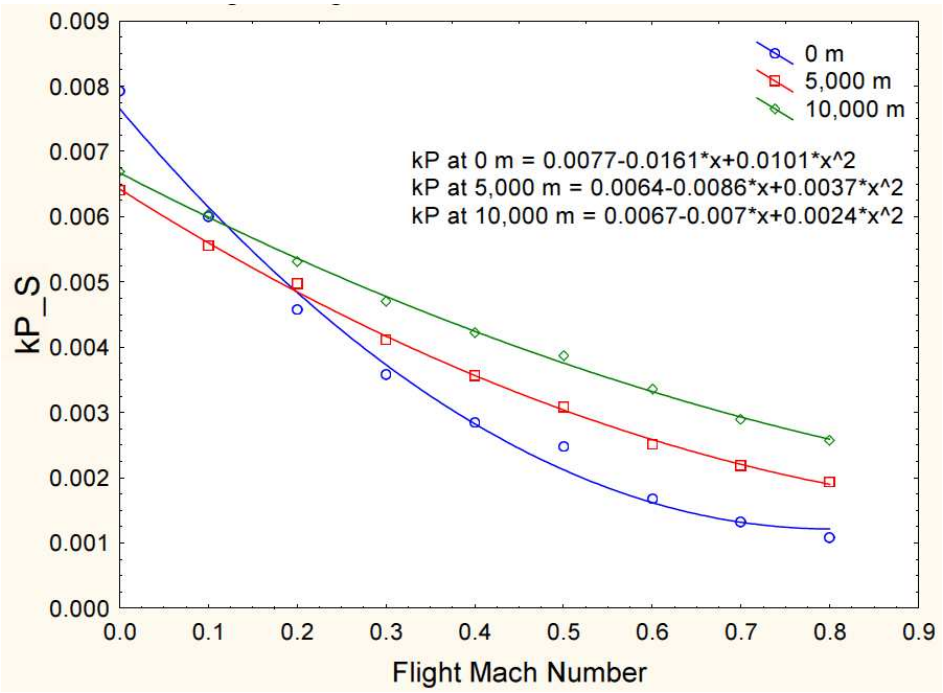

Figure 6-14: IP shaft off-take extraction penalty (2-D) representation

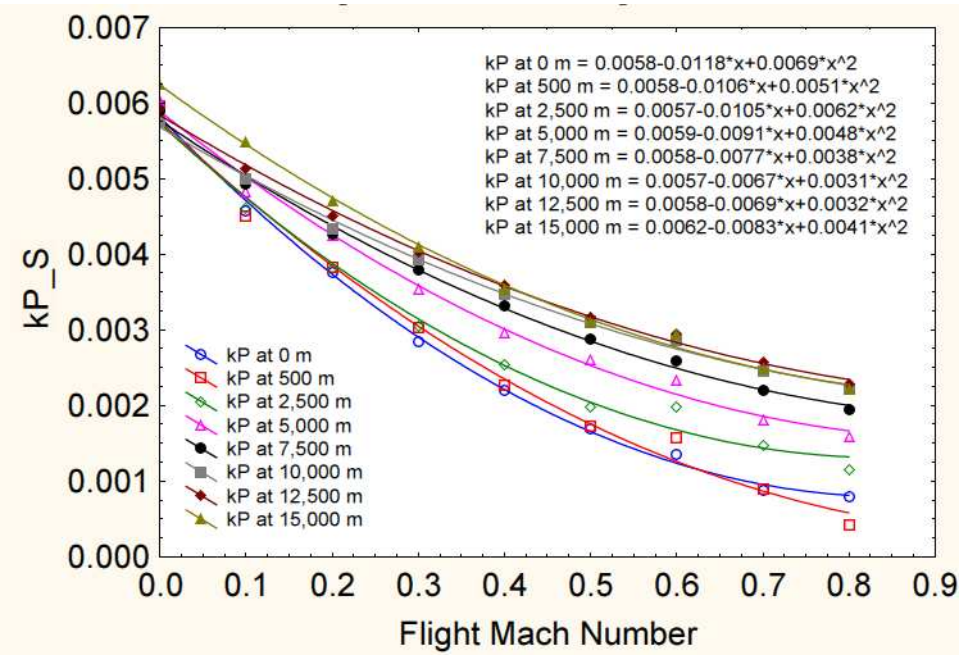

Figure 6-15: LP shaft off-take extraction penalty (2-D) representation

In summary, the following relationships can be derived.

HP shaft off-takes;

$$k_{P\_S} = 0.0061 - 0.0126M + (1.9751 \times 10^{-7})h + 0.0071M^2 + (1.0159 \times 10^{-7})Mh - (7.2301 \times 10^{-12})h^2 \quad (31)$$

IP shaft off-takes;

$$k_{P\_S} = 0.0071 - 0.0121M - (8.1519 \times 10^{-8})h + 0.0054M^2 + (2.9455 \times 10^{-7})Mh + (5.4392 \times 10^{-12})h^2 \quad (32)$$

LP shaft off-takes;

$$k_{P\_S} = 0.0055 - 0.0098M + (1.0572 \times 10^{-7})h + 0.0046M^2 + (1.2261 \times 10^{-7})Mh - (4.8865 \times 10^{-12})h^2 \quad (33)$$

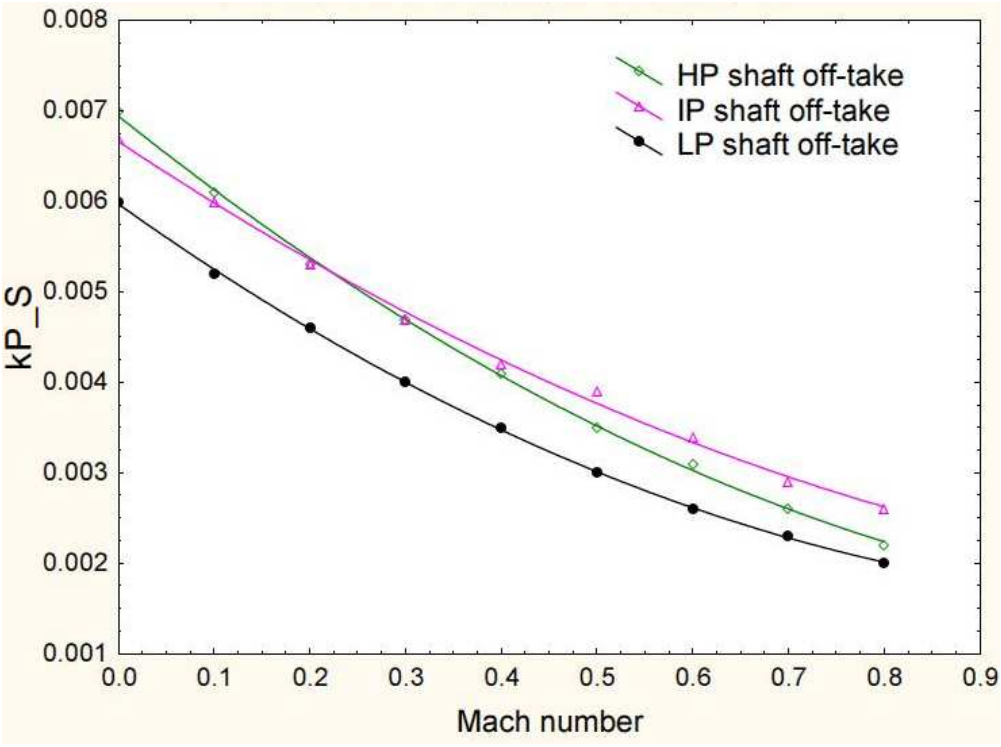

Figure 6-16: Comparison of the "*shaft power extraction* impact" from different shafts of the engine at 10,000 m

The results in Figure 6-16 suggest that, the LP shaft power extraction offers the least penalty over a majority of the flight envelop and is especially true for typical cruising altitudes for large commercial turbofan aircraft as shown in Figure 6-16.

6.4 Verification

The numerical method was verified for its robustness and accuracy by applying it to other commercial turbofan engines. The GE90-85B by General Electrics, regarded as one of the larger commercial turbofan engines and the Snecma CF56-5B2 which is at the other end of the spectrum in terms of thrust rating, were chosen. Random performance points were defined which included extremes for the bleed off-takes and shaft off-takes as well as combined off-takes of bleed and shaft power. These points are listed below in Table 6-1.

Table 6-1: Control points for testing generalness and applicability

Altitude (m)	Mach number	ISA deviation (K)	Net thrust (N)	Bleed air (kg/s)	Shaft power off-take (kW)
GE-90-85B					
0	0.2	10	167813.4	1.061	100
3000	0.45	-10	163861	0	120
6000	0.6	0	119963.6	4.96	0
8000	0.77	0	115918	0.48	200
10000	0.89	25	79958	0	1500
CFM56-5B2					
0	0.2	10	56707.12	0.401	100
3000	0.45	-10	51550	0	120
6000	0.6	0	32046.98	2.483	0
8000	0.77	0	28144.33	0.926	200
10000	0.89	25	12914.68	0	1500

The performance conditions were tested using TURBOMATCH, to establish the benchmark specific fuel consumption. The numerical method was then applied to the engines under the same performance conditions to calculate the SFC with off-takes. The results are tabulated below in Table 6-2;

Table 6-2: Results of generalness and applicability tests

TURBOMATCH SFC (mg/N.s)	Numerical k_P method SFC (mg/N.s)	Deviation%
	GE-90-85B	
9.19648	9.17433	-0.24
11.9949	11.953	-0.35
14.7734	15.8609	7.36
15.987	15.879	-0.68
18.2905	18.1799	-0.6
	CFM56-5B2	
11.8593	11.6335	-1.9
13.7649	13.6805	-0.18
17.1746	15.4523	-10.02
17.859	17.32	-3.02
24.8634	25.1914	1.32

The results show that the numerical method can consistently predict the specific fuel consumption with a satisfactory level of accuracy. The largest deviation is observed at the control point where the largest bleed extraction is made.

6.5 Implementation

The method discussed in this research is a set of equations, hence it can be efficiently implemented in design and optimisation problems without compromising simulation run times. Moreover, the method has been tested over a vast performance envelopes and the accuracy has been proven against fully fledged gas turbine performance codes. Due to the simplicity of the method, it can be coupled with complex gas turbine performance codes, or with estimation methods which predict the engine SFC (without any off-take), to then be corrected for off-take extraction. The work here was done with the intention of representing airframe systems penalties in trajectory optimisation problems. But the method can also be used in preliminary

aircraft sizing (to estimate range with systems off-takes), airframe systems design and analysis, and aircraft engine design.

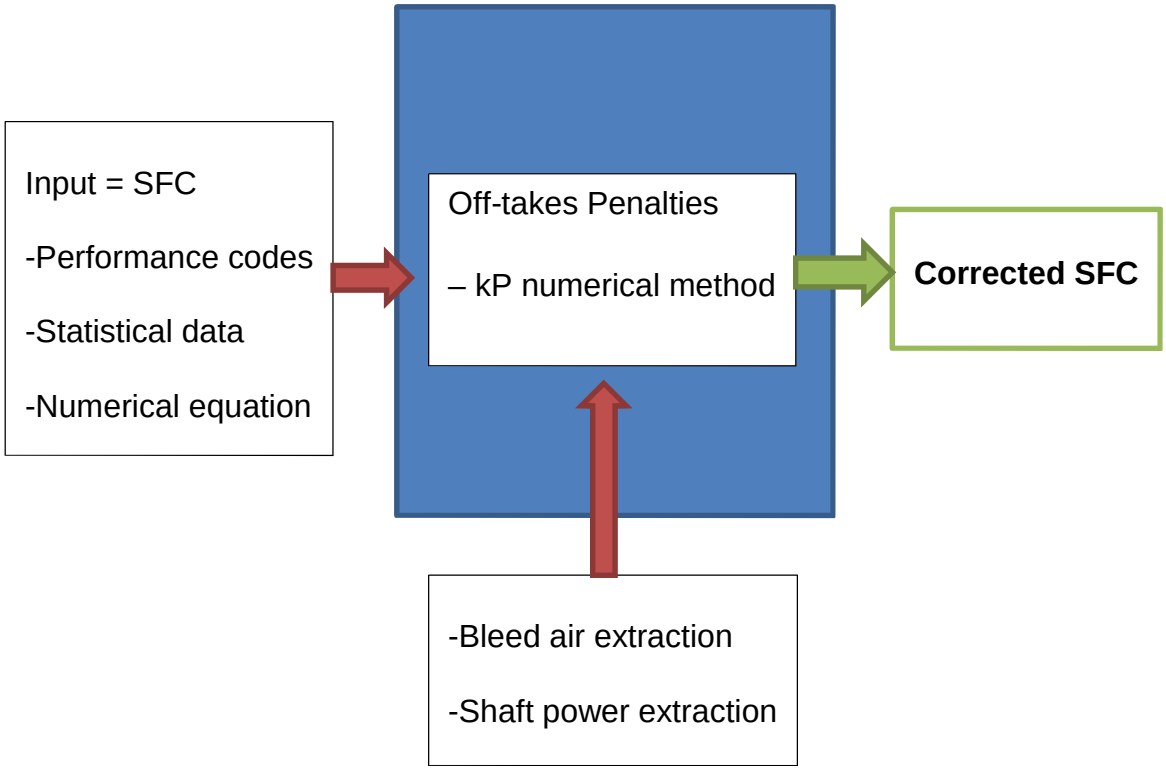

Figure 6-17: Implementation of k_P method

6.6 Summary

The extensive simulations provided a numerical solution to predict the bleed air off-take and shaft power off-take fuel penalties in large commercial turbofan engines. The work gave an insight to the behaviour of turbofan engines when there are power off-takes. It also gives an indication of penalties associated to off-takes. The numerical method developed, can be coupled with generic SFC equations and used as a substitute for high fidelity performance codes, in computationally time exhaustive applications such as trajectory optimisation. This will also give the ability to definitively establish whether the “more electric aircraft” has a significant advantage for various flight missions.

7 Airframe Systems Performance and Power Off-take modelling in Conventional and More-Electric Large Commercial Aircraft for Use in Trajectory Optimisation within the GATAC Framework

The power to operate the airframe systems is extracted from the aircraft engines. Commercial turbofan aircraft engines provide shaft power and bleed air power which is regulated and converted as required to operate the airframe systems. These power extractions can have a significant fuel penalty on the engines. [81] The magnitude of the effect depends on the amount of power extracted, the operating conditions of the engine the type of power extracted and also the point of power extraction within a turbofan engine.

The amount of power extracted is a function of the airframe systems and the functionalities within. The operating conditions of the engine are closely related to the aircraft flight and thus the aircraft trajectory. The point of power extraction is usually a design parameter and is not discussed within the research scope here. The type of power extracted typically depends on the configuration of the airframe systems. An aircraft equipped with an all-electric secondary power system would only require shaft power extractions from the aircraft engine.

Hence the effect of the airframe systems on the trajectory is quite complex and cannot be generalised. The type of trajectory flown and the configuration of the secondary power system influence the power extractions, while the power extractions influence the fuel burn and thus trajectory optimisation. [74] shows that the conventional secondary power system and the more electric secondary power system are both influenced by the trajectory flown. The more electric secondary power system is affected more than the conventional system. More importantly, it was established that the systems influence the trajectory optimisation.

This has been the motivation for the methodology discussed in this research which aims to provide airframe systems models which can be easily integrated with aircraft dynamics models and optimisation frameworks.

7.1 Classical approach to trajectory optimisation

The classical approach to trajectory optimisation has been typically to use an optimiser coupled with aircraft performance/dynamics models, fuel flow models and emissions models. In this sense the airframe systems impact is not accounted for. This research focuses on developing models which can be integrated within the optimisation loop as shown in Figure 7-1, thereby

enhancing the classical approach. It also gives the ability to define the “more electric aircraft trajectory optimisation” problem.

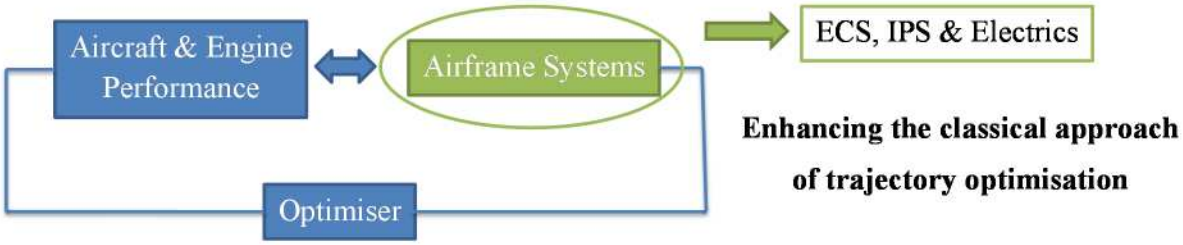

Figure 7-1: Enhanced approach to aircraft trajectory optimisation

7.2 Methodology

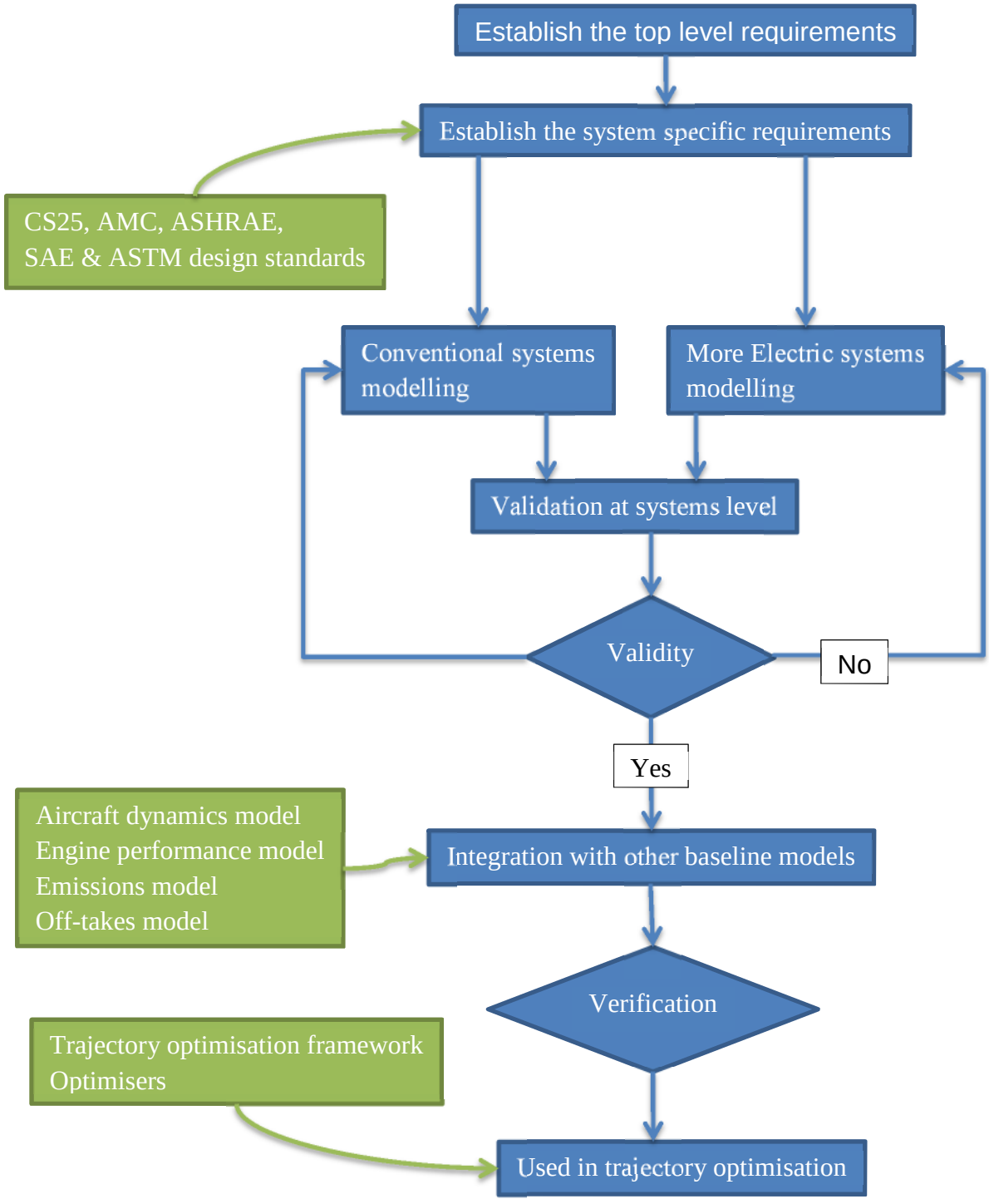

Figure 7-2: Modelling methodology

The methodology which was applied in the modelling process is shown in Figure 7-2. A top level requirements study for the airframe systems model was carried out to identify which systems were to be modelled to achieve the research goal. Moreover, the characteristics to be

modelled were also established. The ECS, IPS and electrics were established as the key systems to be modelled. It was established that the performance characteristics in terms of energy usage should be the key focus in each model. The actuators were not taken into account due to the instantaneous nature of power usage. The same is true for intermittent loads in the electrical system which last for less than 5 minutes once activated.

The systems specific requirements were based on certification standards which affected the energy usage of the overall systems. Aspects such as reliability or safety were not modelled unless they had a direct impact on the power usage of the system.

Both more electric and conventional systems were modelled so that comparative studies could be performed. The performance of the systems was validated with published data. The integration with other models and the optimisation framework was a key driver in establishing the software requirements for the integrate systems model. From the onset the modelling approach was driven by the requirements of execution speed and ease of integration.

7.3 Airframe systems model

The baseline for the airframe systems model was a 180 passenger twin engine turbofan short haul aircraft which was similar to the Airbus A320. The objective of the airframe systems models was to provide the bleed air requirement and shaft power requirement to operate the secondary power system at any given operating condition. As mentioned, the ECS, IPS and the electrics were modelled in detail to represent the majority of the power requirement within the secondary power system.

The model was constructed in Matlab/Simulink and converted to a dynamic link library in order to improve execution times and integration capabilities. This model was based on the preliminary systems performance modelling discussed in §4.2. The overall specification for the airframe systems model is documented in [82] and the software description is documented in [83].

7.3.1 Environmental control system

The main function of the ECS is to provide a comfortable environment for passengers, crews and avionics equipment. In order to achieve these requirements several sub-systems built in the system. The different sub-systems include;

- Ventilation

- Thermal regulation
- Pressurisation and control
- Humidity control
- Avionics ventilation
- Indication
- Emergency ram air systems
- Distribution control
- Supplemental cooling

The ventilation, pressurisation and thermal regulation sub-systems are the main drivers in terms of the ECS power usage.

A conventional ECS is principally integrated with four sections; the air or pneumatic energy sources, the air conditioning pack, the cabin and the control unit. Other components like filters, intakes and ozone reduction packs are included in the ECS conditioning pack. Such components do not represent a considerable impact on the thermodynamics and it can be assumed that these equipment do not affect the performance in terms of power requirement; specifically the bleed air mass flow requirements. The pneumatic energy source provides the flow with an internal energy, which can be measured in terms of mass flow for thermal balance calculations. This mass flow is associated with the respective temperature, pressure and density. Depending on the type of pneumatic source and the mission status, the mass flow can be delivered with different characteristics. The pneumatic energy source in the conventional aircraft could be the engine, an Auxiliary Power Unit (APU) or a ground services cart when the aircraft is stationary at the airport.

The CS25 standards clearly specify the minimum requirements for ventilation in order to provide a safe environment for the passengers and crew. CS25.831, AMC25.8319(a), CS25.831[B(2)] and CS25.841 were some of the airworthiness requirements that were considered in the modelling approach.

Moreover, Commercial airplanes normally fly over a wide range of operating temperatures ranging from -70°C to +50°C or more. As per the recommendation of ASHRAE 55-1992 the comfort zone for human being lies between 19.5°C to 27°C.

The cabin pressurisation and control system is mainly required to isolate the occupants from low pressure effects. Low pressures associated with high altitudes leads to health related disorders such as hypoxia, hypothermia, and decompression sickness.

7.3.1.1 ECS – conventional

The conventional model was based on an air cycle systems which would use bleed air from the aircraft engines as the primary power source. This is a typical configuration which is commonly found on large commercial aircraft. The modelling focused on the required mass flow rate for adequate ventilation, pressurisation and thermal regulation.

The model included the following sub-modules;

- Mass flow calculation as per the ventilation requirements
- Calculation and control of the cabin altitude
- Calculation of the cabin heat loads
- Mass flow calculation for thermal regulation
- Modelling of the mixing manifold with provision for re-circulation

Detailed modelling of the dynamics in the ECS conditioning pack was avoided and assumptions were made to simplify the modelling. The main simplification was that the cabin inlet temperature of the flow was set as an input variable rather than an output of the ECS conditioning pack.

This was adequate for this research since, the objective was to quantify the overall power requirement rather than the performance characteristics of the ECS. The ECS model had the following inputs;

- Operating altitude
- Flight Mach number
- ISA deviation of temperature
- Maximum number of passengers for the aircraft variant
- Airframe systems thermal load
- Night or day (for the calculation of solar radiation)
- Cabin temperature
- Cabin inlet temperature
- Cockpit window area
- Windscreen heat exchange co-efficient
- Cabin window area
- Cabin window heat exchange co-efficient
- Cabin wall area
- Wall heat exchange co-efficient
- Metabolic heat load per crew
- Number of crew
- Metabolic heat load per passenger

- Temperature of air at the bleed regulation valve
- Re-circulation %

The kinetic heating, solar radiation, systems heat loads, passenger and crew heat loads and avionics heat loads were considered in the thermal regulation calculation. The necessary thermal regulation was achieved applying the steady state energy balance equation, which is reported as follows):

$$\dot{m}_a C_p(T_i - T_e) - U.A(T_c - T_s) + H_s + H_p + H_e = 0 \quad (34)$$

The ECS model was validated using data obtained from [68]. An ECS system (with re-circulation) with similar requirements to an Airbus A320 (150 passenger) variant was simulated (at a cabin pressure of 1 atm and an average cabin temperature of 293 K) and the difference in the "*ventilation capacity per passenger (L/s)*" was observed as 2.31%. The same was done for an ECS (without re-circulation) with similar requirements to a Boeing 727-100 ECS and the deviation was observed as 1.6%.

Moreover, [81]provides data for off-takes for an Airbus A320 flight from Hamburg to Toulouse. The ECS model was configured to represent a similar model to the A320 ECS and simulated to perform a comparison study. Since there was uncertainty as to the average cabin temperature, a range of between 293 K and 298 K was simulated. Initial experimentation with the ECS model showed that the cabin temperature influenced the ECS power requirement more than some others, hence this approach was followed. After experimentation with the cabin inlet and average temperatures (shown in Table 7-1), the inlet temperature was fixed to 275 K and the cabin average temperature was set at 295 K.

Table 7-1: ECS comparison study

Simulated Cabin T (K)	Calculated bleed flow requirement (kg/s)	Deviation %
Climb (1,500 ft to 31,00 ft), maximum HP compressor off-take = 0.710 kg/s		
293	0.7683	8.21%
295	0.7186	1.21%
298	0.6605	6.97%

Cruise (31,00 ft at M=0.78), HP compressor off-take = 0.481 kg/s		
293	0.5635	17.15%
295	0.4965	3.22%
298	0.4181	13.08%
Approach (1,500 ft to ground), maximum HP compressor off-take = 0.429 kg/s		
293	0.4814	12.21%
295	0.4227	1.47%
298	0.3539	17.51%

The results suggest that at a cabin temperature of 295 K, the flow requirements agree very well with the measured data from Airbus.

7.3.1.2 ECS – more electric

The system requirements for the more electric ECS were similar to those of the conventional ECS. The ventilation, pressurisation and thermal regulation requirements were set to be the same. The difference was the source of power; the electrical ECS comprised of an electrically powered compressor to draw and compress ram air rather than extracting bleed air from the engine. The air mass flow calculation remained the same as the conventional ECS. The electrical compressor was modelled in a simplified manner to represent only the compressor work needed to supply the required mass flow.

The equations used to represent the electrical compressor work is stated in § 5.4.

The efficiency of the heat exchanger was assumed to be constant. A major simplification of the modelling was that the aft temperature of the compressor was set as equal to the regulated bleed temperature of the conventional ECS. This simplification meant that the two systems, the more electric ECS and the conventional ECS, had similar performance constraints and that the overall system had comparable characteristics other than the source of energy. So the conventional and more electric baseline aircraft can be compared without having to make adjustments for major changes in design philosophy.

From [71] a benchmark for an electrical ECS power demand was derived. It suggested that for a typical hot day cruise at 40,000 ft, a typical electrical ECS will consume about 1.17 kW/per passenger for ventilation, pressurisation and cooling of the cabin.

The model developed calculated a ratio of 1.21 kW/per passenger for the baseline aircraft during a hot day cruise flight at 40,000 ft. It was a deviation of 3.8% thus the model was accurate to be used in further analysis.

7.3.2 Electrics

The aircraft electrical system requirements are heavily dependent on all other aircraft systems. The consumer components of the electrical system are solely dependent on other aircraft systems. The generation and distribution architecture is decided upon the technology level and power consumption of the components required for the systems. The ASTM F2490-05e1 (standard guide for aircraft electrical load and power source capacity analysis) sets the standard for the aircraft electrical system sizing. An example is given by the Civil Aviation Authority (CAA) UK in [49] and it can be seen that each component needs to be listed and then a full analysis carried out.

The electrical loads were derived by using a model developed for electrical load sizing and analysis described in §5 and documented in [84]. The tool was used to derive the electrical load profile so that it could be applied within the integrated model to represent the electrical generator loads. Engine shaft power off-takes provided the energy source for the electrical loads.

The electrical load sizing tool also gave inputs such as the airframe systems load and the avionics cooling load, for the ECS model. The airframe systems thermal load was calculated by analysing equipment in the cabin such as; the in-flight entertainment and galley equipment.

The conventional large aircraft has systems run purely on electricity as well as systems which require electrical power but use pneumatic or hydraulic power as the primary type of power. In the environmental control system equipment such as the re-circulation fans, many pressure regulating valves, the monitoring and controlling computers, and a variety of controllers are powered electrically. In the anti-icing system the anti-icing of probes, the wipers, the ice detectors, the anti-icing and de-misting of cockpit windows, and the operation of some valves

and most controllers, are powered electrically. Certain pumps and monitoring systems in the hydraulic system and fuel system are powered electrically as well.

The electrical model listed component loads for equipment in the following ATA chapters; ATA 36, ATA 21, ATA 22, ATA 23, ATA 25, ATA 27, ATA 28, ATA 29, ATA 30, ATA 31, ATA 32, ATA 33, ATA 34, ATA 35, ATA 38, ATA 45, and ATA 49.

The model developed in [84] has been validated at the systems level for a Boeing 777-300 using data in [70], at the aircraft level for an Airbus A300 using data in [27] and for a Lockheed L-1011 Tristar using data in [21].

In the more electric aircraft, the definition of the electric system covers all systems on board. The conventional electrics as well as the electric ECS, electric IPS, electric actuators contribute to the total electrical load.

7.3.3 IPS

The IPS was modelled based on the Messinger method. The method utilises convection, sensible heating, evaporation/sublimation, kinetic energy, and viscosity terms in the conservation energy equation to find the equilibrium temperature of an unheated icing surface. A detailed description of the conventional IPS modelling philosophy, equations, validation and verification is listed in [85]. The electrical IPS modelling approach is described in [86].

Typically icing mostly occurs between 7,000 ft and 22,000 ft during flight. Icing heavily depends on the atmospheric conditions and predicting real weather icing clouds was beyond the scope of this study. So as a compromise, CS 25 Appendix C was used to formulate an artificial icing cloud. As a baseline, it was assumed that there would be an icing cloud between 7,000 ft and 10,000 ft at a uniform temperature of 253 K with a liquid water content of 0.23 g/m^3.

7.4 Integrated model

The integrated model consists of the Aircraft Dynamics model, Engine performance model, Airframe Systems Model, Emissions model and the Off-takes model. A modular approach was followed such that more models can be easily linked in future to form a comprehensive model which wasn't computationally exhaustive. The architecture of the integrated model is shown in Figure 7-3.

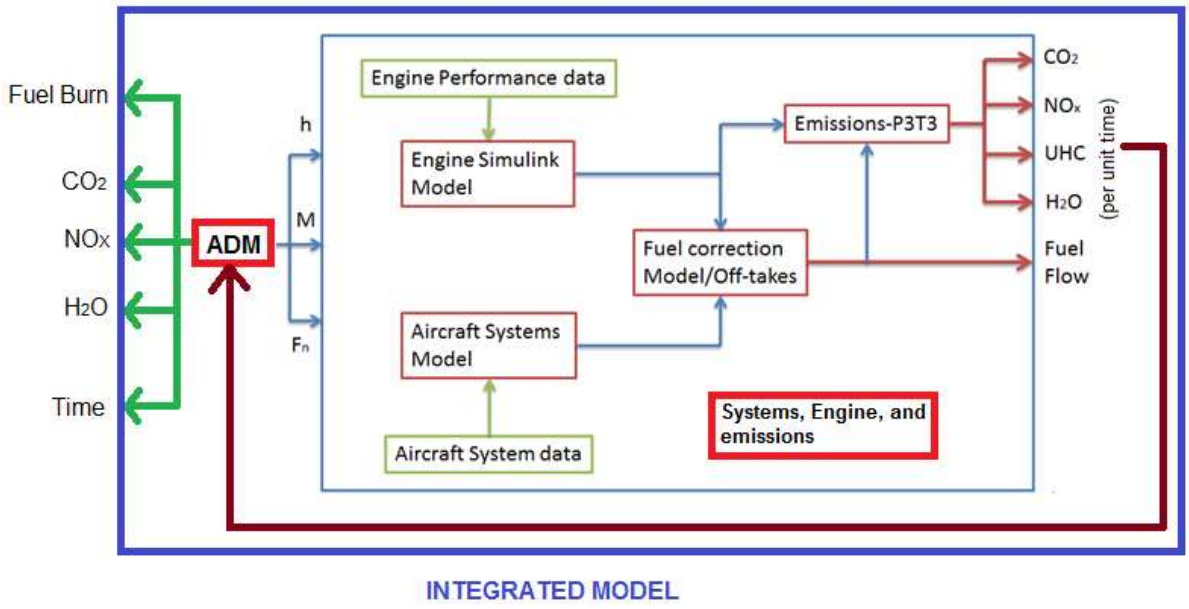

Figure 7-3: Architecture of the integrated model

7.4.1 Aircraft dynamics model

The Aircraft Dynamics Model (ADM) is capable of aircraft trajectory generation for a generic aircraft between two pre-defined positions in a 3D space. The generic aircraft is modelled using the rigid body idealisation with a varying mass under aerodynamic, propulsive and gravitational forces with assumption of symmetrical aircraft with thrust force parallel to the aircraft motion. In addition the assumptions of spherical, non-rotating Earth and no wind atmosphere are also introduced to simplify the problem. The aircraft motion is described by using point mass with three degrees of freedom and the resulting differential algebraic equations are listed in (35).

$$\begin{cases} m\dfrac{dV}{dt} = T - D - mg\sin(\gamma) \\ mV\cos(\gamma)\dfrac{dX}{dt} = L\sin(\mu) \\ mV\dfrac{d\gamma}{dt} = L\cos(\mu) - mg\cos(\gamma) \\ \dfrac{dm}{dt} = -c\,T \\ (R_E + h)\dfrac{d\varphi}{dt} = V\cos(\gamma)\cos(\chi) \\ (R_E + h)\dfrac{d\lambda}{dt} = V\cos(\gamma)\sin(\chi) \\ \dfrac{dh}{dt} = V\sin(\gamma) \end{cases} \tag{35}$$

The aerodynamic forces are modelled by drag polar characteristic provided by the BADA dataset [87] and the gravitational forces are modelled by using the International Standard Atmosphere (ISA) model with constant gravity acceleration.

The ADM generates 3D trajectories based on input variables. The baseline ground track of the aircraft is specified using waypoints (latitude and longitude). Altitude and aircraft speed are used as variables to generate trajectories. Several other parameters such as initial and final positions speed and aircraft initial mass are required set up an optimisation problem. The optimisation process will evaluate many possible trajectories by varying the trajectory input variables and refine the search by trying to minimise the specified objectives.

7.4.2 Interface with engine – Off-takes model

The power required for the airframe systems are extracted in terms of bleed air or shaft power from the aircraft engines in large commercial aircraft. This power extraction causes an increase in the fuel consumption. Accounting for these power extractions was identified as a key issue in this research.

The interface needed to be robust and calculate the fuel penalty by being independent of time. It also needed to calculate the penalty in a manner that detailed modelling of the engine components and efficiencies were not required. These requirements meant that methods suggested in [60] and [7] were not suited for the task. A new calculation approach was developed within the study which was established by studying the trends within turbofan engine performance which provided a method of calculating the fuel penalty due to off-takes based on the aircraft operating conditions, engine operating conditions and systems operating conditions. The initial findings and formulae are presented in [81]. The methodology of the off-takes are explained in §6.

7.4.3 Engine and Emissions

Two turbofan engines were modelled for this research.

The first is a high by-pass ratio twin spool engine with a maximum static take-off thrust of 121 kN. The engine is capable of providing both bleed air and shaft power for secondary power systems. The engine performance was modelled such that it was similar to the CFM-56-5B4 turbofan engine which is used on the Airbus A320. The engine model was constructed in TURBOMATCH, which was developed at Cranfield University. TURBOMATCH is gas turbine

performance software developed for engine performance simulation and fault diagnostics in which the engine is modelled to a very high detail. The high detail of modelling and computational accuracy has a significant computational penalty. In order to have the optimum balance of accuracy and executional speed, the engine was simulated over a vast envelop and the resulting database was incorporated in the Matlab/Simulink environment. Interpolation/extrapolation and polynomial evaluation techniques were used within the Simulink database to create a complete performance model of the engine.

The second engine was a high by-pass ratio (BPR of 6.4) turbofan engine which would be capable of producing 151 kN of thrust at sea level in ISA conditions at the maximum static take-off setting. This model is similar to the CFM-56-5C turbofan engine which is used on the Airbus A340. The same approach as for the 121 kN engine was followed in this instance. The off-design performance of the engine is shown is Figure 7-4.

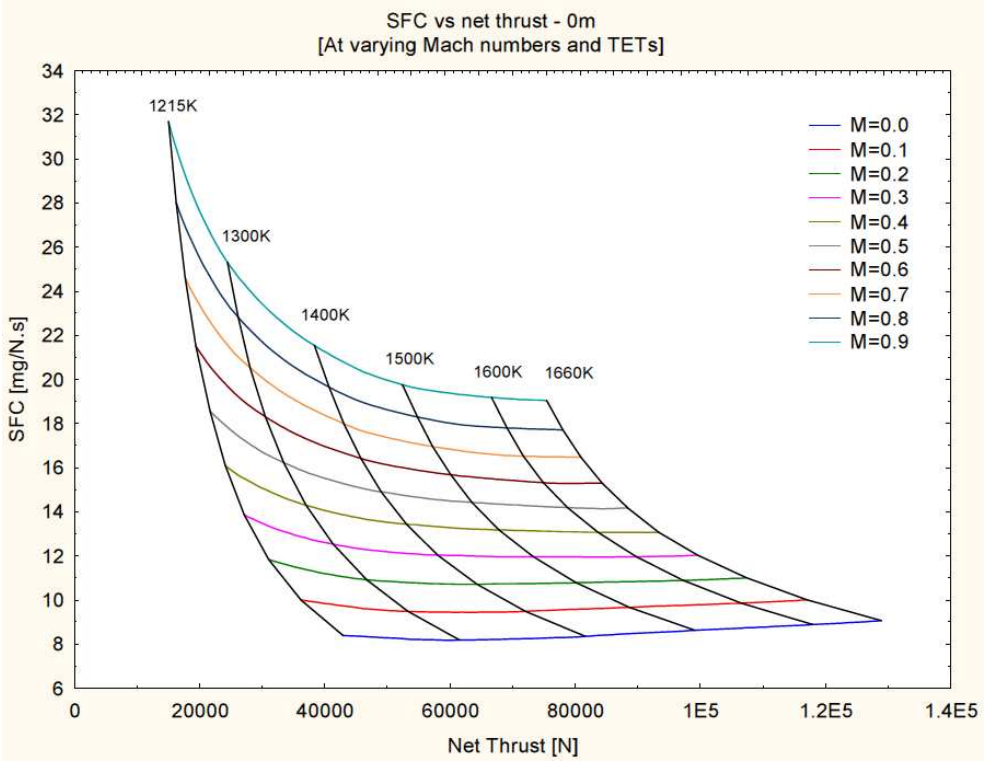

Figure 7-4: Off-design performance of the 151 kN engine

Initially three methods were considered for the emissions modelling. These included; the Boeing-2 Fuel Flow [88] method, the DLR Fuel Flow method [89] and the P3T3 method. For this study, the P3T3 method was implemented to analyses the emissions. The P3T3 method relies upon the pressure and temperatures at the combustion stage and uses a correction

based calculation method. The methodology is explained in [90] and [89]. The ground level indices for the emissions were taken from [91] for the short range aircraft engine and [92] for the long range aircraft engine.

7.5 Other models and tools

7.5.1 INMTM noise model

The INMTM noise model calculates the noise exposure on a user-defined grid below a flight trajectory. Four noise metrics which include the SEL, $L_{A,max}$, EPNL and PNLTM are used in the model. The model is based on the Integrated Noise Model developed by the FAA. [93]

The INMTM noise model is coupled with a user-defined population grid which gives the capability to calculate the number of “awakenings” due to the noise exposure. In the scope of the trajectory optimisation for noise, the number of awakenings is an important parameter since it relates directly to the environmental impact.

7.5.2 D3 tool

The D3 model exploits demographics data from standard publically available demographic databases and formats the data such that it can be used with the INMTM noise model. It manipulates data and transforms the latitude, longitude and altitude to local co-ordinates thereby creating a population grid to be used with the noise calculation model. [94]

7.6 Results

In order to test the behaviour of the integrated model throughout the flight envelope a test case with conventional systems on-board, was devised. The flight profile is shown in Figure 7-5 and Figure 7-6. The flight profile was based on a real aircraft flight on the 14th of April 2014, between Heathrow and Schiphol. The baseline icing condition (see §7.3.3) as well as the baseline ECS cabin configuration (see§7.3.1.1) was used in the simulations.

The ADM was set to represent an A320 using BADA aerodynamic co-efficient. The airframe systems were configured to represent a similar secondary power system to that of the A320 and engine which is similar to the CFM-56-5B4 was used.

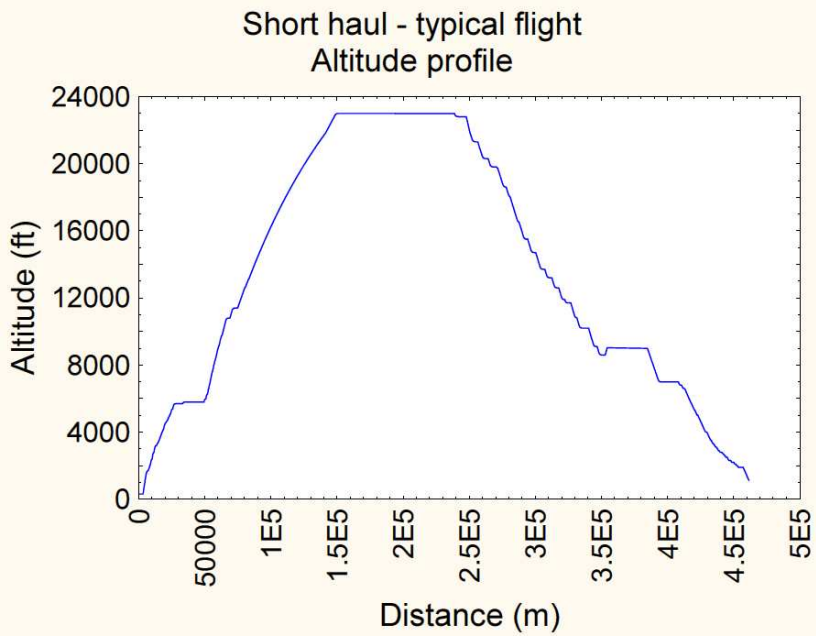

Figure 7-5: London to Amsterdam typical flight; Altitude profile

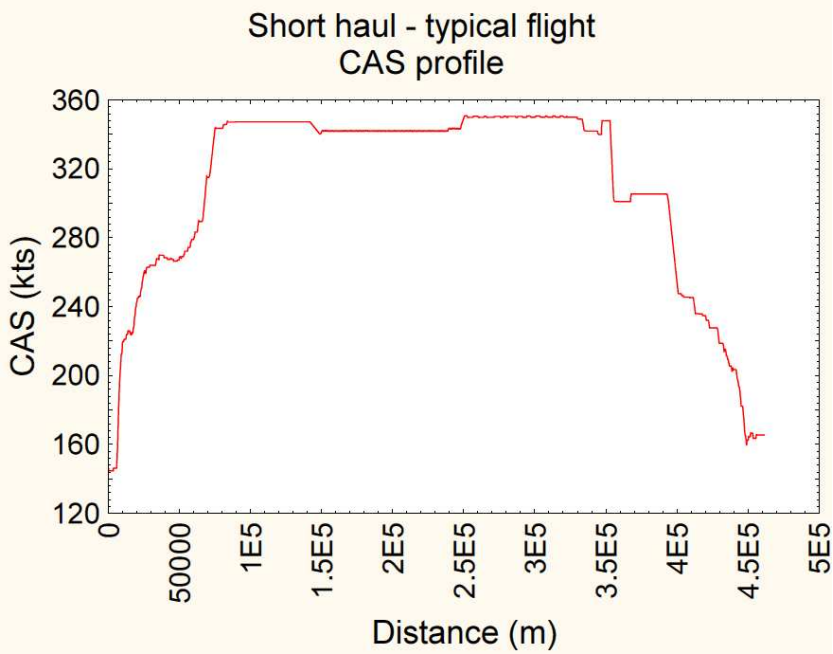

Figure 7-6: London to Amsterdam typical flight; CAS profile

Table -7-2: Results summary of a typical flight

Trajectory definition	Fuel burn (kg)	Flight time (s)	Increase in fuel burn due to systems
Zero power off-takes	2330	2575	

With conventional systems	2565	2575	10.1%
MEA	2352	2575	0.9%

The conventional systems causes an 10.1% increase in fuel burn for this particular trajectory.

With the more electric systems the total fuel burn was calculated as 2352 kg which was 9.2% less than the conventional systems.

For the departure phase of the flight shown above, the effects due to the systems were significantly different when compared with the en-route and arrival phases. The conventional configuration increased the fuel burn by 1.82% and the more-electric configuration increased the fuel burn by 0.38%. This was a clear indication that the flight conditions effect the systems operation and hence the penalty due to systems operation.

When comparing the “approach” to trajectory optimisation, the baseline case is the “zero power off-takes” in which, the airframe systems power off-take penalties are not accounted for within the problem definition. For the comparison of the gains achieved by trajectory optimisation, the baseline cases are configuration dependant.

7.7 Summary

A robust methodology to model the airframe systems penalties within the trajectory optimisation scope has been presented in this research. The effect on systems due to the flying conditions and the airframe technology level has been demonstrated.

Moreover, the study clearly demonstrated the need for the representation of the airframe systems penalties within the optimisation loop. It established and defined the problem; “*more electric aircraft trajectory optimisation*”.

8 Results and discussions

This section presents the final results of the research. It presents the gains that are achieved by including airframe systems penalties within the optimisation loop and compares the optimum flight operations for conventional and more-electric aircraft in terms of fuel burn, flight time and emissions.

8.1 Case study – short haul

8.1.1 Aircraft, engine and systems set-up

The baseline aircraft and engine for the short haul study was similar to the Airbus A320 (150 passenger variant) and the CFM-56-5B. The operational environment for the airframe systems were set according to the baseline conditions described in §7 and the systems were similar to the A320 systems.

8.1.2 Framework and Optimiser Setup

GATAC trajectory optimisation software framework was used to run the simulation. GATAC has a set of optimisers which include a genetic-based optimiser called NSGAMO, and a multi-objective tabu-search (MOTS) and also an hybrid optimiser. For this study the NSGAMO was used.

The setup is as follows:

- The flight trajectory was divided into three phases. Each flight phase was optimised with and without considering airframe systems power off-take penalties
- Optimiser used: NSGAMO (Genetic Algorithm developed by Cranfield University and based on NSGA-2 algorithm)
- Optimisation objectives were fuel burn and flight time for all three flight phases.

Table 8-1: Conditions of the optimisation studies

Flight phase	Objective 1	Objective 2	Generations	Population	Initialization factor
Departure	Fuel	Time	250	100	50
En-route	Fuel	Time	250	100	50
Arrival	Fuel	Time	250	100	50

The starting mass for the aircraft was;

- At the start of departure – 66,000 kg
- At the stat of the en-route – 65,406 kg
- At the start of the arrival – 63,000 kg

8.1.3 Mission route

The mission case chosen for this study is from London Heathrow (LHR) airport to Amsterdam Schiphol (AMS) airport. The mission was divided into three flight phases (departure, en-route and arrival). Departure phase begins at 83ft (Above Ground Level) AGL with an airspeed of 140 kts and terminates at the end of the Standard Instrumental Departure (SID). The SID selected for the departure phase is BPK7G.

Figure 8-1: Short haul ground track

Table 8-2: Departure way points and constraints – short haul

WP name	Latitude	Longitude	Altitude min/max (ft)	CAS min/max (kt)
LHR	51 27 53.25 N	000 28 54.99 W	83	140
WP2	51 27 52.51 N	000 31 35.75 W	83/10,000	140/310
WP3	51 31 08.00 N	000 40 38.00 W	83/10,000	140/310
WP4	51 35 07.13 N	000 36 29.69 W	83/10,000	140/310
WP5	51 37 23.00 N	000 31 07.00 W	83/10,000	140/310

BPK	51 44 59.00 N	000 06 24.00 W	10,000	310

The en-route phase starts after the aircraft has reached the BPK VOR waypoint and ends when the aircraft enters the Amsterdam Schiphol STAR procedure. During this phase a minimum altitude of FL100 and a maximum of FL390 are used. These bounds give the optimiser the freedom to choose an optimum flight level within both lower and upper airspaces. The airspeed during the en-route is limited to KCAS 310 for the lower boundary and by the maximum operation Mach number for the upper boundary. The route selected for the en-route is shown in Table 8-3.

Table 8-3 : En-route way points and constraints - short haul

WP name	Latitude	Longitude	Altitude min/max (ft)	CAS min/max (kt)
BPK	51 44 59.00 N	000 06 24.00 W	10,000	310
WP6	51 46 30.00 N	000 11 48.00 E	10,000/39,000	310/400
WP7	51 46 45.00 N	000 15 00.00 E	10,000/39,000	310/400
WP8	51 48 40.00 N	000 39 06.00 E	10,000/39,000	310/400
WP9	51 49 19.00 N	000 47 39.00 E	10,000/39,000	310/400
WP10	51 50 55.00 N	001 08 51.00 E	10,000/39,000	310/400
WP11	51 54 19.00 N	001 25 33.00 E	10,000/39,000	310/400
WP12	52 06 52.51 N	002 29 16.61 E	10,000/39,000	310/400
WP13	52 26 52.00 N	003 25 15.00 E	10,000/39,000	310/400
SUGOL	52 31 31.00 N	003 58 02.00 E	10,000	310

The arrival phase starts when the aircraft passes over SUGOL and terminates at 2,000 ft AGL. The STAR used in this phase for Amsterdam Schiphol airport is RNAV-Night RWY06 and the entry altitude is set to FL100. The route and the related parameters for the arrival phase are listed in Table 8-4. The aerodrome charts are attached in Appendix D: Departure and Arrival charts.

Table 8-4 : Arrival way points and constraints – short haul

WP name	Latitude	Longitude	Altitude min/max (ft)	CAS min/max (kt)
SUGOL	52 31 31.00 N	003 58 02.00 E	10,000	310
WP14	52 25 20.00 N	004 23 16.00 E	2,000/10,000	150/310

WP15	52 14 14.00 N	004 21 51.00 E	2,000/10,000	150/310
WP16	52 12 33.00 N	004 27 45.00 E	2,000/10,000	150/310
WP17	52 12 28.00 N	004 31 35.00 E	2,000/10,000	150/310
WP18	52 13 14.00 N	004 33 27.00 E	2,000	150

8.1.4 Terminology used to discuss results

The terminology used in the section needs to be clarified.

- *Min. fuel* = Trajectory optimised for minimum fuel burn.
- *Min. time* = Trajectory optimised for minimum flight time.
- *Zero power off-take* = No account is made for systems power off-takes.
- *With systems power* = Conventional systems power off-takes are modelled in the optimisation.
- *Systems power post processed* = Conventional systems power off-takes are not included in the optimisation, but are added on in post processing.
- *MEA* = More-electric systems power off-takes are modelled in the optimisation.

8.1.5 Results and analysis – short haul flight

8.1.5.1 Departure results

Figure 8-2 shows the pareto fronts obtained at the end of the optimisations for the departure phase. It is possible to see that the setup with systems included is shifted to higher values of fuel consumption; this is obviously due to the consumption the systems introduce. However the results regarding the minimum time aren't so different between the two setups. It should be noted that better pareto fronts could be obtained by increasing the number of evaluations which the optimiser performs. However, the objective of the research was to reach acceptable pareto fronts with the ability to assess the impact of the airframe systems, therefore the optimiser settings where set equal for both the setups.

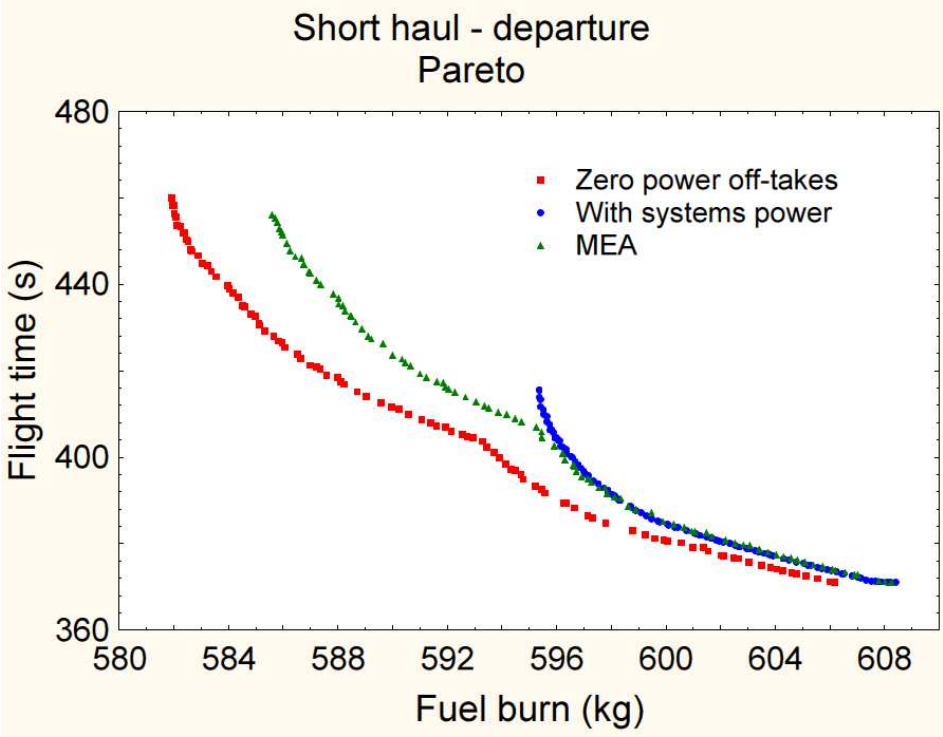

Figure 8-2: Pareto fronts - departure, short haul

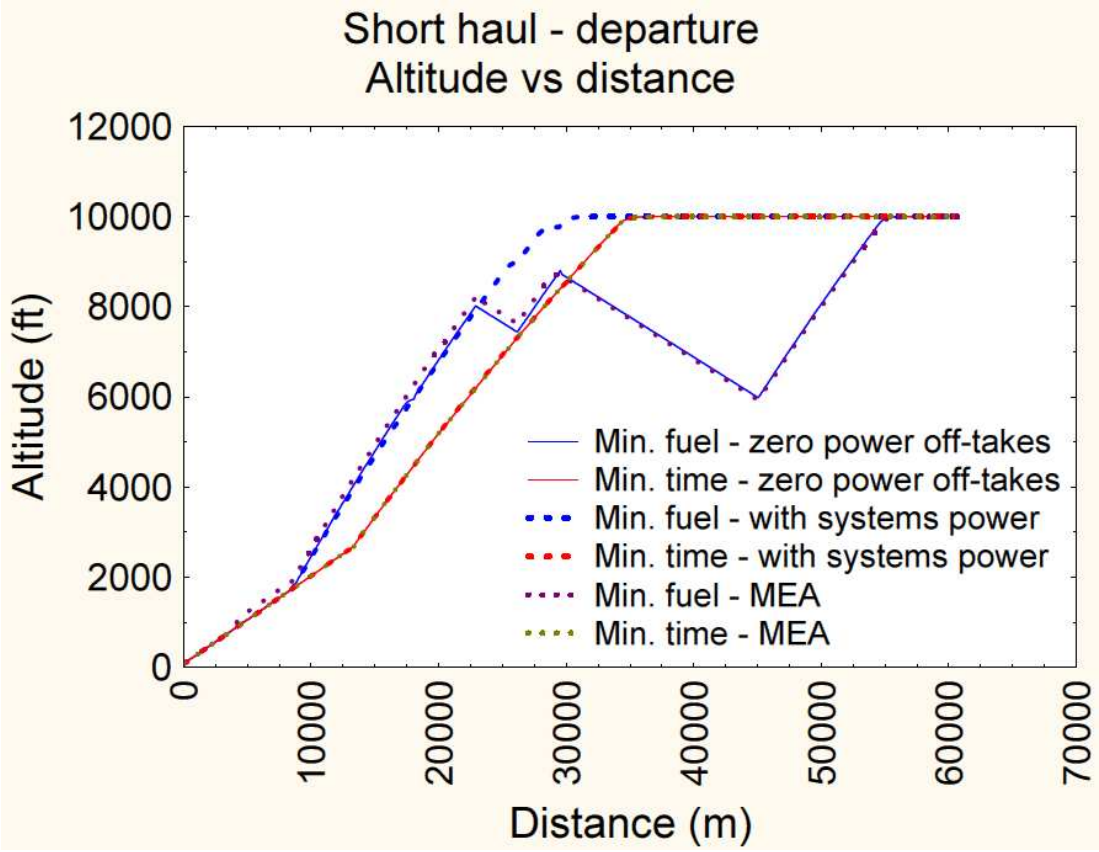

Figure 8-3: Altitude vs distance – departure, short haul

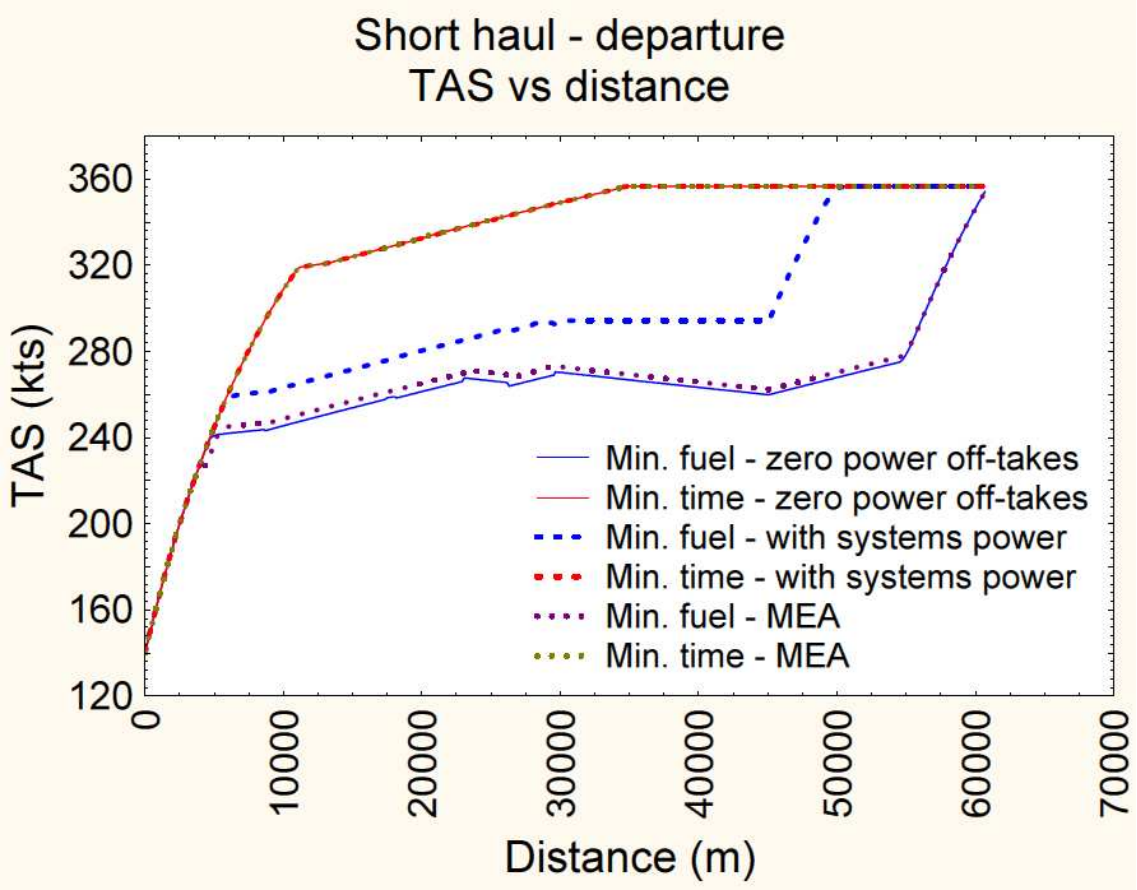

Figure 8-4: True air speed vs distance – departure, short haul

Figure 8-3 and Figure 8-4 show the aircraft altitude and aircraft true airspeed for the “Min. fuel” and “Min. Time” results. The “Min. fuel – with systems power” case climbs continuously to 10,000 ft and then flies level. It also flies faster at the beginning and it continuously at a higher speed than the other two cases. The “Min. fuel – MEA” and “Min. fuel – zero power off-takes” are similar. The “Min. fuel – MEA” flies faster than the “Min. fuel – zero power off-takes” case but both fly at a lower speed than the “Min. fuel – with systems power” and accelerate towards the end to meet the final conditions as specified.

There is a distinct difference in the “Min. fuel” trajectories. The reason for the difference is the effect of the systems, which is shown in Figure 8-5.

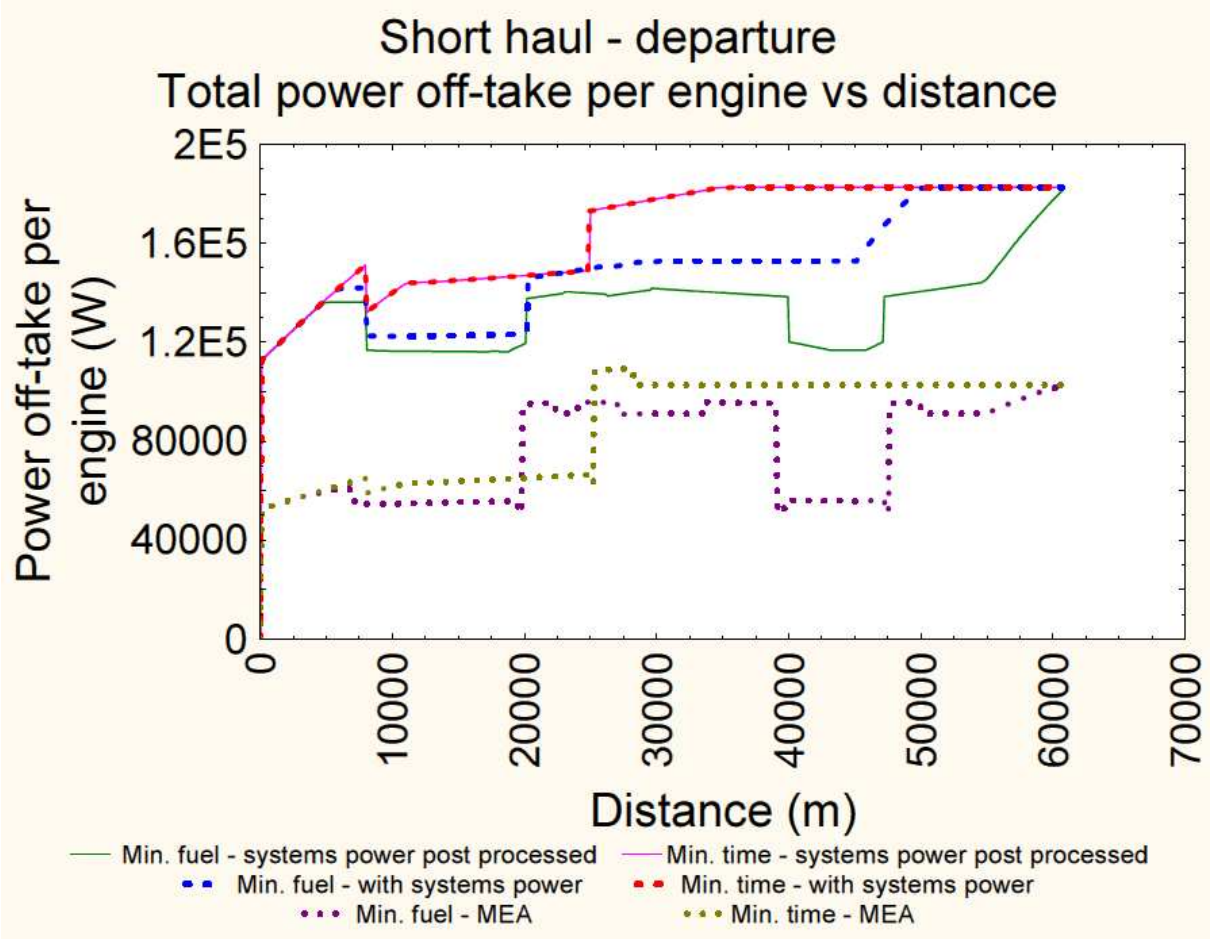

Figure 8-5: Total power off-take per engine vs distance – departure, short haul

As can be seen in Figure 8-5, the MEA power off-take is much less than that of the conventional aircraft. The “Min. fuel – systems power post processed” and “Min fuel – with systems power” have similar power off-take requirements during the first half of the phase. In the second half of the phase, the “Min. fuel – with systems power” has a larger power off-take. However, the fuel penalty due to power off-take is dependent on the throttle setting of the engine as well. Large off-takes at lower throttle settings will cause large fuel penalties than large off-takes at higher throttle settings.

The fuel penalty due to systems is not significant enough to change the trajectory when the setup is optimised for time. However, when the objective is to fly with the minimum fuel burn, the effect of the systems are significant.

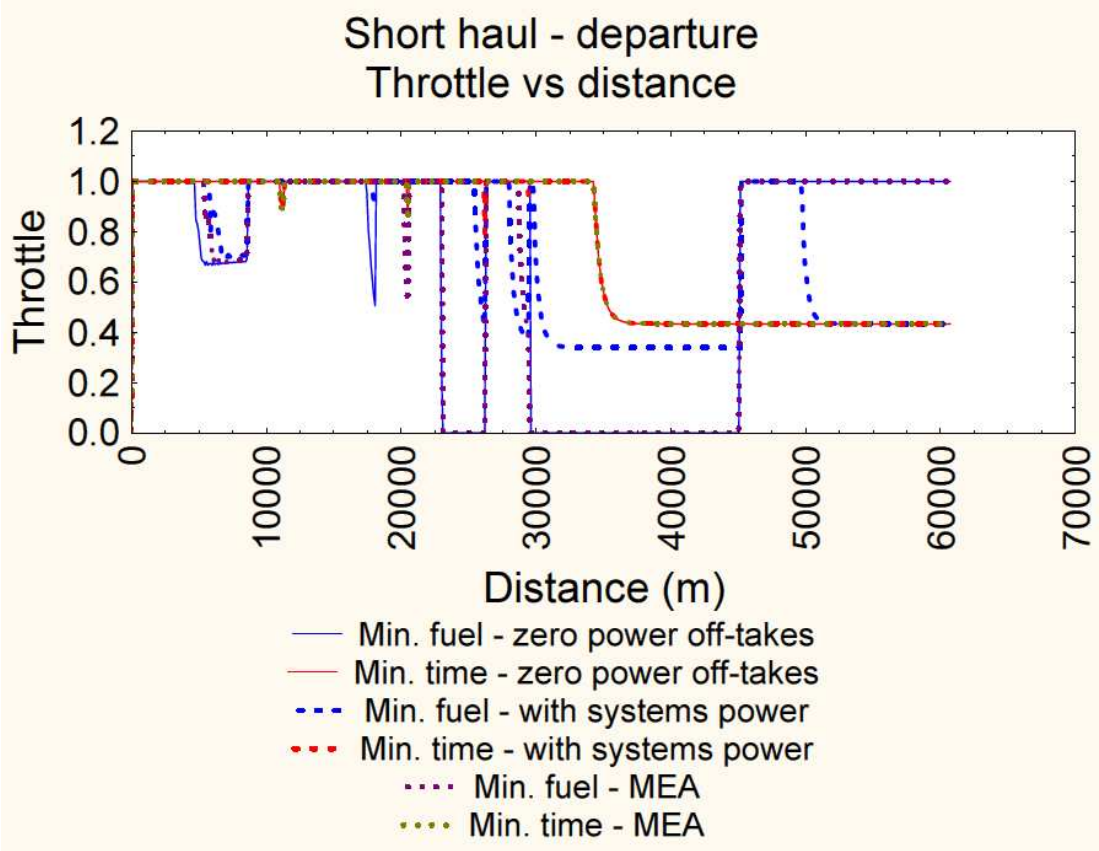

Figure 8-6: Throttle vs distance –departure, short haul

By studying the trajectory using Figure 8-5 and Figure 8-6, it was observed that for the "systems power post processed" trajectories, there was a relatively high off-take at lower thrust conditions which caused a significant fuel penalty. It should be noted that the total power off-take is the sum of the shaft power off-take and the bleed air off-take. The bleed air flow is converted to a power by using

$$\dot{Q} = \dot{m}_a C_p (T_e - T_i) \tag{36}$$

The exit temperature of air for the secondary power system is arguable. For this study the exit temperature of air has been established as the ambient temperature at the operating environment of the aircraft. Even though the exit temperature of the ECS is the cabin temperature and the exit temperature for the IPS is the temperature at the exit of the piccolo tubes, at the point of exit for both systems, there is still energy stored within the air. Hence only a proportion of the actual energy within the bleed flow is exhausted by the ECS and IPS. Since there is no energy recovery within the typical conventional secondary power system, using exit

temperatures of the systems cannot be justified and cannot be used to calculate the energy extracted from the engine to operate the pneumatic based systems.

"Min. fuel – zero power off-takes" and "Min. fuel – MEA" represent a "saw-tooth" shape. Firstly it has to be noted that the results are obtained by a constrained optimisation. The performance of the aircraft also gives some indication as to why the shape is as it is. Typically the fuel consumption is lower at lower throttle settings. However, when there are significant off-takes during lower throttle conditions the fuel consumption is increased exponentially. In the "zero power off-takes" and "MEA" cases, the power off-take levels are smaller than the conventional aircraft. Hence the "Min. fuel with systems power" climbs to 10,000 ft and stays level, rather than having decent segments where the there is a combination of lower throttle and high power off-take. But the in the other cases the aircraft saves fuel by having descent segments with zero or lower power off-takes and can afford to accelerate at the end. Hence the shape of the trajectory is a result of the power off-take to throttle ratio and corresponding fuel penalties.

A key difficulty in interpreting the results was that the behaviour of the optimised trajectory cannot be easily predicted since there are numerous parameters significantly influencing the optimisation process. This is especially true for the effect of airframe systems since the relationship between the airframe systems operation and optimum flight trajectory is twofold; the systems off-takes influences the trajectory due to fuel burn but the trajectory and the ambient conditions also influences the power requirements of the overall systems.

However, the summary of the results in

Table 8-5 indicates the advantage in using the enhanced approach to aircraft trajectory optimisation; which is to include the airframe systems within the optimisation loop. The systems add a penalty of 5.15% on the fuel burn if the "Min. fuel - zero power off-takes" trajectory is applied in and aircraft with systems. The fuel burn can be reduced by 2.78% by using the enhanced optimisation approach. Figure 8-7 and Figure 8-8 illustrates the advantage in terms of emissions. CO_2 and NO_X emissions are lower for the "Min. fuel - with systems power" than the "Min. fuel - system power post processed", which establishes the environmental gains that the enhanced approach offers.

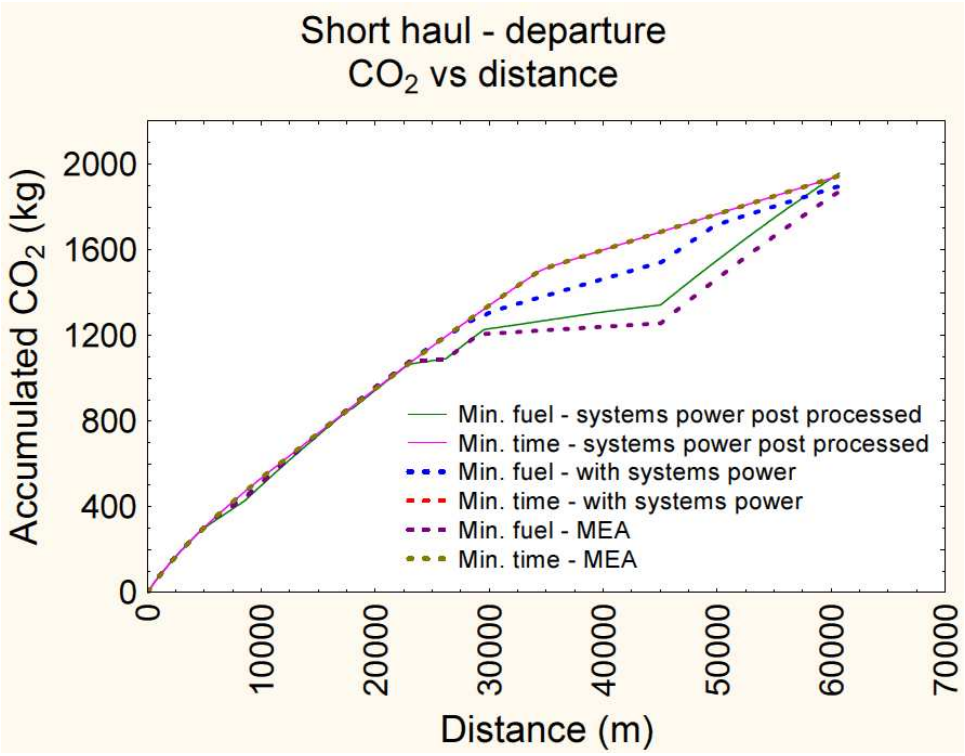

Figure 8-7: Total CO_2 emissions vs distance – departure, short haul

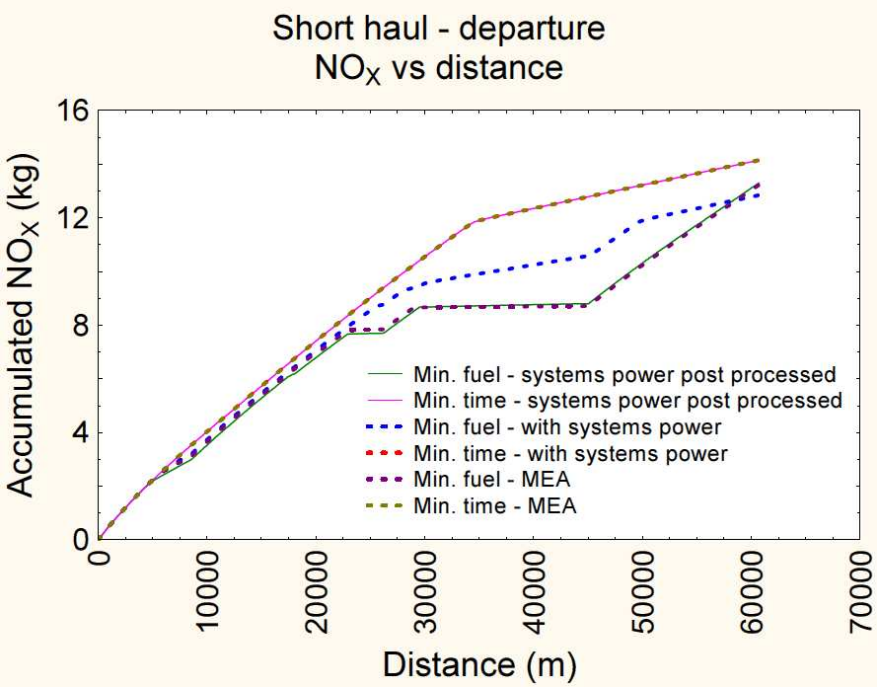

Figure 8-8: Total NO_X emissions vs distance – departure, short haul

Table 8-5: Results summary of the departure segment, short haul

Trajectory definition	Fuel burn (kg)	Flight time (s)	Penalty due to systems (%)	Fuel saving due to enhanced approach
Min. fuel – zero power off-takes	582	460	-	-
Min. fuel – systems power post processed	612	460	5.15%	-
Min. fuel - with systems power	595	416	-	2.78%
Min. time – zero power off-takes	606	371	-	-
Min. time – systems power post processed	608	371	0.33%	
Min. time - with systems power	608	371	-	0.00%

The enhanced approach to optimisation provided the platform to define and study the problem of "*more-electric aircraft trajectory optimisation*". The same city pair and constraints were applied to a more electric aircraft. The results showed that there was significant reduction in the fuel burn. The work presented here focuses on the minimum fuel burn trajectories, since one of the advantages of the MEA is the expected environmental gain in terms of fuel efficiency. The starting mass of the aircraft was the same as for the conventional aircraft. There were many reasons for this. Firstly the increase in mass compared to the overall aircraft mass will likely be small. Furthermore, the systems mass is a fixed mass and is not a variable mass such as the fuel. This limits the effect the MEA mass increase has on the overall trajectory optimisation procedure. Finally, with the current trends in technology development, it could be assumed that the power to weight ratio of more electric aircraft components would improve to a level where the mass penalty is a minimal.

It was inferred that the combined effect of the throttle setting and power off-take, allows the more electric aircraft to fly lower and accelerate heavily at the end of the phase to reach the final condition without a significant fuel penalty in the last segments. The power off-takes for the MEA are comparatively lower and that enables the aircraft to fly at lower throttle conditions (in the descending sections) without a heavy fuel penalty. Whereas the aircraft with conventional systems climbs constantly at a lower gradient until it reaches 10,000 ft and then levels off. This is further evidence on the importance of combining the systems operation and

aircraft operation in optimisation studies and indicates that more electric aircraft operations should be different to conventional aircraft within trajectory optimisation.

The total fuel burn for the “Min. fuel – MEA” was 586 kg. This is 1.5% less than “Min fuel – with systems power”. This results in lower CO_2 emissions but higher NO_X emissions as shown in Figure 8-7 and Figure 8-8. The higher NO_X is a result of the engine operating at a much higher temperature during the later stages of the departure to climb to 10,000 ft, whereas in the aircraft with conventional systems, the aircraft reaches 10,000 ft much quicker and flies level as shown in Figure 8-3.

Table 8-6: Comparison of MEA to conventional aircraft, short haul departure

Fuel burn			Flight time		
Conv.	MEA	%	Conv.	MEA	%
Optimised for minimum fuel burn					
595	586	1.5	416	456	-9.6
Optimised for minimum flight time					
608	608	0.0	371	371	0.0

8.1.5.2 En-route results

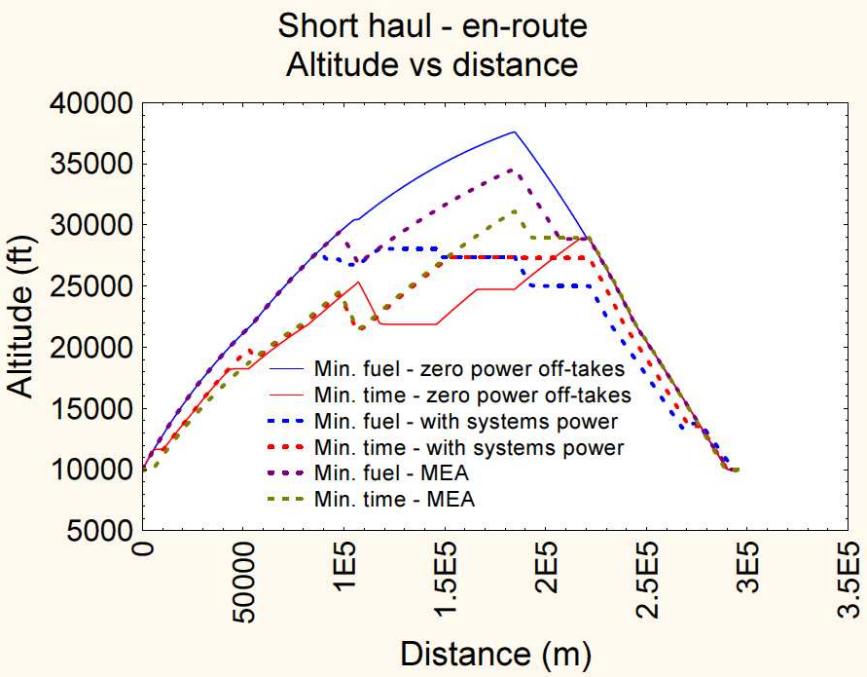

Figure 8-9: Altitude vs distance – en-route, short haul

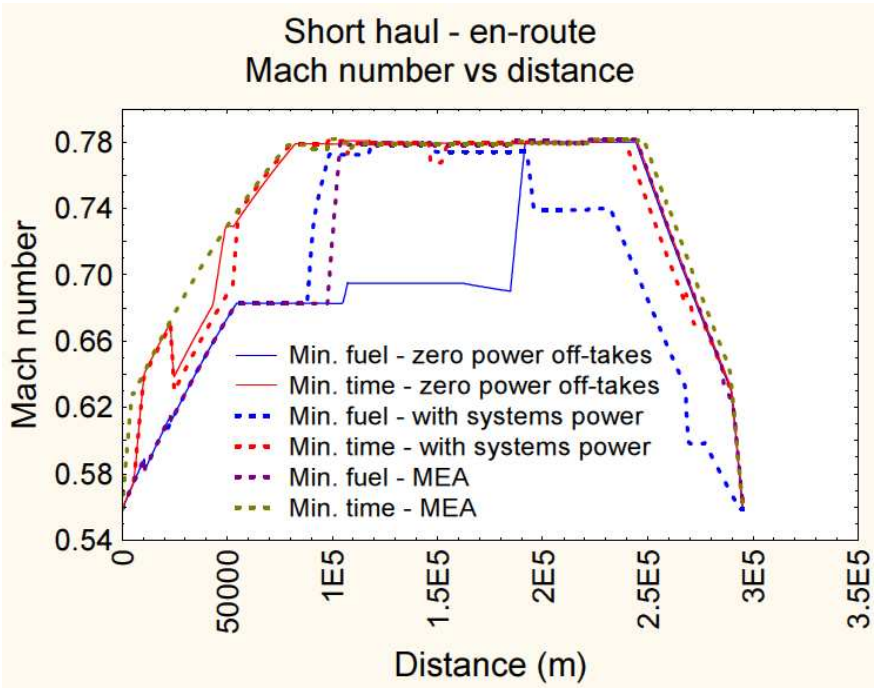

Figure 8-10: Flight Mach number vs distance – en-route, short haul

Figure 8-9 and Figure 8-10 show the aircraft altitude and aircraft Mach number profiles for the minimum fuel burn and minimum flight time trajectories for the two different setups.

The altitude profile of the simulation “Min. fuel - zero power off-takes” where the aircraft systems are not considered keeps climbing till top of descent and then descending to the end point of the phase. Instead the simulation “Min. fuel - with systems power” where the aircraft systems are considered generates a profile where it is possible to see several cruise levels flight before start the descending to the end point of the phase. It is therefore noticeable that the setup without systems in-the-loop for minimum fuel climbs at lower Mach number till top of descent and then accelerates and descends at higher speed. The setup with systems in-the-loop for minimum fuel instead cruises at higher speed and then decelerates and descends at lower speed.

This is quite an important characteristic, since some theoretical studies show that for minimum fuel burn, an aircraft should have a continuous climb and then a continuous descent. Yet from an aircraft systems operational point of view, a continuous climb and a continuous descend would cause a higher operational load. For example a continuous climb would cause a heavy load on the ECS pressurisation and thermal regulation, whereas a continuous descent would cause a significantly higher power off-take to thrust ratio, which causes higher fuel penalties. Hence it was interesting to observe the compromise reached when the systems were operational.

Moreover, the MEA shows intermediate characteristics. In the “Min. fuel” trajectories the MEA shows the tendency to have a continuous climb but also shows signs of levelling off and starts to descend much quicker than the “Min. fuel – zero power off-takes” trajectory. The “Min. time” trajectories tend to fly faster at lower altitudes and this is observed in Figure 8-9 and Figure 8-10.

The environmental gains are shown in Figure 8-11 and Figure 8-12. For both CO_2 and NO_X, the MEA has an advantage over the conventional aircraft. The characteristics are very similar to those observed during the departure phase.

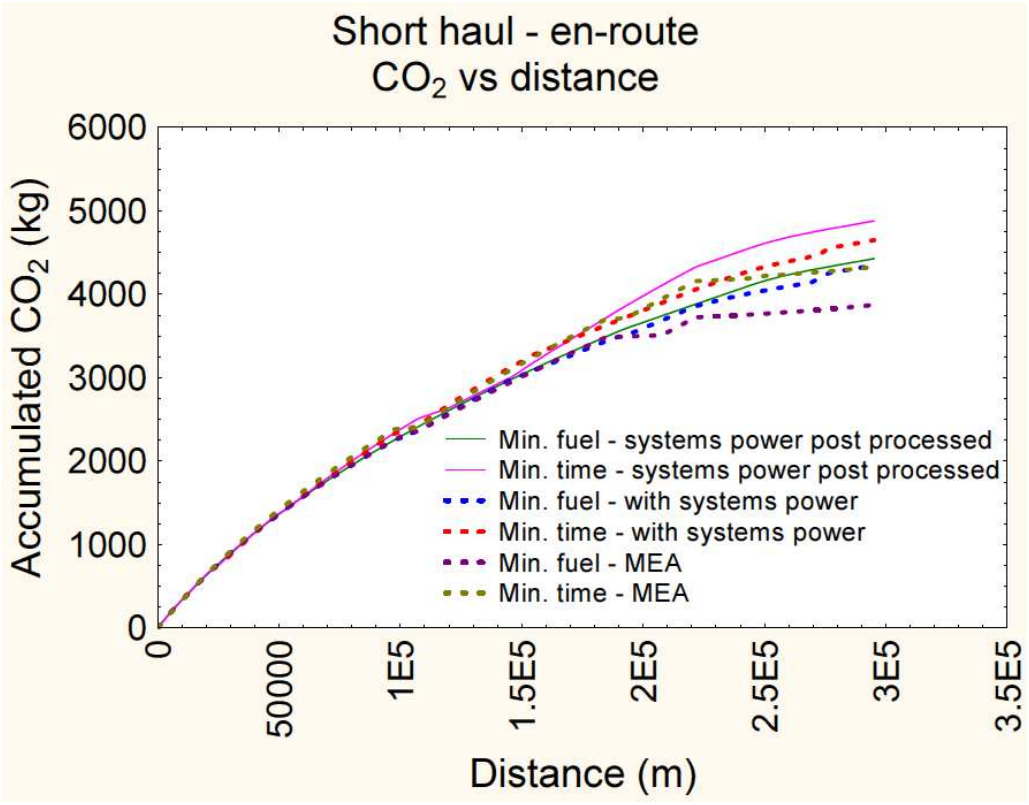

Figure 8-11: Total CO_2 emissions vs distance – en-route, short haul

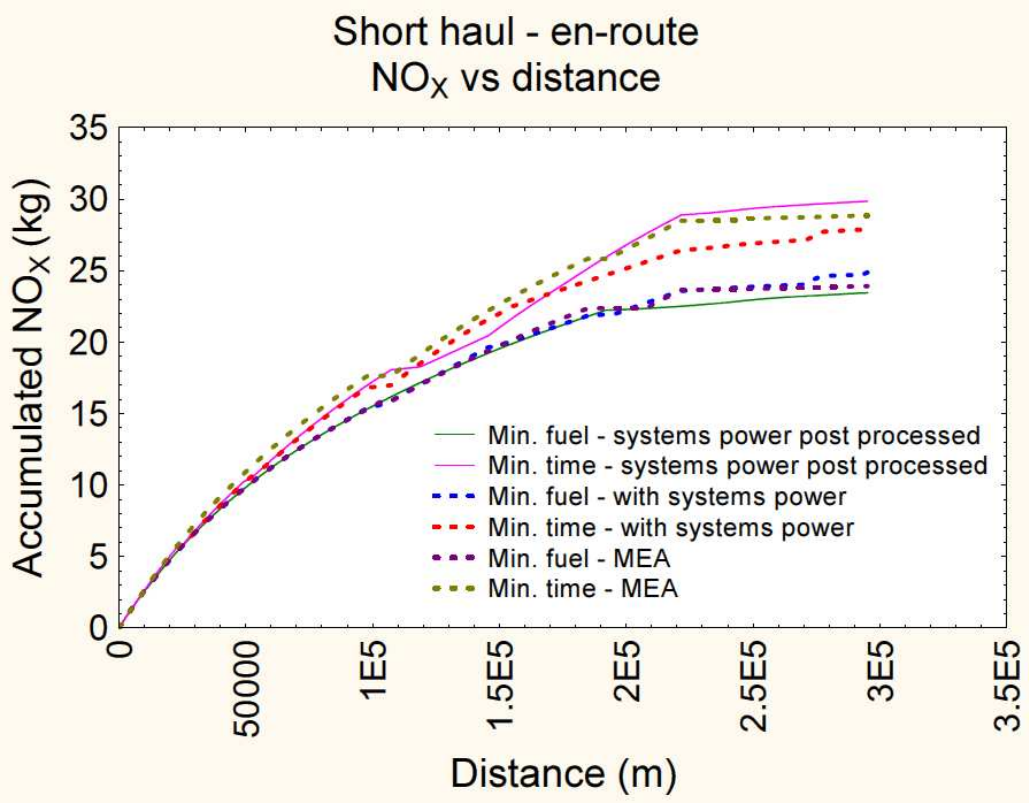

Figure 8-12: Total NO_X emissions vs distance – en-route, short haul

Table 8-7: Results summary of the en-route segment, short haul

Trajectory definition	Fuel burn (kg)	Flight time (s)	Penalty due to systems (%)	Fuel saving due to enhanced approach
Min. fuel – zero power off-takes	1180	1387	-	-
Min. fuel – systems power post processed	1403	1387	18.9	-
Min. fuel - with systems power	1367	1356	-	2.6%
Min. time – zero power off-takes	1348	1274	-	-
Min. time – systems power post processed	1531	1276	13.6%	-
Min. time - with systems power	1475	1285	-	3.7%

Table 8-8: Comparison of MEA to conventional aircraft, short haul en-route

Fuel burn			Flight time		
Conv.	MEA	%	Conv.	MEA	%
Optimised for minimum fuel burn					
1367	1211	11.4	1356	1333	1.7
Optimised for minimum flight time					
1531	1332	13	1276	1269	0.5

During the en-route the enhanced approach of including airframe systems within the optimisation loop, gave a 2.6% (from Table 8-7) fuel saving, when trajectories were optimised for fuel burn. When the trajectories were optimised for flight time, the fuel saving was 3.7%. The MEA showed a significantly lower fuel burn than the conventional aircraft offering an 11.4% (from Table 8-8) reduction in fuel burn for the “Min. fuel” trajectories.

8.1.5.3 Effects due to systems studied in detail for the en-route segment

The en-route segment, due to the higher impact on the total mission flight time, was analysed in detail to study the behaviour of the systems and the consequent effects. The “Min. fuel - system power post processed”, was compared to the “Min. fuel - with systems power” trajectory.

Figure 8-13 shows the difference in the fuel flow rates, while the CO_2, NO_X, throttle and the total power off-take is shown in Figure 8-11, Figure 8-12, Figure 8-14, and Figure 8-15 respectively. One characteristic of importance is that the systems power off-take effect the fuel burn heavily during lower engine operating conditions. This can be clearly identified by studying the power off-take, throttle and fuel flow in conjunction with each other. At the later stages of the en-route when the aircraft is in the initial descent stages, there is a distinct peak in the fuel flow rates. This is partly due to the fact that the “Min. fuel - system power post processed” trajectory is at a higher altitude (refer Figure 8-9) and higher speed (refer Figure 8-10) during this stage. But it is also due to the effect that the power off-take has on low throttle engine operating conditions. During this stage it was observed that the throttle required for both flight procedures was low. The off-take influences the fuel flow more than it would do in higher throttle settings and is an expected characteristic in large commercial turbofan engines.

When comparing the two flight procedures, it was observed that the “Min. fuel - with systems power” had a comparatively higher average throttle rating. This is also reflected in the NO_X emissions in Figure 8-12. The higher throttle settings indicate that the engine is operating at a higher temperature and it is expected that the NO_X emissions would be comparatively higher. By studying Figure 8-11 and Figure 8-12 it is clear that the there is a trade-off between NO_X and CO_2 as is expected in large commercial turbofan engines.

With regard to the MEA, the power off-takes were lower than the conventional aircraft as expected. The en-route was simulated in ISA atmospheric conditions; hence the major consumer which is the ECS did not reach the design limits. The lower off-take combined with the throttle, altitude and speed profiles enabled the MEA to achieve a more efficient procedure for flight and presents significant environmental gains. The CO_2 reduction was 11.4% and the NO_X reduction was 3.8%.

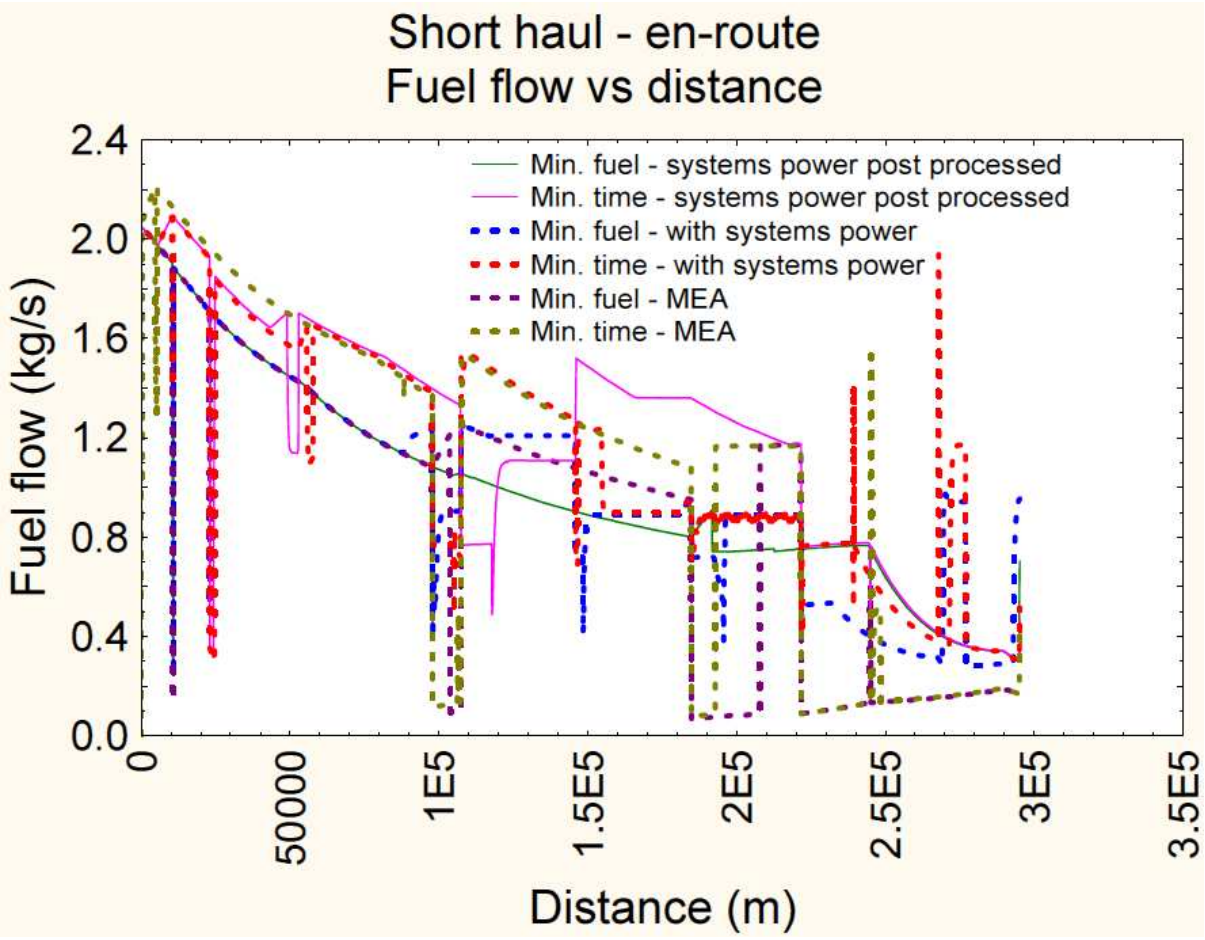

Figure 8-13: Fuel flow vs distance - en-route, short haul

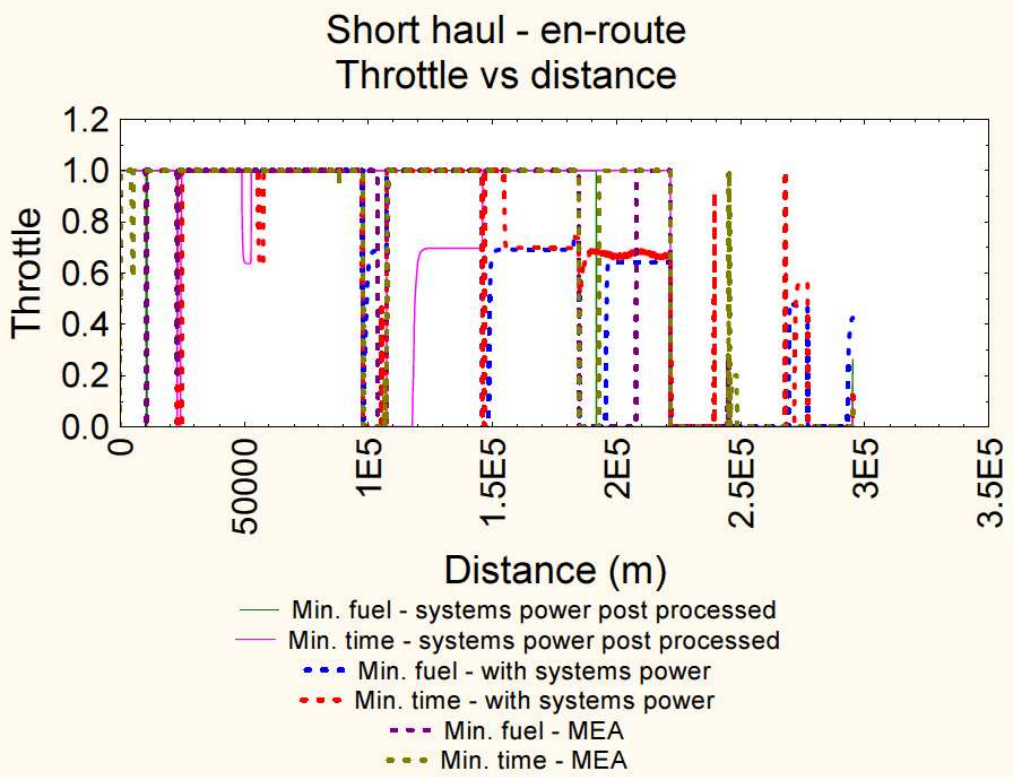

Figure 8-14: Throttle vs distance – en-route, short haul

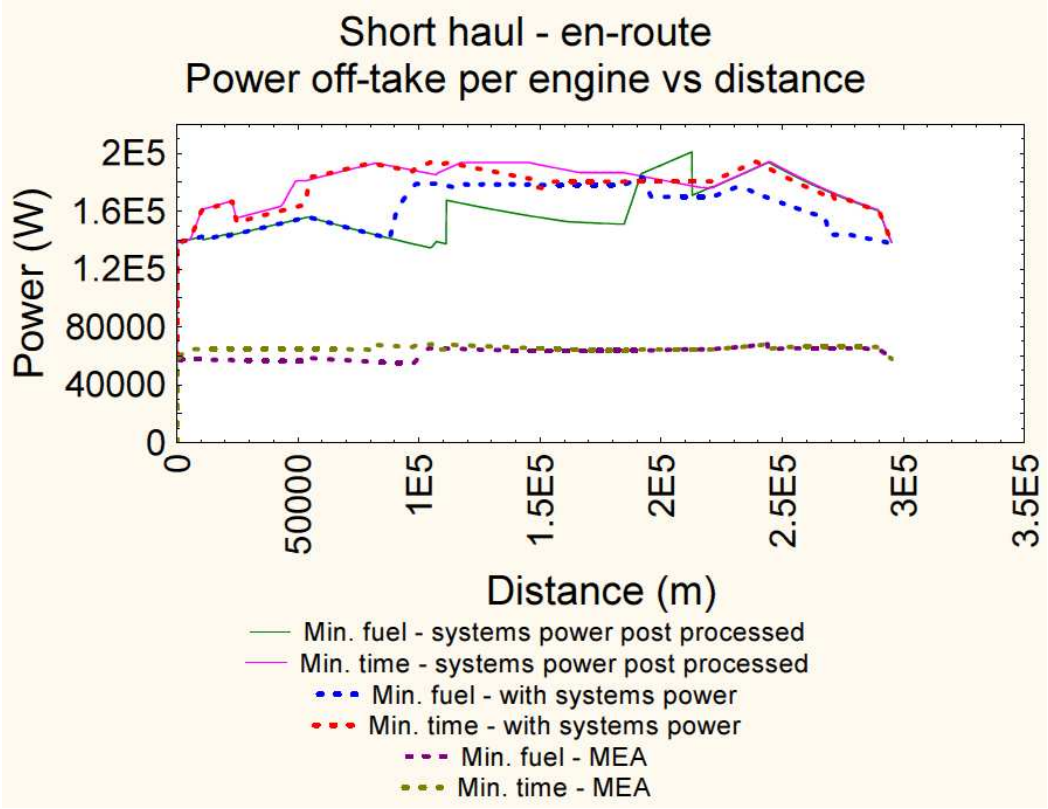

Figure 8-15: Power off-take per engine vs distance – en-route, short haul

The power off-take profiles obtained was subjected to a sanity check. Even though the individual models were validated, the combined effect is complex to comprehend prior to a study as such as this. The Boeing 787 aircraft in operation currently has two 250 kVA generators on each of the two engines. This adds up to 1,000 kVA. Assuming a typical power factor of 0.8 for the generation and distribution system, it is estimated that the maximum available power (from engine mounted generators) is 800 kW. The maximum number of passengers is 242, which gives a power per passenger value of 3.3 kW/per passenger. If this ratio is directly applied to the short haul case study aircraft of 150 passengers, then the aircraft should be limited to a total power off-take capacity of 496 kW. This would equate to 248 kW per engine. From Figure 8-15 it is clear that the more electric aircraft consumes less than the estimated maximum. However, it should be noted that power for the flight control actuators have not been accounted for in this study. Neither is the overall system operating at its design limits. For example, the short haul baseline aircraft doesn't include in-flight entertainment nor does it consider galley loads which have significant power requirements.

8.1.5.4 Arrival results

Due to the nature of the problem, it was observed that the number of feasible results were far less than the departure and en-route phase. The cause of this issue was inherent in the definition of the problem as mentioned in §2.5.

With regard to the specific setup used in this study it presented a significant challenge in defining the "arrival" phase optimisation. The optimisation set-up tries to find the best route possible, in terms of the objective, between two given points in 3-D space. Due to this nature, it was observed that occasionally the setup was not able to converge on feasible arrival trajectories. It was observed that the aircraft descended rapidly and then flew level just above ground for a great distance. Even though in theory this consumes less fuel, it is not accepted in an aircraft operational environment. Hence steps were taken to limit the final point of the aircraft arrival phase to an altitude of 2,000 ft. This ensured that the set-up always produced feasible flight procedures. The final descent (from 2,000 ft to final altitude of the airport) was calculated manually, assuming a constant glide angle.

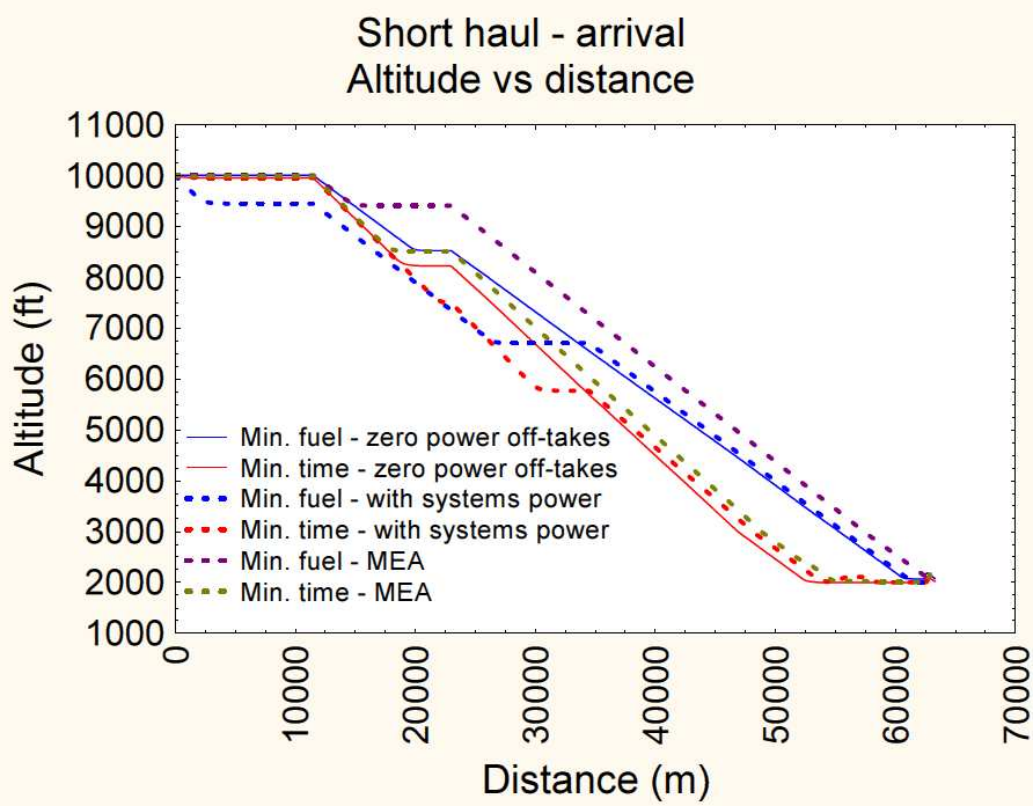

Figure 8-16: Altitude vs distance – arrival, short haul

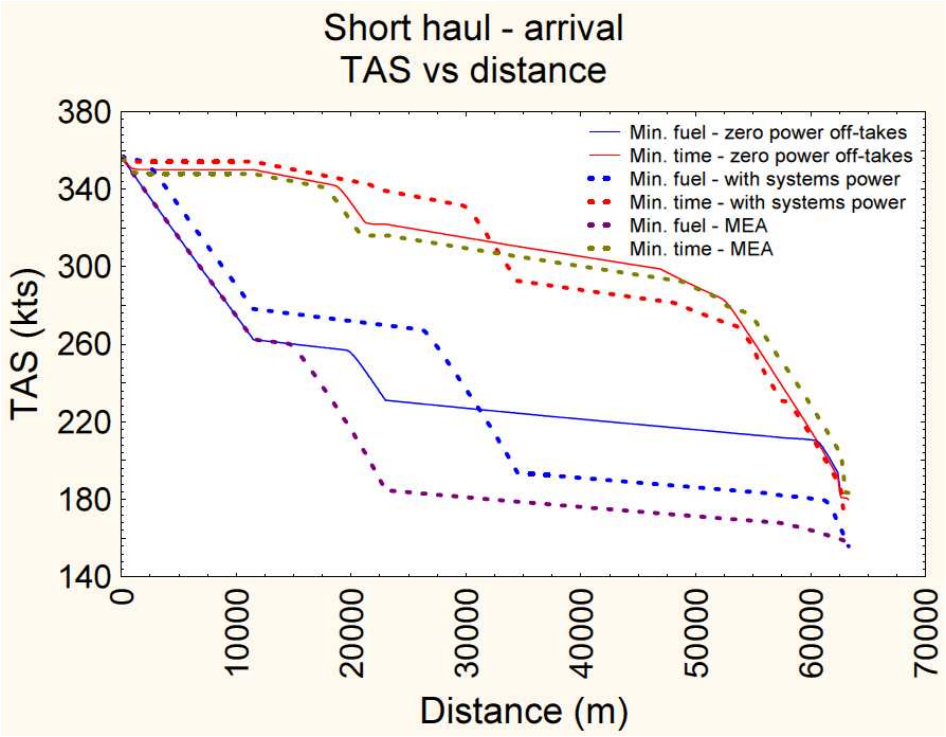

Figure 8-17: True air speed vs distance – arrival, short haul

Figure 8-16 and Figure 8-17 show the aircraft altitude and aircraft true airspeed as function of arrival phase for the minimum fuel burn and minimum flight time trajectories. As expected the minimum fuel burn trajectories tend to descend slower and reach the final point while descending whereas the minimum time trajectories descend faster and then fly level to reach the final point.

Unlike in the previous flight phases, the “Min. time” trajectories are quite different from each other. However, the “Min. time” trajectories all prefer to descend as soon as possible and fly level at the minimum altitude whereas the “Min. fuel” trajectories prefer to reach the final condition through a continuous descent.

Figure 8-18 and Figure 8-19 show the CO_2 and NO_X emissions for the arrival phase. The emissions for the MEA are significantly less than the conventional aircraft. The lower throttle settings and the comparatively lower off-takes result in a lower fuel burn for the MEA.

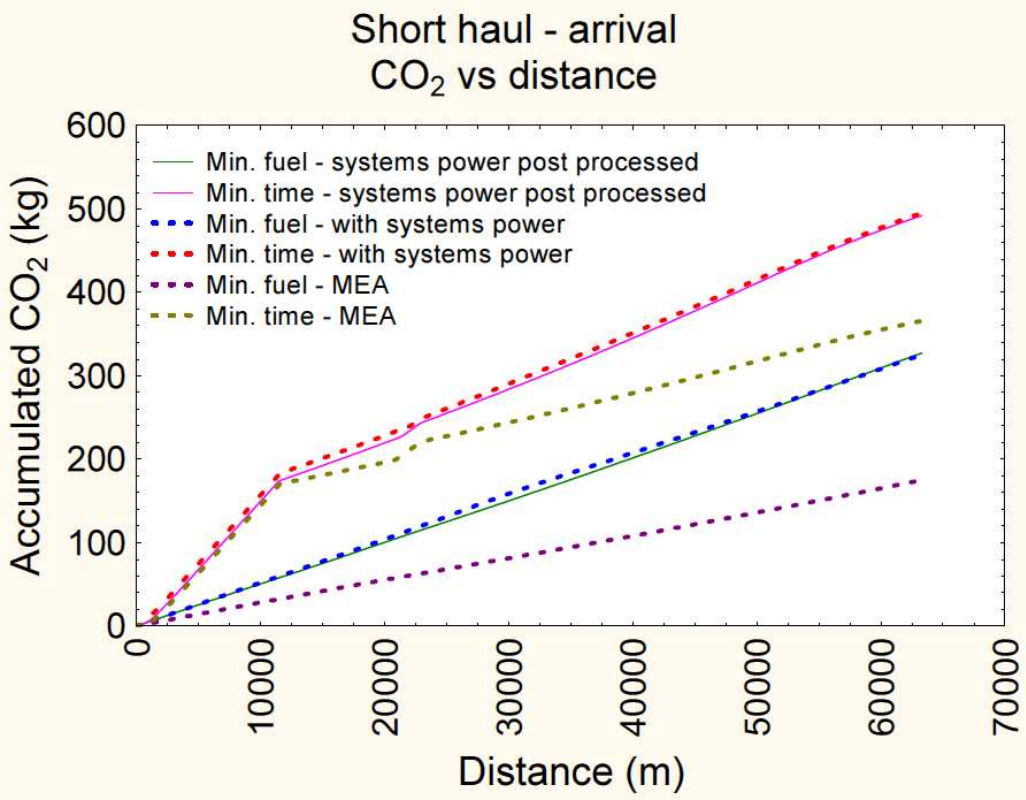

Figure 8-18: Total CO_2 emissions vs distance – arrival, short haul

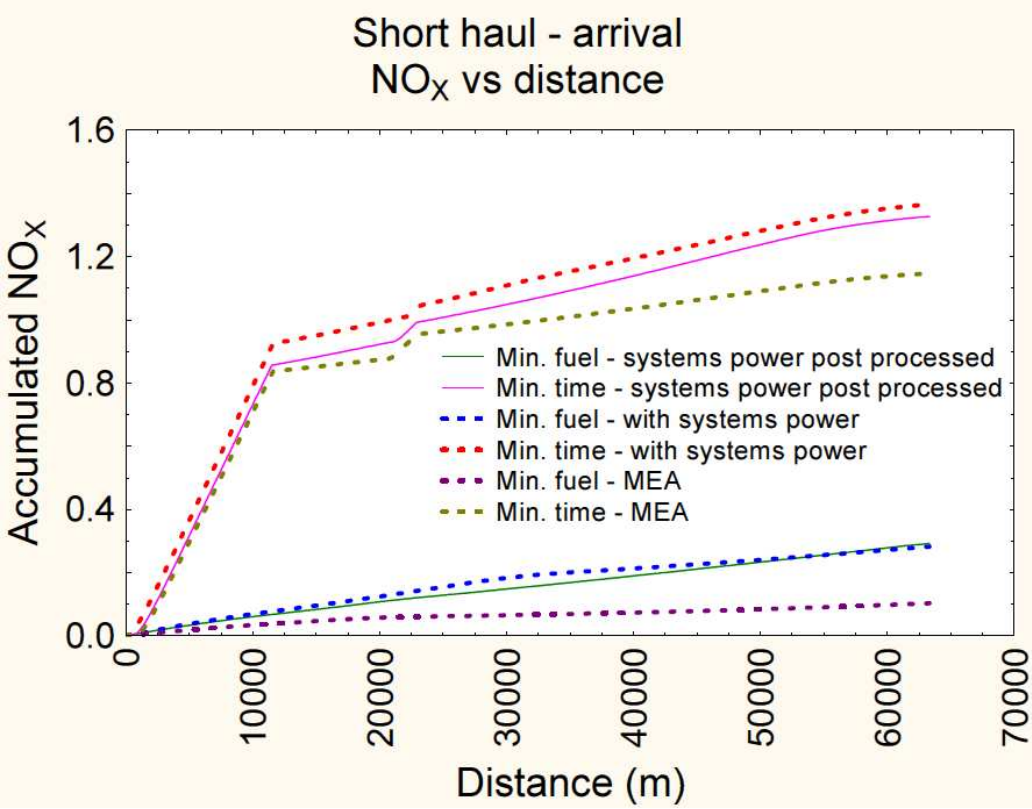

Figure 8-19: Total NO_X emissions vs distance – arrival

Table 8-9: Results summary of the arrival segment, short haul

Trajectory definition	Fuel burn (kg)	Flight time (s)	Penalty due to systems (%)	Fuel saving due to enhanced approach
Min. fuel – zero power off-takes	55	520		
Min. fuel – systems power post processed	104	520	89%	
Min. fuel - with systems power	103	546		0.96%
Min. time – zero power off-takes	116	409		
Min. time – systems power post processed	161	409	29%	

Min. time - with systems power	158	413	1.9%

Table 8-10: Comparison of MEA to conventional aircraft, short haul arrival

Fuel burn			Flight time		
Conv.	MEA	%	Conv.	MEA	%
Optimised for minimum fuel burn					
103	55.4	46	546	620	-13.6
Optimised for minimum flight time					
158	120	24	413	409	0.97

A summary of the results for the complete mission (departure, en-route, arrival) is shown in Table 8-11**.**

Table 8-11: Results summary of the short haul flight, conventional aircraft

Parameter	Min. fuel - zero power off-takes	Min. fuel - system power post processed	Min. fuel - with systems power
Fuel burn for optimised phases (kg)	1817	2119	2065
% increase due to systems – fuel burn		16.6%	
% reduction in fuel burn due to enhanced approach		2.5%	
Environmental gain in CO_2 due to enhanced approach		2.5%	
NOX emissions (kg)	-	36.93	38.01
Environmental gain in NO_X due to enhanced approach		-2.9%	

	Min. time - zero power off-takes	Min. time - system power post processed	Min. time - with systems power
Fuel burn for optimised phases (kg)	2070	2300	2241
% increase due to systems – fuel burn		11.1%	
% reduction in fuel burn due to enhanced approach		2.6%	
Environmental gain in CO_2 due to enhanced approach		2.6%	
NOX emissions (kg)	-	45.34	43.4
Environmental gain in NO_X due to enhanced approach		4.3%	

Table 8-12: Results summary of the short haul flight, MEA

Parameter	Min. fuel - with systems power	Min. fuel - MEA
Fuel burn for optimised phases	2065	1852
% reduction in fuel burn due to MEA	9.9%	
Environmental gain in CO_2 due to MEA %	9.9%	
NOX emissions (kg)	38.01	37.26
Environmental gain in NO_X due to MEA %	1.97%	

	Min. time - with systems power	Min. time - MEA
Fuel burn for optimised phases	2241	2060
% reduction in fuel burn due to MEA	8.1%	
Environmental gain in CO_2 due to MEA %	8.1%	
NOX emissions (kg)	43.4	44.17
Environmental gain in NO_X due to MEA %	-1.77%	

Table 8-13: Gains by optimizing for fuel burn and flight time

Parameter	Zero power off-takes	Conventional Aircraft	MEA
Fuel burn for typical trajectory	2330	2565	2352
Flight time for typical trajectory	2575	2575	2575
Fuel burn for “Min. fuel” trajectories	1817	2119	2065
Gain by optimizing for fuel burn	22%	17.4%	12.2%
Flight time for “Min. time” trajectories	2054	2069	2049
Gain by optimizing for time	20.2%	19.7%	20.4%

Table 8-13 summarizes the gains achieved by using trajectory optimisation. Each aircraft configuration was compared to the respective baseline case. The “zero power off-takes” showed the biggest gain for fuel efficiency while the “MEA” had the lowest gain. The result here shows that the classical approach to trajectory optimisation may exaggerate the gains due to optimisation.

From the overall results it was observed that, had the “Min. fuel” results obtained through the classical approach been applied in a real aircraft, the conventional airframe systems would have caused the flight to consume 16.6% more fuel than was calculated. However, by considering the conventional systems power requirements

within the optimisation loop, this penalty was reduced by 2.5%. The optimal way (with regard to the optimisation constraints) to fly the aircraft with consideration of the conventional systems off-takes was significantly different from an aircraft with zero power off-takes. The minimum fuel burn trajectory for the MEA consumed 9.9% less fuel than the minimum fuel burn trajectory for the conventional aircraft. However, it should be noted that phenomena which haven't been considered here; such as induced drag due to more electric compressors and extra weight due to the heavier electrical components, will reduce this advantage. The enhanced approach, as discussed above, provided a fuel reduction of 2.5% which directly results in a 2.5% reduction of CO_2 emissions but the NO_X emissions increased by 2.9%. However, the optimisation objectives were fuel and time. With the inversely proportional relationship between CO_2 and NO_X this is an expected phenomenon. The MEA proved to have 9.9% lessCO_2 emissions and 1.97% less NO_X emissions.

When the objective was the minimum flight time, the results in terms of the altitude and speed profiles didn't vary as much as the "Min. fuel" trajectories. Nevertheless, applying the enhanced optimisation approach to conventional aircraft showed that overall fuel burn can be reduced by 2.6%, the CO2 emissions can be reduced by 2.6% and the NOX emissions reduced by 4.3%. This is significant enough to challenge the validity of the optimality of the classical approach even when the optimisation objective is different to the fuel burn. When optimised for the minimum flight time, the MEA showed 8.1% reduction in fuel burn, 8.1% reduction in CO_2 and a 1.77% increase in NO_X emissions. The flight time of the MEA was less, which was due to the MEA flying faster at a higher throttle. The lower off-takes of the MEA configuration allowed the aircraft to operate at a higher throttle without causing a significant penalty on the fuel flow. But the higher throttle meant that the engine operating temperatures, especially the combustor inlet temperature was higher for longer periods resulting in an increase in the NO_X emissions.

The increase in NO_X is in contrast to the "Min. fuel" results and show that the complex dependencies within the systems aircraft dynamics, airframe system performance, and engine performance have to be accounted for to have valid results for trajectory optimisation.

Overall, the results show the importance of including the airframe systems off-takes in the optimisation loop. Furthermore, the MEA proves to be more fuel efficient than the conventional aircraft. More importantly, the results establish that the optimum methods to operate conventional aircraft and MEA are significantly different and that these studies can be done by including the airframe systems in the problem definition.

8.2 Case study – long haul

8.2.1 Aircraft, engine and systems set-up

The baseline aircraft and engine for the long haul study was similar to the Airbus A340-300 (295 passenger variant) and the CFM-56-5C. The operational environment for the airframe systems were set according to the baseline conditions described in §7 and the systems were similar to the A340 systems.

8.2.2 Framework and Optimiser setup

The overall set-up was similar to the short-haul setup in Table 8-1. The mass for the aircraft varied as such;

- At the start of departure – 250,000 kg
- At the stat of the en-route – 247,000 kg
- At the start of the arrival – 162,000 kg

8.2.3 Mission route

The mission case chosen for this study is a gate-to-gate flight from London Heathrow (LHR) airport to Colombo Bandaranaike International (CMB) airport. The mission was divided into three flight phases (departure, en-route and arrival). Departure phase begins at 83ft (Above Ground Level) AGL with an airspeed of 140 kts and terminates at the end of the Standard Instrumental Departure (SID). The SID selected for the departure phase is DVR6K.

Figure 8-20: Long haul ground track

Table 8-14: Departure way points and constraints – long haul

WP name	Latitude	Longitude	Altitude min/max (ft)	CAS min/max (kt)
LHR	51 27 53.33 N	000 27 20.46 W	83	140
WP2	51 27 52.94 N	000 23 50.68 W	83/10,000	140/310
WP3	51 26 36.05 N	000 20 05.61 W	83/10,000	140/310
WP4	51 18 14.00 N	000 35 50.00 E	83/10,000	140/310
DVR	51 09 45.00 N	001 21 33.00 E	10,000	310

The en-route phase starts after the aircraft has reached the DVR/VOR waypoint and ends when the aircraft enters the Colombo Bandaranaike STAR procedure. During this phase a minimum altitude of FL100 and a maximum of FL390 are used. These bounds give the optimiser the freedom to choose an optimum flight level within both lower and upper airspaces. The airspeed during the en-route is limited by KCAS 310 for the lower boundary and by the maximum operation Mach number for the upper boundary. The route selected for the en-route is shown in Table 8-20.

Table 8-15 : En-route way points and constraints - long haul

WP name	Latitude	Longitude	Altitude min/max (ft)	CAS min/max (kt)
DVR	51 09 45.00 N	001 21 33.00 E	10,000	310
WP5	51 05 40.86 N	002 39 05.85 E	10,000/39,000	310/400
WP6	50 30 53.10 N	005 37 25.00 E	10,000/39,000	310/400
WP7	49 14 10.37 N	010 22 59.33 E	10,000/39,000	310/400

WP8	47 25 39.41 N	016 35 58.95 E	10,000/39,000	310/400
WP9	41 27 12.00 N	032 59 34.00 E	10,000/39,000	310/400
WP10	38 42 29.80 N	039 13 26.70 E	10,000/39,000	310/400
WP11	29 52 31.00 N	048 29 44.00 E	10,000/39,000	310/400
WP12	25 37 00.00 N	054 55 34.00 E	10,000/39,000	310/400
WP13	20 37 00.00 N	060 57 00.00 E	10,000/39,000	310/400
WP14	12 15 47.20 N	074 16 06.20 E	10,000/39,000	310/400
WP15	11 08 05.50 N	075 57 17.50 E	10,000/39,000	310/400
WP16	09 49 51.90 N	078 05 20.50 E	10,000/39,000	310/400
WP17	08 17 06.30 N	078 35 55.30 E	10,000/39,000	310/400
ENRE	07 42 43.00 N	079 14 32.00 E	10,000	310

The arrival phase starts when the aircraft passes over ENRE and terminates at 3,500 ft AGL at VOR/DME. The route and the related parameters for the arrival phase are listed in Table 8-16. The aerodrome charts are attached in Appendix D: Departure and Arrival charts.

Table 8-16 : Arrival way points and constraints – short haul

WP name	Latitude	Longitude	Altitude min/max (ft)	CAS min/max (kt)
ENRE	07 42 43.00 N	079 14 32.00 E	10,000	310
WP18	07 30 32.32 N	079 42 11.10 E	3,500/10,000	180/310
WP19	07 20 30.00 N	080 00 30.00 E	3,500/10,000	180/310
DME	07 09 41.00 N	079 52 07.00 E	3,500	180

8.2.4 Terminology used to discuss results

- *Min. fuel* = Trajectory optimised for minimum fuel burn.
- *Min. time* = Trajectory optimised for minimum flight time.
- *Zero power off-take* = No account is made for systems power off-takes.
- *With systems power* = Conventional systems power off-takes are modelled in the optimisation.
- *Systems power post processed* = Conventional systems power off-takes are not included in the optimisation, but are added on in post processing.
- *MEA* = More-electric systems power off-takes are modelled in the optimisation.

8.2.5 Results and analysis – long haul flight

8.2.5.1 Departure results

The *Min. fuel* and *Min. time* trajectories (altitude and speed profiles) for the long haul departure case are shown in Figure 8-21and Figure 8-22. The difference between the Min. fuel and Min. time trajectories is visible. But when the Min. fuel trajectories are compared with each other the difference is minimal. This is the case for the Min. time trajectories as well. As expected, the aircraft flies faster to achieve the Min. time trajectories.

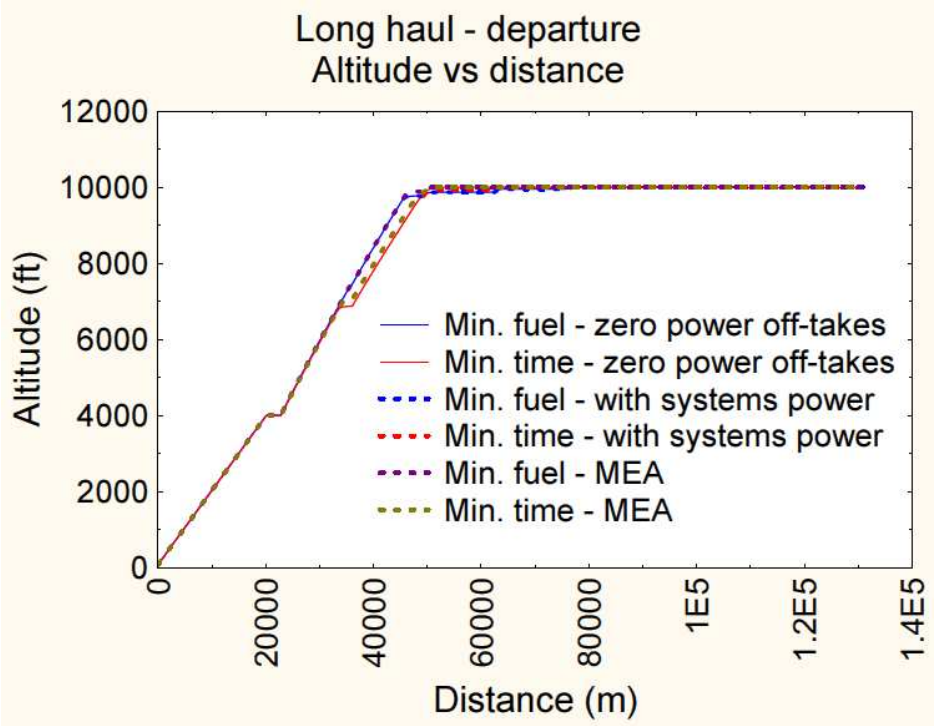

Figure 8-21: Altitude vs distance – departure, long haul

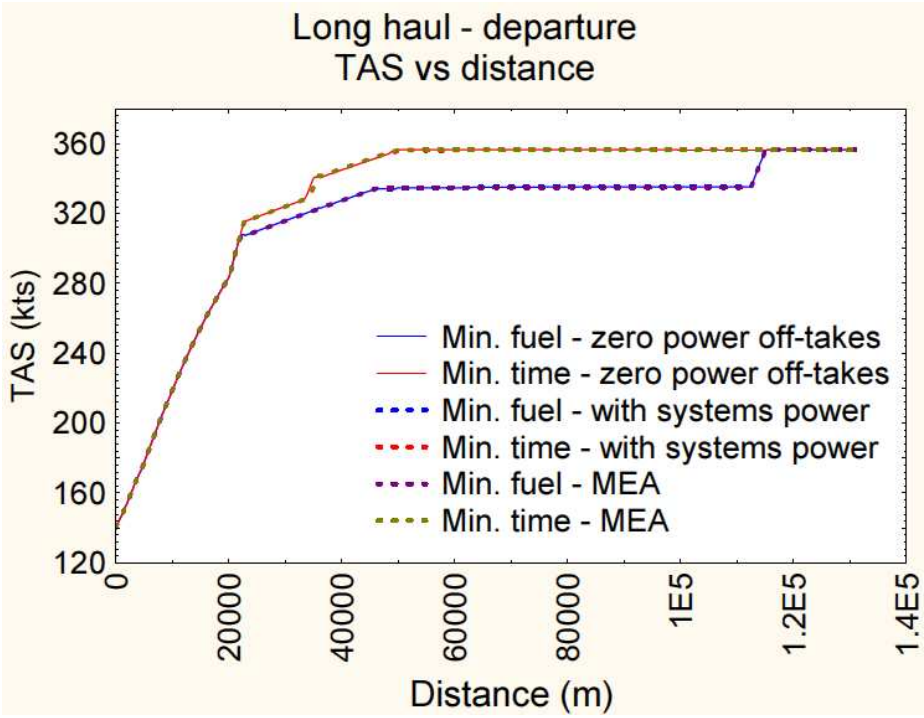

Figure 8-22: True air speed vs distance – departure, long haul

The power off-take profiles are shown in Figure 8-23. As expected the MEA has a significantly lower power requirement than the conventional aircraft. The bleed power component for the conventional aircraft has been calculated as explained is §8.1.5.1.

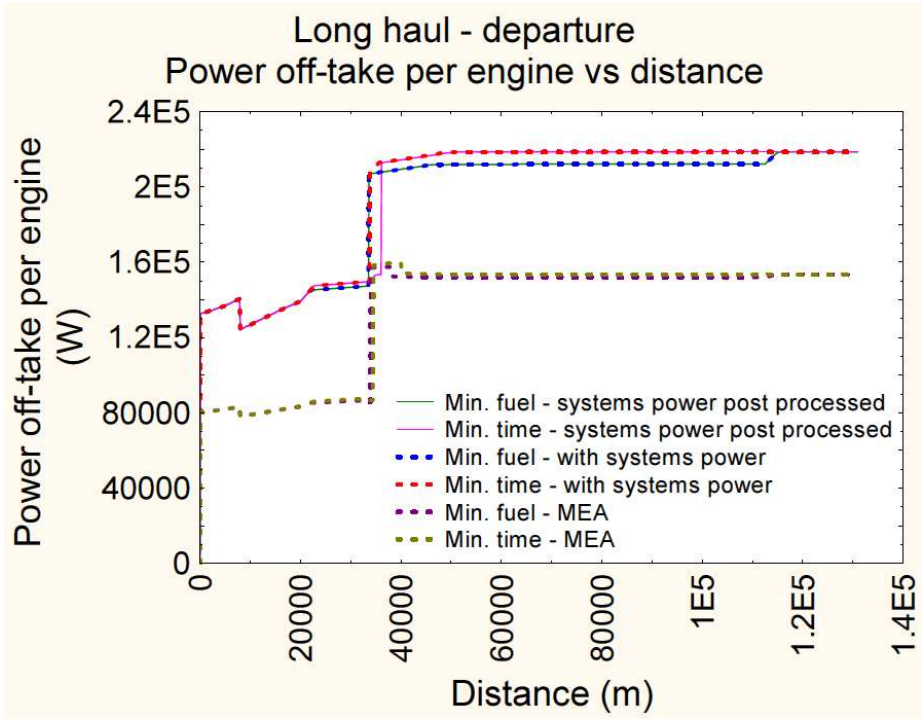

Figure 8-23: Total power off-take per engine vs distance – departure, long haul

Table 8-17: Results summary of the departure segment, long haul

Trajectory definition	Fuel burn (kg)	Flight time (s)	Penalty due to systems (%)	Fuel saving due to enhanced approach
Min. fuel – zero power off-takes	3049	835		
Min. fuel – systems power post processed	3061	835	0.39	
Min. fuel - with systems power	3061	835		0.0
Min. time – zero power off-takes	3061	806		
Min. time – systems power post processed	3071	806	0.33	
Min. time - with systems power	3070	806		0.03

Table 8-18: Comparison of MEA to conventional aircraft, long haul departure

Fuel burn			Flight time		
Conv.	MEA	%	Conv.	MEA	%
Optimised for minimum fuel burn					
3061.2	3060.7	0.01	835	835	0.0
Optimised for minimum flight time					
3070	3070	0	806	806	0.0

As can be seen from Table 8-17and Table 8-18, which lists the summary of the long haul departure optimisation study, the difference between the fuel burn and flight times for all three aircraft configurations are similar to each other. The improvements shown by the MEA are significantly less than the short haul case. This holds true for the impact that the airframe systems have as well. This leads to the conclusion that the impact due to the airframe systems is heavily dependent on a number of factors and that it is difficult to be generalised. By modelling and representing the systems within

the trajectory optimisation scope, this generalisation is avoided. In the long haul departure case, the airframe systems impose a 0.39% fuel penalty (when optimised for fuel burn) whereas in the short haul departure case, the penalty due to the airframe systems was 5.15%. Moreover, the fuel burn for the MEA was 1.5% lower than the conventional aircraft for the short haul departure case, whereas the MEA doesn't seem to offer a competitive advantage in terms of fuel burn for the long haul departure. This also emphasises that the when design concepts such as MEA are discussed it is important to discuss the operational aspects as well.

8.2.5.2 En-route results

The en-route segment was optimised using the same approach as for the departure. The ceiling altitude for the aircraft was limited to 39,000 ft. The results for the altitude profiles and speed profiles are shown in Figure 8-24 and Figure 8-25 respectively.

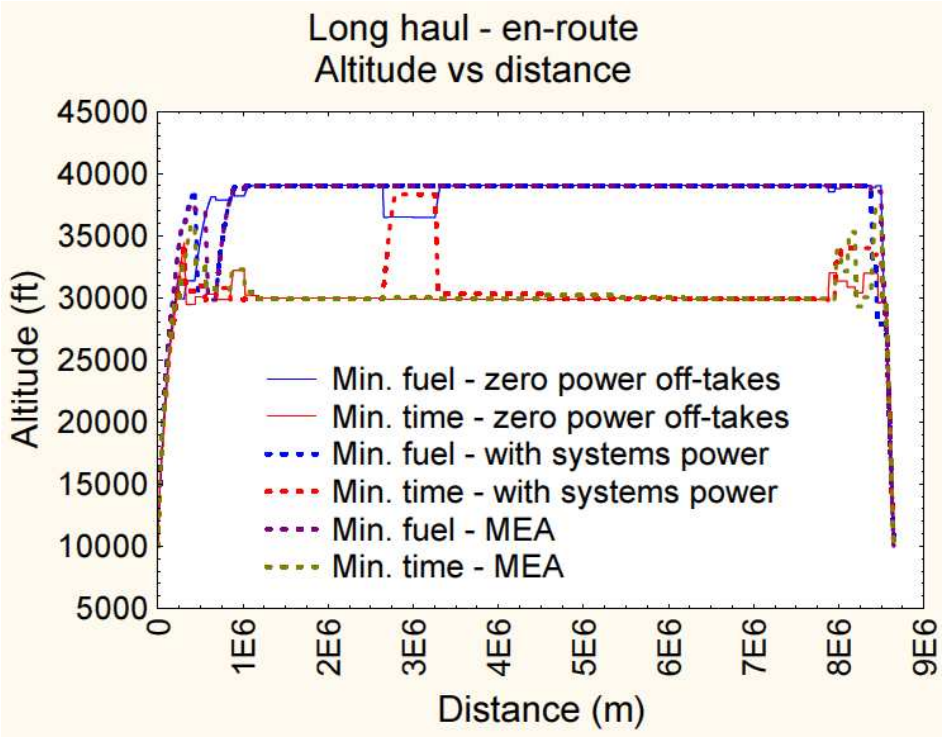

Figure 8-24: Altitude vs distance – en-route, long haul

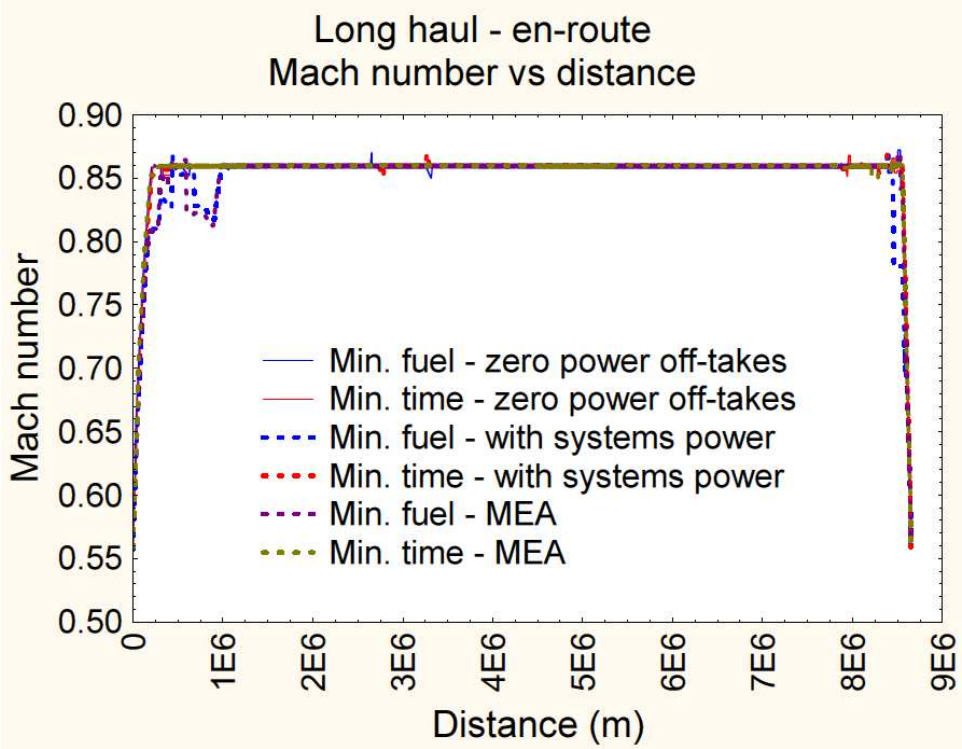

Figure 8-25: Mach number vs distance – en-route, long haul

The results shown that for the Min. fuel trajectories the aircraft tend to accelerate to the highest permissible altitude and then fly level. For the Min. time trajectories the aircraft cruises at between 30,000 ft to 31,000 ft. The cruise Mach number for both objectives is 0.85 which is the maximum permissible as set in this problem. With regard to the “Min. fuel – with systems power” trajectory, the aircraft once reaching 39,000 ft, descends to 31,000 ft and then climbs back to 39,000 ft. This was an unexpected characteristic and is thought to be a product of the optimisation process. The en-route segment is long with many way points and it is anticipated that increasing the generations and population for the optimisation will give a much smoother result. But in order to regulate the study, the same optimisation conditions were applied throughout the study. The “Min. time – with systems power” trajectory also shows an unexpected climb and descend characteristic between $2x10^6$ m and $4x10^6$ m. It is anticipated that this is also due to the optimisation needing more evaluations to reach the optimum time result for the aircraft with conventional systems. There are some differences between the different aircraft configurations for both the Min. fuel and Min. time results at the top of climb and start of descent. These indicate that the different aircraft configurations should be flown differently to achieve the objectives. However,

the results clearly show that for long cruise segments, the best fuel results are obtained when the aircraft flies as high as possible. The power off-take profiles are shown in Figure 8-26.

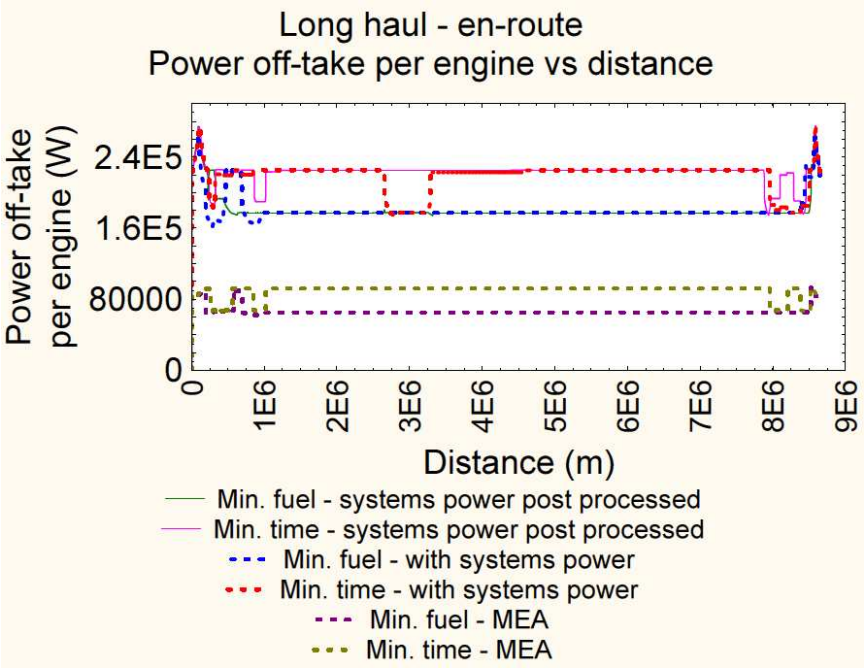

Figure 8-26: Total power off-take per engine vs distance, long haul

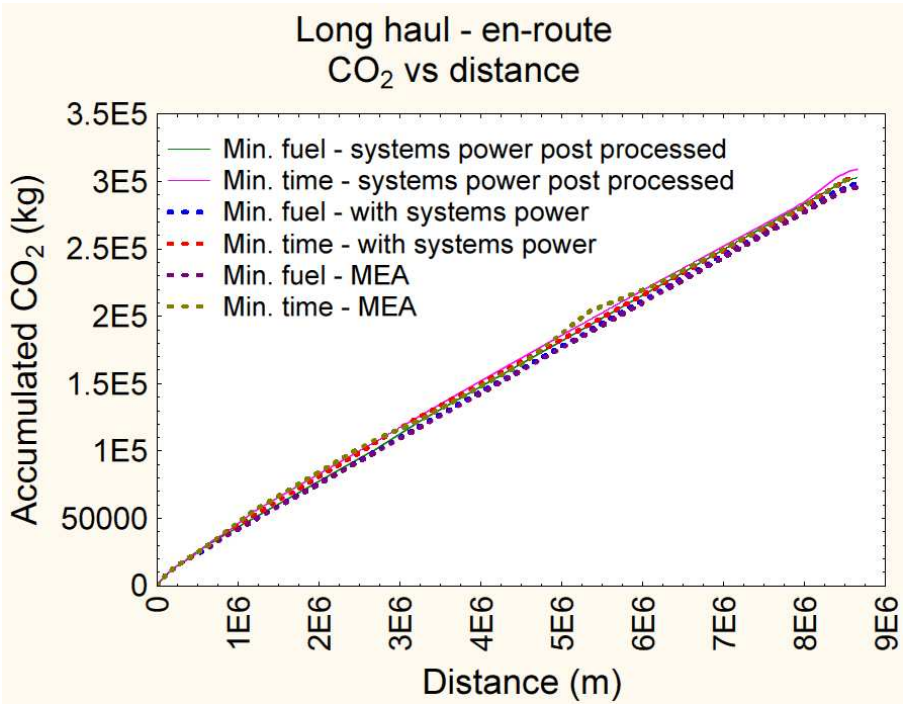

Figure 8-27: Total CO_2 emissions vs distance – en-route, long haul

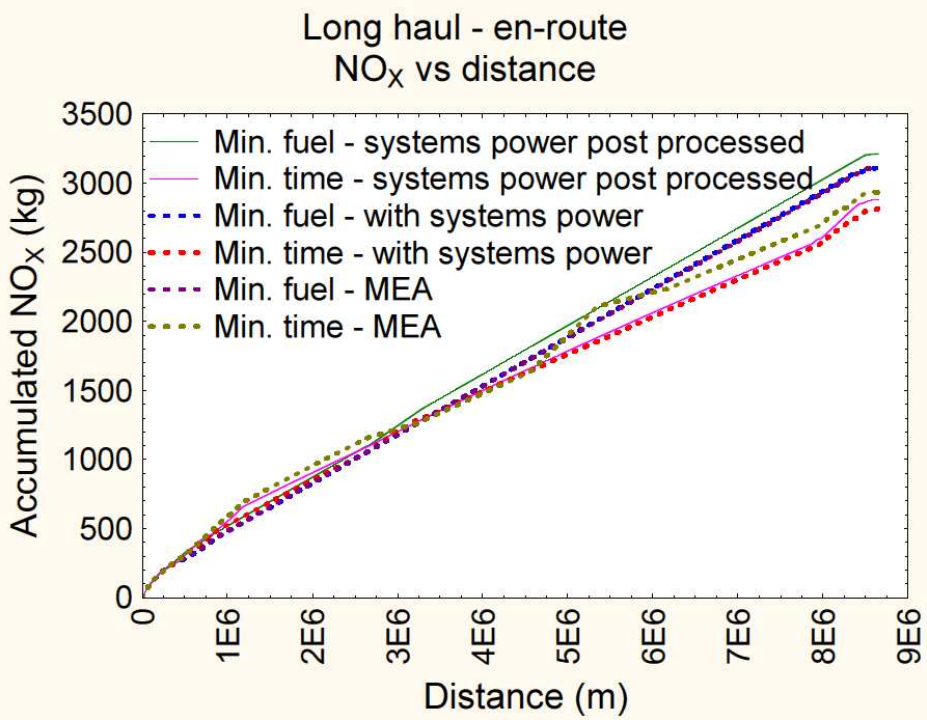

Figure 8-28: Total NO_X emissions vs distance – en-route, long haul

Hence the visual differences of the trajectory profiles are less significant than the short haul case. But by observing the results summary in Table 8-19 and Table 8-20 it is clear that the advantage for optimising long haul flights is much greater in terms of environmental impacts shown in Figure 8-27 and Figure 8-28, fuel burn and flight time.

Moreover, it should be noted that phenomena of weather such as the wind, temperature, icing clouds and relative humidity will have significant effects on long haul trajectories.

Table 8-19: Results summary of the en-route segment, long haul

Trajectory definition	Fuel burn (kg)	Flight time (s)	Penalty due to systems (%)	Fuel saving due to enhanced approach
Min. fuel – zero power off-takes	81806	34208		
Min. fuel – systems power post processed	87015	34208	6.4	

Min. fuel - with systems power	86602	34354		0.5
Min. time – zero power off-takes	93700	33387		
Min. time – systems power post processed	95822	33387	2.3	
Min. time - with systems power	94599	33471		1.27

Table 8-20: Comparison of MEA to conventional aircraft, long haul en-route

Fuel burn			Flight time		
Conv.	MEA	%	Conv.	MEA	%
Optimised for minimum fuel burn					
86602	81832	5.5	34354	34333	0.06
Optimised for minimum flight time					
94599	94683	-0.08	33471	33397	0.22

It is interesting to note that the fuel penalty due to the conventional airframe systems in the long haul en-route case is 6.4% whereas in the short haul en-route case the effect due to the airframe systems was 18.9% for the minimum fuel burn result. This difference is important to note since it shows that the effect of the airframe systems should not be generalised. Hence in an optimisation problem, the airframe systems operation should be modelled as accurately as possible to achieve results applicable to real aircraft. In the long haul study when the minimum fuel burn trajectories are considered, the advantage of the MEA as a percentage is reduced to 5.5% from 11.4% for the short haul study. But in terms of real saving on fuel mass, the long haul case is more prominent, which signifies the importance of extending the advantage of the MEA by optimising MEA operation.

8.2.5.3 Arrival results

The arrival segment of the long haul trajectory ends at 3,500 ft with a speed of 180 kts. The altitude profiles are shown in Figure 8-29 and the speed profiles in Figure 8-30. As expected the Min. fuel trajectories have step descents whereas the Min. time trajectories descent continuously and fly level at 3,500 ft. With regard to the speed profiles, the Min fuel trajectories tend to reduce speed rapidly at the start of the

descent. There onwards the speed drops more gradually. The Min. time trajectories have higher speeds throughout the initial descent as expected. The speed reduces gradually at the start of the descent and then rapidly drops towards the end to reach the final conditions. There are distinct differences for both the Min. fuel and Min. time trajectories where different aircraft configurations are concerned.

The power off-take profiles are shown in Figure 8-31. These results yet again underline the different flight operations needed to achieve optimum flight conditions for minimum fuel burn and minimum flight time.

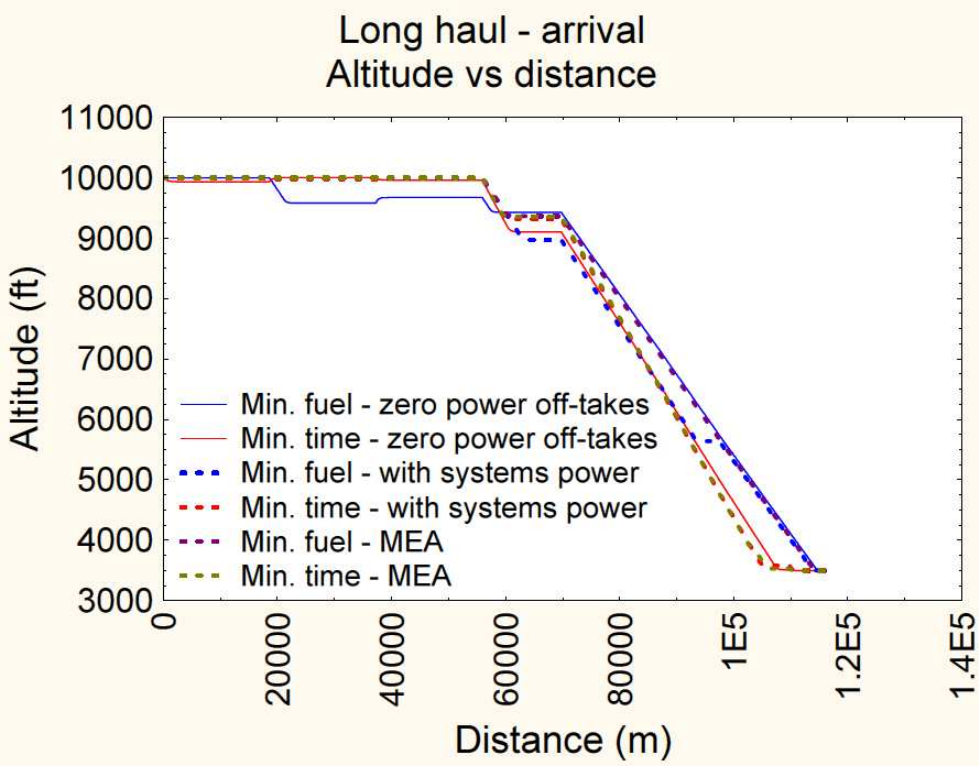

Figure 8-29: Altitude vs distance – arrival, long haul

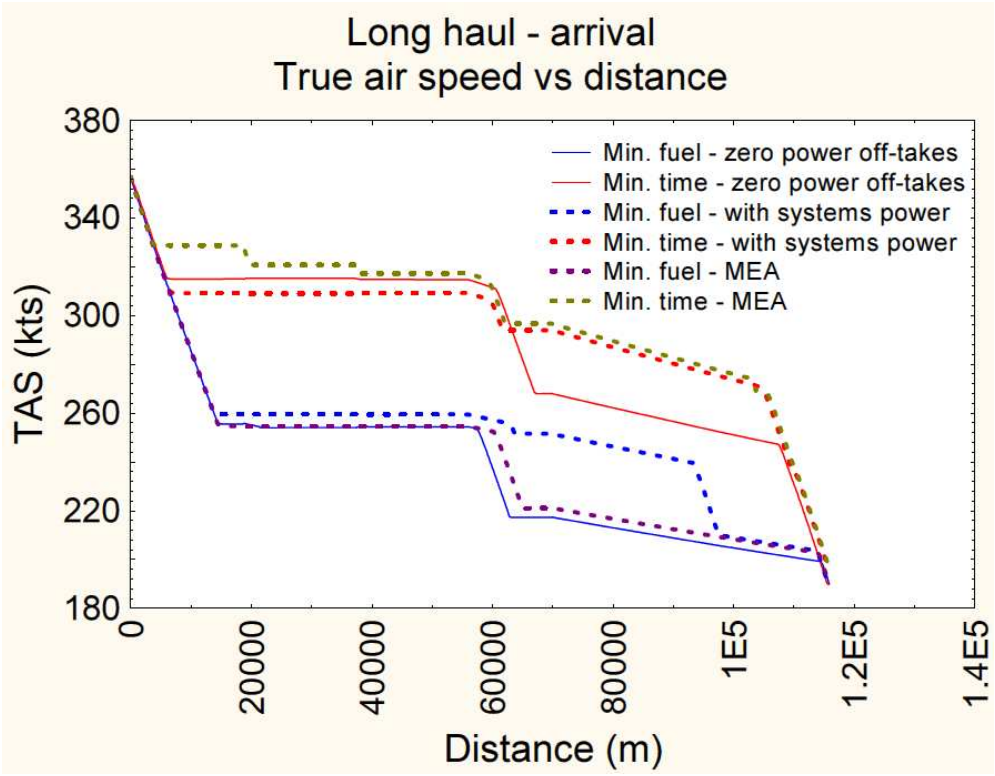

Figure 8-30: True airspeed vs distance – arrival, long haul

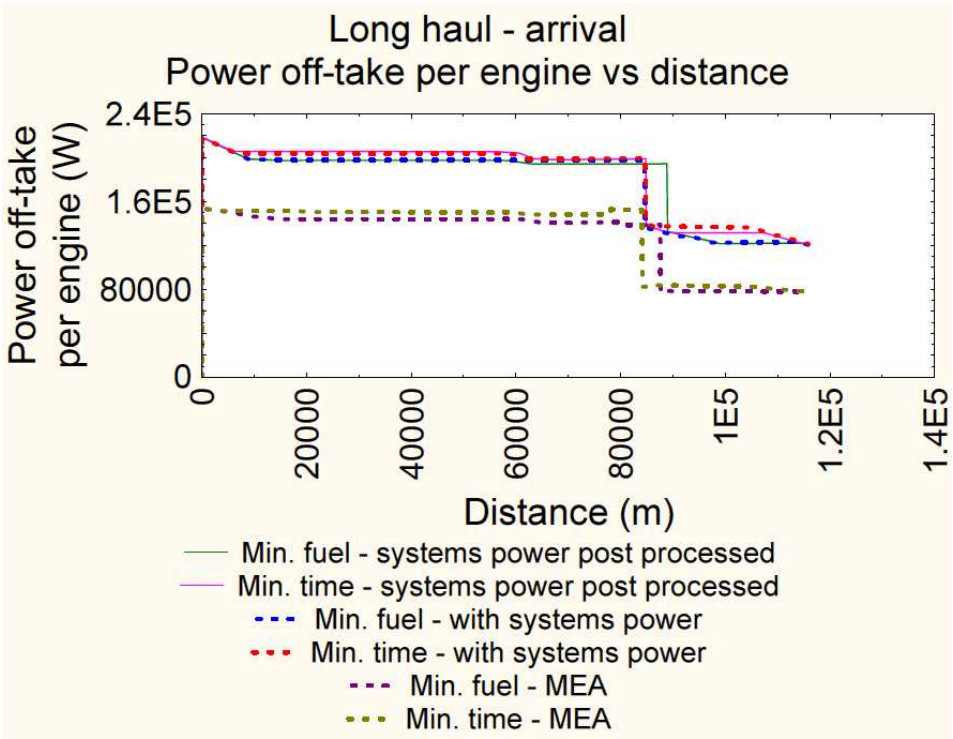

Figure 8-31: Power off-take per engine vs distance – arrival, long haul

The arrival segment is summarised in Table 8-21 and Table 8-22.

Table 8-21: Results summary of the arrival segment, long haul

Trajectory definition	Fuel burn (kg)	Flight time (s)	Penalty due to systems (%)	Fuel saving due to enhanced approach
Min. fuel – zero power off-takes	811	960		
Min. fuel – systems power post processed	934	960	15.2	
Min. fuel - with systems power	912	906		2.4
Min. time – zero power off-takes	890	795		
Min. time – systems power post processed	961	795	8.0	
Min. time - with systems power	976	773		-1.6

Table 8-22: Comparison of MEA to conventional aircraft, long haul en-route

Fuel burn			Flight time		
Conv.	MEA	%	Conv.	MEA	%
Optimised for minimum fuel burn					
912	835	8.4	906	948	-4.6
Optimised for minimum flight time					
976	951	2.6	773	757	2.1

The arrival segment presents the biggest variation in terms of airframe systems impact. For the short haul case, when the trajectory was optimised for fuel burn, the impact of the conventional airframe systems was 89% whereas in the long haul arrival, the impact due to airframe systems is 15.2%. The advantage of the MEA concept is also reduced from 46% to 8.4% in the Min. fuel trajectories. In terms of fuel mass, the long haul arrival saves more than the short haul arrival.

The summary of the long haul case study is shown in Table 8-23.

Table 8-23: Results summary of the long haul flight, conventional aircraft

Parameter	Min. fuel - zero power off-takes	Min. fuel - system power post processed	Min. fuel - with systems power
Fuel burn for optimised phases (kg)	85666	91010	90575
% increase due to systems – fuel burn		6.24	
% reduction in fuel burn due to enhanced approach		0.5	
Environmental gain in CO_2 due to enhanced approach %		0.5	
NOX emissions (kg)		3321.4	3222.6
Environmental gain in NO_X due to enhanced approach %		2.97	
	Min. time - zero power off-takes	Min. time - system power post processed	Min. time - with systems power
Fuel burn for optimised phases (kg)	97650	99854	98646
% increase due to systems – fuel burn		2.26	
% reduction in fuel burn due to enhanced approach		1.2	
Environmental gain in CO_2 due to enhanced approach		1.2	
NOX emissions (kg)		2996.9	2930.3

Environmental gain in NO_X due to enhanced approach	2.22

Table 8-24: Results summary of the long haul flight, MEA

Parameter	Min. fuel - with systems power	Min. fuel - MEA
Fuel burn for optimised phases	90575	85728
% reduction in fuel burn due to MEA	5.35	
Environmental gain in CO_2 due to MEA %	5.35	
NOX emissions (kg)	3222.6	3222.4
Environmental gain in NO_X due to MEA %	0.01	
	Min. time - with systems power	Min. time - MEA
Fuel burn for optimised phases	99854	98704
% reduction in fuel burn due to MEA	1.15	
Environmental gain in CO_2 due to MEA %	1.15	
NOX emissions (kg)	2930.3	3049.7
Environmental gain in NO_X due to MEA %	-4.07	

8.3 Effect of mission profile on trajectory, systems configuration and systems operation

During the study it became clear that the effect of the airframe systems was far more complex than initially envisaged at the literature review stage. By analysing the results

for the two case studies it became apparent that the effect due to the airframe systems was not only dependant on the aircraft type but also the mission. Moreover, the advantage of the more-electric aircraft was also dependant on the aircraft mission. To have a clear view of the interwoven effects of trajectory optimisation, systems configuration and systems operation, the results of the Min. fuel trajectories for the long haul and short haul flight are compared to each other.

The penalty due to conventional airframe systems has been of fundamental importance to this study. The initial findings documented in [74] suggested that the impact of the systems cannot be thought of as a constant effect which would not affect trajectory optimisation. This has been one of the primary bases of the study. By comparing the “Min. fuel – zero power off-takes” to “Min. fuel – systems power post processed”, the impact of conventional systems can be analysed. The result is shown in Figure 8-32 and Figure 8-33.

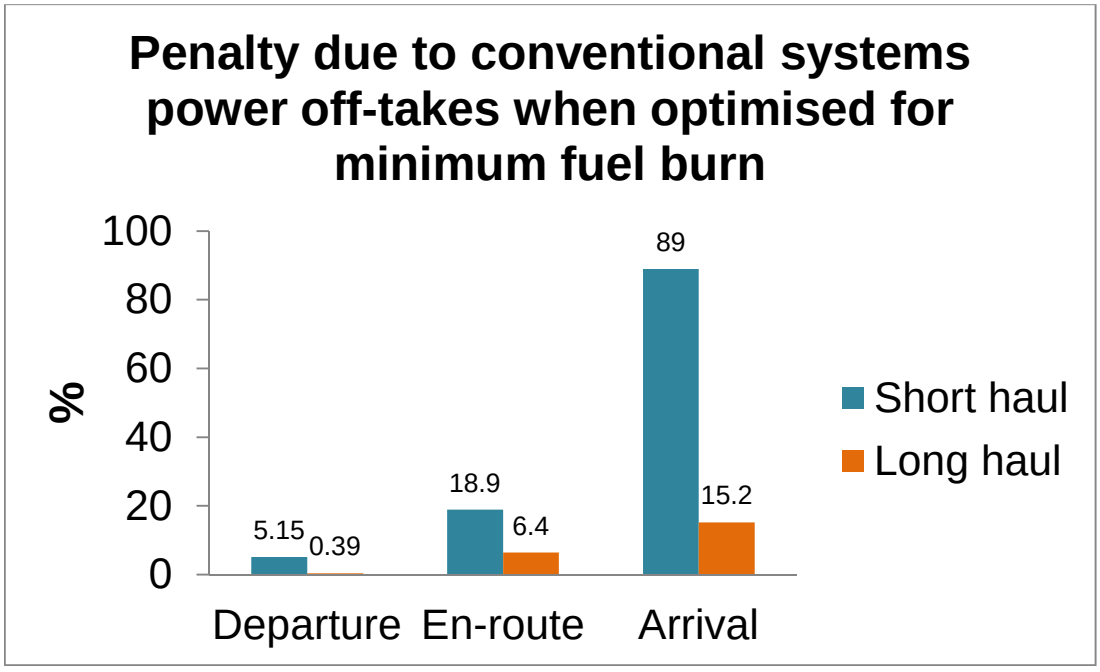

Figure 8-32: Comparison of the effect due to conventional systems under different flight durations

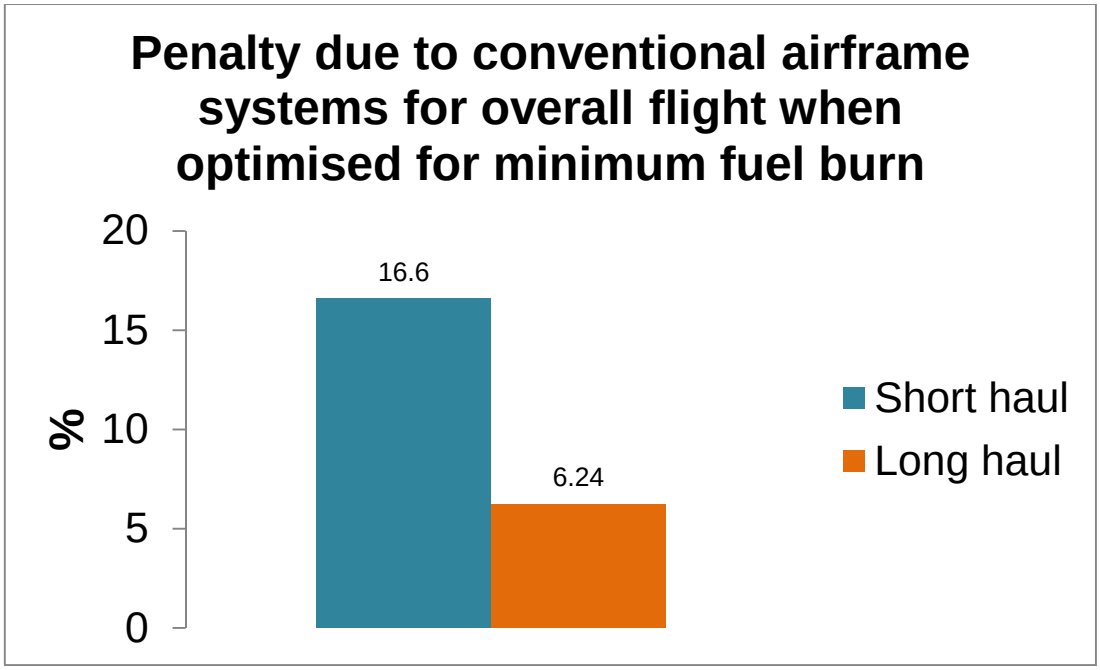

Figure 8-33: Comparison of the effect due to conventional systems on the two trajectory cases

As can be seen the airframe systems have a greater impact on shorter durations of flight. As expected the impact of the systems off-takes are greater during low throttle conditions such as those encountered during a typical arrival phase. A key observation is that the variation of the penalty due to systems is not uniform. This is due to the impact the trajectory has on the systems. This is further proof that when studying the scope of real-aircraft trajectory optimisation, the airframe systems penalties have to be represented as closely as possible. The effect on fuel burn and emissions are influenced by a number of top level parameters such as the flying conditions, operating procedure, and aircraft technology level. None of these should be singled out as the main contributor due to the sheer complexity of the entire system.

One of the key arguments throughout this study was that if results obtained through the classical trajectory optimisation approach were applied in real-aircraft, the fuel burn and emissions output would be higher than expected. These are shown in “Min. fuel – systems post power processed” trajectory results. With the enhanced approach of including airframe systems penalties in the loop, behaviour which is closer to real aircraft are represented. The fuel saving due to the enhanced approach is shown in Figure 8-34.

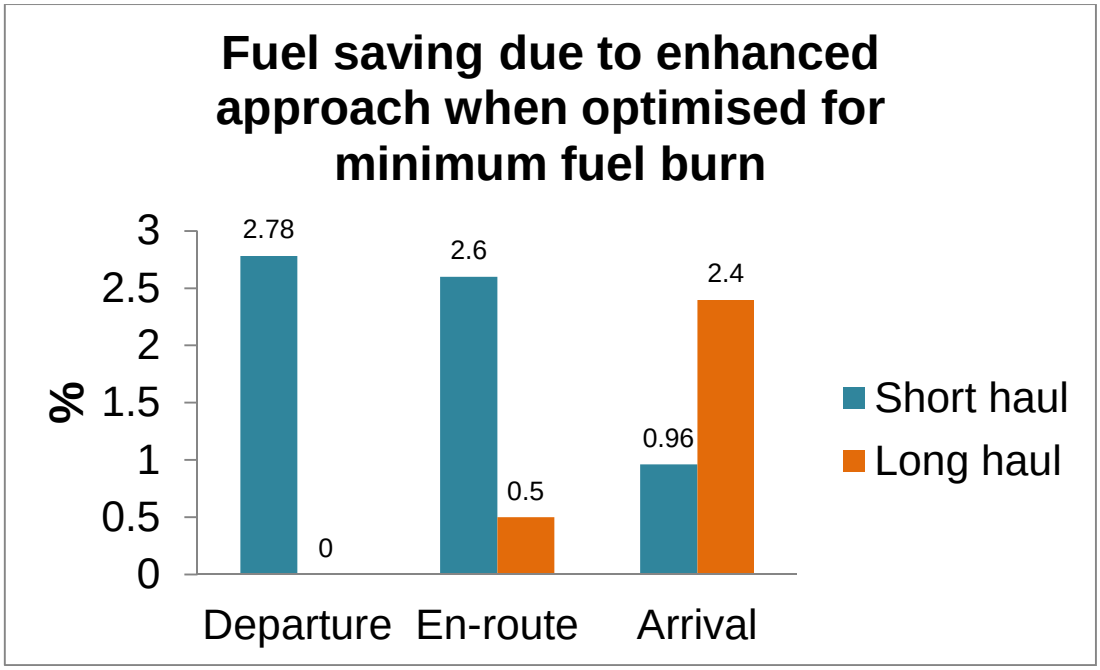

Figure 8-34: Fuel saving due to the enhanced trajectory optimisation

The fuel savings through the enhanced approach are higher for the short-haul but on average the enhanced approach accounts for a 2.5% and 0.5% reduction in fuel for the short haul and long haul trajectories, respectively, as shown in Figure 8-35. When considering the actual fuel burn of about 80,000 to 90,000 kg, on a long haul flight such as the one simulated here, the fuel saving in kilograms is quite significant. The same applies for the short haul trajectory. And once the numbers of annual flights are taken into consideration the savings in fuel, costs and emissions increase exponentially.

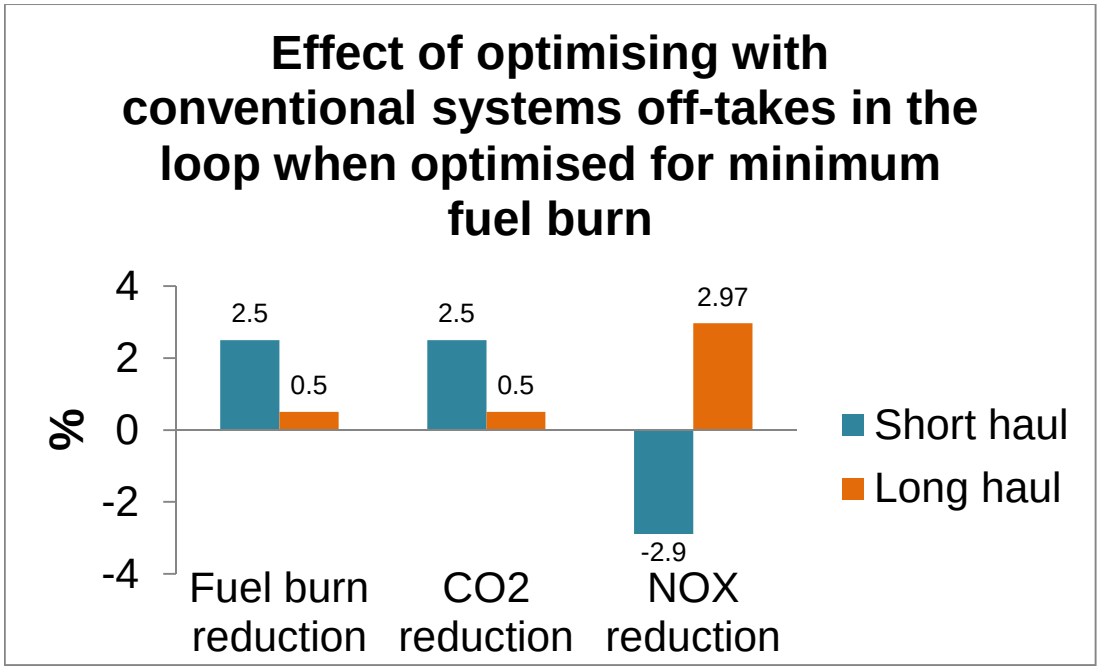

Figure 8-35: Advantage of the enhanced approach to trajectory optimisation

Apart from the fuel and emissions savings achieved by using the enhanced approach, the enhanced approach also establishes the basis for studying more electric aircraft in the trajectory optimisation domain. It is of vital importance to quantify the gain over the conventional aircraft in terms of fuel efficiency but also creates the environment to fuse and study novel design and novel operational procedures. The more electric aircraft is expected to be more efficient than the conventional aircraft. When a typical short haul trajectory was simulated for both the conventional and MEA [95], the MEA showed an 8.3% reduction in fuel burn. During the research the MEA concept was coupled with trajectory optimisation to increase the efficiency of the MEA through optimised operation. The results are shown in Figure 8-36 and Figure 8-37.

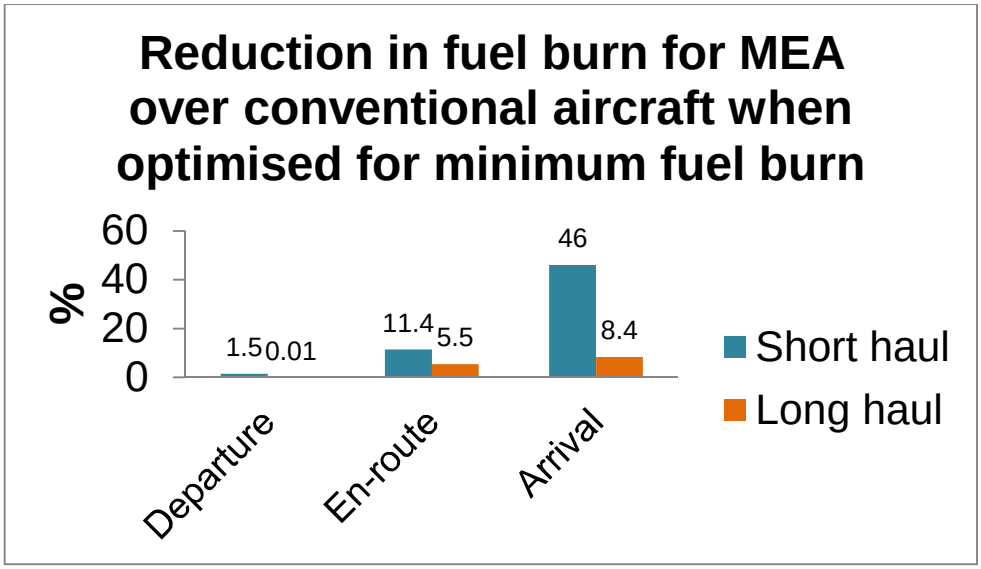

Figure 8-36: Reduction in fuel burn of the MEA during various flight durations

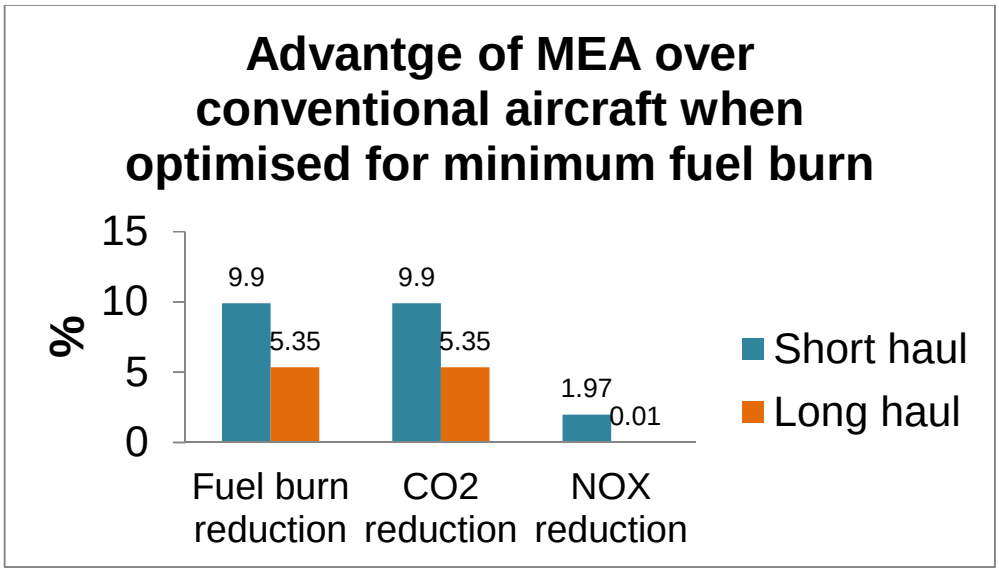

Figure 8-37: Comparison of optimised trajectories for MEA and conventional aircraft

The results show that optimising MEA operation will increase the advantage over conventional aircraft. The reduction in fuel burn and emissions are significant considering the volume of air traffic and the expected growth in years to come. By combining the domain of aircraft design and aircraft operation such as this study has done, the advantages of novel concepts can be evaluated in a broader scope.

8.4 Impact on noise and extension of study to 3-D optimisation

The ADM as described in §7.4.1 is cable of performing 3-D optimisation. To demonstrate this feature as well as to observe the noise impact of the trajectories, 3-D optimisation was performed with the objective of minimising noise levels. The number of awakenings was used as the noise index and the objective was to minimise the number of awakenings.

8.4.1 Long haul departure – noise optimisation

The noise grid that was constructed using the D3 tool described in §7.5.2, cover the area shown in Figure 8-38. The population density is shown as a contour map.

Figure 8-38: Long haul departure noise grid and population density

The problem setup which was optimised for minimum noise impact included freedom for waypoint displacement. WP3 and WP4 in Table 8-14 were given the freedom to move its position by 0.01 degrees in longitude (East or West) and 0.05 degrees in latitude (North or South). None of the other constraints were changed. The noise index summary is shown below in Table 8-25.

Table 8-25: Awakenings summary – long haul departure

Trajectory	Awakenings
Min. fuel – zero power off-takes	40950
Min. time – zero power off-takes	41343
Min. fuel – with systems power	40956

Min. time – with systems power	41450
Min. fuel - MEA	40932
Min. time - MEA	41352
Min. noise – with systems power	18082

The improvement by optimising for the noise levels is clearly significant. The “Min. noise – with systems power” is 55.85% quieter than the “Min. fuel – with systems power”. The effect is due to a combination of the lateral movement in the ground track, different altitude profile and significantly lower flying speed.

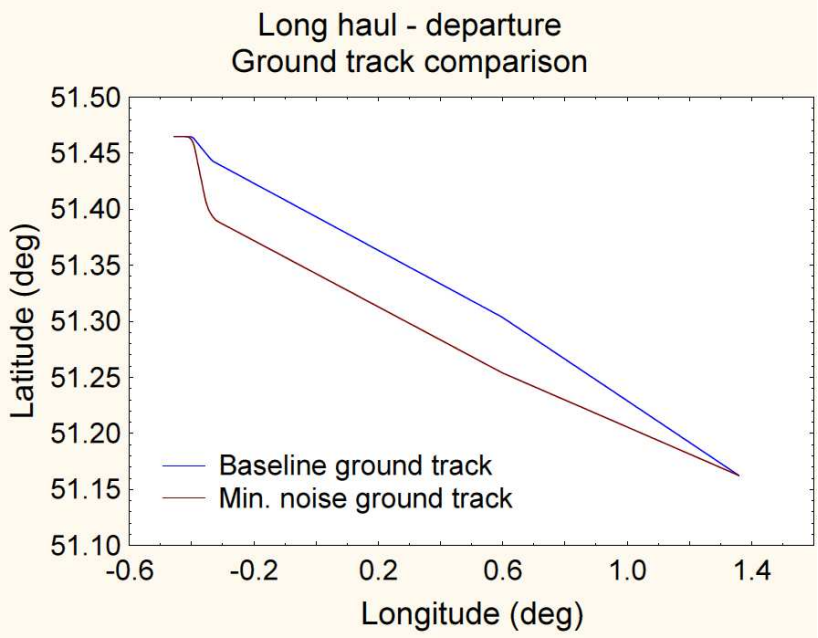

a) Latitude vs longitude

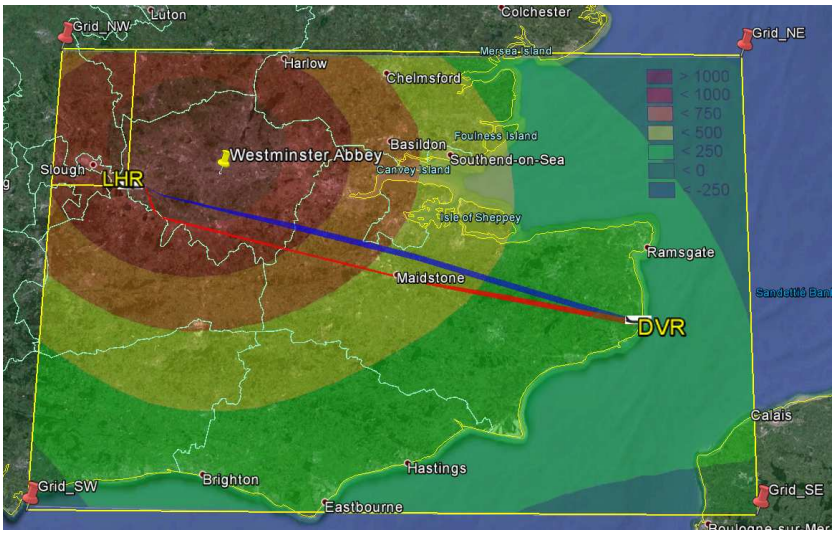

b) Projection on population density

Figure 8-39: Ground track variation when optimised for noise – long haul

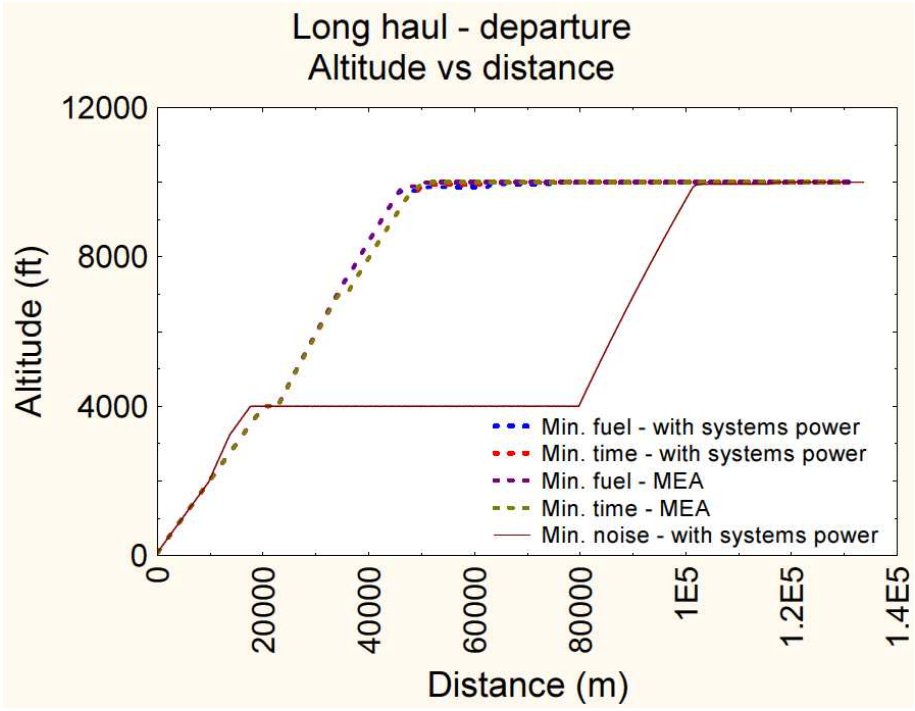

Figure 8-40: Altitude variation when optimised for noise – long haul

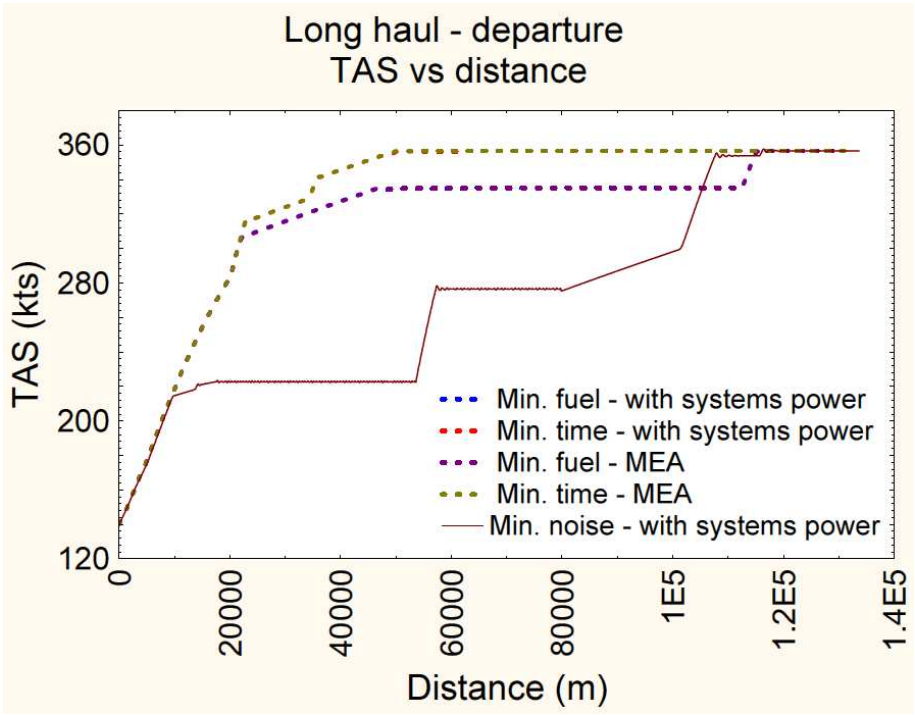

Figure 8-41: TAS variation when optimised for noise – long haul

The “Min. noise” characteristic profiles are shown in Figure 8-39, Figure 8-40, and Figure 8-41. The sound exposure level, measured in A-weighted decibel has been plotted to illustrate the difference in the number of awakenings.

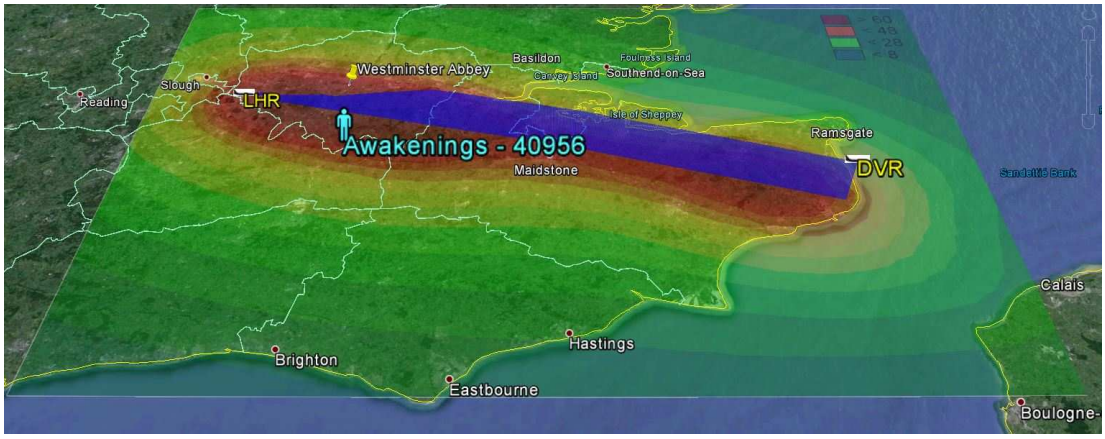

a) Min. fuel – with systems power

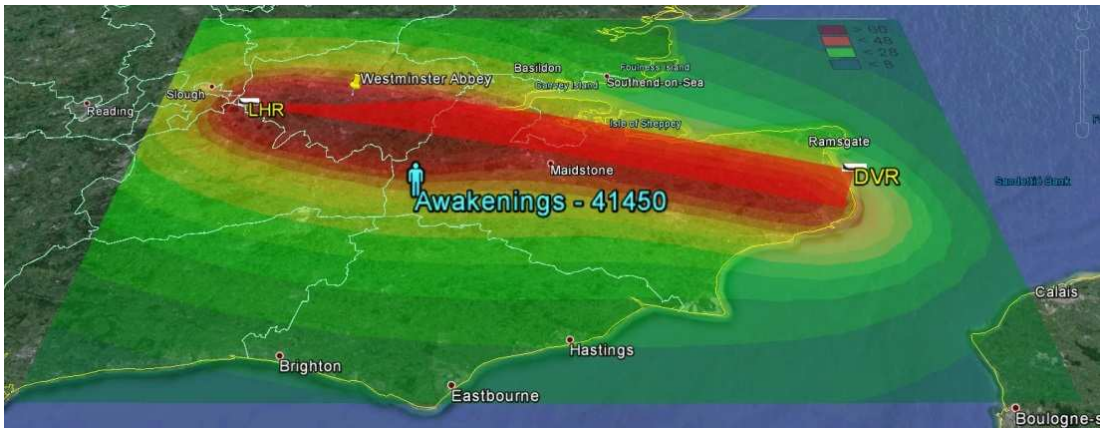

b) Min. time – with systems power

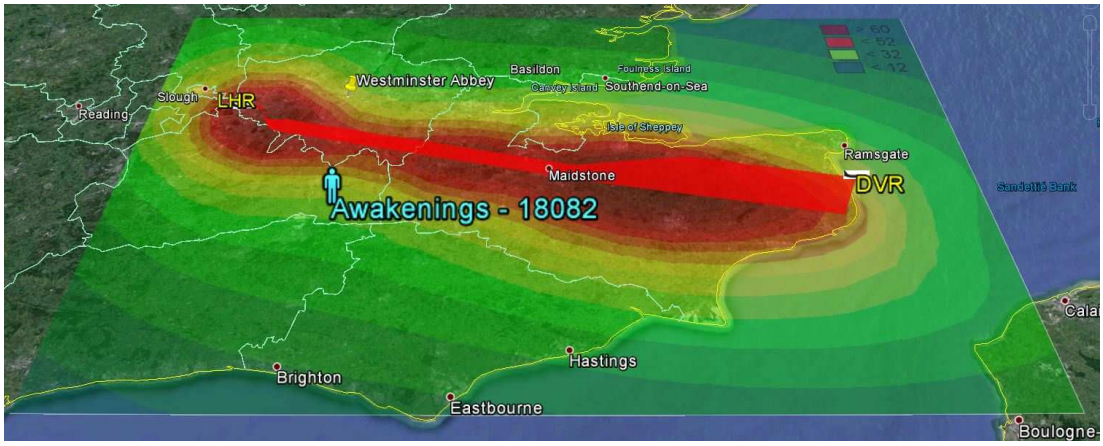

c) Min. noise – with systems power

Figure 8-42: Noise contours (SEL in dBA) for conventional aircraft under different operating conditions – long haul

The noise contours in Figure 8-42 show that for the “Min. noise – with systems power” trajectory the area around Westminster Abbey (marked with a yellow place mark) has a lower exposure level. The place mark gives indication to Central London which is

heavily populated. The trajectory of the aircraft has shifted to the south to avoid the heavily populated areas and flies lower and slower to reduce the exposure levels. The sound exposure levels in the Greater London area for the “Min. fuel –with systems power” and “Min. time – with systems power” trajectories are red in colour and are more than 60 dBA. But for the “Min. noise trajectory” the sound exposure level in the Central London area as well as most of the Greater London area is less than 38 dBA. As a consequence there is a drastic reduction in the number of awakenings.

The advantage in the noise reduction comes at the cost of fuel and flight time. The “Min. noise – with systems power” trajectory burns 8% more fuel than the “Min. fuel – with systems power” trajectory. It has a 24.9% longer flight time than the “Min. time – with systems power” trajectory. Optimising for noise in this instance poses an emissions penalty. The CO_2 output is 8% higher and the NO_X output is 86.4% higher than the “Min. fuel – with systems power” trajectory.

The noise calculation model which is discussed in §7.5.1 is mainly influenced by the engine and aircraft noise measurements. In the conventional aircraft, the airframe systems have no significant impact on the noise generated. There is a case to be made that systems such as electric ECS with high ram air intake may influence the noise generation. But this is beyond the scope of both the noise calculation model used and this research. There is a slight difference in the number of awakenings between the Min. fuel and Min. time trajectories for the conventional aircraft and MEA. This is due to the variations in aircraft speed and thrust levels. Since noise generation of systems cannot be represented accurately, the MEA has not been optimised for minimum noise operation. The research suggests no indication that there would be a significant difference between the conventional and MEA for noise operation when both aircraft types use the same airframe and engine.

8.4.2 Short haul departure – noise optimisation

The short haul departure was subjected to a similar study as above. Wp3, WP4, and WP5 in Table 8-2 was given the freedom to displace by 0.01 degree in longitude (East or West) and latitude (North or South). Other constraints were kept the same.

The population grid and population density projection is shown in Figure 8-43.

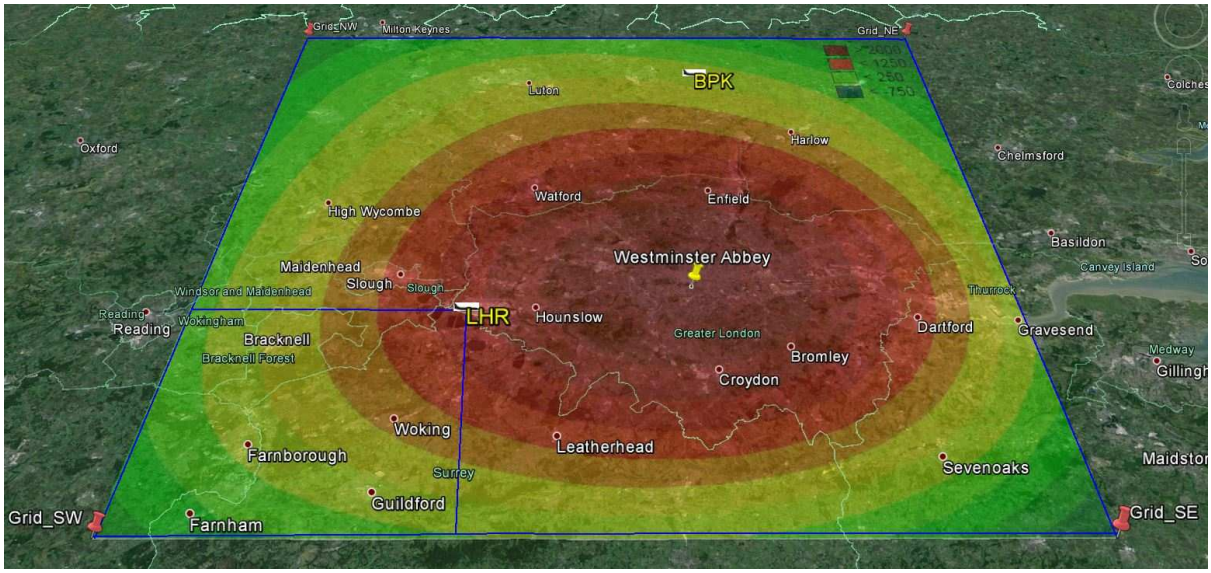

Figure 8-43: Short haul departure noise grid and population density

The awakenings summary is shown in Table 8-26.

Table 8-26: Awakenings summary – short haul departure

Trajectory	Awakenings
Min. fuel – zero power off-takes	10163
Min. time – zero power off-takes	12882
Min. fuel – with systems power	13012
Min. time – with systems power	12882
Min. fuel - MEA	10251
Min. time - MEA	12882
Min. noise – with systems power	8867

The reduction in the number of awakenings when optimised for noise is 31.9% in comparison to the “Min. fuel – with systems power” trajectory. The improvement is lower than that observed in the long haul case. But the numbers of awakenings are far lower than the long haul case. The baseline ground track itself avoids most of Greater London; hence the population density is significantly lower. The sound exposure levels are shown in Figure 8-44.

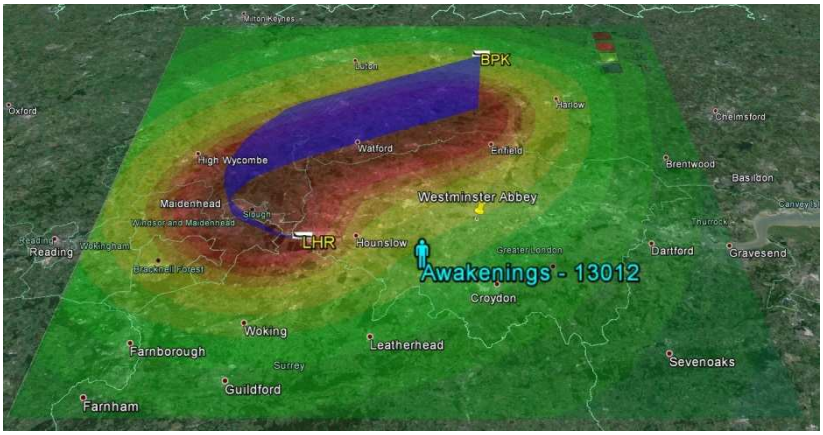

a) Min. fuel – with systems power

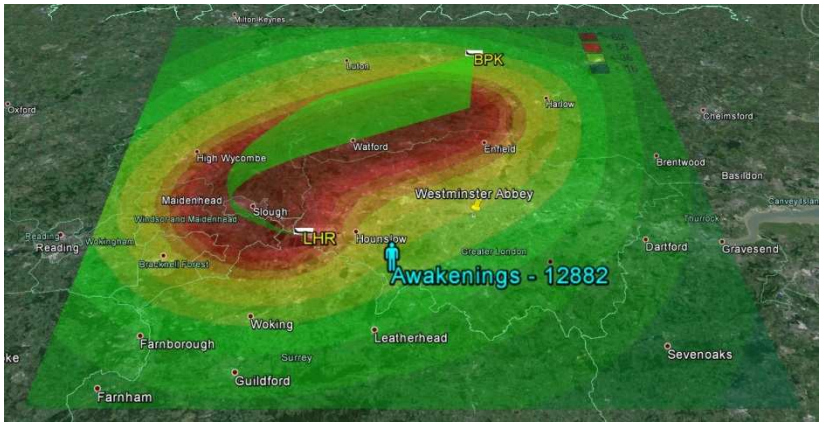

b) Min. time – with systems power

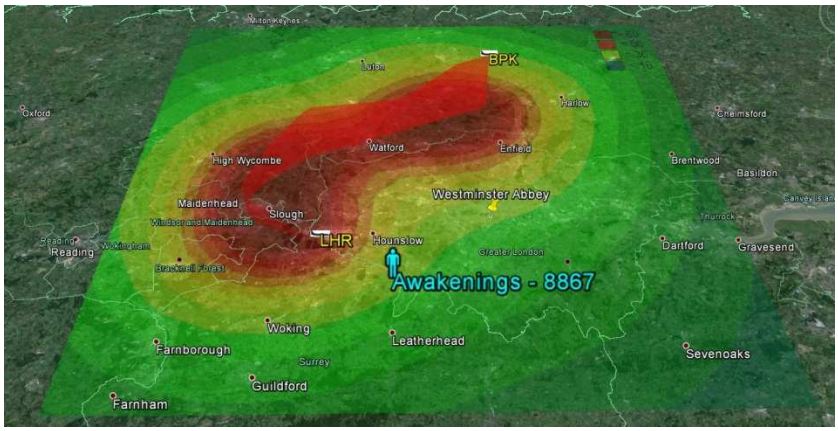

c) Min. noise – with systems power

Figure 8-44: Noise contours (SEL in dBA) for conventional aircraft under different operating conditions – short haul

The altitude profile, speed profile and the ground track variation for the “Min. noise – with systems power” trajectory is shown in Figure 8-45, Figure 8-46, and Figure 8-47 respectively.

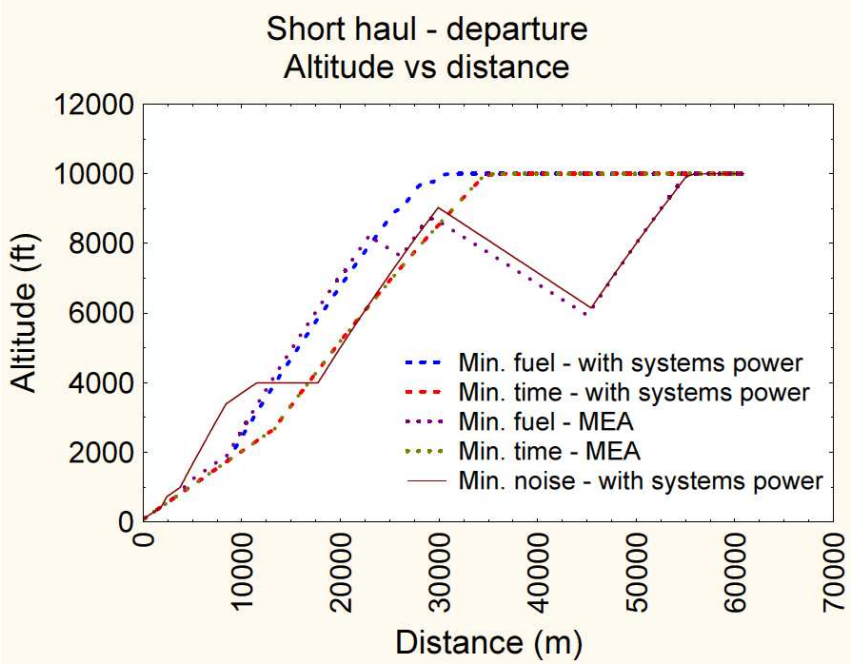

Figure 8-45: Altitude variation when optimised for noise – short haul

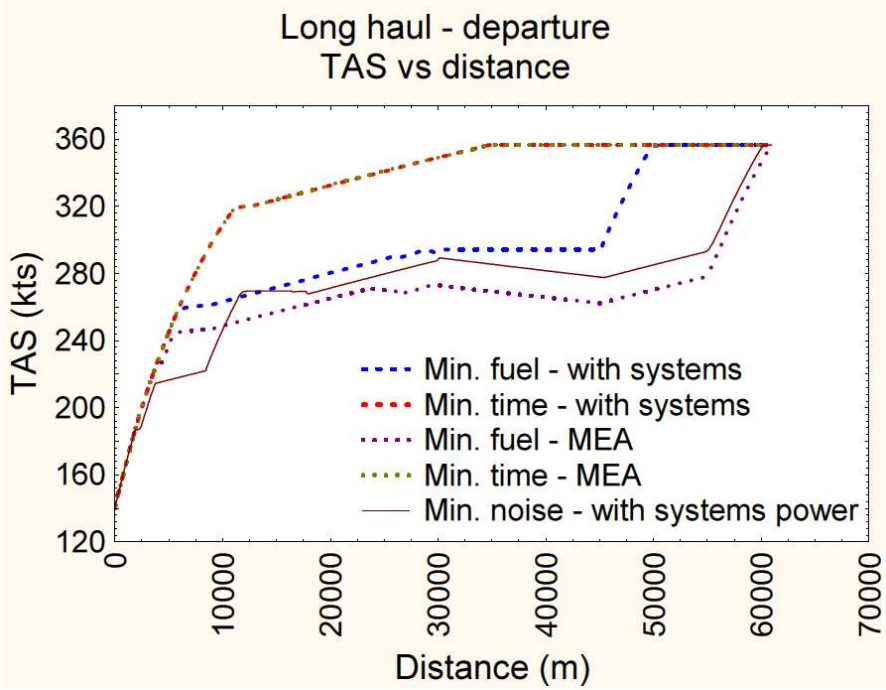

Figure 8-46: TAS variation when optimised for noise – short haul

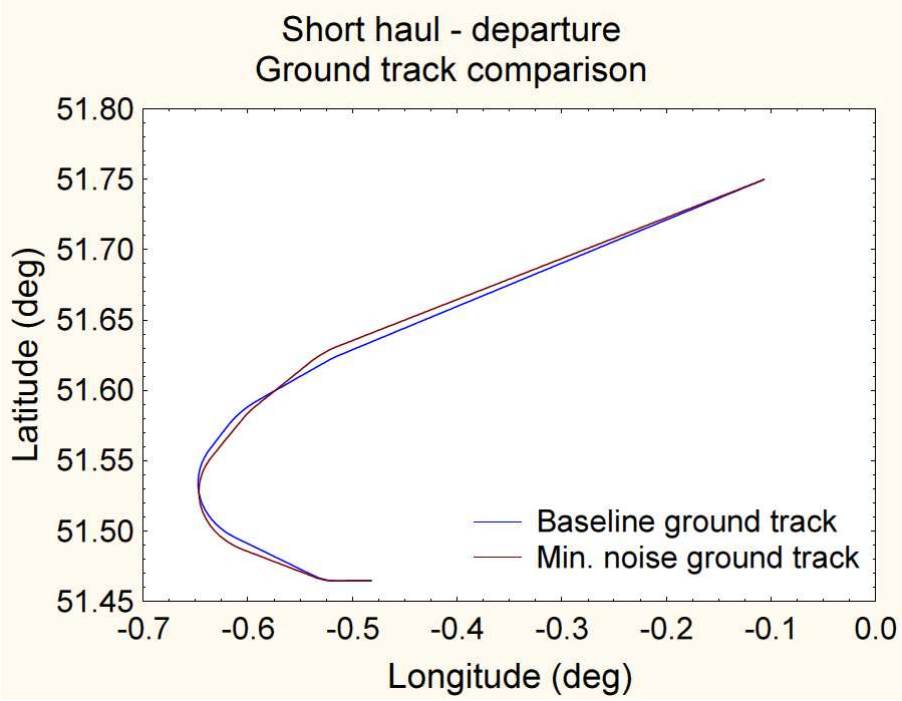

Figure 8-47: Ground track variation when optimised for noise – short haul

The results of the short haul case show that the numbers of “awakenings” appear to be sensitive to the operation of the airframe systems. The numbers of awakenings relative to one another vary between the different trajectories much more than the levels observed in the long haul case. The noise calculation doesn’t consider the operation of the systems in any form. So this is because the airframe systems influence the short haul trajectories more than the long haul trajectories in terms of fuel burn as observed in Figure 8-35 and Figure 8-37. The influence on the fuel burn ultimately has an effect on the altitude, speed and thrust profile which influence the sound exposure levels. However, these differences cannot be used to discuss the advantages and disadvantages between the conventional and MEA in terms of noise produced. More accurate noise modelling which takes into account the airframe systems need to be used to make such an assessment.

The lateral movement seen in this particular case is less significant than that observed in the long haul case. This is partly due to the less degree of freedom in the short haul study but also due to the fact that the population along the baseline ground track being similar in density. The long haul case was much more sensitive to noise in terms of the number of awakenings since the baseline ground track went through Greater London which is a heavily populated area with varying population density.

The “Min. noise – with systems power” had a 4.2% increase in fuel burn when compared to the “Min. fuel – with systems” trajectory. It had a 20.2% longer flight time compared to the “Min. time – with systems power” trajectory. The CO_2 emissions were 4.2% higher and the NO_X was 0.7% higher than the “Min. fuel – with systems power” trajectory.

9 Conclusion and future work

9.1 Conclusion

The research reviewed the evolution of the electrical loading in commercial aircraft by discussing the electrical load and distribution system qualitatively and detailed the electrical load profiles where data were available. It was concluded that the electrical load on-board the aircraft is the key driver for the generator size and rating and with current design going in favour of the MEA concept, it is no longer acceptable not to consider the design of the electrical loads and distribution system at the conceptual and preliminary design stages. This established the need for a clear concise methodology to estimate and size the electrical loading, distribution and generation system for the MEA concept at a conceptual and preliminary aircraft design stage.

Consequently a tool was developed to size the electrical loads of an aircraft (at the preliminary design stage) with relation to aircraft level, system level and operational level inputs and constraints. As part of the validation procedure, a sensitivity analysis was incorporated in to the tool itself, thereby showing the user the impact of an over-rating or under-rating of a component compared to the baseline calculation using the generic component database. The methodology was successfully validated at component, system and aircraft level. Observations from case study results revealed that the conventional electric load is only 33% of the total load of a comparative MEA.

To fulfil the aim of the study, fuel penalties due to airframe systems loads needed to be represented satisfactorily. The extensive simulations done using a thoroughly validated aircraft engine model on TURBOMATCH provided a numerical solution to predict the bleed air off-take and shaft power off-take fuel penalties in large commercial turbofan engines. The work also gave an insight to the behaviour of turbofan engines when there were power off-takes. The numerical method developed, could be coupled with generic SFC equations and used as a substitute for high fidelity performance codes, and was highly suited for computationally time exhaustive applications such as trajectory optimisation. This gave the ability to definitively establish whether the “more electric aircraft” had a significant advantage for various flight missions. It also provided the basis for MEA trajectory optimisation.

Having created a tool to model the conventional electric loads as well as an efficient model to act as an interface between the engine and airframe systems, a complete integrated model was developed which included other sub-systems (apart from the conventional electrical loads) such as the ECS and IPS. The ECS and IPS models were capable of representing the conventional or more electric configurations. These models were validated. The integrated model also included engine performance data, and a P3T3 emissions model. The integrated model was then configured to match two case study aircraft; a short haul aircraft and a long haul aircraft. To test the functionality a real trajectory between London Heathrow and Amsterdam Schiphol, which is typically flown by an Airbus A320 was simulated. It was observed that for this particular mission, the conventional airframe systems increased the fuel burn by 10.1%. The MEA increased the fuel burn by 0.9%. When considering only the departure phase of the trajectory, the conventional systems caused a fuel burn increase of 1.82% and the more-electric systems caused a fuel burn increase of 0.38%. Further studies were done on trajectory optimisation results obtained using the classical approach to optimisation which didn't include the airframe systems penalties in the optimisation loop. The airframe systems model was used as a post processor. The systems operation had significant power off-take demands of varying magnitudes during the different flight phases. This resulted in a significant fuel penalty due to airframe systems. It was concluded that the optimality of the computed aircraft trajectories (without the airframe systems penalties in the optimisation loop) can be significantly improved by representing the aircraft systems requirements within the optimisation loop, particularly for MEA applications.

Having coupled the integrated model with an aircraft dynamics model, the two case studies were studied in detail using the GATAC optimisation framework developed under the Clean Sky program. The optimiser used in the study was a GA based on the NSGA-2. One of the primary observations was that the airframe systems operation had a significant impact on the optimum way to fly (within the set constraints) in order to achieve a given objective. The penalty due to the systems varied according to the flight duration as well as the conditions of flying. More significantly, the MEA had different optimum operating procedures (within the set constraints) to those of the

conventional aircraft. This validated the enhanced approach to trajectory optimisation that has been used in the methodology of the study.

The conventional airframe systems account for a 16.6% fuel burn increase than expected in the short haul case and a 6.2% fuel burn increase than expected in the long haul case if results obtained for minimum fuel burn through the classical approach are applied in a real conventional aircraft. By using the enhanced approach to trajectory optimisation of representing the airframe systems in the optimisation loop, the study was able to prove that a 2.6% reduction in fuel burn for the short haul case and a 0.5% reduction in fuel burn for the long haul case could be achieved compared to the scenario mentioned above. The baseline for the comparison was the fuel burn that would occur if results from the classical trajectory optimisation approach (without systems penalties in the loop) were applied in aircraft with airframe system operational penalties. The MEA had 9.9% lower fuel burn during the shot haul case study and 5.4% lower fuel burn in the long haul case study than the conventional aircraft when the objective was the minimum fuel burn.

To demonstrate the capability of the models and the framework the optimisation was extended to included lateral trajectory optimisation thereby creating the environment to perform 3-dimensional trajectory optimisation. By using this approach, the long haul case study departure phase was optimised for minimum noise. The result was a different ground track which had 55.9% less “awakenings” (the noise index which was minimised) than the corresponding minimum fuel burn trajectory.

Optimising for noise caused other environmental penalties. The “Min. noise – with systems power” trajectory but 8% more fuel than the “Min. fuel – with systems power” trajectory. It had a 24.9% longer flight time than the “Min. time – with systems power” trajectory. The CO_2 output was 8% higher and the NO_X output was 86.4% higher than the “Min. fuel – with systems power” trajectory.

The short haul departure case showed that by optimising for noise levels, a 31.9% quieter trajectory than when optimised for fuel can be achieved. However, the “Min. noise – with systems power” had a 4.2% increase in fuel burn when compared to the “Min. fuel – with systems” trajectory. It had a 20.2% longer flight time compared to the

“Min. time – with systems power” trajectory. The CO_2 emissions were 4.2% higher and the NO_X was 0.7% higher than the “Min. fuel – with systems power” trajectory.

9.2 Contribution to knowledge

The research has provided a methodology to enhance the classical approach to aircraft trajectory optimisation by including the airframe systems power off-take penalties within the optimisation loop; thereby assessing optimum operations for novel more-electric aircraft.

9.3 Milestones achieved

- Development of a tool to size the conventional electrical loads at the conceptual and preliminary design stage. Moreover, the methodology developed can be used to assess airline modification programmes which affect the overall electrical loading.
- Integrated models which represent the majority of the secondary power system in both conventional and more-electric aircraft.
- Equations to study the impact on fuel consumption due to secondary power off-take. The model developed has a high accuracy which matches complex gas turbine performance codes but is not computationally exhaustive and can be used in optimisation problems.
- Establishment of the impact that the airframe systems have on the operation of the aircraft.
- Optimal trajectories for both conventional and more – electric aircraft for pre-defined case studies.

9.4 Future work

The scope of the work that can be achieved by implementing this methodology is vast. The GATAC framework is based on a modular architecture. Moreover, since the methodology presented uses genetic algorithms as optimisers, the system for optimisation doesn’t require discretisation or parameterisation. This provides the ability to treat models as “black boxes”. These facts combined, enables to add countless number of models which represent different aspect of aircraft design and aircraft operation.

Cost based optimisation, weather based optimisation, and airline scheduling based operation are some of the examples for further study.

With regard to the models presented in this study, further improvements can be made to the airframe systems models. By using industry level data accurate systems models can be incorporated into the problem setup. The same is true for the aircraft performance and dynamics. By using industry level data, parameters such as the aerodynamic co-efficient and aircraft weight can be adjusted to real aircraft.

The methodology to calculate the penalty due to off-takes is limited to large commercial turbofan engines. This can be extended to cover turbo prop engines and more importantly novel engine concepts such as open rotor engines. This would enable to combine and study novel aircraft concepts, novel airframe systems concepts, novel engine concepts and novel air traffic operation concepts in one framework.

The noise evaluation methodology used in this study is limited to conventional aircraft. By using improved noise evaluation tools which are based on the aircraft dynamics, drag and thrust levels the conventional aircraft can be compared to the MEA. This would help understand the overall impact of the MEA for a multi-disciplinary scope.

The results presented in the research are limited to two flight missions. By evaluating more flight missions comprising of different durations and flying conditions, the impact of the airframe systems can be understood better. This holds true with regard to the impact of the MEA.

Even though this study has demonstrated multi-disciplinary multi-objective optimisation the optimisation objectives, have been limited to fuel burn, time and noise. As demonstrated in the results the models are capable of calculating other emissions such as NO_X. The fuel burn directly corresponds to CO_2 emissions but the NO_X is dependent on the operating temperatures of the engine. Further optimisation studies can be done to find efficient procedures to reduce the NO_X not only during the departure and arrival phases but also during the cruise phase.

The demonstration of 3-D trajectory optimisation was limited to optimising the noise. But this concept can be expanded to cover a vast envelop of air traffic management concepts including “free-flight” where there are no restrictions and ATM constraints.

The final aim is to expand this methodology and produce a framework and model suite which creates and environment to design and evaluate novel aircraft concepts for novel air traffic management concepts. And also to create and test laboratory setups and/or flight test data for verification and validation of individual models but also the top level concepts and methodology proposed in this study.

10 Publications

10.1 Journal publications:

Ravinka Seresinhe, and Craig Lawson, "*The MEA Evolution in Commercial Aircraft and the Consequences for Initial Aircraft Design"*; Journal of Aerospace Engineering and Technology, Volume 3, 2013, STM Journals, ISSN: 2231-038X

Ravinka Seresinhe, Craig Lawson and Roberto Sabatini, *"Environmental Impact Assessment, on the Operation of Conventional and More Electric Large Commercial Aircraft"*; SAE International Journal of Aerospace, Volume 6, Issue 1, 2013, SAE International, DOI: 10.4271/2013-01-2086

Ravinka Seresinhe and Craig Lawson, *"Electrical load-sizing methodology to aid conceptual and preliminary design of large commercial aircraft"*; Proceedings of the Institution of Mechanical Engineers, Part G: Journal of Aerospace Engineering, OnlineFirst, 2014, SAGE Publications DOI: 10.1177/0954410014534638

Ravinka Seresinhe, Craig Lawson, Ahmed Shinkafi, Daniele Quaglia and Irfan Madani, "*Improving the operating efficiency of the more-electric aircraft concept through optimised flight procedures"*; Optimizing and Engineering (under review)

Ravinka Seresinhe, Craig Lawson and Dieter Scholz, "*Simplified regression model to account for SFC penalties due to power off-takes in large turbofan aircraft*"; Proceedings of the Institution of Mechanical Engineers, Part G: Journal of Aerospace Engineering (under review)

Ravinka Seresinhe, Craig Lawson, Daniele Quaglia, Ahmed Shinkafi and Irfan Madani, "*Comparison of short and long haul trajectory optimisation for conventional and more-electric large aircraft"*; AIAA Journal of Aircraft (under review)

Ravinka Seresinhe, Daniele Quaglia, Craig Lawson, Ahmed Shinkafi and Irfan Madani, *"Multi-disciplinary approach to multi-objective aircraft trajectory optimisation"*; AIAA Journal of Aircraft (under review)

10.2 Conference publications:

Dieter Scholz, Ravinka Seresinhe, Ingo Staack and Craig Lawson, *"Fuel consumption due to shaft power off-takes from the engine"*; AST 2013: Workshop of Aircraft System Technologies, 2013, Hamburg, Germany, AST 2013

Ravinka Seresinhe, Craig Lawson, Ahmed Shinkafi, Daniele Quaglia and Irfan Madani, *"Airframe systems power off-take modelling in more-electric large aircraft for use in trajectory optimisation"*; 29th Congress of the International Council of Aeronautical Sciences, 2014, St Petersburg, Russia, ICAS 2014

Ahmed Shinkafi, Craig Lawson, Ravinka Seresinhe, Daniele Quaglia and Irfan Madani, *"An intelligent ice protection system for next generation aircraft trajectory optimisation"*; 29th Congress of the International Council of Aeronautical Sciences, 2014, St Petersburg, Russia, ICAS 2014

10.3 Clean Sky reports;

Aircraft Systems Modelling – Specification Document – WP3.1:O_3.1_40_a; R Seresinhe, M Cooper, R Vega Diaz and A Shinkafi, Clean Sky, 2012

Aircraft Systems Model – Description Document – WP3.1:O_3.1_40_b; Ravinka Seresinhe, Clean Sky, 2012

D_3.2.2_7 Report on the Performance Analysis of Trajectories Using GATAC Version 3 – Ravinka Seresinhe, Daniele Quaglia, Mathruin Pelletier de Chambure, Lorenzo Virgili, Siti Nur Mariani Mohd Yunos, Clean Sky, 2014

Works Cited

1. **Clean Sky.** Aviation & Environment. *Clean Sky.* [Online] [Cited: 13 March 2013.] http://www.cleansky.eu/content/homepage/aviation-environment.

2. **AIRBUS.** *DELIVERING THE FUTURE - Global market Forecast 2011-2030.* s.l. : AIRBUS, 2011.

3. **Waitz, Ian, et al.** Report to the United States Congress - AVIATION AND THE ENVIRONMENT - A National Vision Statement, Framework for Goals and Recommended Actions. *MIT.edu.* [Online] [Cited: 13 March 2013.] http://web.mit.edu/aeroastro/partner/reports/congrept_aviation_envirn.pdf.

4. **ICAO - Chief Economic Analysis & Policy Section.** AVIATION STATISTICS & DATA: A VITAL TOOL FOR THE DECISION MAKING PROCESS. *ACI Airport Statistics and Forecasting Worksop.* London : ICAO, 2011.

5. **Arguelles, P, et al.** *EUROPEAN AERONAUTICS: A VISION FOR 2020 - Meeting society's needs and winning global leadership.* Luxembourg : European Commission, 2001.

6. **Peacock, N J.** *Engine Design and Systems Integration for Propfan and High Bypass Turbofan Engines.* San Diego, California : American Institue of Aeronautics and Astronautics (AIAA), 1987. AIAA-87-1730.

7. **Giannakakis, Panagiotis, Laskaridis, Panagiotis and Pilidis, Pericles.** *Effects of Offtakes for Aircraft Secondary-Power Systems on Jet Engine Efficiency.* s.l. : American Institute of Aeronautics and Astronautics (AIAA), 2011. JOURNAL OF PROPULSION AND POWER. doi: 10.2514/1.55872.

8. **Rosero, J.A, et al.** *Moving Towards a More Electric Aircraft.* s.l. : IEEE, 2007.

9. **Feiner, L.J.** *POWER-BY-WIRE AIRCRAFT SECONDARY POWER SYSTEMS.* s.l. : AIAA/IEEE, 1993. ISBN:0-7803-1343-7.

10. **ACARE.** *Strategic Research Agenda Volume 2.* s.l. : ACARE, 2002.

11. **Moir, Ian and Seabridge, Allan.** *Aircraft Systems - Mechanical, electrical, and avionics subsystems integration.* s.l. : John Wiley & Sons, 2008. ISBN: 978-0-470-05996-8.

12. **Cronin, M J, et al.** *Integrated Digital/Electric Aircraft Concepts Study.* Scientific and Technical Information Brach, National Aeronautics and Space Administration (NASA). s.l. : NASA, 1985. NASA Contractor Report 3841.

13. **Hoffman, Anthony C, et al.** *Advanced Secondary Power System for Transport Aircraft.* Scientific and Technical Information Branch, National Aeronautics and Space Administration (NASA). s.l. : NASA, 1985. NASA TECHNICAL PAPER 2463.

14. **Tagge, G E, Irish, L A and Bailey, A R.** *Systems Study for an Integrated Digital/Electric Aircraft (IDEA).* Scientific and Technical Information Branch, National Aeronautics and Space Administration (NASA). s.l. : NASA, 1985. NASA Contractor Report 3840.

15. **Cross, A.M., Forsyth, A.J. and Mason, G.** *Modelling and SImulation Strategies for the Electric Systems of Large Passenger Aircraft.* s.l. : SAE-2002-01-3255, 2002.

16. **Times Higher Education.** 'POA' - research project works to optimise aircraft power use. *Times Higher Education.* [Online] 26 October 2004. [Cited: 12 October 2011.] http://www.timeshighereducation.co.uk/story.asp?storyCode=192017&sectioncode=26.

17. **MOET Technologies.** More Open Electrical Technologies. *eutrd.* [Online] 14 December 2009. [Cited: 13 10 2011.] http://www.eurtd.com/moet/.

18. **Anderson, Robert H.** *Secondary Power Generation System Considerations for Advanced Aircraft.* s.l. : SAE - 841604, 1984.

19. **Beauchamp, Edward D.** *Secondary Power Generation - Tomorrow's Concepts and Today's Risks.* s.l. : SAE - 942113, 1994.

20. **Lockheed Aircraft Corporation.** L-1011-500 TRISTAR TECHNICAL PROFILE. *Tristar 500.net.* [Online] [Cited: 27 June 2012.] http://www.tristar500.net/features/technicalprofile.pdf.

21. **Lockheed - California Company.** *Engineering Description Series - Volume 7, Electrical, L-1011 TriStar.* s.l. : Lockeed - California Company, 1970.

22. **Hannan, W.P.** *Secondary Power Systems.* s.l. : SAE - 740465, 1974.

23. **Roskam, Jan.** *Airplane Design.* s.l. : Roskam Aviation and Engineering Corporation, 1989. ISBN:978-1884885242.

24. **Airbus Training.** AIRBUS 300/310 SERIES - Systems - Hydraulic System. *SMARTCOCKPIT.* [Online] [Cited: 28 June 2012.] http://www.smartcockpit.com/pdf/plane/airbus/A300A310/systems/0014/.

25. —. AIRBUS 300/310 SERIES - Systems - Pneumatic System. *SMARTCOCKPIT.* [Online] [Cited: 28 June 2012.] http://www.smartcockpit.com/pdf/plane/airbus/A300A310/systems/0018/.

26. —. AIRBUS 300/310 SERIES - Systems - Electrical System. *SMARTCOCKPIT.* [Online] [Cited: 28 June 2012.] http://www.smartcockpit.com/pdf/plane/airbus/A300A310/systems/0007/.

27. **Airbus.** *Airbus A300 Engineering Notes Edition 2 Volume 2.* s.l. : Airbus, 1975.

28. **Airbus Training.** Airbus 320 Series - Systems - Hydraulic. *SMARTCOCKPIT.* [Online] [Cited: 10 November 2011.] http://www.smartcockpit.com/pdf/plane/airbus/A320/systems/0033/.

29. **Airbus Industrie.** *Airbus Industrie briefing : A320.* s.l. : Airbus Industrie, 1993.

30. **Airbus Training.** Airbus 320 Series - Systems - Pneumatics. *SMARTCOCKPIT.* [Online] [Cited: 10 November 2011.] http://www.smartcockpit.com/pdf/plane/airbus/A320/systems/0042/.

31. —. Airbus 320 Series - Systems - Electrical. *SMARTCOCKPIT.* [Online] [Cited: 10 November 2011.] http://www.smartcockpit.com/pdf/plane/airbus/A320/systems/0037/.

32. **AIRBUS TRAINING.** AIRBUS 340 - Systems - Pneumatics. *SMARTCOCKPIT.* [Online] [Cited: 03 July 2012.] http://www.smartcockpit.com/pdf/plane/airbus/A340/systems/0021/.

33. —. AIRBUS 340 - Systems - Hydraulics. *SMARTCOCKPIT.* [Online] [Cited: 03 July 2012.] http://www.smartcockpit.com/pdf/plane/airbus/A340/systems/0012/.

34. —. AIRBUS 340 - Systems - Electrical. *SMARTCOCKPIT.* [Online] [Cited: 03 July 2012.] http://www.smartcockpit.com/pdf/plane/airbus/A340/systems/0007/.

35. **SMARTCOCKPIT.** BOEING 777 - Systems - Electrical NEW. *SMARTCOCKPIT.* [Online] [Cited: 03 July 2012.] http://www.smartcockpit.com/pdf/plane/boeing/B777/systems/0005/.

36. **Moir, Ian.** *The All-Electric Aircraft - Major Challenges.* s.l. : IEEE, 1998.

37. **Rajashekara, Kaushik.** *Converging Technologies for Electric/Hybrid Vehicles and More Electric Aircraft Systems.* Fort Worth, TX, USA : SAE, 2010. pp. 2010-01-1757.

38. **Boeing Commercial Airplanes.** 787 No-Bleed Systems: Saving Fuel and Enhancing Operational Efficiencies. *AERO.* 2007, 28_Quater 04.

39. **Jackson, Paul, Munson, Kenneth and Peacock, Lindsay.** *JANE'S - All the world's Aircraft 2006-2007.* s.l. : Jane's Information Group Limited, 2006.

40. **AIRBUS.** Aircraft families. *Airbus.* [Online] [Cited: 02 July 2012.] http://www.airbus.com/aircraftfamilies/.

41. **BOEING.** Commercial Airplanes/About Our Products. *Boeing.* [Online] [Cited: 02 July 2012.] http://www.boeing.com/commercial/products.html.

42. **Lambert, Mark, Munson, Kenneth and Taylor, Michael.** *JANE'S - All the world's Aircraft 1991-92.* s.l. : Jane's Information Group Limited, 1991.

43. **Lambert, Mark and Munson, Kenneth.** *JANE'S - All the world's Aircraft 1994-95.* s.l. : Jane's Information Group Limited, 1994.

44. **Howe, Denis.** *Aircraft Conceptual Design Synthesis.* s.l. : Professional Engineering Publishing Limited, 2005. ISBN:978-1860583018.

45. **Kundu, Ajoy Kumar.** *Aircraft Design.* s.l. : Cambridge University Press, 2010. ISBN: 978-0521885164.

46. **Raymer, Daniel P.** *Aircraft Design: A Conceptual Approach.* Fourth Edition. s.l. : AIAA, 2006. ISBN:978-1563478291.

47. **Tooley, Mike and Wyatt, David.** *AIRCRAFT ELECTRICAL AND ELECTRONIC SYSTEMS - PRINCIPLES, MAINTENANCE AND OPERATION.* s.l. : Elsevier Ltd., 2009. ISBN: 978-0750686952.

48. **Fielding, John P.** *Introduction to Aircraft Design.* s.l. : CAMBRIDGE UNIVERSITY PRESS, 1999.

49. **CAA - Safety Regulation Group.** AIRWORTHINESS INFORMATION LEAFLET - AIRCRAFT ELECTRICAL LOAD AND POWER SOURCE CAPACITY ANALYSIS. *CAA.* [Online] 25 March 2004. [Cited: 05 July 2012.] http://www.caa.co.uk/docs/33/AIL0194.PDF. ISBN 1 904862 64 0.

50. **Renz, David D.** *COMPARISON OF ALL-ELECTRIC SECONDARY POWER SYSTEMS FOR CIVIL TRANSPORT.* s.l. : SAE-929493, 1992.

51. **Lee, J.C.** *Aircraft transformer-rectifier units.* s.l. : IET, 1972. pp. 69-71, Students' Quaterly Journal, Volume 42, Issue 169. doi: 10.1049/sqj.1972.0044.

52. **IEEE.** History: Origins of the Inverter - IEEE Industry Applications Magazine. *IEEE.* [Online] January/February 1996. [Cited: 21 November 2011.] ieeexplore.ieee.org/iel1/2943/10203/00476602.pdf.

53. **Kanokbannakorn, W, Saengsuwan, T and Sirisukprasert, S.** *The modeling of AC magnetic contactor for immunity studies and voltage sag assessment.* Khon Kaen : IEEE, 2011. pp. 621-624, 8th International Conference on Electrical Engineering/Electronics, Computer, Telecommunications and Information Technology (ECTI-CON). doi: 10.1109/ECTICON.2011.5947916.

54. *Electrical Systems Architectures for Future Aircraft.* **Emadi, Ali and Ehsani, Mehrdad.** s.l. : SAE - 1999-01-2645, 1999. Intersociety Energy Conversion Engineering Conference.

55. **Izquierdo, D, et al.** *Modeling methods for Solid State Power Controllers (SSPC).* s.l. : IEEE, 2009. pp. 265-270, Compatibility and Power Electronics.

56. *A comparative study of various motor drive systems for aircraft applications .* **Krishnan, R. and Bharadwaj, A.S.** s.l. : IEEE , 1991. Industry Applications Society Annual Meeting. pp. 252 - 258 vol.1.

57. **Maldonado, Miguel A, et al.** *Power Management and Distribution System for a More-Electric Aircraft (MADMEL).* Washington : IEEE, 1999. pp. 148-153, IEEE AES Systems Magazine. doi: 10.1109/IECEC.1997.659198.

58. **Rolls-Royce.** *THE JET ENGINE.* s.l. : Rolls-Royce plc, 1986. ISBN 0902121235.

59. **Boeing Commercial Airplane Company.** *Integrated Application of Active Controls (IAAC) Technology to an Advanced Subsonic Transport Project - Initial Act Configuration Design Study, Summary Report.* Scientific and Technical Information Branch, National Aeronautics and Space Administration (NASA). s.l. : NASA, 1980. NASA Contractor Reprt 3304.

60. **SAE INTERNATIONAL.** *Aircraft Fuel Weight Penalty Due to Air Conditioning - AIR 1168/8.* s.l. : SAE, 1989. SAE AIR 1168/8.

61. **Betts, John T.** *Survey of Numerical Methods for Trajectory Optimisation.* s.l. : AIAA, 1998. Journal of Guidance, Control and Dynamics, Volume 21, Issue 2.

62. **Sammut, Matthew, et al.** *Systems for Green Operations (SGO) ITD: GATAC V3 User Manual.* s.l. : Clean Sky, 2013.

63. **Chircop, Kenneth, et al.** *A GENERIC FRAMEWORK FOR MULTI-PARAMETER OPTIMISATION OF FLIGHT TRAJECTORIES.* s.l. : ICAS 2010, 2010. 27th International Congress of the Aeronautical Sciences.

64. **Pervier, Hugo, et al.** *Application of Genetic Algorithm for Preliminray Trajectory Optimisation.* s.l. : SAE, 2011. SAE International Journal of Aerospace Volume 4, Issue 2.

65. **Tsotskas, Christos, Kipouros, Timoleon and Savill, Anthony Mark.** *The Design and Implementation of a GPU-enabled Multi-Objective Tabu-Search intended*

for Real World and High-Dimensional Applications. s.l. : Elsevier B.V., 2014. Procedia Computer Science, Volume 29.

66. **Hartjes, Sander, et al.** *Systems for Green Operations (SGO) ITD - Report on the Performance Analysis of the Trajectories - Cycle 1 - WP3.2.* s.l. : Clean Sky - SGO ITD (Internal), 2012.

67. **Cooper, M, et al.** *Aircraft Systems Modelling - Specification Document - WP3.1:O_3.1_40_a.* s.l. : Clean Sky - SGO ITD (Internal), 2012.

68. **Hocking, M.B.** *Passenger aircraft cabin air quality: trends, effects, societal costs, proposals.* s.l. : Elsevier Ltd, 2000. pp. 703-704, Volume 45,Issue 4-5. ISSN: 0045-6535.

69. **SAE Aerospace.** *Ice, Rain, Fog, and Frost Protection - AIR1168/4.* s.l. : SAE International, 1990.

70. **Andrade, Luiz and Tenning, Carl.** *Design of Boeing 777 electric system.* s.l. : IEEE, 1992. IEEE AES MAGAZINE, Volume 7, Issue 7.

71. **Herzog, Jacques.** *ELECTRIFICATION OF THE ENVIRONMENTAL CONTROL SYSTEM.* s.l. : ICAS 2006, 2006.

72. **Schneider, M.G, et al.** *Test Results of Reflux-Cooled Electromechanical Actuator.* s.l. : SAE, 1994. SAE 942176.

73. **de Tenorio, Cyril, et al.** *METHODOLOGY FOR AIRCRAFT SYSTEM ARCHITECTURE SIZING.* s.l. : ICAS 2008, 2008.

74. **Seresinhe, Ravinka, Lawson, Craig and Sabatini, Roberto.** *Environmental Impact Assessment, on the Operation of Conventional and More Electric Large Commercial Aircraft.* s.l. : SAE International, 2013. SAE International Journal of Aerospace Engineering, Volume 6, Issue 1. doi: 10.4271/2013-01-2086.

75. **Esdras, Gustavo Franco and Liscouet-Hanke, Susan.** *An Electrical Load Estimation Tool for Aircraft Conceptual Design.* Montreal, Canada : SAE International, 2013. 2013-01-2206.

76. **Kayton, Myron and Fried, R Walter.** *Avionics Navigation Systems.* Second Edition. s.l. : John Wiley & Sons, Inc, 1997. ISBN:978-0471547952.

77. **Kendal, Brian.** *Manual of Avionics.* Third Edition. s.l. : Blackwell Scientific Publications, 1993. ISBN:978-0632034727.

78. **Eaton Aerospace Limited.** *Fuel Boost Pump Type 8810 and Canister Type 8811.* 2013. Data Sheet. 568-1-28300, 568-1-28301.

79. —. *Fuel Boost Pump Type 20004 and Canister Type 20005.* 2013. 568-1-30685, 568-1-30690.

80. **Walsh, Philip P and Fletcher, Paul.** *Gas Turbine Performance.* Second Edition. Oxford : Blackwell, 1998. ISBN :978-0791800676.

81. **Scholz, Dieter, et al.** *FUEL CONSUMPTION DUE TO SHAFT POWER OFF-TAKES FROM THE ENGINE.* s.l. : Workshop on Airframe Systems Technologies (AST) 2013, 2013.

82. **Seresinhe, Ravinka, et al.** *Aircraft Systems Modelling - Specification Document.* s.l. : Clean Sky (Confidential), 2012. WP3.1:O_3.1_40_a.

83. **Seresinhe, Ravinka.** *Aircraft Systems Model - Description Document.* s.l. : Clean Sky (Confidential), 2012. WP3.1:O_3.1_40_b.

84. **Seresinhe, Ravinka and Lawson, Craig.** *Electrical load sizing methodology to aid conceptual and preliminary design of large commercial aircraft.* s.l. : SAGE Publications, 2014. Proceedings of the Institution of Mechanical Engineers, Part G: Journal of Aerospace Engineering. doi: 10.1177/0954410014534638.

85. **Shinkafi, Ahmed, Lawson, Craig, Seresinhe, Ravinka, Quaglia, Daniele and Madani, Irfan.** *AN INTELLIGENT ICE PROTECTION SYSTEM FOR NEXT GENERATION AIRCRAFT TRAJECTORY OPTIMISATION.* St Petersburgh : ICAS 2014, 2014.

86. **Shinkafi, Ahmed and Lawson, Craig.** *Enhanced Method of Conceptual Sizing of Aircraft Electro-Thermal De-icing System.* s.l. : World Academy of Science,

Engineering and Technology, 2014. International Journal of Mechanical, Aerospace, Manufacturing, Industrial Science and Engineering, Volume 8, Issue 6.

87. **Nuic, A.** *User Manual for the Base of Aircraft Data (BADA) revision 3.10.* s.l. : Eurocontrol, 2012.

88. **DuBois, Doug and Paynter, Gerald.** *"Fuel Flow Method2" for Estimating Aircraft Emissions.* s.l. : SAE International, 2006. SAE Technical Paper 3006-01-1987. doi: 10.4271/2006-01-1987.

89. **SAE International.** *AIR5715.* s.l. : SAE International, 2009. Technical Standard.

90. **Norman, P D, et al.** *Development of the technical basis for a New Emissions Parameter covering the whole AIRcraft operation: NEPAIR.* 2003. Final Technical Report; NEPAIR/WP4/WPR/01. EC Contract Number G4RD-CT-2000-00182.

91. **ICAO.** *ICAO ENGINE EMISSIONS DATA BANK - CFM56-5B4.* s.l. : ICAO, 1992.

92. —. *ICAO ENGINE EMISSIONS DATA BANK - CFM56-5C4.* s.l. : ICAO, 1992. 7CM047-CFM56-5C4_P SAC.

93. **Delft University of Technology.** *INMTM v3 Noise Calculation Tool Specification.* s.l. : CleanSky (Confidential), 2010. SGO-WP 3.1.2-TUD-SPEC-0053-A.

94. **Quaglia, Daniele, Ramasamy, Subramanian and Gardi, Alessandro.** *Software Design Description - Demographic Distribution Database (D3) Model Exploitation and Integration in GATAC.* s.l. : Clean Sky (Confidential), 2014. SGO-WP 3.1-C-U-OUT-0333.

95. **Seresinhe, Ravinka, et al.** *AIRFRAME SYSTEMS POWER OFF-TAKE MODELLING IN MORE-ELECTRIC LARGE AIRCRAFT FOR USE IN TRAJECTORY OPTIMISATION.* St. Petersburgh, Russia : 29th Congress of the International Council of Aeronautical Sciences, ICAS 2014, 2014.

96. **UK CIVIL AVIATION AUTHORITY.** *ENGINE TYPE CERTIFICATE DATA SHEET NO. 1044.* s.l. : UK CAA, 2003. ISSUE 24.

97. **UK CIVIL AVAITION AUTHORITY.** *ENGINE TYPE CERTIFICATE DATA SHEET NO. 1043.* s.l. : UK CAA, 1988. ISSUE 36.

98. **EUROPEAN AVIATION SAFETY AGENCY.** *EASA TYPE-CERTIFICATE DATA SHEET - E.060.* s.l. : EASA, 2007. ISSUE 01.

99. —. *EASA TYPE-CERTIFICATE DATA SHEET - E.042.* s.l. : EASA, 2006. ISSUE 01.

100. **UK CIVIL AVIATION AUTHORITY.** *ENGINE TYPE CERTIFICATE DATA SHEET NO. 1051.* s.l. : UK CAA, 2004. ISSUE 14.

101. **EUROPEAN AVIATION SAFETY AGENCY.** *EASA TYPE-CERTIFICATE DATA SHEET - E.012.* s.l. : EASA, 2013. ISSUE 05.

102. —. *EASA TYPE-CERTIFICATE DATA SHEET - E0.36.* s.l. : EASA, 2011. ISSUE 03.

103. —. *EASA TYPE CERTIFICATE DATA SHEET - IM.E.021.* s.l. : EASA, 2013. ISSUE 05.

104. **U.S. DEPARTMENT OF TRANSPORTATION - FEDERAL AVIATION ADMINISTRATION.** *TYPE CERTIFICATE DATA SHEET E13NE.* s.l. : U.S DEPARTMENT OF TRANSPORTATION - FAA, 2005. REVISION 20.

105. **EUROPEAN AVIATION SAFETY AGENCY.** *EASA TYPE CERTIFICATE DATA SHEET - E.003.* s.l. : EASA, 2012. ISSUE 03.

106. —. *ENGINE TYPE CERTIFICATE DATA SHEET EASA.IM.E.002.* s.l. : EASA, 2004. ISSUE 02.

107. —. *EASA TYPE CERTIFICATE DATA SHEET - IM.E.102.* s.l. : EASA, 2012. ISSUE 04.

108. —. *EASA TYPE CERTIFICATE DATA SHEET - IM.E.069.* s.l. : EASA, 2013. ISSUE 02.

109. —. *EASA TYPE CERTIFICATE DATA SHEET - IM.E.026.* s.l. : EASA, 2013. ISSUE 03.

110. —. *EASA TYPE-CERTIFICATE DATA SHEET - IM.E.043.* s.l. : EASA, 2013. ISSUE 02.

Appendix A: List of inputs for the A300 case study for the ELA

AIRCRAFT LEVEL INPUTS	
No. of engines	2
No. of APU	1
No. of wings	2
No. of pilots	2
APU capacity (kVA)	90
No. of RAT	1
No. of passengers (maximum density)	269
No. of passengers (aircraft variant)	269
Maximum range(km)	7500
No. of lavatories	4
No. of galleys	6
No. of exits	8
Cabin volume(m3)	289
SYSTEM LEVEL INPUTS	
ECS - ATA 21	
No. of conditioning packs	2

No. of cabin compartments (incl. cockpit)	3
No. of avionics compartments	1
No. of cargo compartments	2
No. of ram air inlets	1
No. of re-circulation fans in cabin	2
No. of zone controllers	1
No. of blowers for avionics ventilation	1
No. of cabin pressure controllers	3

Landing Gear - ATA 32

No. of wheels with fans	0
No. of brake pressure indicators	1

IPS - ATA 30

No. of heated windows	2
No. of heated drain masts	0

Maintenance - ATA 45

No. of maintenance computers	1
No. of displays for maintenance	1

Hydraulics - ATA 29

No. of hydraulic pumps per engine	1
No. of hydraulic systems	3
No. of HSMU	0
No. of electric pumps in hydraulic systems	2

Fuel - ATA 28

No. of transfer valves to outer tanks	2

Fuel functionality matrix

	Tanks	Refuel	Jettison	Trim transfer	Gravity XFR to feed tank	Pump XFR to feed tank	Engine Feed
Outer	2	y	n	n	y	n	n
Inner	2	n	n	n	n	n	y
Centre	1	y	n	n	n	y	y
Trim	0	n	n	n	n	n	n

FCS - ATA 27

No. of primary computers	0
No. of secondary computers	0
No. of flight data concentrators	0

No. of flight augmentation computers	0
No. of flap/slat computers	0
No. of pitch trim actuators	3
No. of rudder trim actuators	2
No. of rudder travel actuators	2
No. of gyroscopes	0
No. of accelerometers	0

Water & Waste - ATA 38

No. of water tanks	1
No. of waste tanks	1

Indicating & recording - ATA 31

No. of digital flight data recorders	0
No. of linear accelerometers	0
No. of weight and balance computers	0

Lighting - ATA 33

Lighting type	Fluorescent
No. of Instrument panels per pilot	5
No. of annunciator lights	100

No. of forward navigation lights	2
No. of rear navigation lights	1
No. of beacon lights	2
No. of landing lights	2
No. of runway turn-off lights	2
No. of taxi and take-off lights	2
No. of logo lights	2
No. of wing inspection lights	2

Consumer Loads

Do passengers have an in-seat power supply	n
Do passengers have in-flight entertainment	n
Are the above two systems integrated	n
Food heating cycles per serving	1

Navigation - ATA34

No. of TCAS	0
No. of PVI	0
No. of AHRS	0

Autopilot - ATA 22

No. of flight management guidance computers	0
No. of FMS display units	0
No. of flight control units	10
No. of FMS data loaders	0

OPERATIONAL LEVEL INPUTS

No. of pitch trim actuators used at a time	1
No. of rudder trim actuators used at a time	1
No. of rudder travel actuators used at a time	1
Fraction of annunciator lights on ground	0.2
Maximum fraction of simultaneous galley operation	1

Appendix B: Characteristics of past and present large commercial turbofan engines

Engine	Manufacturer	Aircraft application	Max. T-O F_n (kN)	Max. Bleed% - normal operation	Gen. PAD continuous rating (kW)	
RB211-535E4-B-37	Rolls Royce	Boeing 757-28A	189.3	2% HPC 2nd stage – max. T-O	-	[96]
RB211-524D4-19	Rolls Royce	Boeing 747-300	231.2	3.4% IPC – max. T-O	-	[97]
Trent 553-61	Rolls Royce	Airbus A340-541	248.1	1% HPC 1st stage – max. T-O	-	[98]
Trent 772-60	Rolls Royce	Airbus A330-300	316.3	2.4% IPC 8th stage – max. T-O	-	[99]
Trent 892-17	Rolls Royce	Boeing 777-300	406.8	2.2% IPC 8th stage – max. T-O	-	[100]
Trent 970-84	Rolls Royce	Airbus A380-841	334.3	1.95% IPC 8th stage – max. T-O	-	[101]
Trent 1000-A	Rolls Royce	Boeing 787-8	307.8	No bleed	-	[102]
CF34-10E5	GE	Embraer E190	83.7	8% HPC 5th stage – max. T-O	74.8	[103]
CF6-80C2-B1F	GE	Boeing 747-428M	254.3	5% HPC 14th stage – max. T-O	164.1	[104]
CFM56-5B1	GE/ Snecma	Airbus A321-111	133.5	7% HPC 9th stage - above 82.5% N1K	135	[105]
GE90-94B	GE	Boeing 777-200ER	432.8	7.8% - combined bleed -	181.3	[106]

				above 96.8% N1K		
Genx-1B54	GE	Boeing 787-8	255.3	No bleed	1032	[107]
V2522-A5	IAE	Airbus A319	102.5	6% HPC 7th stage - above 97% of N2K	131	[108]
GP7270	P&W/ GE	Airbus A380-800	332.4	5.8% HPC 4th stage - above 2319 rpm (N1K)	186	[109]
PW4164	P&W	Airbus A330-300	286.9	4% 8th stage bleed	130	[110]

Appendix C: Design and off-design performance points used in validation of engine simulation

Point No.	Condition	Description
1	Design point	Datum point, specified thrust of 51,980 lbf, SLS, ISA, 100% intake efficiency, no off-takes
2	Off-design	Specified thrust of 47,230 lbf, otherwise as point 1.
3	Off-design	Specified thrust of 11,230 lbf, 35,000 ft altitude, 0.85 M, ISA, and 100 HP off-take.
4	Off-design	Specified thrust of 10,110 lbf, otherwise as point 3.
5	Off-design	Specified thrust of 8,980 lbf, otherwise as point 3.
6	Off-design	Specified thrust of 7,860 lbf, otherwise as point 3.
7	Off-design	Rating code of 50, SL, 0.1 M, ISA and 100 HP off-take
8	Off-design	Rating code of 50, 5,000 ft altitude, 0.3 M, ISA +15, otherwise as point 7.
9	Off-design	Rating code of 45, 5,000 ft altitude, 0.3 M, ISA +39.4, otherwise as point 7.
10	Off-design	Rating code of 40, 15,000 ft altitude, 0.65 M, ISA +10, otherwise as point 7.
11	Off-design	Rating code of 40, 25,000 ft altitude, 0.75 M, ISA +10, otherwise as point 7.
12	Off-design	Rating code of 40, 35,000 ft altitude, 0.85 M, ISA +10, otherwise as point 7.

13	Off-design	Rating code of 40, 10,000 ft altitude, 0.3 M, ISA +10, otherwise as point 7.
14	Off-design	Specified thrust of 15,050 lbf, 25,000 ft altitude, 0.7 M, ISA, otherwise as point 7.
15	Off-design	Specified thrust of 40,000 lbf, SLS, ISA +15, no off-takes.
16	Off-design	Specified power lever angle of 85.0, otherwise as point 15.
17	Off-design	Specified power lever angle of 89.49, 5 lb/s IP cabin airflow, otherwise as point 15.
18	Off-design	Specified power lever angle of 89.49, 5 lb/s HP cabin airflow, otherwise as point 15.
19	Off-design	Specified power lever angle of 89.49, 15 lb/s HP cabin airflow, otherwise as point 15.
20	Off-design	Specified thrust of 4,000 lbf, 35,000 ft altitude, 0.84 M, ISA +15, 100 HP off-take, 2.5 lb/s IP cabin airflow.
21	Off-design	Specified thrust of 6,500 lbf, 35,000 ft altitude, 272.6 kts VEAS*, no cabin bleed, otherwise as point 20.
22	Off-design	Specified thrust of 6,500 lbf, 35,000 ft altitude, 490.0 kts VTAS**, otherwise as point 21.
23	Off-design	Rating code of 52, SL, 0.22 M, ISA +20, 100 HP off-takes, no bleeds.

M – Mach number

HP – Horse Power

ISA – International Standard Atmospheric conditions

SLS – Sea Level Static

SL – Sea Level

*VEAS – Equivalent Air Speed

**VTAS – True Air Speed

Appendix D: Departure and Arrival charts

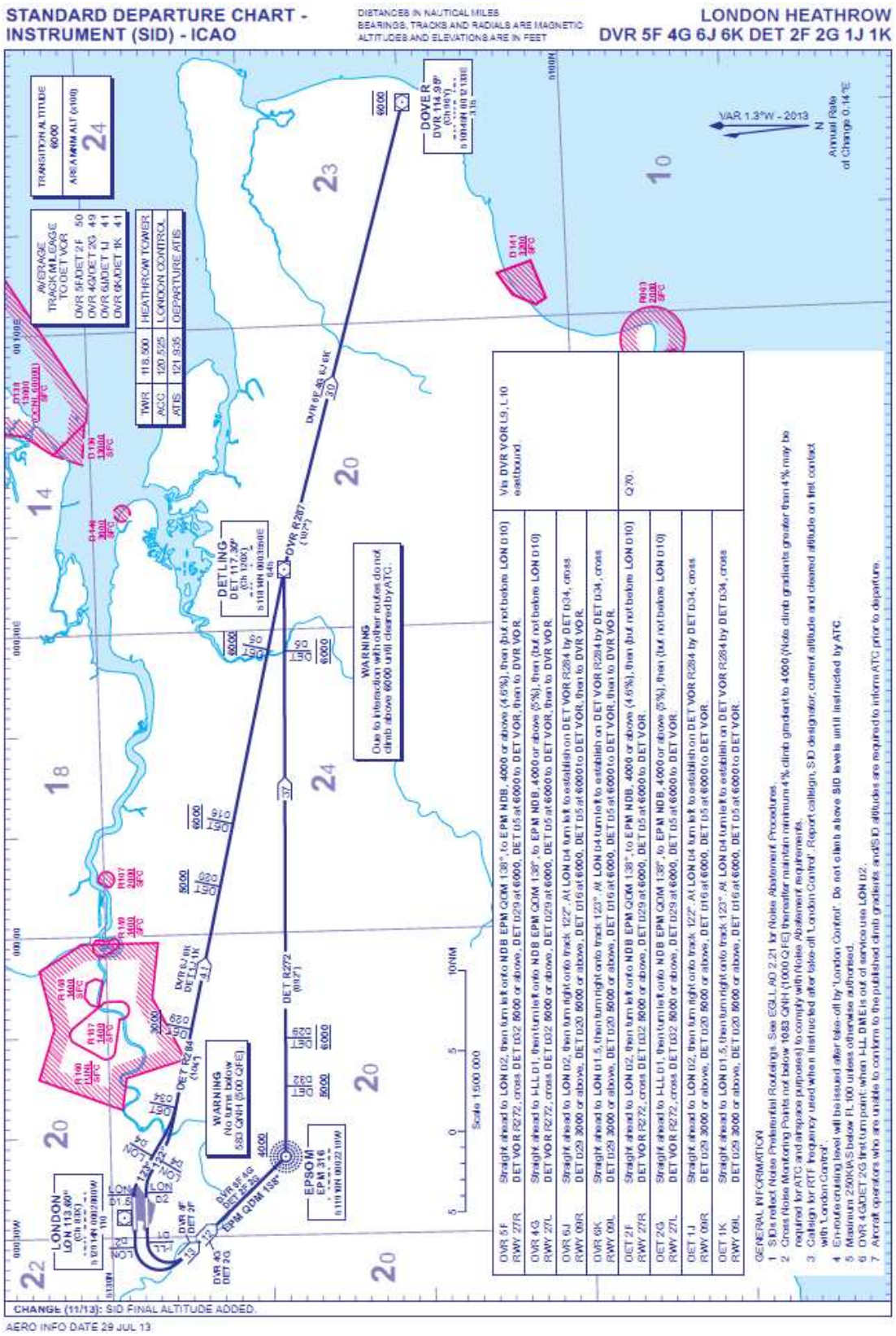

Figure D-0-1: SID at Heathrow - Dover departure

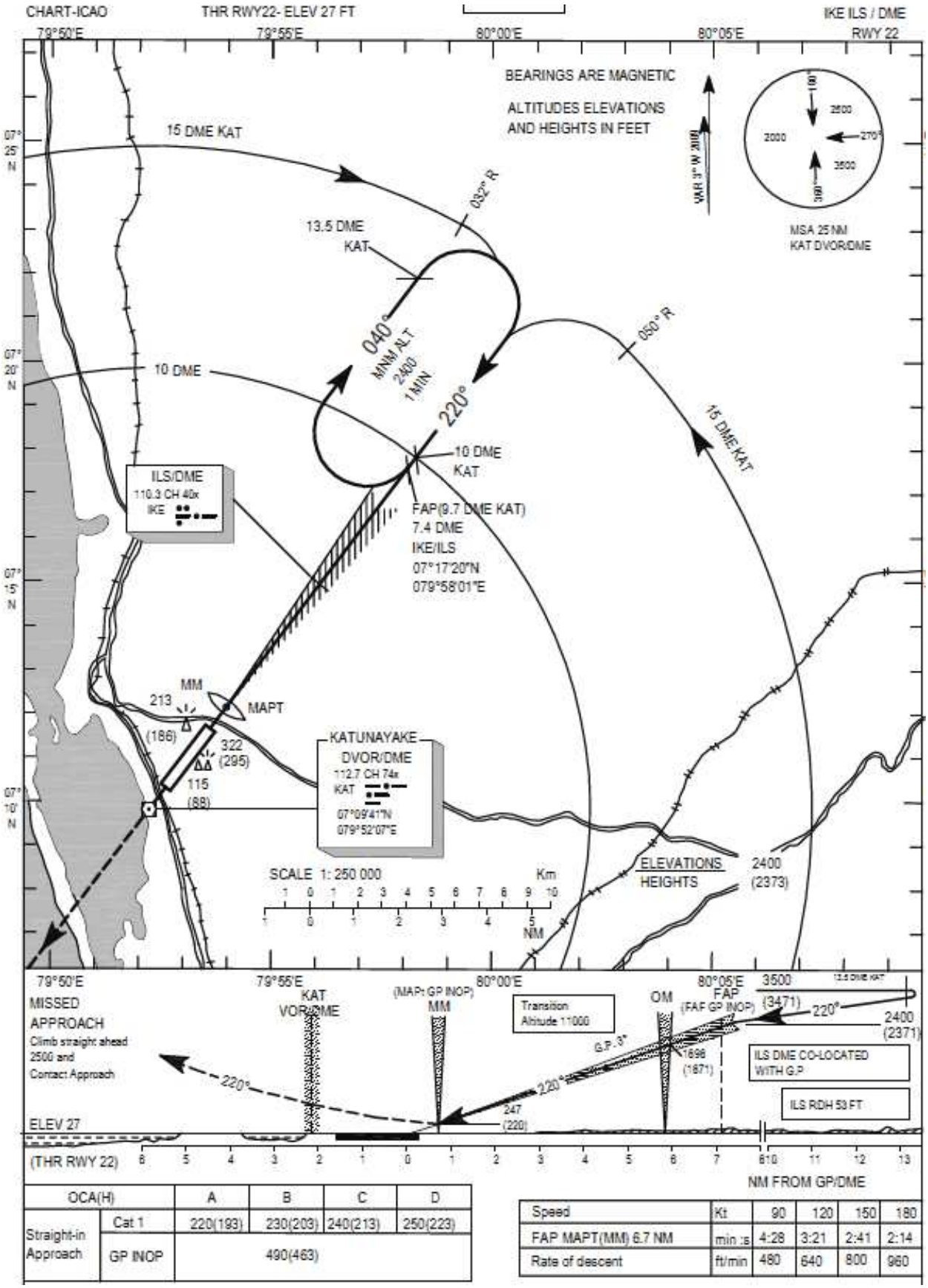

OCA(H)		A	B	C	D
Straight-in Approach	Cat 1	220(193)	230(203)	240(213)	250(223)
	GP INOP	490(463)			

Speed	Kt	90	120	150	180
FAP MAPT(MM) 6.7 NM	min :s	4:28	3:21	2:41	2:14
Rate of descent	ft/min	480	640	800	960

Figure D-0-2: Arrival Procedure at Colombo, Sri Lanka

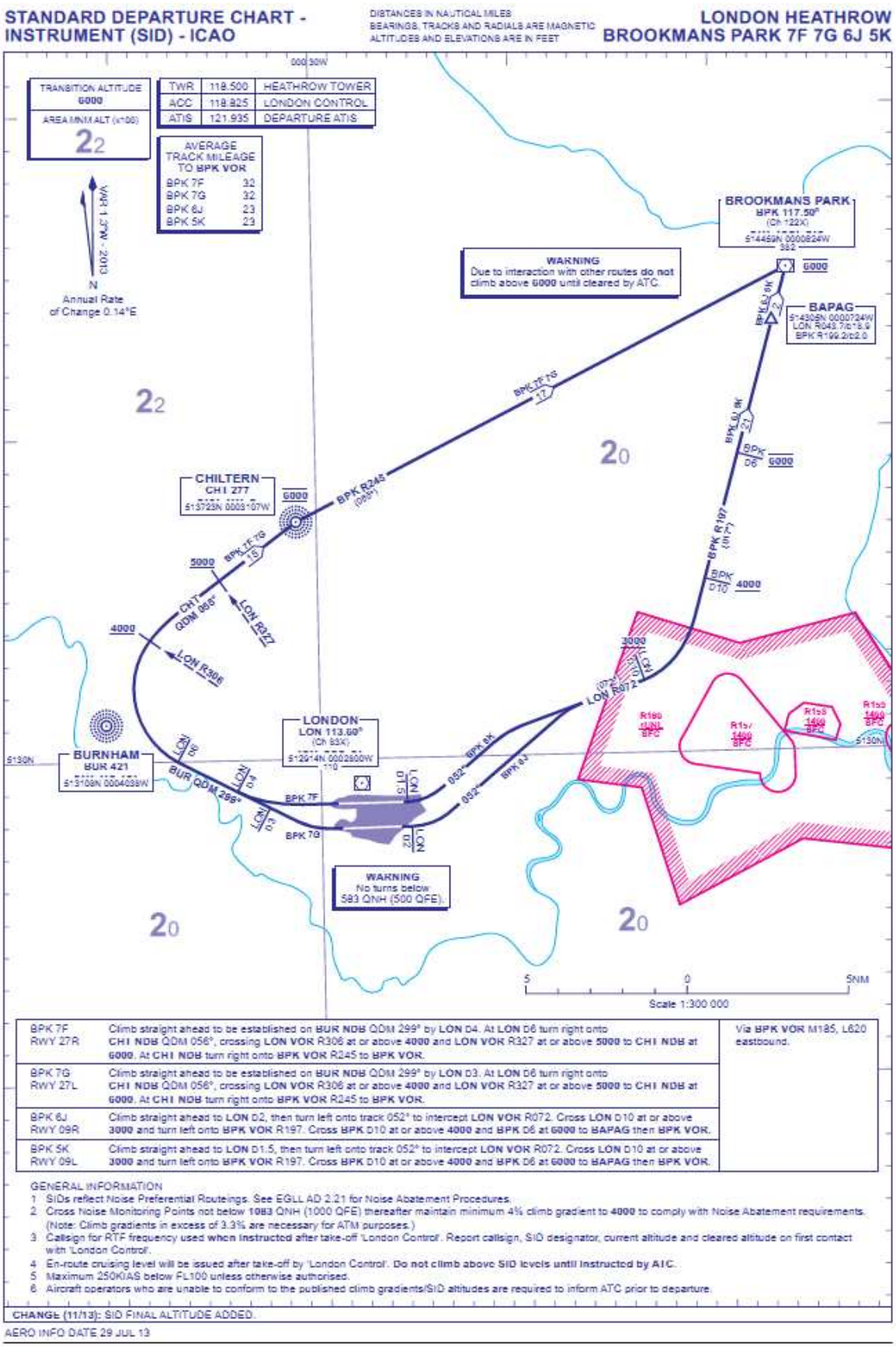

Figure D-0-3: SID at Heathrow – Brookmans Park departure

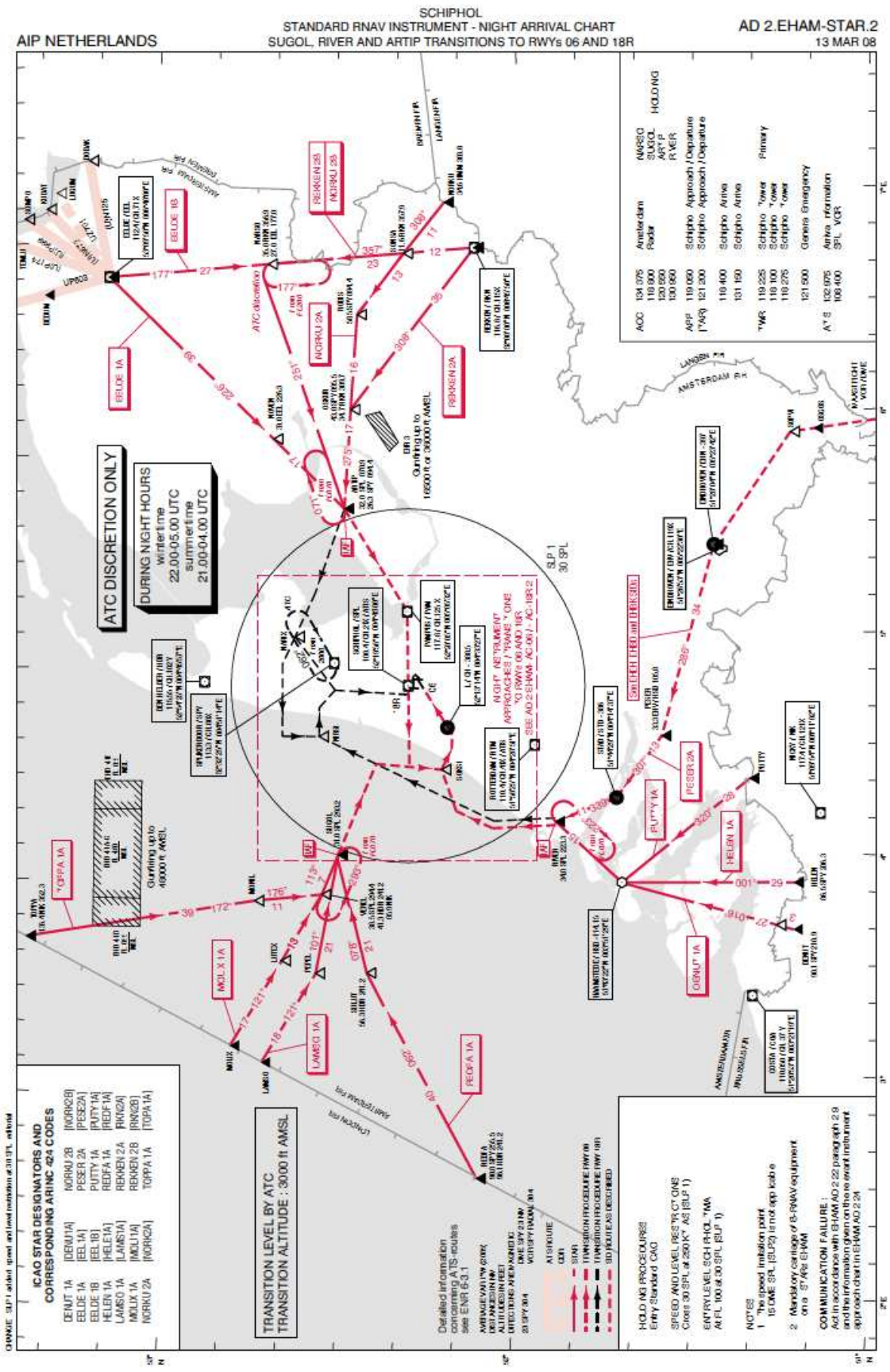

Figure D-0-4: Arrival procedure at Amsterdam, Schiphol